

# Merge Two into One: Multispecific Symmetric Antibodies for Cancer Immunotherapy



TECHNISCHE  
UNIVERSITÄT  
DARMSTADT

Vom Fachbereich Chemie  
der Technischen Universität Darmstadt

zur Erlangung des Grades  
Doctor rerum naturalium  
(Dr. rer. nat.)

Dissertation  
von  
Julia Harwardt, M. Sc.

Erstgutachter: Prof. Dr. Harald Kolmar  
Zweitgutachter: PD Dr. Stefan Schülke

Darmstadt 2024

---

---

Harwardt, Julia: Merge Two into One: Multispecific Symmetric Antibodies for Cancer Immunotherapy  
Darmstadt, Technische Universität Darmstadt,

Jahr der Veröffentlichung der Dissertation auf TUpriints: 2024

URN: urn:nbn:de:tuda-tuprints-278482

URI: <https://tuprints.ulb.tu-darmstadt.de/id/eprint/27848>

Tag der Einreichung: 10. Juni 2024

Tag der mündlichen Prüfung: 22. Juli 2024

Urheberrechtlich geschützt:

<https://rightsstatements.org/page/InC/1.0/>

Die vorliegende Arbeit wurde unter der Leitung von Herrn Prof. Dr. Harald Kolmar am Clemens-Schöpf-Institut für Organische Chemie und Biochemie der Technischen Universität Darmstadt im Zeitraum von Januar 2021 bis Februar 2024 angefertigt.

---

---

## Publications derived from this work

---

**Harwardt J\***, Bogen JP\*, Carrara SC, Ullitzka M, Grzeschik J, Hock B, Kolmar H (2022). A Generic Strategy to Generate Bifunctional Two-in-One Antibodies by Chicken Immunization. *Frontiers in Immunology*, 10.3389/fimmu.2022.888838.

**Harwardt J**, Carrara SC, Bogen JP, Schoenfeld K, Grzeschik J, Hock B, Kolmar H (2023). Generation of a symmetrical trispecific NK cell engager based on a two-in-one antibody. *Frontiers in Immunology*, 10.3389/fimmu.2023.1170042.

**Harwardt J**, Geyer FK, Schoenfeld K, Baumstark D, Molkenhuth V, Kolmar H (2024). Balancing the Affinity and Tumor Cell Binding of a Two-in-One Antibody Simultaneously Targeting EGFR and PD-L1. *Antibodies*, 10.3390/antib13020036.

Schoenfeld K\*, **Harwardt J\***, Kolmar H (2024). Better safe than sorry: Dual targeting antibodies for cancer immunotherapy. *Biological Chemistry*, 10.1515/hsz-2023-0329.

\* shared first authorship

---

---

## Patent application derived from this work

---

Kolmar H, **Harwardt J**, Bogen JP, Carrara SC, Ullitzka M (2023). TWO IN ONE – ANTIBODIES BINDING TO EGFR/PD-L1-DOUBLE POSITIVE CELLS. EP4238992A1.

---

---

## Contributions to Publications

---

Pekar L, Klewinghaus D, Arras P, Carrara SC, **Harwardt J**, Krah S, Yanakieva D, Toleikis L, Smider VV, Kolmar H, Zielonka S (2021). Milking the Cow: Cattle-Derived Chimeric Ultralong CDR-H3 Antibodies and Their Engineered CDR-H3-Only Knobby Counterparts Targeting Epidermal Growth Factor Receptor Elicit Potent NK Cell-Mediated Cytotoxicity. *Frontiers in Immunology*, 10.3389/fimmu.2021.742418.

Carrara SC, **Harwardt J**, Grzeschik J, Hock B, Kolmar H (2022). TriTECM: A tetrafunctional T-cell engaging antibody with built-in risk mitigation of cytokine release syndrome. *Frontiers in Immunology*, 10.3389/fimmu.2022.1051875.

Schoenfeld K, **Harwardt J**, Habermann J, Elter A, Kolmar H (2023). Conditional activation of an anti-IgM antibody-drug conjugate for precise B cell lymphoma targeting. *Frontiers in Immunology*, 10.3389/fimmu.2023.1258700.

Ulitzka M, **Harwardt J**, Lipinski B, Tran H, Hock B, Kolmar H (2024). Potent Apoptosis Induction by a Novel Trispecific B7-H3xCD16xTIGIT 2+1 Common Light Chain Natural Killer Cell Engager. *Molecules*, 10.3390/molecules29051140.

---

---

## Contributions to Conferences

---

**Harwardt J**, Bogen JP, Carrara SC, Grzeschik J, Hock B, Kolmar H. A generic strategy to generate trifunctional two-in-one antibodies by chicken immunization (Poster). *Protein Engineering Summit Europe*, Barcelona, Spain (14 – 16 November 2022).

Ulitzka M, **Harwardt J**, Mattes B, Hock B, Kolmar H. A streamlined process for the generation of humanized multispecific common light chain NK cell-engaging mABs (Poster). *Protein Engineering Summit Europe*, Barcelona, Spain (14 – 16 November 2022).

**Harwardt J**, Schoenfeld K, Carrara SC, Bogen JP, Kolmar H. The potential of 2in1 antibodies: affinity maturation & trifunctionalization (Poster). *Protein Engineering Summit Europe*, Lisbon, Portugal (14 – 16 November 2023).

Schoenfeld K, **Harwardt J**, Habermann J, Elter A, Kolmar H. Precise targeting of B cell lymphoma by a conditionally activated anti-IgM antibody-drug conjugate (Poster). *Protein Engineering Summit Europe*, Lisbon, Portugal (14 – 16 November 2023).

Meiser F, **Harwardt J**, Kolmar H. Engineering bispecific antibodies targeting CD89 for macrophage-mediated tumor eradication (Poster). *Protein Engineering Summit Europe*, Lisbon, Portugal (14 – 16 November 2023).

Baumstark D, Wörle E, Mehringer J, **Harwardt J**, Schubert T, Plach M, Gellert J, Kolmar H, Molkenhuth V. Real-time binding kinetics on cells (Poster). *Protein Engineering Summit Europe*, Lisbon, Portugal (14 – 16 November 2023).

---

---

## Table of Contents

---

<b>Publications derived from this work</b>	<b>ii</b>
<b>Patent application derived from this work</b>	<b>ii</b>
<b>Contributions to Publications</b>	<b>iii</b>
<b>Contributions to Conferences</b>	<b>iv</b>
<b>Table of Contents</b>	<b>v</b>
<b>Zusammenfassung und wissenschaftlicher Erkenntnisgewinn</b>	<b>vi</b>
<b>Scientific Novelty and Significance</b>	<b>viii</b>
<b>Individuelle Beiträge von J. Harwardt zum kumulativen Teil der Dissertation</b>	<b>x</b>
<b>1. Introduction</b>	<b>1</b>
1.1. Antibody structure, function, and diversification	2
1.2. Antibodies as therapeutic agents	5
1.2.1. Therapeutic antibodies in immuno-oncology	8
1.3. Generation of therapeutic antibodies	9
1.3.1. Yeast surface display	10
1.3.2. Chicken-derived antibodies	12
1.4. Antibody engineering	13
1.4.1. Fc engineering	14
1.4.2. Affinity maturation	15
1.5. Bispecific antibodies	16
1.5.1. Two-in-One antibodies	18
1.5.2. Dual tumor targeting antibodies	19
1.5.3. Immune cell engagers	20
1.6. Trispecific antibodies	22
<b>2. Objective</b>	<b>25</b>
<b>3. References</b>	<b>27</b>
<b>4. Cumulative Section</b>	<b>44</b>
4.1. A Generic Strategy to Generate Bifunctional Two-in-One Antibodies by Chicken Immunization	44
4.2. Generation of a symmetrical trispecific NK cell engager based on a two-in-one antibody	64
4.3. Balancing the Affinity and Tumor Cell Binding of a Two-in-One Antibody Simultaneously Targeting EGFR and PD-L1	84
4.4. Better safe than sorry: Dual targeting antibodies for cancer immunotherapy	110
<b>5. Danksagung</b>	<b>128</b>
<b>6. Affirmations</b>	<b>131</b>

---

## Zusammenfassung und wissenschaftlicher Erkenntnisgewinn

---

Diese Arbeit befasst sich mit der Herstellung und Charakterisierung von multispezifischen symmetrischen Antikörpern für die Krebsimmuntherapie. Im Gegensatz zu asymmetrischen Antikörpern, bei denen *Protein Engineering* Technologien angewendet werden müssen, um die korrekte Paarung der verschiedenen Polypeptidketten zu gewährleisten, bestehen symmetrische Antikörper aus zwei identischen schweren und leichten Ketten. Folglich weisen diese Moleküle hinsichtlich der etablierten Herstellung und des konventionellen Zulassungsverfahrens ähnliche Eigenschaften wie monoklonale Antikörper (mAb) auf. *Two-in-One* Antikörper sind symmetrische tetravalente IgG-ähnliche bispezifische Antikörper (bsAbs), bei denen jedes Antigenbindungsfragment (*fragment antigen binding*, Fab) zwei verschiedene Antigene adressiert. Die gleichzeitige Bindung von zwei tumorassoziierten Antigenen (TAAs) auf derselben bösartigen Zelle bietet Vorteile wie erhöhte Spezifität und geringere Immunevasion. Die Optimierung der Affinität kann die Wirksamkeit von Arzneimittelkandidaten weiter verbessern und unerwünschte Nebenwirkungen begrenzen.

Die erste Untersuchung im Rahmen dieser kumulativen Dissertation befasste sich mit der Generierung eines symmetrischen *Two-in-One* Antikörpers, der den epidermalen Wachstumsfaktor-Rezeptor (EGFR) und den programmierten Zelltod-Liganden-1 (PD-L1) bindet, zwei therapeutische Zielmoleküle, die in vielen soliden Tumoren hochreguliert sind. Dazu wurde die schwere Kette eines vom Huhn stammenden anti-PD-L1 *common light chain* (cLC) Antikörpers mit einer vom Huhn stammenden anti-EGFR Hefe-Display (YSD) Antikörperbibliothek kombiniert und anschließend auf Bindungseigenschaften an beide Antigene untersucht. Der isolierte *Two-in-One* Antikörper HCP-LCE adressierte EGFR und PD-L1 gleichzeitig mit demselben Fab-Fragment und wies vorteilhafte biophysikalische Eigenschaften auf. BLI-Messungen und zellbasierte Assays ergaben, dass HCP-LCE die EGFR-Signalübertragung durch Bindung an die EGFR Dimerisierungsdomäne II hemmt und die PD-1/PD-L1-Interaktion blockiert. Bemerkenswerterweise wurden beide Antigene mit vergleichsweise geringen Bindungsaffinitäten im zweistelligen bis dreistelligen nanomolaren Bereich adressiert, jedoch wurden spezifische und hochaffine zelluläre Bindungseigenschaften auf EGFR- und PD-L1-doppelpositive Tumorzellen nachgewiesen. HCP-LCE ist der erste *Two-in-One* Antikörper ohne *complementarity-determining region* (CDR) *Engineering*, der mit einem einzigen Fab-Fragment zwei Antigene gleichzeitig bindet. Dieser Ansatz der Bibliotheksgenerierung ebnet den Weg für die weitere Entwicklung von aus der Vogelimmunisierung stammenden *Two-in-One* Antikörpern mit maßgeschneiderten Bindungseigenschaften.

In dem zweiten Projekt wurde ein symmetrischer trispezifischer natürlicher Killer (NK) Zell-Engager (NKCE) auf der Grundlage des zuvor isolierten *Two-in-One* Antikörpers entwickelt. Durch die

---

gleichzeitige Adressierung eines TAA und eines spezifischen Markers auf der Oberfläche von NK-Zellen wird die Immunfunktion von NK-Zellen zur Eliminierung von Tumorzellen für die Tumorthherapie nutzbar gemacht. Zum Aufbau eines solchen Antikörpers wurde die cLC-Technologie eingesetzt, eine etablierte Methode zur Vermeidung von Fehlpaarungen der leichten Kette in multispezifischen Antikörpern. Dazu wurde die leichte Kette des *Two-in-One* Antikörpers HCP-LCE als cLC für die Herstellung einer vom Huhn stammenden anti-CD16a YSD-Bibliothek verwendet. Das isolierte cLC Fab-Fragment, das an CD16a bindet, wurde in einer *Head-to-Tail*-Konfiguration mit dem parentalen *Two-in-One* Antikörper fusioniert, wodurch ein symmetrischer trispezifischer 2+2 Antikörper entstand, der gleichzeitig EGFR, PD-L1 und CD16a mit sechs unabhängigen Paratopen auf vier Fabs adressierte. Der Antikörper zeigte eine spezifische zelluläre Bindung an EGFR- und PD-L1-doppelpositive Tumorzellen und verursacht eine NK-Zell-vermittelte Tumorzellabtötung (ADCC) bereits bei niedrigen Konzentrationen. Diese Studie leistet Pionierarbeit bei der unkomplizierten Herstellung trispezifischer cLC Immunzell-aktivierender Antikörper in einem 2+2 Design, die aufgrund ihrer symmetrischen Architektur die nachfolgende Prozessentwicklung erleichtern.

Der dritte Teil dieser Arbeit befasste sich mit der Affinitätsoptimierung des *Two-in-One* Antikörpers hinsichtlich der EGFR-Bindung durch zielgerichtete Mutagenese und YSD in Kombination mit fluoreszenzaktivierter Zellsortierung (FACS). Einzelne Aminosäuren der CDR1 und CDR3 der leichten Kette wurden randomisiert, und die resultierende YSD Bibliothek lieferte eine *Two-in-One* Variante, die eine 60-fache Verbesserung der EGFR-Bindungsaffinität durch den Austausch einer einzelnen Aminosäure an Position drei der CDR3 der leichten Kette aufwies, während die PD-L1-Bindung nicht beeinträchtigt wurde. Die AlphaFold2-basierte Modellierung sagte voraus, dass der Austausch der neutralen Aminosäure Tyrosin gegen die saure Aminosäure Glutaminsäure die Bildung einer zusätzlichen Salzbrücke zwischen der eingeführten Glutaminsäure und einem Arginin an EGFR-Position 165 verursacht. Die erhöhte Affinität wurde durch BLI-Messungen, Echtzeit-Antigenbindungsmessungen auf Oberflächen mit einer Mischung aus beiden rekombinanten Proteinen und zellulären Bindungsstudien mittels Durchflusszytometrie und Echtzeit-Interaktionszytometrie nachgewiesen. Dieser Ansatz zur Affinitätsoptimierung bietet eine breit anwendbare generische Strategie für die Affinitätsreifung von *Two-in-One* Antikörpern.



---

---

## Scientific Novelty and Significance

---

This work is focused on the generation and characterization of multispecific symmetric antibodies for cancer immunotherapy. In contrast to asymmetric antibodies, where protein engineering technologies need to be applied to ensure the correct pairing of the different polypeptide chains, symmetric antibodies consist of two identical heavy and light chains. Consequently, these molecules exhibit monoclonal antibody (mAb)-like characteristics in terms of established manufacturing and a conventional approval process. Two-in-One antibodies are symmetrical tetravalent IgG-like bispecific antibodies (bsAbs) in which each fragment antigen binding (Fab) addresses two distinct antigens. Simultaneous targeting of two tumor-associated antigens (TAAs) on the same malignant cell offers advantages like increased specificity and reduced immune escape. Affinity optimization can further improve the efficacy of drug candidates and limit adverse effects.

The first investigation within this cumulative thesis was dedicated on the generation of a symmetrical Two-in-One antibody targeting epidermal growth factor receptor (EGFR) and programmed cell death ligand-1 (PD-L1), two therapeutic targets upregulated in many solid tumors. To this end, the heavy chain of a chicken-derived anti-PD-L1 common light chain (cLC) antibody was combined with a chicken-derived anti-EGFR light chain yeast surface display (YSD) library, followed by subsequent screening for binding properties towards both antigens. The isolated Two-in-One antibody HCP-LCE simultaneously targeted EGFR and PD-L1 at the same Fab fragment and exhibited favorable biophysical characteristics. BLI measurements and cell-based assays revealed that HCP-LCE inhibited EGFR signaling by binding to EGFR dimerization domain II and blocked the PD-1/PD-L1 interaction. Remarkably, both antigens were addressed with comparatively low binding affinities in the double- to triple-digit nanomolar range, but specific and high-affinity cellular binding properties were demonstrated on EGFR and PD-L1 double positive tumor cells. HCP-LCE represented the first Two-in-One antibody without complementarity-determining region (CDR) engineering, targeting two antigens simultaneously with a single Fab fragment. This approach of library generation paves the way for the further development of Two-in-One antibodies derived from avian immunization with tailor-made binding properties.

In a second project, a symmetrical trispecific natural killer (NK) cell engager (NKCE) was generated based on the previously isolated Two-in-One antibody. By the simultaneous targeting of a TAA and a specific marker on the surface of NK cells, the immune function of NK cells to kill tumor cells is harnessed for tumor therapy. For the generation of such an antibody, the cLC technology was applied, an established method to circumvent light chain mispairing in multispecific antibodies. To this end, the light chain of the Two-in-One antibody HCP-LCE was used as cLC for the generation of a chicken-derived anti-CD16a YSD library. The isolated CD16a engaging cLC Fab fragment was fused in a head-to-tail setup

---

with the parental Two-in-One antibody, resulting in a symmetrical trispecific 2+2 antibody that simultaneously bound EGFR, PD-L1 and CD16a with six independent paratopes on four Fabs. The antibody exhibited specific cellular binding on EGFR and PD-L1 double positive tumor cells and induced NK cell-mediated tumor cell killing (ADCC) already at low concentrations. This study pioneers the straightforward generation of trispecific cLC immune cell engager molecules in a 2+2 design, which facilitates subsequent process development due to the symmetrical architecture.

The third part of this work focused on the affinity maturation of the Two-in-One antibody for EGFR binding by site-directed mutagenesis and YSD in combination with fluorescence-activated cell sorting (FACS). Individual amino acids of the light chain CDR1 and CDR3 were randomized and the resulting YSD library provided a Two-in-One variant that exhibited a 60-fold improvement in EGFR binding affinity due to the replacement of a single amino acid at position three of the light chain CDR3, while PD-L1 binding was not impaired. AlphaFold2-based modeling predicted that the exchange of the neutral amino acid tyrosine to the acidic amino acid glutamic acid causes the formation of an additional salt bridge between the introduced glutamic acid and an arginine at EGFR position 165. The increase in affinity was demonstrated by BLI measurements, real-time antigen binding measurements on surfaces with a mixture of both recombinant proteins and cellular binding studies using flow cytometry and real-time interaction cytometry. This easily adaptable approach provides a generic strategy for the affinity maturation of Two-in-One antibodies.

---

---

## Individuelle Beiträge von J. Harwardt zum kumulativen Teil der Dissertation

---

- 1) **Harwardt J\***, Bogen JP\*, Carrara SC, Ullitzka M, Grzeschik J, Hock B, Kolmar H (2022). A Generic Strategy to Generate Bifunctional Two-in-One Antibodies by Chicken Immunization. *Frontiers in Immunology*, 10.3389/fimmu.2022.888838.

(\*Geteilte Erstautorenschaft)

### Beiträge von J. Harwardt:

- Design und Planung der Experimente mit J. P. Bogen
- Generierung und Screening der Bibliothek
- Reformatierung und Charakterisierung des resultierenden Antikörpers
- Design und Anfertigung der im Artikel dargestellten Abbildungen
- Verfassen des Manuskripts mit J. P. Bogen und H. Kolmar

**Der Anteil von J. Harwardt an dieser Publikation beläuft sich auf 40%.** Der Anteil von J.P. Bogen beläuft sich als Co-Erstautor ebenfalls auf 40%. Die verbleibenden 20% verteilen sich auf die übrigen Co-autoren für die experimentelle Beteiligung an Zellkultivierung und chromatographischer Reinigung, kritische Anmerkungen und das Korrigieren des Manuskripts.

- 2) **Harwardt J**, Carrara SC, Bogen JP, Schoenfeld K, Grzeschik J, Hock B, Kolmar H (2023). Generation of a symmetrical trispecific NK cell engager based on a two-in-one antibody. *Frontiers in Immunology*, 10.3389/fimmu.2023.1170042.

### Beiträge von J. Harwardt:

- Literaturrecherche und konzeptionelles Design
- Design und Planung der Experimente
- Generierung und Screening der Bibliothek
- Reformatierung und Charakterisierung der trispezifischen Varianten
- Design und Anfertigung der im Artikel dargestellten Abbildungen
- Verfassen des Manuskripts mit H. Kolmar

**Der Anteil von J. Harwardt an dieser Publikation beläuft sich auf 80%.** Die verbleibenden 20% verteilen sich auf die übrigen Co-autoren für die experimentelle Beteiligung an Zellkultivierung, kritische Anmerkungen und das Korrigieren des Manuskripts.

- 
- 3) **Harwardt J**, Geyer FK, Schoenfeld K, Baumstark D, Molkenhain V, Kolmar H (2024). Balancing the Affinity and Tumor Cell Binding of a Two-in-One Antibody Simultaneously Targeting EGFR and PD-L1. *Antibodies*, 10.3390/antib13020036.

Beiträge von J. Harwardt:

- Literaturrecherche und konzeptionelles Design
- Design und Planung von 70% der im Manuskript beschriebenen Experimente
- Generierung und Screening der Bibliothek
- Reformatierung und Charakterisierung der Varianten mittels BLI-Messungen und zellulären Bindungsexperimenten
- Design und Anfertigung von 70% der im Artikel dargestellten Abbildungen
- Verfassen des Manuskripts mit V. Molkenhain und H. Kolmar

**Der Beitrag von J. Harwardt an dieser Publikation beläuft sich auf 70%.** Die verbleibenden 30% verteilen sich auf die übrigen Co-autoren für die experimentelle Beteiligung an Proteinbindungsstudien, AlphaFold basierter Modelling, kritische Anmerkungen und das Korrigieren des Manuskripts.

- 4) Schoenfeld K\*, **Harwardt J\***, Kolmar H (2024). Better safe than sorry: Dual targeting antibodies for cancer immunotherapy. *Biological Chemistry*, 10.1515/hsz-2023-0329.

(\*Geteilte Erstautorenschaft)

Beiträge von J. Harwardt:

- Literaturrecherche mit K. Schoenfeld
- Zusammenfassung der Literaturdaten und Planung des Manuskripts mit K. Schoenfeld
- Verfassen des Manuskripts und Erstellung der Abbildungen mit K. Schoenfeld

**Der Beitrag von J. Harwardt an dieser Publikation beläuft sich auf 45%.** Der Anteil von K. Schoenfeld beläuft sich als Co-Erstautor ebenfalls auf 45%. Die verbleibenden 10% belaufen sich auf H. Kolmar für das kritische Korrigieren des Manuskripts.

---

## 1. Introduction

---

Host defense is one of the most important functions of living organisms, as they are constantly exposed to microbial pathogens and viral infections (1). In higher organisms such as vertebrates, the immune system is divided into two entities determined by the speed and specificity of the response: the innate and the adaptive immune system (2). While the innate immune system is activated as the first line of defense shortly after infection enabling a rapid, general immunological response, the adaptive immune system requires more time to develop an antigen-dependent, highly specific response (3).

The innate immune system is based on physical and chemical barriers to infection, including the epidermis and the mucosal epithelia, as well as on different cell types that recognize invading pathogens and activate antimicrobial immune responses (4, 5). It is restricted to a limited number of genetically predetermined, germline-encoded receptors, the so-called pattern-recognition receptors (PRRs), which are specific for distinct conserved structures on pathogens, termed pathogen-associated molecular patterns (PAMPs). Upon recognition of PAMPs, PRRs induce proinflammatory and antimicrobial responses by activating a variety of intracellular signaling pathways resulting in the secretion of inflammatory mediators such as cytokines, chemokines, interferons, and antimicrobial peptides (6, 7). The cellular components of the innate immune system include antigen-presenting dendritic cells (DCs), phagocytotic macrophages and granulocytes, and cytotoxic NK cells (4). NK cells are able to kill virus-infected somatic cells and tumor cells by releasing perforins and granzymes, while their activation depends on a variety of inhibitory and activating receptors that interact with the surface of healthy and malignant cells (8). Moreover, NK cells recognize cells with downregulated major histocompatibility complex (MHC) class I expression (“missing self”), leading to their killing, the release of cytokines, and the activation of macrophages, which eliminate infected cells via phagocytosis (9–11).

The adaptive immune system is activated by antigen-presenting DCs and has evolved to enable specific pathogen detection by providing a broader repertoire of recognizing self- and non-self-antigens (12, 13). It relies on B lymphocytes, which arise in the bone marrow, on T lymphocytes, which mature in the thymus, and on the diversity and specificity of their antigen receptors, the B cell receptors (BCRs), and the T cell receptors (TCRs), respectively (13, 14). The diversity of these receptors is generated by somatic recombination of gene fragments encoding for variable receptor structures, which is described in more detail in chapter 1.1. (15). Besides specificity, another essential feature of adaptive immunity is the formation of an immunological memory. During the first exposure to a pathogen, sets of long-lived memory T and B cells are established, which are rapidly activated upon subsequent exposure to the same pathogen to elicit a fast, specific, and effective protective immune response (13). The adaptive immune response can be further subdivided into the humoral immune response, which is mediated by the secreted form of BCRs, termed antibodies, and the cell-mediated immune response, in which TCRs are involved. The humoral immune response is initiated by recognition of an antigen via the BCR and the

---

subsequent activation of immature B cells (16). Antigen recognition leads to internalization of the complex and antigen degradation in the proteasome. The resulting peptides are displayed on the surface of the B cell via MHC class II molecules (17). These complexes are recognized by activated CD4<sup>+</sup> T helper cells, which subsequently stimulate the B cell, leading to B cell proliferation and differentiation into antibody-secreting plasma cells or memory cells (3, 18).

### **1.1. Antibody structure, function, and diversification**

Antibodies are heterotetrametric glycoproteins composed of two identical light chains (LCs) and two identical heavy chains (HCs). Each heavy and light chain as well as the two HCs are linked via disulfide bonds. All antibody domains exhibit the characteristic immunoglobulin (Ig) fold comprising two tightly packed, anti-parallel  $\beta$ -sheets that are covalently linked by an intra-domain disulfide bridge (Figure 1A) (19, 20). Human LCs belong to one of two functionally similar classes,  $\kappa$  (kappa) or  $\lambda$  (lambda), with both LC classes consisting of a C-terminal constant domain (CL) and an N-terminal variable domain (VL). The HCs belong to one of the five isotypes IgA, IgD, IgE, IgG, and IgM, each of which has an independent role in the adaptive immune system. IgA, IgD, and IgG consist of one N-terminal variable domain (VH) and three C-terminal constant domains (CH1, CH2, CH3), while IgE and IgM exhibit one N-terminal VH and four C-terminal CH domains (CH1, CH2, CH3, CH4). Besides, IgA and IgM contain an additional joining (J) chain which enables the formation of dimers or pentamers, respectively (19). The immunoglobulin isotype IgG, which is further subdivided into IgG1, IgG2, IgG3, and IgG4, is the most prevalent in human serum (70-85% of the total serum Igs) (21). The overall structure of the four human IgG subclasses, of which IgG1 is the most common, is very similar, however there are differences that affect binding to accessory molecules and receptors and thus functionality (22). In contrast to the other isotypes, in which glycosylation is found in almost all constant domains, IgG antibodies have a single glycosylation site at position N297 within the CH2 domain (23).

One IgG antibody molecule consists of three functional components, two Fabs represented by a protein complex of VH-CH1 and VL-CL, and the crystallizable fragment (Fc) consisting of CH2-CH3 (Figure 1A-C). The two Fabs are connected to the Fc by a hinge region, which enables high flexibility of the Fabs in conformation. However, the flexibility differs between the various IgG subclasses. The antigen binding paratope is formed by certain residues located in the fragment variable (Fv) region, consisting of VH and VL. Each domain contributes three CDRs, which are characterized by a high structure and sequence diversity. These six loops, CDR-L1, CDR-L2, CDR-L3 for VL and CDR-H1, CDR-H2, CDR-H3 for VH, are located in close proximity to each other (Figure 1D). CDR-H3 is the most diverse loop and is often considered the most important CDR for antigen binding. The framework regions (Fr), which are located between the CDRs, are relatively conserved and are numbered Fr1 to Fr4 (19, 24, 25).

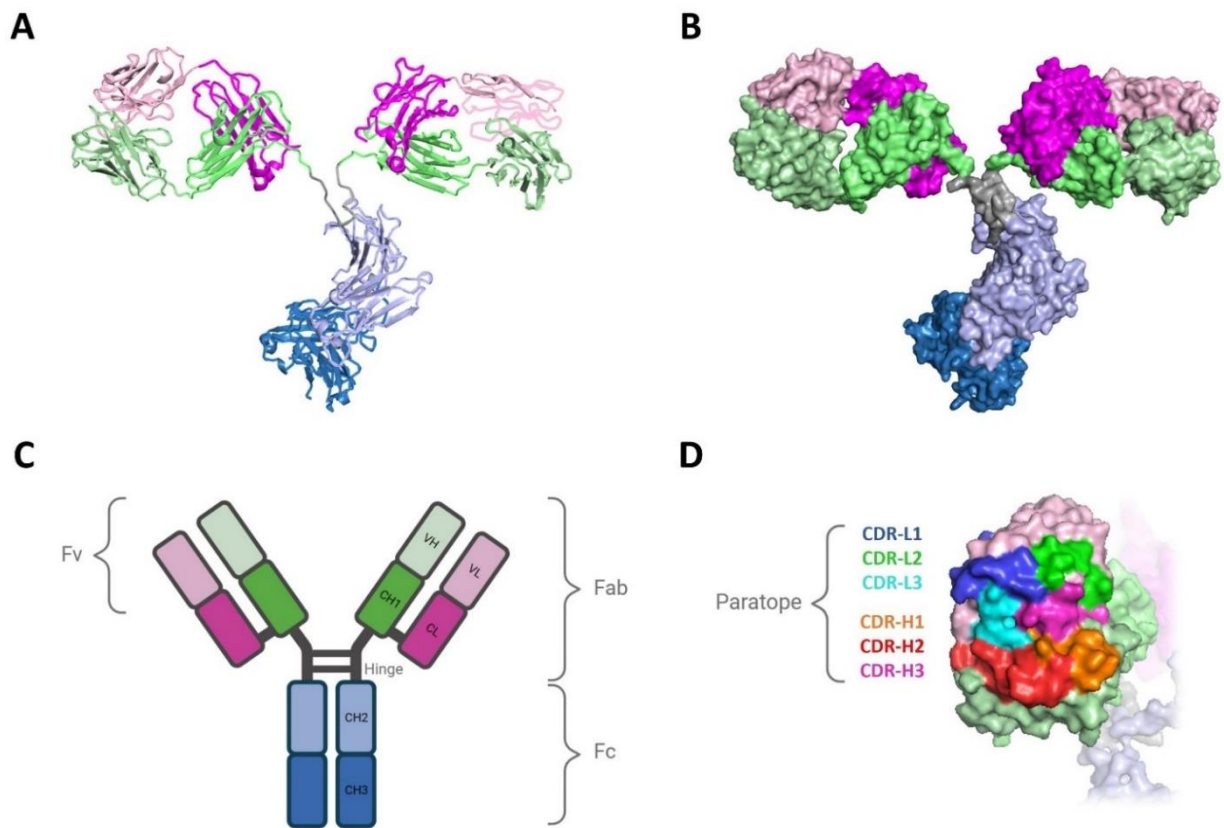


**Figure 1: Structural and schematic representation of an IgG1 antibody.** A) Structural model of an IgG1 antibody in the ribbon view. B) Structural model of an IgG1 antibody in a space-filling view. C) Schematic structure of an IgG1 antibody. Variable regions are shown in light green and light pink for VH and VL, respectively, making up the variable fragment. Constant domains are depicted in dark green and blue for the heavy chain and in dark pink for the light chain. D) Structural model of the six complementarity-determining regions that form the paratope. Structure models are based on PDB 1IGT and were created with PyMol. Abbreviations: fragment variable: Fv; fragment crystallizable: Fc; fragment antigen binding: Fab; complementarity-determining region: CDR. Figure created with BioRender.com.

While the Fv fragment of an antibody is involved in antigen binding, the Fc region is essential for the interaction with effector molecules and cells involved in the stimulation of immune defense mechanisms. The Fc region of an IgG antibody interacts with Fc gamma receptors (FcγR) and the first subcomponent of the C1 complex (C1q) to mediate mechanisms such as antibody-dependent cellular cytotoxicity (ADCC), complement-dependent cytotoxicity (CDC), and antibody-dependent cellular phagocytosis (ADCP) (19, 26). ADCC can be mediated by three types of receptors: FcγRI (CD64) expressed on monocytes, macrophages, and DCs, FcγRII (CD32) expressed on most myeloid cells, and FcγRIIIA (CD16) primarily expressed on NK cells. While FcγRI targets IgG with high affinity, FcγRII and FcγRIIIA are low-affinity receptors (27–30). Binding of FcγRIIIA, often referred to as the main receptor for ADCC, to antibody-opsionized target cells induces cellular cytotoxicity through the NK cell-mediated release of perforins and granzymes. The potency of ADCC is influenced by the IgG subclass, the epitope, the flexibility and affinity of the antibody, the fucosylation and glycosylation pattern, and the FcγR polymorphisms (21, 31). CDC is triggered by the binding of C1q to the Fc region of cell-bound antibodies,

---

resulting in subsequent recruitment of a number of complement proteins and the formation of a membrane attack complex (MAC) that mediates the lysis of target cells (32, 33). ADCP is the mechanism by which target cells opsonized with antibodies activate the FcγRs on the surface of macrophages to trigger phagocytosis, leading to internalization and degradation of the target cell by acidification of the phagosome (34).

Besides mediating effector functions, the Fc part of an IgG antibody is targeted by the neonatal Fc receptor (FcRn) expressed on endothelial cells, prolonging the serum half-life of IgGs to approximately 20-23 days. Since the FcRn exhibits a significantly higher affinity for the Fc domain of an IgG at acidic pH than under neutral conditions, the antibody is bound in the acidified endosome after uptake via pinocytosis and is subsequently recycled to the cell surface and released into the bloodstream (35, 36). The diversity of the human antibody repertoire is estimated to comprise more than  $10^{11}$  unique antibody sequences (3). This theoretical diversity is a result of the somatic recombination of antibody gene segments during B cell development. The exons encoding for the antibody VH region are assembled from variable (V), diversity (D), and joining (J) gene segments, whereas for the VL region, V and J gene segments are combined, a process termed V(D)J recombination (37, 38). Conserved DNA sequences flank each gene segment and serve as recognition sites for the joining process, which is mediated by an enzyme complex. This complex includes the proteins recombination activating gene 1 and 2 (RAG1 and RAG2), which introduce double-strand breaks at the flanking DNA sequences, and enzymes that are involved in general DNA double-strand repair which together with the RAG proteins perform the DNA rejoining (37, 39, 40). In addition, the joining mechanism itself increases the number of possible antigen binding sites through the random loss and addition of nucleotides at the junction sites, which is referred to as junctional diversification. This significantly increases the diversity of coding sequences, particularly in CDR-H3 (38, 40). In mature B cells, somatic hypermutation (SHM) further increases diversity of antibodies in response to antigen stimulation by introducing several single nucleotide substitutions into the rearranged V(D)J gene segment. SHM is triggered by activation-induced deaminase (AID), an enzyme that induces cytosine to uracil deamination (41, 42). Another diversification mechanism, which is also initialized by AID, is the class switch recombination (CSR). In naïve B cells, the BCR is of the IgM or IgD isotype (43). CSR is a process of recombinational deletion in which the exons of the IgM or IgD constant region are removed and the functional VDJ segment is brought into proximity of the exons of downstream Ig constant regions allowing the switch to IgG, IgA, or IgE. Thus, within a few days after the first contact with an antigen, the genes encoding for low-affinity antigen-specific IgM antibodies are converted into genes that code for high-affinity antibodies (41, 44).



---

## 1.2. Antibodies as therapeutic agents

Based on the innate properties of antibodies, including high affinity and specificity, Fc-mediated effector functions, and the ability to modulate biological responses, mAb therapies have emerged as a powerful class of therapeutics. The importance of antibodies in combating diseases has been known since 1890, when Emil von Behring showed that the symptoms of diphtheria in animals can be reduced by transferring sera from rabbits infected with attenuated pathogens (45, 46). However, it quickly emerged that polyclonal animal sera have significant limitations in terms of the quantities that can be produced, the variability of batches, and immunological complications associated with the administration of repeated doses of exogenous proteins (47, 48). In 1975, Georges Köhler and César Milstein invented the hybridoma technology, which revolutionized biomedical research and diagnostics and paved the way for mAb-based therapies (49). The hybridoma technology is based on the fusion of a short-lived antibody-producing B cell from immunized rodents with an immortalized myeloma cell, resulting in the generation of long-lasting hybridoma cells that constitutively express a large amount of one specific mAb (50). Mabs are defined as “monospecific antibodies that are made by identical immune cells that are all clones of a unique parent cell” (51). This platform led to the discovery of the first therapeutic mouse hybridoma mAb, Muromonab-CD3, which was approved for human use by the Food and Drug Administration (FDA) in 1986. However, it has been shown that mAbs of murine origin are highly immunogenic and cause the formation of human anti-mouse antibodies (HAMAs), which also shortens the serum half-life of these antibodies (52, 53). Muromonab-CD3 triggered a HAMA response that caused neurotoxicity in treated patients (54). In addition, the ability of the murine Fc region to induce ADCC in patients is limited (55). To overcome these limitations of murine mAbs, various strategies have been developed to increase their sequence similarity to human antibodies while maintaining binding affinity and specificity. First, chimeric antibodies were generated in which murine variable domains were combined with human constant regions (Figure 2A) (56). In 1994, Abciximab was approved as the first chimeric antibody for the treatment of platelet aggregation (57). In many cases, chimeric antibodies exhibited reduced immunogenicity and were capable of mediating ADCC, but still induced HAMA responses (58). Later, humanization of antibodies was introduced by grafting the CDRs of murine antibodies into a human acceptor framework sequence (Figure 2A) (59). Besides CDR grafting, alternative humanization methods such as resurfacing (60), super-humanization (61), or human string content optimization (62) have been developed. Resurfacing preserves the non-exposed residues of the non-human antibody, as only the surface residues are replaced by residues present in human germlines (63). The first humanized antibody, Daclizumab, generated via CDR grafting, was approved by the FDA for the treatment of transplant rejection in 1997 (64). Since then, humanized antibody therapies have accounted for a high proportion of approved antibody therapies each year. While approximately 40% of chimeric antibodies induce anti-drug antibody (ADA) responses *in vivo*, only 9% of humanized antibodies do so (58). The

current state of the art are fully human antibodies where antigen specificity has been selected either *in vivo* using transgenic animals exhibiting a human antibody repertoire or by antibody engineering processes combined with screening (65, 66). The first fully human IgG antibody, Adalimumab, was approved by the FDA in 2002 for the treatment of rheumatic diseases (67). However, even fully human sequence derived antibodies can induce an ADA response (68). Currently, nearly 200 antibody therapeutics have received marketing approval or are under regulatory review, and more than 130 antibody therapeutics are being investigated in late-stage clinical studies (phase 2, phase 2/3, or phase 3) for the treatment of various diseases (69). The majority of antibody therapeutics in the United States or the European Union are approved for the treatment of cancer, followed by immune-mediated disorders and infectious diseases (Figure 2B) (70).

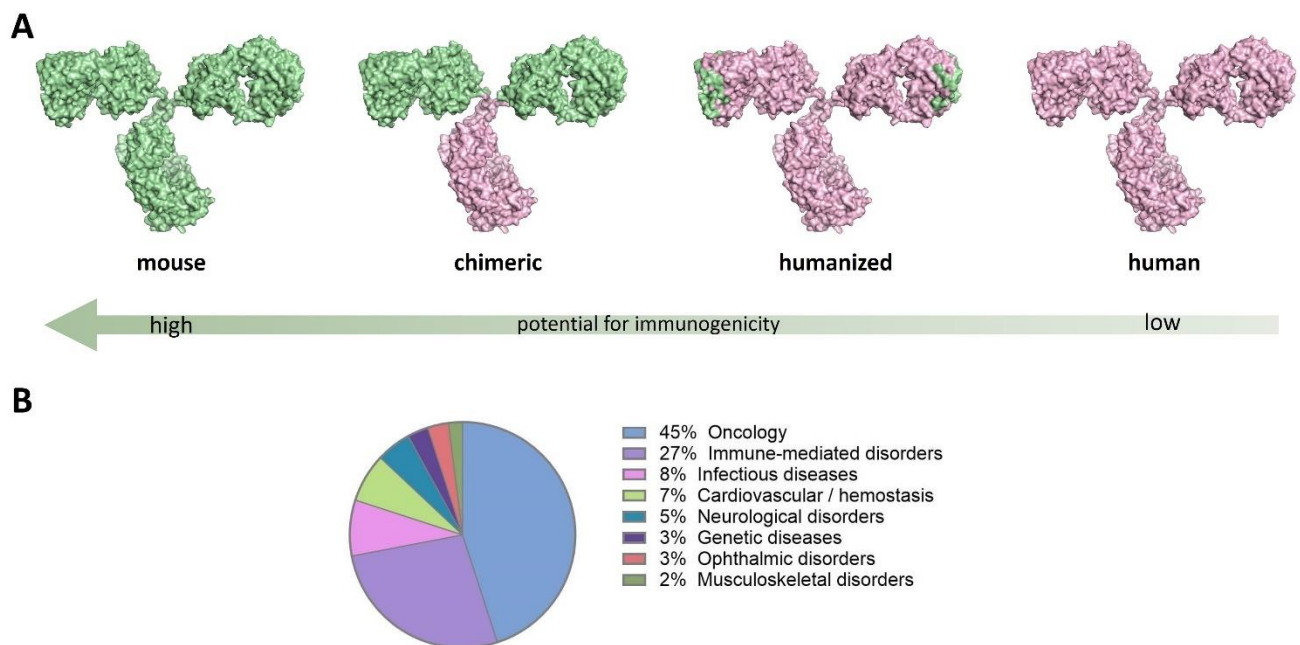


**Figure 2: Different degrees of monoclonal antibody humanization and the primary indications of approved antibody therapeutics.** A) Mouse-derived antibody domains are shown in green, human-derived antibody domains are colored pink. A chimeric antibody combines the Fc region of a human antibody with the Fab fragment of a murine antibody. By grafting of mouse-derived CDRs into a human framework, a humanized antibody variant is generated. The immunogenicity potential decreases with the number of mouse-derived amino acids present. Structure models are based on PDB 1IGT and were created with PyMol. B) Primary indications for antibody therapeutics approved or in regulatory review in the United States or European Union according to (70).

Despite the great success of antibodies for the treatment of various disease, there are certain limitations of their use in clinical applications, including poor tissue penetration and Fc-mediated bystander activation of the immune system (71). To avoid the latter, antibody engineering approaches have been developed that prevent the binding of Fc domains to FcγRs, which will be discussed in chapter 1.4.1..

Antibody fragments such as Fabs (50 kDa), single chain variable fragments (scFvs, 25 kDa), camelid-derived nanobodies ( $V_{HHs}$ , 15 kDa), and shark-derived  $V_{NARs}$  (13 kDa) are much smaller than full-length IgGs (150 kDa) (Figure 3), which promotes their penetration into tissues, including solid tumors (71, 72). Fab fragments consist of the variable domains  $V_H$  and  $V_L$  and the constant domains  $CH_1$  and  $CL$  of an IgG molecule, whereas scFvs are composed of the variable domains  $V_H$  and  $V_L$  connected by a flexible polypeptide linker (72).  $V_{HHs}$  and  $V_{NARs}$  are the antigen binding domains of heavy chain only antibodies (HcAbs) which are naturally produced by camelids and sharks, respectively (73). Antibody fragments retain antigen specificity of the full-length antibody, while elimination from the body occurs faster (71). To date, several Fab fragments have been FDA approved, of which Abciximab, a Fab fragment of a chimeric mAb, was the first to be approved in 1994 (74). However, the use of antibody fragments in therapy also shows limitations, such as possible immunogenicity, insufficient affinity due to monovalent target binding, lower stability compared to full-length antibodies, and short half-life (71). The fusion of two Fabs or scFvs results in bivalent  $F(ab')_2$  antibody variants or tandem scFvs, respectively (Figure 3). In addition to the use of antibody fragments as single or multimeric molecules, fusions to different termini of full-length IgGs can be generated, resulting in bispecific or multispecific antibodies which are addressed in chapter 1.5. and 1.6..

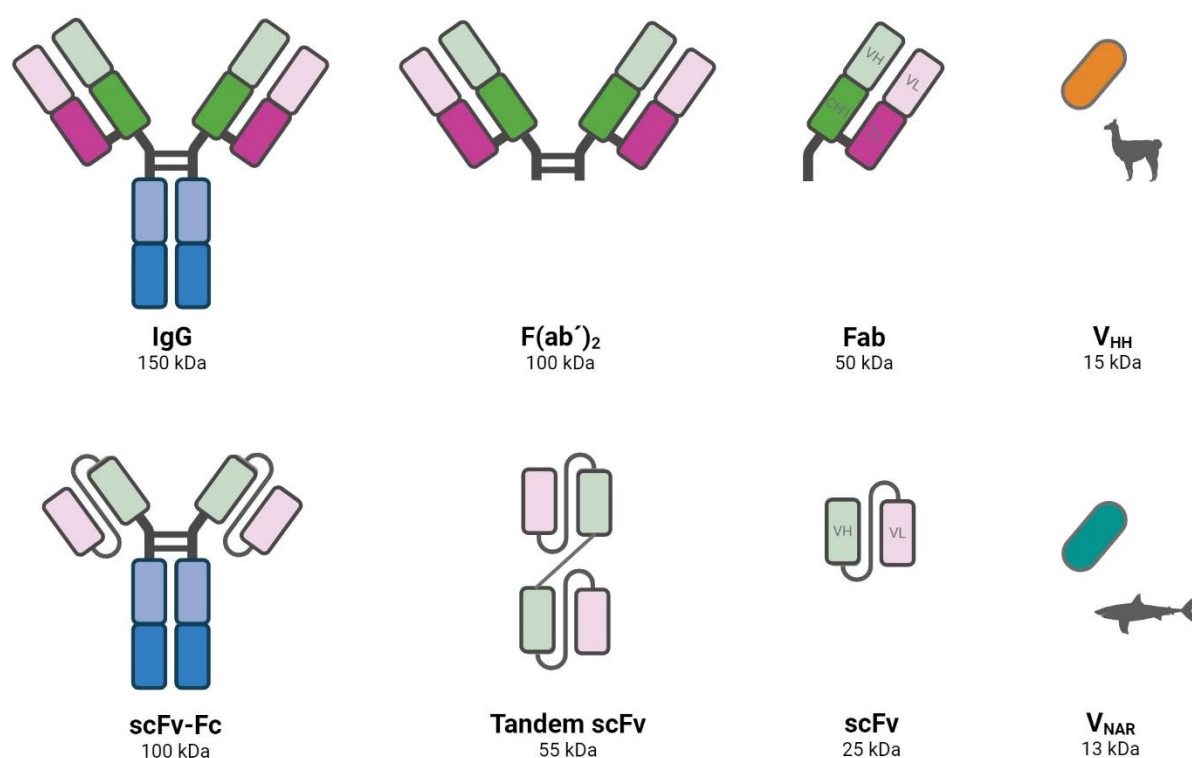


**Figure 3: Schematic representation of antibody fragment structures.** The constant domains are depicted in dark green for  $CH_1$ , blue for  $CH_2$  and  $CH_3$  and dark pink for  $CL$ . The variable chains are shown in light green and light pink for  $V_H$  and  $V_L$ , respectively. Abbreviations: Immunoglobulin: Ig; single chain variable fragment: scFv; fragment crystallizable: Fc; fragment antigen binding: Fab. Figure created with BioRender.com.

---

### 1.2.1. Therapeutic antibodies in immuno-oncology

Cancer is a leading cause of death worldwide, accounting for almost 10 million deaths in 2020. The most commonly diagnosed cancers were female breast cancer, lung cancer, and prostate cancer, with the most common causes of death being lung, liver, and stomach cancers (75). Along with conventional treatment methods like surgery, chemotherapy, and radiotherapy, mAb-based immunotherapy is considered one of the most important components of cancer therapy (76). The advantages of targeted therapy are fewer adverse effects, higher efficacy, and reduced off-target toxicity (77). However, the safety and efficacy of therapeutic mAbs in oncology depends on the type of target antigen. In 1998, the protein CD20 was identified, which is abundantly expressed on cancerous B cells in non-Hodgkin's lymphoma, but not on healthy, immature B cells. This made CD20 the first target for mAb-based cancer therapy and the chimeric anti-CD20 antibody Rituximab the first mAb to be approved for the treatment of cancer in 1997 (78). TAAs targeted by therapeutic mAbs in oncology may belong to different categories, including hematopoietic differentiation antigens, glycoproteins expressed by solid tumors, antigens involved in angiogenesis, antigens of growth and differentiation signaling, and stromal and extracellular matrix antigens (79). Growth factor receptors are one of the most common TAAs identified in a variety of cancer patients, among them EGFR and the human epidermal growth factor receptor 2 (Her2) (80–82). Four anti-EGFR antibodies (Cetuximab, Panitumumab, Nimotuzumab, and Necitumumab) and three anti-Her2 antibodies (Trastuzumab, Pertuzumab, and Margetuximab) have already been FDA approved (83, 84). Anti-EGFR antibodies block the ligand-induced EGFR tyrosine kinase signaling and thus inhibit malignant cell proliferation and differentiation. In addition, the antibodies are able to trigger effector functions like ADCC, which leads to tumor cell killing (85). Another promising type of mAb cancer therapy is the blockade of immune checkpoint proteins. Cytotoxic T lymphocyte antigen-4 (CTLA-4) and programmed cell death-1 (PD-1) are co-inhibitory receptors expressed on the surface of T cells that negatively regulate T cell-mediated immune responses to maintain self-tolerance and limit collateral tissue damage (86, 87). However, tumor cells take advantage of these inhibitory molecules to induce tumor tolerance and T cell exhaustion (88). Accordingly, immune checkpoint inhibitors (ICIs) targeting CTLA-4, PD-1, or PD-L1 have the potential to reactivate the immune response against tumor cells (89). In 2011, the anti-CTLA-4 antibody Ipilimumab was approved as the first checkpoint inhibitor for the treatment of metastatic melanoma (76, 90). Many mAbs addressing the PD-1/PD-L1 axis have been evaluated in clinical trials for cancer treatment, of which nine have been approved by the FDA, including Atezolizumab, Avelumab, and Durvalumab targeting PD-L1 and Pembrolizumab, Nivolumab, Cemiplimab, Dostarlimab, Retifanlimab, and Toripalimab targeting PD-1 (87, 91–93). Immunotherapies with PD-1 or PD-L1 blockers have been used successfully in many types of cancer, including melanoma, non-small cell lung cancer, renal cell carcinoma, ovarian cancer, bladder cancer, and lymphoma (94, 95). Lymphocyte activation gene-3 (LAG-3), T cell immunoglobulin and mucin-domain containing-3

---

(TIM-3), and T cell immunoglobulin and ITIM domain (TIGIT) are considered the next generation of co-inhibitory receptors that have expanded the repertoire of potential immunotherapeutic targets in various types of cancer (96). In recent years, antibodies targeting “innate immune checkpoints”, such as CD47, have been developed. CD47 is ubiquitously expressed in human cells and binds to the signal regulatory protein  $\alpha$  (SIRP $\alpha$ ), which is expressed on macrophages to prevent macrophage-mediated phagocytosis (97). Although CD47 is a promising target for cancer therapy and clinical trials with anti-CD47 mAbs have shown excellent results, toxicity issues need to be considered as adverse events such as anemia and thrombocytopenia have been reported (98).

### 1.3. Generation of therapeutic antibodies

To date, various techniques have been developed for the discovery and generation of antibodies with desired biological properties from non-human, human, and transgenic human antibody repertoires, including the hybridoma technology described in chapter 1.2. and library-based antibody display approaches (99, 100). The main feature that enables the isolation of a desired candidate using antibody display technologies is based on the linkage of the protein of interest (i.e. the phenotype) to its genetic information (i.e. the genotype). This principle of genotype phenotype coupling enables the selection of binders from several billion different protein variants via a high-throughput screening process (101). For the construction of antibody libraries, different sources of diversity can be utilized. Immune libraries are typically derived from immunized animals and are thus predisposed for recognition of certain antigens (102). Since the antibody repertoire has already been affinity optimized *in vivo*, these libraries usually contain high-affinity antibody variants (100). The first immunization hosts described were mice, rats, and rabbits (103, 104). More recently, chicken immunization has shown great promise and is therefore discussed in detail in chapter 1.3.2.. Regardless of the immunization host, humanization of the antibody candidates is required to avoid immunogenic reactions (68). However, the immunization of transgenic animals that harbor the human Ig variable region gene repertoire enables the generation of fully human antibodies (105, 106). In contrast to an immune library, which is predisposed for recognizing certain antigens, a single naïve library derived from primary B cells from non-immunized or healthy donors is of general use for the generation of antibodies targeting all types of antigens, including toxins and self-antigens. The random combination of heavy and light chains increases the antibody diversity of the donors by multiple orders of magnitude (102, 107). However, antibodies isolated from naïve libraries usually exhibit lower affinities compared to antibodies isolated from immune libraries (108). A method for antibody repertoire generation that is independent of a natural source is the design of a synthetic library in which antibody diversity is designed *in silico* and subsequently synthesized in a controlled manner. This enables the use of a highly optimized human framework and the introduction of a defined diversity at the CDRs (102). Using this method, complex libraries can be designed that contain synthetic

---

antibodies with affinities and specificities beyond the capacity of natural antibodies (109). In semi-synthetic approaches, natural and synthetic antibody sequences are usually combined (67).

Numerous molecular display technologies have been established for protein engineering, in which the libraries of protein variants are connected to ribosomes or mRNA (110, 111), or to the surface of phages (112, 113), bacteria (114), mammalian (115, 116), or yeast (117) cells. Prokaryotic display, especially phage display, is the most commonly used display technology due to its simplicity, high efficiency, and low cost. The origin of phage display dates back to 1985, when George P. Smith showed that filamentous phages are able to display a peptide of interest on their surface after inserting a foreign DNA fragment into the filamentous phage coat protein gene (112). McCafferty and Winter were the first to utilize this technology in antibody discovery (113, 118). M13, one of the filamentous bacteriophages of *Escherichia coli*, is the most widely used phage for antibody display while most phage display systems are based on pIII-antibody fusion proteins due to the structural flexibility of the coat protein pIII and its ability to display large proteins without loss of function (119–121). Antibody candidates with the desired characteristics can be enriched in a process referred to as “panning” by incubating the library with the respective antigen (121). Nevertheless, this technology relies on the bacterial expression, secretion, and folding apparatus, not allowing correct protein folding and glycosylation of mammalian proteins (122). Therefore, alternative cellular display systems such as yeast display (117), which is described in chapter 1.3.1., bacterial display (114), or mammalian display (116) have been developed. Ribosome display and mRNA display are cell-free *in vitro* methods where the number of library members is not limited by the transformation efficiency of the host, allowing the generation and screening of large diversities ( $10^{12}$  –  $10^{15}$  variants) (110). However, the accessibility of functional ribosomes per library reaction is a limiting factor of ribosome display which can reduce the library size on protein level (111).

### **1.3.1. Yeast surface display**

YSD combines the advantages of eukaryotic systems such as post-translational modifications and correct protein folding and glycosylation with low technical and time requirements (123). This method, developed by Eric T. Boder and K. Dane Wittrup in 1997, is based on the display of recombinant proteins on the surface of *Saccharomyces cerevisiae* by genetic fusion of the protein of interest (POI) to a microbial cell surface protein (117). Several different anchor proteins have been evaluated for the efficient display of the POI, with the most commonly used being the  $\alpha$ -agglutinin mating complex, consisting of two subunits referred to as Aga1p and Aga2p (124, 125). In nature,  $\alpha$ -agglutinin acts as an interaction partner for  $\alpha$ -agglutinin, which mediates cell-cell interactions between haploid yeast cells of opposite mating types to facilitate fusion into diploid yeast cells (126). Using the Aga2p system, up to  $10^5$  copies of the fusion protein are displayed on a single yeast cell (117). Genetically, the Aga2p fusion protein is encoded on a plasmid, whereas the Aga1p protein is encoded in the yeast genome. The expression of both proteins

is under the control of a galactose-inducible promoter (125). Induction of protein expression results in surface presentation of the fusion protein by the formation of two disulfide bonds between Aga2p and the  $\beta$ 1,6-glucan-anchored Aga1p domain (127, 128). Various antibody fragments, among them scFvs, Fab fragments, and camelid V<sub>HH</sub> domains, were successfully displayed on yeast (129). The earliest studies reported the display of scFv mutants in the context of affinity maturation (117). However, YSD has also successfully been used for the isolation of antibodies from Fab libraries. Large Fab libraries with a diversity of more than 10<sup>9</sup> variants can be generated by yeast mating of two haploid yeast strains of opposing mating types that contain plasmids with orthogonal selection markers encoding VH-CH1-Aga2p and VL-CL, respectively (130, 131). The resulting diploid yeast cells present functional Fab fragments on their surface (Figure 4).

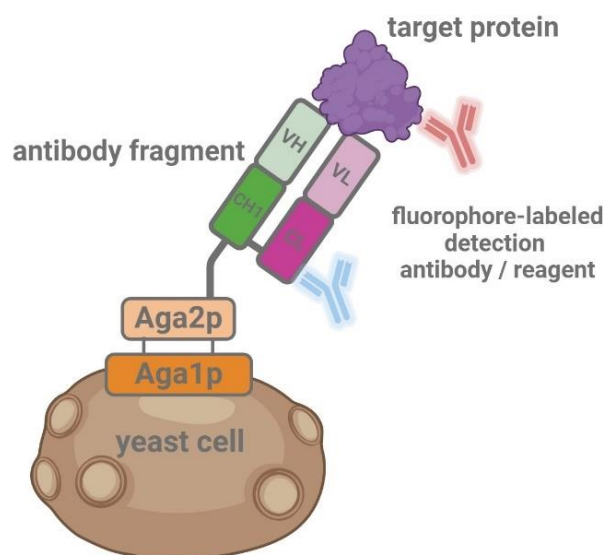


**Figure 4: Schematic representation of a yeast surface displayed Fab fragment.** The VH-CH1-Aga2p fusion protein is connected to the Aga1p by two disulfide bridges. The light chain (pink) is expressed as a solitary polypeptide chain that associates to the VH-CH1 fusion protein. Fluorophore-labeled detection reagents are used to identify yeast cells that display a functional Fab fragment and simultaneously bind to the antigen. Figure created with BioRender.com.

One of the main advantages of YSD is its compatibility with FACS, which enables online and real-time analysis of library candidates and thus precise control of selection on a quantitative basis (132). A two-dimensionally sorting strategy enables the gating of clones with structural integrity that bind the labeled target protein. The detection of functional clones without frame shifts or stop codons is achieved by employing epitope tags or by using fluorescently labeled detection reagents directed against constant domains of the displayed protein (100). Using FACS, it is possible to discriminate finely in terms of affinity, enabling the isolation of mutants with only slightly improved affinity compared to wild-type proteins when screening for affinity maturation (133).

### 1.3.2. Chicken-derived antibodies

During antibody generation, the choice of the immunization host depends on various factors, such as antigen conservativity in different species and the availability of facilities for animal-related work (134). Although most antibodies are derived from mammalian immunization, the generation of antibodies targeting well-conserved mammalian proteins by immunization of mammals is challenging as they are weakly immunogenic. The phylogenetic and evolutionary divergence of avians, including chickens (*Gallus gallus*; 310 million years), from mammals circumvents the problems associated with antigen self-tolerance and increases the likelihood for the production of antibodies that target human antigens (Figure 5A). Furthermore, the immune system of chickens recognizes epitopes on a human protein that would not be addressed by the mammalian immune system (135–137). While only 15% of human drug targets are highly conserved in chickens, the proportion is significantly higher in mice (48%) (138–140). Avians only produce antibodies of the IgA, IgM, and IgY isotype, with IgY being the most abundant serum antibody in chickens (141). The nomenclature of IgY is derived from its high concentration found in egg yolk (142). IgY shares structural homology with the mammalian isotype IgE and functional similarity with mammalian IgG (143). Similar to IgE, an additional CH4 region is observed in IgY, resulting in a molecular weight of about 180 kDa (Figure 5B). Due to the absence of the hinge region between CH1 and CH2, IgY is less flexible than IgG (144–146).

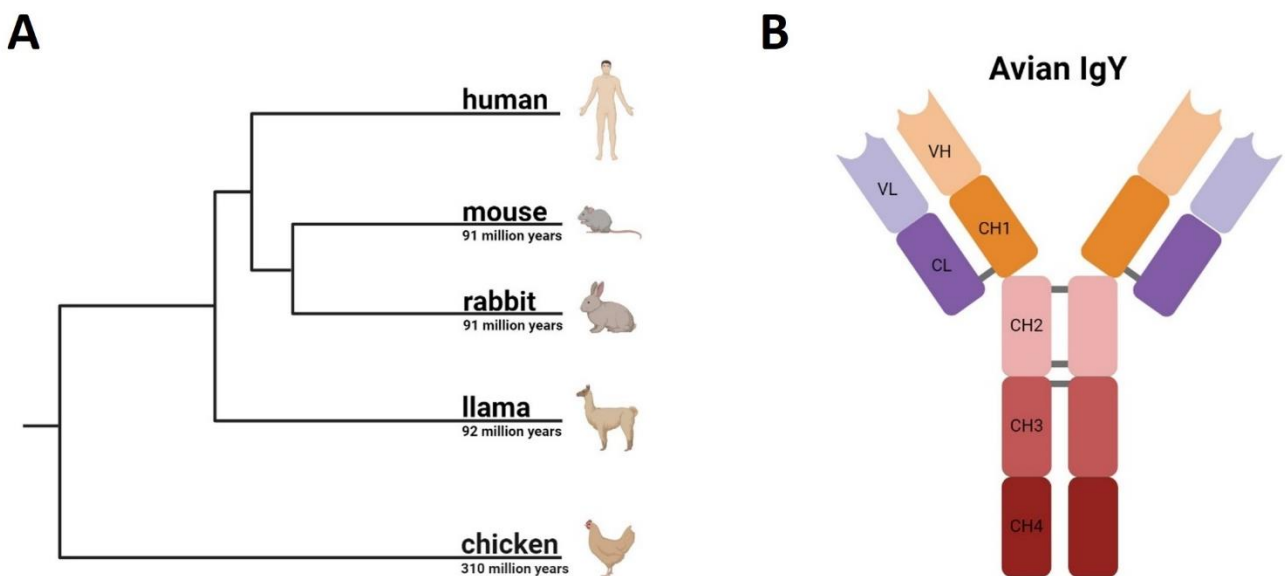


**Figure 5: Phylogenetic tree and avian IgY antibody structure.** A) Phylogenetic tree of different species (mice, rabbits, llama, and chicken) used as hosts for immunization in terms of evolutionary distance to humans according to (140). B) Schematic representation of an avian IgY antibody. Variable regions are shown in light orange and light purple for VH and VL, respectively. Constant domains are depicted in red and orange for the heavy chain (CH1 – CH4) and in purple for the light chain (CL). Figure created with BioRender.com.



---

The variable genes of chicken IgYs are also subdivided into four framework regions and three CDR regions, with hypervariability predominantly found in the CDRs. Compared to human IgG, chicken IgY exhibit a significantly longer and less hydrophobic CDR-H3, with non-canonical cysteine residues incorporated, which are hypothesized to form intrachain disulfide bonds conferring additional structural stability (147, 148). Based on the cysteine-pattern, chicken antibodies are divided into six different types (147). While human light chains belong to one of two classes ( $\lambda$  or  $\kappa$ ), only the  $\lambda$  light chain is expressed in avians. Apart from the fact that the IgY CDR-L1 is significantly shorter than that of IgG, the  $\lambda$  VL domains of IgY and IgG exhibit sequence and structural homology (149–151).

The generation of antibody diversity in chickens differs from the diversification of antibodies in humans which is described in chapter 1.1.. In contrast to the human Ig germline, in which several gene families exist for the heavy and light chains, chickens comprise only one functional germline-encoded heavy and light chain gene segment (152). Consequently, chicken VH and VL coding genes share the identical 3' and 5' leader sequence, which enables the amplification of these genes and thus the generation of chicken-derived immune libraries with two sets of oligonucleotides (153). Although V(D)J rearrangement occurs in chickens, it provides only minimal sequence diversity, as only one single locus undergoes rearrangement (134). The mechanism responsible for diversity incorporation into the chicken Ig repertoire is known as somatic gene conversion. Here, non-reciprocal upstream located pseudogene segments are transferred onto the recipient germline gene segment. This process, in which 80 – 100 heavy chain and 25 light chain pseudogenes can be rearranged, relies on high DNA homology between the pseudogene and the germline gene acting as the acceptor in the recombination event (148, 152, 154, 155). Repeated somatic gene conversion together with heavy and light chain pairing potentially results in a repertoire of  $3 \times 10^9$  antibody variants (156). AID-mediated single point mutations introduce additional diversity (148).

Symphogen's PD-1 targeting antibody Sym021 is the first humanized chicken-derived mAb to enter clinical trials in 2019 (NCT03311412, NCT04641871, NCT04672434) (157). Numerous chicken-derived antibodies are in preclinical development, some of which target proteins that are highly conserved in mammals, such as Pfizer's anti-BDNF antibody and the anti-KCNA3 antibody developed by Ligand and Tetragenetics, a trend that is expected to accelerate as more alternatives to conventional rodent immunization emerge (140, 158, 159).

#### **1.4. Antibody engineering**

Antibody engineering involves the demand-oriented modification of the biochemical and biophysical properties of antibodies. These modifications often only affect a small subgroup of the amino acids within the protein (160). For molecular engineering, random or targeted mutagenesis can be applied (161). Targeted (structure-guided) engineering is based on structural knowledge, which is essential for the

---

identification of the amino acid residues to be modified. Specific amino acid substitutions at particular positions are introduced by site-directed mutagenesis, whereas semi-rational engineering involves multiple amino acid substitutions at contiguous or non-contiguous positions (162). During random mutagenesis, the DNA encoding the entire protein or a structural domain is modified by error-prone PCR (ep-PCR), with the mutations occurring randomly rather than selectively (161, 163). The resulting libraries of mutants are recombinantly expressed and screened to identify variants with the desired properties (162).

#### **1.4.1. Fc engineering**

As described in chapter 1.1., the antibody Fc region induces immune effector functions by interacting with FcγRs and the complement system. This is a significant characteristic, since Fc-mediated effector functions have shown to be an important mechanism contributing to the therapeutic effect of many approved antibodies (164). Therefore, Fc engineering strategies have been developed to increase the FcγR binding affinity in order to enhance the Fc effector functions and thus increase the efficacy of the antibody (165, 166). Since almost all approved therapeutic mAbs belong to the IgG class (mostly IgG1), research focused mainly on Fc engineering of this isotype (165). The key Fc residues involved in the interaction with FcγRs, which were found to be in the lower hinge and proximal CH2 region, were focused in mutational studies (167). A Trastuzumab variant carrying the mutations S239D, A330L, and I332E (according to the EU numbering scheme) showed an increased binding affinity to FcγRIIIA and FcγRIIB, resulting in a significant enhancement of ADCC (168). Combination of the mutations F243L, R292P, Y300L, V305I, and P396L caused a 10-fold increase in FcγRIIIA binding, but only a minimal increase in binding to FcγRIIB, enhancing the activating-to-inhibitory (A:I) ratio and thus Fc effector functions (169). In addition to mutational studies, glycoengineering emerged as a powerful tool for the modification of Fc-mediated cellular effector functions, as glycosylation at the N297 residue was found to be critical for the induction of ADCC (170, 171). Afucosylation is the most common glycoengineering technique to improve effector functions, since the fucose at position N297 impairs the optimal interaction of IgG with FcγRIIIA (23, 172). The CD20 targeting mAb Obinutuzumab developed using the Glycart GlycoMab® technology was the first glycoengineered antibody approved for cancer therapy in 2015 (165, 173). However, not all antibodies engineered for enhanced effector function achieved the expected patient benefit (165).

For some indications, such as the blockade of surface receptors or cytokines, Fc-receptor functions may be more detrimental than beneficial (174). This is particularly important for immune checkpoint inhibiting antibodies used in cancer therapy, as depletion of the target cells is not desirable. Consequently, Fc-silenced antibody formats were developed. OKT3 antibodies with IgG1 and IgG4 L234A/L235A (abbreviated as LALA) Fc domains were not able to target the low affinity FcγRs and C1q,

---

leading to a significant reduction in ADCC and CDC (175). Schlothauer *et al.* coupled the novel mutation P329G with the previously described LALA variant, creating the triple mutant LALA-PG, which resulted in abrogated ADCC when introduced into an IgG1 anti-EGFR antibody (176). Glycoengineering techniques removing the glycan at position 297 (N297A, N297Q, and N297G) also reduce binding to all FcγRs and C1q (177–179). Beyond preventing Fc-mediated bystander activation of the immune system, Fc-silenced antibodies are of great value for investigating the mode of action of therapeutic antibodies (176). In addition to the modulation of Fc-mediated effector functions, Fc engineering is utilized to enhance FcRn binding or to promote heavy chain heterodimerization in the context of multispecific antibodies, which will be described in chapter 1.5..

### 1.4.2. Affinity maturation

Isolated antibodies often do not exhibit the binding properties required for their therapeutic application. For the development of drug candidates, affinity optimization is crucial as it can impact the efficacy of the mAb and thus the dose and dosing regime, limit adverse effects, and reduce therapy costs (180, 181). Even antibodies derived from immunized animals that have undergone several rounds of SHM *in vivo* may need to be optimized in their affinity to the antigen of interest (161, 182). *In vitro* affinity maturation usually involves the diversification of variable antibody domains followed by the selection of high-affinity binders, a direct evolution process similar to SHM that occurs naturally in mammalian B cells (41, 183). Mutation sites can be located at the center of the antigen binding interface, although peripheral residues have also proven to be advantageous for affinity maturation. The key residues of the binding site are usually hydrophobic and already optimized for specific antigen interactions while the surrounding residues are rather hydrophilic and solvent-exposed, so that the incorporation of charged residues might improve antigen interactions (19). Depending on the length and number of interactions with the antigen, mutations in CDR-H3 and CDR-L3 offer promising opportunities for affinity maturation, as demonstrated in several studies. By randomizing several amino acids in CDR-H3 and CDR-L3, an anti-VEGF scFv variant with 18-fold improved binding affinity was isolated via phage display (184). Based on a similar randomization approach, a variant of an anti-complement protein receptors C5aR1/2 mAb containing four mutations in CDR-H3 and three mutations in CDR-L3 was generated, resulting in an affinity improvement by three orders of magnitude compared to the parental antibody (185). The generation of an antibody library containing all possible combinations of single and multiple mutations in all CDRs of a usual variable domain would require a library size of more than  $10^{39}$  variants, making it infeasible to screen using a common display technology (161). To improve CDR diversification efficiency and reduce library size, hot-spot mutagenesis (186), look-through mutagenesis (187), or simultaneous mutagenesis (188) can be applied. Simultaneous mutagenesis of all six CDRs of an anthrax toxin neutralizing antibody enabled the selection of an antibody variant with 19-fold improved affinity

---

from a phage display library with an average mutation rate of four (188). Li *et al.* showed that affinity-enhancing mutations cluster at sites where somatic mutations often occur *in vivo*, referred to as hotspots (189). In recent years, different strategies of computer-assisted *in silico* affinity maturation have been developed, including homology modelling (190), molecular dynamics simulation (191), molecular docking (192), mutation hotspots design (193), and interface residues analysis (194, 195). Clark *et al.* reported an improvement in the affinity of an integrin VLA1 targeting antibody by an order of magnitude applying structure-based computational methods (196). Computer-aided methods have the advantage of identifying variants from large virtual libraries ( $\sim 10^{40}$  members) in a short time and at low cost (161). As the different approaches indicate, the choice of an optimal diversification strategy together with a suitable display and screening method is an important determinant of the success of affinity maturation (183).

### 1.5. Bispecific antibodies

BsAbs represent an attractive class of therapeutics that hold great potential for the treatment of complex diseases such as cancer involving various factors and multiple signaling pathways (197–200). These molecules target either two distinct antigens or two distinct epitopes of the same antigen, enabling unique therapeutic modes of action (201). Cell-bridging bispecifics are designed to link immune cells to malignant cells, whereas non-cell-bridging (antigen-crosslinking) bsAbs usually block two signals of cell survival and cell growth simultaneously, enhancing inhibitory or stimulatory effects in malignant cells or immune cells, respectively (202). Compared to conventional mAbs, this offers advantages in terms of specificity, efficacy, toxicity, and drug resistance (200).

Although the concept of bsAbs was proposed by Nisonoff and colleagues in the 1960s (203, 204), the first bsAbs were generated in the 1980s using the hybrid-hybridoma (quadroma) technology pioneered by Milstein and Cuello (205). Since the approval of the first bsAb in 2009, 14 bsAbs were approved for marketing to date, including eleven for cancer therapy (206). More than 85% of bsAbs in clinical trials are cancer therapeutics and the number of new clinical trials is steadily increasing, expecting a large number of bsAbs to be approved in the next three to five years (202, 207). Notably, two approved bsAbs (Emicizumab and Faricimab) have already achieved blockbuster status, underlining the commercial promise of this class of therapeutics (208).

The main challenge during the development of bsAbs is the correct pairing of the two different heavy and light chains, which when mismatched produce a variety of side products (209, 210). In order to achieve correct heavy and light chain pairing, several strategies have been developed (Figure 6). The Knobs-into-Holes (KiH) technology proposed by Ridgway *et al.* in 1996 is based on the replacement of a smaller amino acid with a larger amino acid (T336Y) in the CH3 domain of one heavy chain to form a “knob” structure, and the substitution of a larger amino acid with a smaller amino acid in the other

heavy chain to form a “hole” structure (Y407T) allowing for heterodimerization of both chains based on steric hindrance (211, 212). Further improvement of the KiH model resulted in the introduction of a T336W mutation at the CH3 knob domain and three mutations (T336S, L368A, Y407V) at the CH3 hole domain, enabling a more stable interaction between both heavy chains (213, 214). Other approaches utilize electrostatic steering to direct heterodimerization by electrostatic attraction. Substitution of the two charge interactions in the wild-type CH3 domains (K409D in one CH3 domain and D339K in the other) was found to favor the formation of heterodimers (215). Heterodimerization is further improved by introducing additional substitutions (K409D, K392D / D399K, E356K; CH3 charge pairs) (216). The DEKK platform introduces both L351D and L368E mutations in one of the heavy chains combined with L351K and T336K substitutions in the other, leading to the formation of stabilizing salt bridge interactions (217). By applying the strand-exchange engineered domain (SEED) technology, complementary CH3 heterodimers are formed. The SEED CH3 domains of the resulting SEEDbodies are composed of alternating segments derived from human IgA and IgG CH3 sequences (AG SEED CH3 and GA SEED CH3) which promote heterodimerization through steric complementary contact surfaces (218).

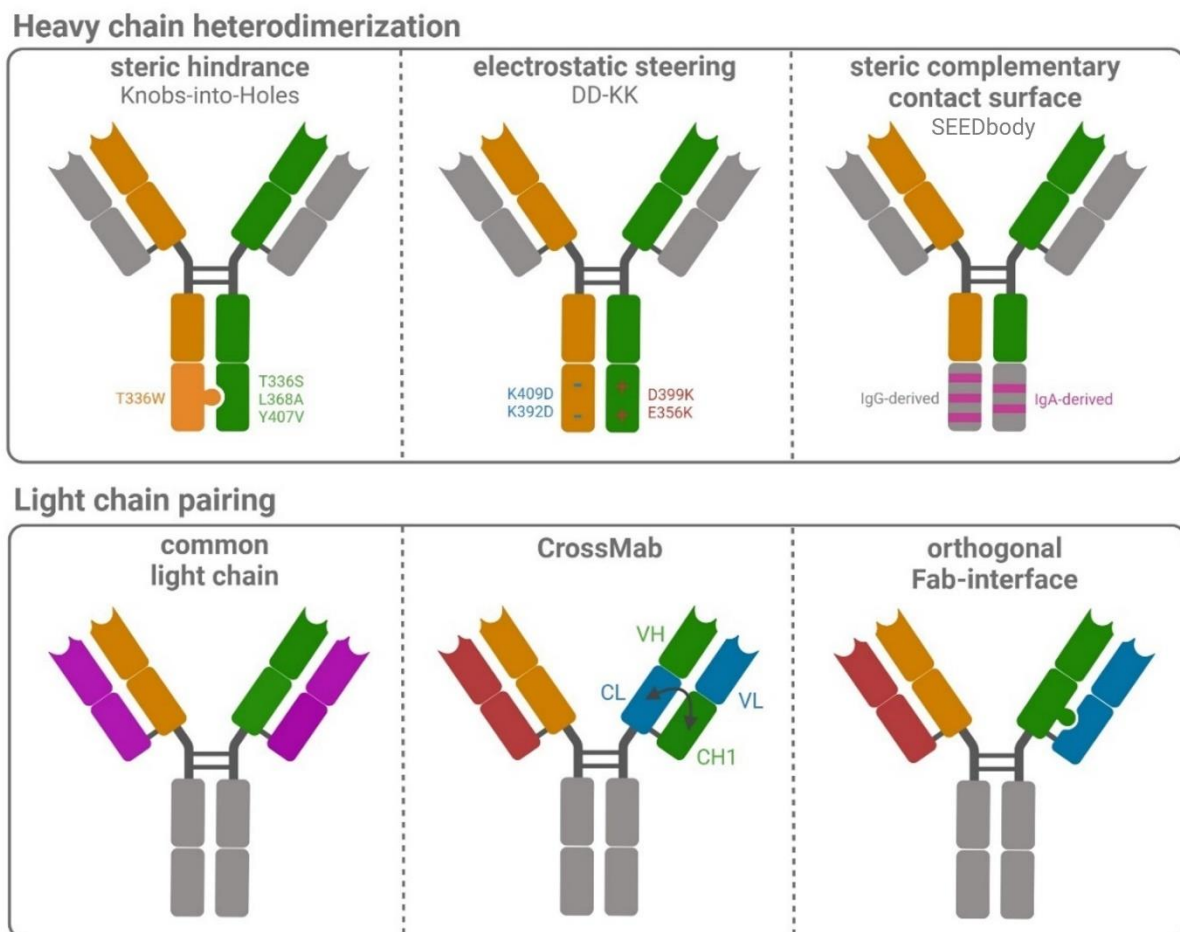


**Figure 6: Schematic overview of engineering strategies to force heterodimerization of heavy chains and correct light chain pairing of IgG-based bispecific antibodies with Y-shaped architecture.** Figure created with BioRender.com.

Protein engineering that forces heterodimerization of heavy chains solves only part of the problem associated with the formation of bispecific IgGs. A straightforward approach described to solve the light chain pairing problem involved the use of a cLC that is compatible with the two distinct heavy chains, so that no additional light chain engineering is required (219). Here, the heavy chain CDRs are mainly involved in antigen recognition and binding, while the light chain mediates a stabilizing effect (220). Roche's CrossMab technology switches the constant domains (CH1 and CL) or the variable domains (VH and VL) of one Fab, causing pairing of the unmodified heavy and light chain as well as pairing of the modified chains (221). Another technology that promotes correct light chain pairing is the engineering of the heavy and light chain interface by introducing a set of mutations. In an ortho-Fab IgG approach, complementary mutations were introduced at the HC and LC interface of one Fab without modifying the other (222).

### 1.5.1. Two-in-One antibodies

Two-in-One antibodies are a subclass of bsAbs that recognize two different antigens with a single Fab fragment (Figure 7) (214, 221). They are also referred to as dual action Fab (DAF) antibodies due to the duality of the high-affinity antigen recognition embedded within one antigen binding site. Consisting of two identical heavy and light chains, these bispecific tetravalent IgG-like molecules exhibit mAb-like characteristics in terms of established manufacturing and a conventional approval process (223).

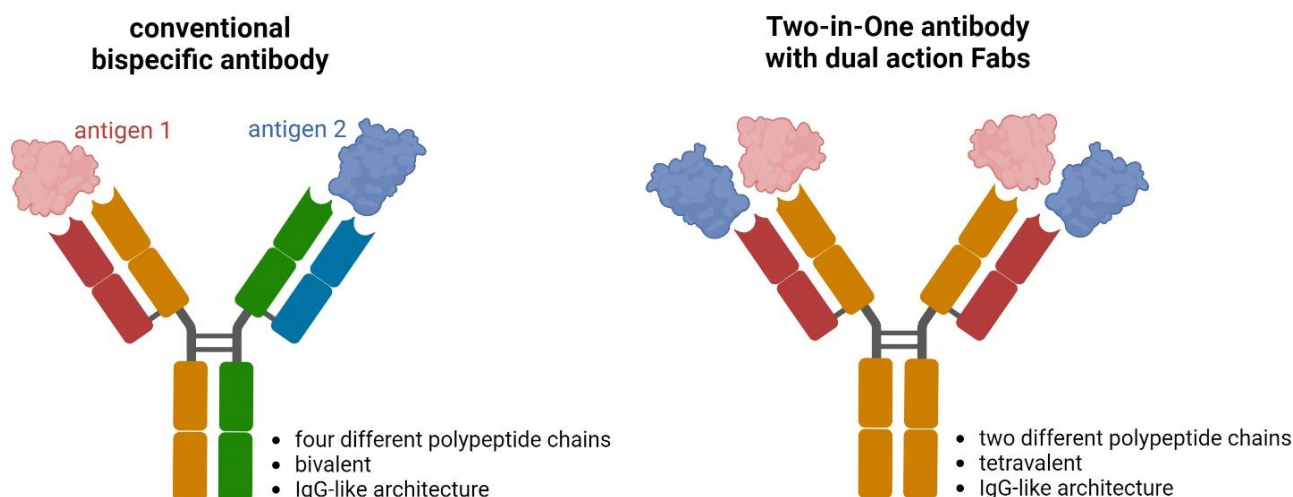


**Figure 7: Schematic representation of a conventional bispecific antibody and a Two-in-One antibody.** The bivalent IgG-like bispecific antibody (left) consist of four different polypeptide chains (heavy chains are shown in orange and green and light chains are shown in red and blue) and targets one antigen with each Fab fragment. The tetravalent IgG-like Two-in-One antibody (right) consist of two different polypeptide chains (heavy chain is shown in orange and light chain is shown in red) and targets two antigens with each antigen binding site. Figure created with BioRender.com.

---

The first Two-in-One antibody was generated based on mutagenesis of the light chain CDRs of the Her2 targeting antibody Trastuzumab, which resulted in Her2 and vascular endothelial growth factor (VEGF) binding (224, 225). The heavy chain CDRs of Trastuzumab dominate the Her2 binding energy, so that the change of eleven residues in the light chain CDRs enabled binding of the unrelated antigen VEGF while preserving Her2 specificity (223, 226). Crystal structures revealed that the antigens are bound with overlapping paratopes. The functional paratope for Her2 is primarily located at the VH CDRs, while the critical sites for VEGF binding mainly include VL residues, as demonstrated via mutational studies (223, 224). Duligotuzumab, a Two-in-One antibody targeting EGFR and Her3, was developed by light chain CDR randomization of an anti-EGFR antibody, maintaining the CDR-L3 sequence important for EGFR binding. Compared with two monospecific anti-EGFR and anti-Her3 antibodies alone or in combination, Duligotuzumab proved to be more effective, most likely due to the avidity effect (227). However, clinical trials (NCT01911598, NCT01986166) generally reported limited activity (228, 229). In the Two-in-One formats described, the six CDRs are modified to bind two antigens with overlapping paratopes. Dual targeting Fab (DutaFab) molecules, in contrast, comprise two independent binding sites, with paratopes restricted to three of the six CDRs. The H-side paratope consists of the CDRs H1, H3, and L2 and the L-side paratope comprises the CDRs L1, L3, and H2. Both paratopes can be independently selected and modularly combined. Therefore, DutaFabs are able to simultaneously bind two different antigens at the same Fv region (230).

### **1.5.2. Dual tumor targeting antibodies**

Dual TAA-targeting antibodies belong to the class of non-cell-bridging (antigen-crosslinking) bsAbs and offer several advantages over antibodies targeting a single TAA, including increased tumor selectivity, simultaneous modulation of two functional pathways in the tumor cell, and circumvention of drug resistance or immune escape mechanisms (231, 232). To increase tumor selectivity and reduce on-target toxicity towards healthy tissue, maximum discrimination between healthy and malignant cells is required. Although dual TAA targeting increases the selectivity for tumor cells compared to healthy cells expressing only one of the two antigens, selectivity can be further improved by affinity optimization of the antigen binding domains (233, 234).

Treatment of a multifactorial disease is always associated with the risk of immune escape and drug resistance (231). The dual TAA-targeting antibody Amivantamab inhibits both EGFR and c-Met, which utilize highly overlapping downstream signaling pathways, potentially restricting the activation of compensatory pathways (235). It is the first-in-class dual TAA-targeting antibody that received FDA approval in 2021 (236). Synergistic effects were also demonstrated for targeting and blocking other TAA combinations. One example for this is the co-targeting of EGFR and PD-L1, combining immune checkpoint blockade with a directed anti-cancer effect for an enhanced anti-tumor response (237, 238).

---

### 1.5.3. Immune cell engagers

Immune cell engagers (ICEs) belong to the class of cell-bridging bsAbs and target both immune effector cells and tumor cells. The recruitment and engagement of immune cells and the formation of an immune synapse between effector and tumor cells promotes the MHC-independent elimination of target tumor cells (239, 240). Depending on the type of immune effector cell to be engaged, ICEs are subdivided into T cell engagers (TCEs) and NKCEs. Most TCEs contain a binding domain directed against CD3, which is associated with the TCR complex and involved in TCR signaling. This leads to the activation of T cells and their redirection against the target tumor cells. Tumor cell lysis is mediated by the release of perforin and granzyme (241, 242). To avoid side effects associated with systemic CD3 cross-linking in the absence of target cancer cells, monovalent CD3 binding is crucial (243, 244). In addition, most IgG-like TCEs entering clinical trials are Fc-silenced to prevent cross-linking of FcγR-bearing immune cells (245). By the end of 2023, nine TCEs have been approved for therapeutic usage (Figure 8). The first was the quadroma-based bsAb Catumaxomab targeting epithelial cell adhesion molecule (EpCAM) and CD3, which was approved for malignant ascites in 2009. The trifunctional antibody with a functionalized Fc was voluntarily withdrawn from the US market in 2013 and for commercial reasons by the European Commission in 2017 (246, 247). In 2014, the FDA approved the bispecific T cell engager (BiTE) Blinatumomab, a CD3 x CD19 scFv-based TCE, for the treatment of acute lymphoblastic leukemia. Since Blinatumomab consists of two tandem scFvs, making the molecule relatively small in size (55 kDa), it has a short half-life of approximately two hours, but penetrates easily into tumor tissue (248, 249). The three bispecific T cell engaging immunotherapies Tebentafusp, Teclistamab, and Mosunetuzumab were FDA approved in 2022. Tebentafusp is a gp100-targeting TCR / anti-CD3 scFv bispecific fusion protein approved for the treatment of unresectable or metastatic uveal melanoma (250, 251). As the first bispecific B cell maturation antigen (BCMA)-directed CD3 TCE, Teclistamab was approved for the treatment of patients with relapsed or refractory multiple myeloma (252, 253). The bispecific CD20 x CD3 IgG-like antibody Mosunetuzumab was approved for relapsed or refractory follicular lymphoma. Mosunetuzumab exhibits an aglycosylated, non-functional Fc domain and was generated using the KiH technology (244, 254). Two additional CD20 and CD3 targeting bispecific TCEs were approved in 2023. The first was Epcoritamab, a full-length Fc-silenced bispecific IgG1 antibody generated by controlled Fab-arm exchange and approved for the treatment of relapsed or refractory diffuse large B cell lymphoma and high-grade B cell lymphoma (255, 256). Subsequently, Glofitamab was approved for selected relapsed or refractory large B cell lymphomas. Glofitamab is a full-length IgG-like bsAb with a 2:1 configuration that enables bivalent binding to CD20 on B cells and monovalent CD3 binding (257, 258). Two other IgG-like TCEs approved in 2023 for relapsed or refractory multiple myeloma are the bispecific BCMA x CD3 antibody Elranatamab, and the G protein-coupled receptor family C group 5 member D (GPRC5D) and CD3 targeting antibody Talquetamab (259, 260).



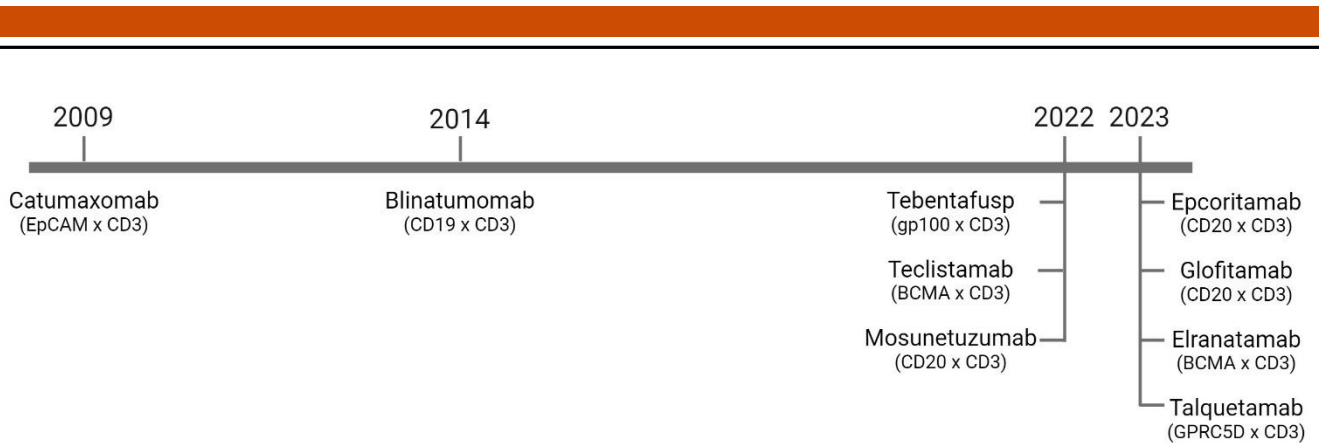


**Figure 8: Timeline of regulatory approved TCEs.** Figure created with BioRender.com.

A number of TCEs with different architectures that address a range of TAAs are currently undergoing clinical trials (206, 240, 242). A limitation observed for many TCEs is the occurrence of side effects like cytokine release syndrome (CRS) and immune effector cell-associated neurotoxicity syndrome (ICANS) (261).

The redirection of NK cells to kill tumor cells represents an alternative to T cell-based therapies, where CRS tends to be much milder (262). Most NKCEs contain an antibody fragment directed against the activating, low-affinity receptor CD16a, which is mainly expressed on NK cells and macrophages. To maximize the potential of NK cell-directed ADCC, the usage of an anti-CD16a moiety offers several advantages over the native Fc domain, including high affinity binding to both CD16a allotypes and conserved NK cell binding in the presence of competing IgG, resulting in enhanced anti-tumor activity (263). However, also immunotherapies targeting different surface molecules on NK cells such as NKG2D, NKp46, or NKp30 have been developed (264). The most advanced NKCEs are developed by Affimed using the redirected optimized cell killing (ROCK<sup>®</sup>) antibody platform (265). The tetravalent bispecific CD30 x CD16 tandem diabody AFM13 showed higher potency and efficacy than a comparable bivalent variant or native IgG and IgG-optimized molecules and has demonstrated anti-tumor activity as monotherapy in a number of clinical trials (266, 267). Another class of bispecific antibody formats that specifically recruit NK cells via antibody binding sites are bispecific killer cell engagers (BiKEs). Like tandem diabodies, they also consist only of variable binding domains connected by flexible linkers (244). In summary, bispecific ICEs represent a promising platform for cancer immunotherapy for the treatment of various tumor types. However, further preclinical and clinical research efforts are needed to overcome challenges like drug resistance, manufacturing difficulties, and adverse effects (240, 242).

---

## 1.6. Trispecific antibodies

It was back in 1991 that Jung *et al.* were the first to describe Fc-free trispecific antibody fragments (268). Eight years later, Hudson *et al.* reported that scFv monomers can be assembled into multimers such as trispecific triabodies (269). In the same year, a trispecific F(ab')<sub>3</sub> antibody conjugate with specificities for CD64, EGFR, and Her2 was developed by Somasundaram *et al.* to redirect effector cell-mediated cytotoxicity against cancer cells expressing either one or both TAAs (270). Since then, the development of trispecific antibodies (tsAbs) has accelerated continuously and the effects of different target combinations, different structural architectures, and different mechanisms of action were investigated (271). The number of articles reporting on tsAbs has increased significantly since 2015, as shown by PubMed's search results. However, no tsAbs has yet been approved for market authorization. Many tsAbs in preclinical development and clinical trials are ICEs. In the case of TCEs, either two TAAs are targeted in addition to CD3, which offers the advantages of dual tumor targeting antibodies described in chapter 1.5.2., or CD28 is targeted together with CD3 and a TAA (271–273). Since CD28 is a key co-stimulatory factor in the T cell response, the later target combination has the advantage of enhancing anti-tumor activity (273). Based on their cross-over dual variable Ig-like (CODV-Ig) antibody platform, Sanofi generated two trispecific CD3 and CD28 binding TCEs which are currently being investigated in phase 1 clinical trials, the CD3 x CD28 x CD38 targeting antibody SAR442257 (NCT04401020) and the CD3 x CD28 x Her2 targeting antibody SAR443216 (NCT05013554) (274–276). The IgG4 isotype Fc domains of the antibodies are silenced to abrogate binding to Fc receptors (277). An example of a dual TAA-targeting trispecific TCE in a 2+1 format is the CD3 x Ly6E x B7-H4 antibody developed by Roche. To ensure correct chain pairing, the KiH technology and charge pairing mutations in two Fab domains were implemented (278). Johnson & Johnson's fully human dual TAA-targeting IgG1-based CD3 x CD79b x CD20 tsAb JNJ-80948543 is currently undergoing a phase 1 clinical trial (NCT05424822). The antibody is composed of an anti-CD79b Fab, an anti-CD3 scFv, and an anti-CD20 scFv, as well as a silenced Fc region (279). Consisting of three common light chain Fab fragments in a 2+1 format, the tsAb ISB 2001 developed by Ichnos Sciences SA targeting CD3 x BCMA x CD38, which is based on the Trispecific Engagement by Antibodies based on the TCR (TREAT) technology, is also investigated in a phase 1 study (NCT05862012) (280). The described IgG-like trispecific TCEs formats are shown schematically in Figure 9A. Other formats of trispecific TCEs such as IL15-based antibodies or molecules containing a moiety for increased serum half-life are described in detail elsewhere (271, 277).

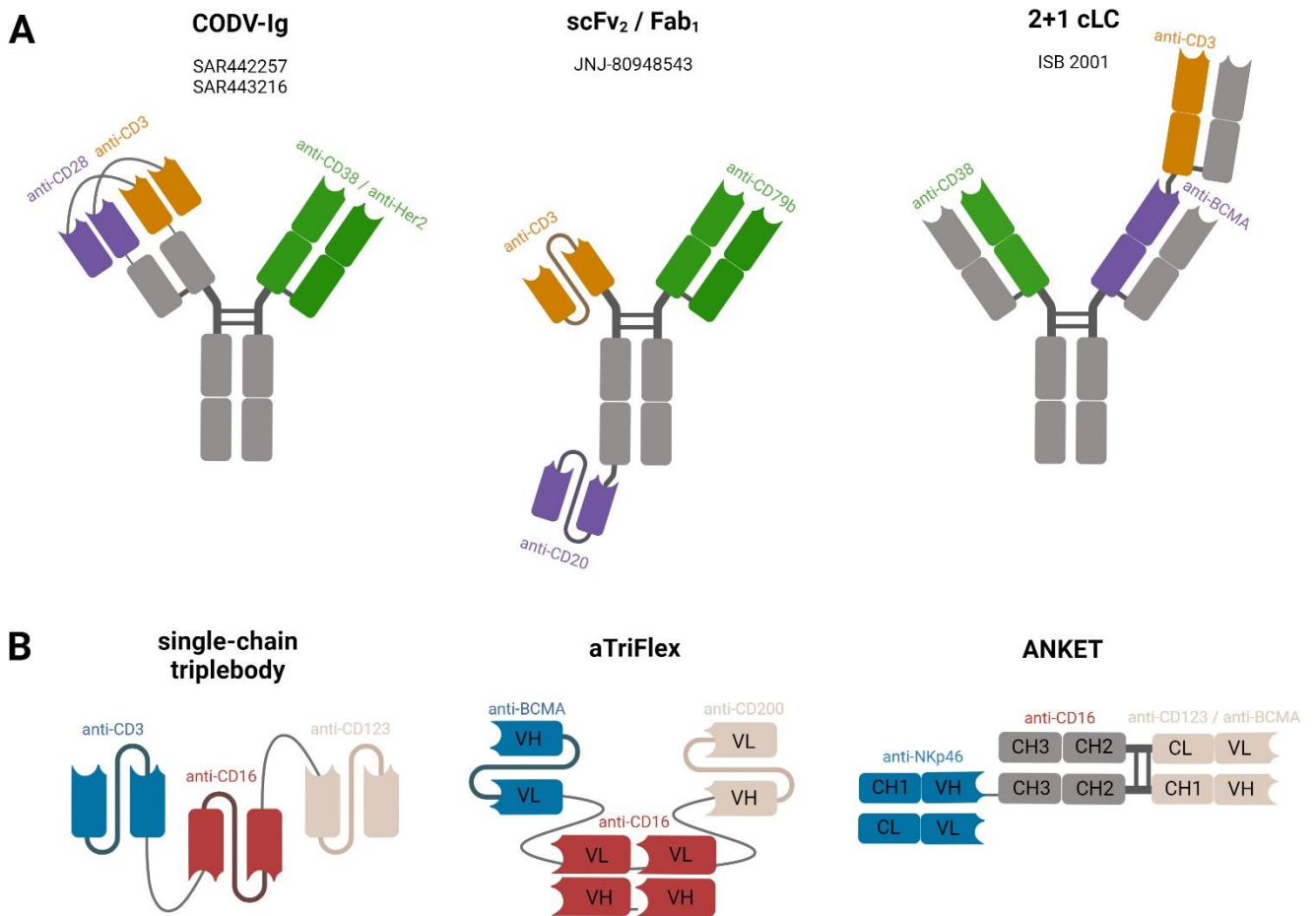


**Figure 9: Schematic overview of selected trispecific antibodies in preclinical development.** A) IgG-like trispecific T cell engager. B) Trispecific NK cell engager. The three antigen binding domains are color-coded. Fc fragments are depicted in grey. Figure created with BioRender.com.

NKCEs can also benefit from improved properties by introducing three binding domains into one molecule. To induce significantly stronger NK lysis of primary leukemic cells, a CD33 x CD16 x CD123 single-chain triplebody was generated (281). Based on this tsAb, the optimized clinical candidate SPM-2 was designed, which carries humanized and disulfide-stabilized scFvs (282). Another dual TAA-targeting CD16-directed trispecific but tetravalent antibody format, termed aTriFlex, consisting of a monospecific anti-CD16 diabody and two TAA-targeting scFvs, was developed to selectively redirect NK cell cytotoxicity to target positive cells. The antigens BCMA and CD200 expressed on the surface of multiple myeloma cells were chosen to demonstrate the increased selectivity of target cell binding and subsequent NK cell cytotoxicity towards target antigen co-expressing cells (283). Bogen *et al.* developed an IgG-like 2+1 tsAb targeting EGFR, PD-L1, and CD16 using the KiH and cLC technology to combine dual tumor targeting, immune checkpoint blockade, and NK cell mediated cytotoxicity (284). In addition to trispecific NKCEs addressing CD16 together with two TAAs, several molecules targeting a TAA and triggering two NK cell activation receptors have been developed. These include molecules based on Innate Pharma’s Antibody-based NK cell Engager Technology (ANKET) platform. Gauthier *et al.*

---

reported the generation of trifunctional NKCEs composed of two Fab fragments targeting NKp46 and a TAA separated by an Fc domain to promote ADCC via CD16 binding. The trifunctional NKCEs were more potent than clinical therapeutic antibodies targeting the same tumor antigen or a mixture of reagents that activate NKp46 and CD16 separately (285, 286). Currently, the ANKET molecules IPH6101/SAR443579 (CD123 x CD16 x NKp46; NCT05086315) and IPH6401/SAR445514 (BCMA x CD16 x NKp46; NCT05839626) are evaluated in phase 1/2 clinical studies. The described trispecific NKCEs formats are shown schematically in Figure 9B. Dragonfly's Trispecific NKCE Therapies (TriNKET) is another platform for the development of multifunctional NKCEs. DF1001 (Her2 x CD16 x NKG2D; NCT04143711) and DF9001 (EGFR x CD16 x NKG2D; NCT05597839) are two of several molecules that belong to this platform (287).

As the described molecules show, tsAbs are capable of addressing multiple mechanisms of action simultaneously by activating immune cells or blocking immune checkpoints and signaling pathways while specifically localizing tumor cells, resulting in an improved anti-tumor efficacy. However, the development of complex therapies such as tsAbs is challenging in terms of manufacturability and the ongoing clinical trials will provide important information on the advantages of tsAbs compared to other immunotherapies. Nevertheless, it is already apparent to date that multispecific antibodies are emerging as a development trend with great potential as next-generation cancer immunotherapy (271, 277).

---

## 2. Objective

---

Over the last three decades, mAbs evolved remarkably from scientific tools to effective human therapeutics. To date, nearly 200 antibody therapies have received marketing approval for the treatment of various diseases, including cancer, immune-related disorders, and infectious diseases. However, due to their monospecificity, mAbs are limited in their mode of action. BsAbs, in contrast, enable unique therapeutic mechanisms of action that can neither be achieved by conventional mAbs nor by their combination, offering advantages in terms of specificity, efficacy, toxicity, and drug resistance. The generation of IgG-like asymmetric bsAbs requires the application of protein engineering technologies to avoid chain mispairing, which complicates the development of these molecules. A subclass of bsAbs that recognize two different antigens with a single Fab fragment, so-called Two-in-One antibodies, consist of two identical heavy and light chains, which is why these symmetrical molecules exhibit mAb-like characteristics in terms of established manufacturing and a conventional approval process. However, the generation of Two-in-One antibodies often involves CDR engineering, and some molecules are unable to target both antigens simultaneously with one Fab fragment.

The first aim of this study was the generation of a Two-in-One antibody derived from immunized chickens without engineering of the antibodies' CDRs. Unlike in rodents, the diversification of avian antibodies is based on gene conversion, and it is not described in the literature whether chicken-derived antibodies are suitable or even advantageous for the generation of Two-in-One antibodies. EGFR and PD-L1, to therapeutic targets that are upregulated in many solid tumors, were selected as target antigens as the simultaneous binding of two cancer-specific targets on the same malignant cell increases the tumor specificity of bsAbs. To generate an EGFR and PD-L1 binding Two-in-One antibody, the heavy chain of a chicken-derived anti-PD-L1 common light chain antibody was combined with a chicken-derived anti-EGFR immune light chain library by yeast mating and the resulting common heavy chain YSD library was screened by FACS. The isolated Two-in-One antibody was analyzed regarding its binding properties by BLI measurements and functional cell-based assays were performed to validate the inhibition of EGFR-dependent signal transduction and the blockade of the PD-1/PD-L1 interaction.

Based on the previously isolated Two-in-One antibody, the second aim of this study was the generation of a trispecific common light chain NK cell engager. TsAbs are considered promising molecules, as the combination of three antigen specificities in one molecule enables unique modes of action. NK cell engagers bridge NK cells with tumor cells to harness the innate immune function of NK cells in tumor therapy. The use of a common light chain is an established method to circumvent light chain mispairing in multispecific antibodies. Different antibody architectures, which varied in their valency towards the target antigens EGFR, PD-L1, and CD16, were investigated and the effect of bivalent target binding was

---

examined by cellular binding experiments. Ultimately, a reporter based ADCC assay was performed to evaluate the effector cell engaging properties of the tsAbs. Since most tsAbs described in the literature consist of three independent monomeric antigen binding units, a hexavalent symmetric 2+2 IgG-like antibody represents a new antibody format, paving the way for the generation of Two-in-One antibody-based tsAbs.

For the development of drug candidates, affinity optimization is crucial as it may impact the efficacy of the drug and limit adverse effects. Even antibodies that have undergone several rounds of somatic hypermutation *in vivo* may not have the desired antigen affinity, which can be optimized by *in vitro* affinity maturation. The third aim of this study was to investigate whether a bispecific Two-in-One antibody can be affinity-matured for one of its two antigens without loss of binding of the other. To improve the EGFR binding affinity of the previously isolated EGFR and PD-L1 binding Two-in-One antibody, site-directed mutagenesis and YSD in combination with FACS were applied. Binding properties of the generated antibody variants were examined by BLI measurements, real time antigen binding experiments on mixed surfaces, and cellular binding assays. In addition, details of the antibody-antigen interaction were predicted by AlphaFold-based modeling.

---

### 3. References

---

1. Alam R. A BRIEF REVIEW OF THE IMMUNE SYSTEM. *Primary Care: Clinics in Office Practice* (1998) **25**:727–38. doi:10.1016/S0095-4543(05)70084-1
2. Parkin J, Cohen B. An overview of the immune system. *Lancet* (2001) **357**:1777–89. doi:10.1016/S0140-6736(00)04904-7
3. Murphy K, Weaver C. *Janeway Immunologie*. Berlin, Heidelberg: Springer Berlin Heidelberg (2018).
4. Basset C, Holton J, O'Mahony R, Roitt I. Innate immunity and pathogen-host interaction. *Vaccine* (2003) **21 Suppl 2**:S12-23. doi:10.1016/S0264-410X(03)00195-6
5. Nochi T, Kiyono H. Innate immunity in the mucosal immune system. *Curr Pharm Des* (2006) **12**:4203–13. doi:10.2174/138161206778743457
6. Mogensen TH. Pathogen recognition and inflammatory signaling in innate immune defenses. *Clin Microbiol Rev* (2009) **22**:240-73, Table of Contents. doi:10.1128/CMR.00046-08
7. Ganz T. The role of antimicrobial peptides in innate immunity. *Integr Comp Biol* (2003) **43**:300–4. doi:10.1093/icb/43.2.300
8. Yokoyama WM, Riley JK. NK cells and their receptors. *Reprod Biomed Online* (2008) **16**:173–91. doi:10.1016/S1472-6483(10)60573-1
9. Raulet DH. Missing self recognition and self tolerance of natural killer (NK) cells. *Semin Immunol* (2006) **18**:145–50. doi:10.1016/j.smim.2006.03.003
10. Gaforio JJ, Ortega E, Algarra I, Serrano MJ, Alvarez de Cienfuegos G. NK cells mediate increase of phagocytic activity but not of proinflammatory cytokine (interleukin-6 IL-6, tumor necrosis factor alpha, and IL-12) production elicited in splenic macrophages by tilorone treatment of mice during acute systemic candidiasis. *Clin Diagn Lab Immunol* (2002) **9**:1282–94. doi:10.1128/cdli.9.6.1282-1294.2002
11. Carayannopoulos LN, Yokoyama WM. Recognition of infected cells by natural killer cells. *Curr Opin Immunol* (2004) **16**:26–33. doi:10.1016/j.coi.2003.11.003
12. Hoebe K, Janssen E, Beutler B. The interface between innate and adaptive immunity. *Nat Immunol* (2004) **5**:971–4. doi:10.1038/ni1004-971
13. Bonilla FA, Oettgen HC. Adaptive immunity. *J Allergy Clin Immunol* (2010) **125**:S33-40. doi:10.1016/j.jaci.2009.09.017
14. Magadán S. Adaptive immune receptor repertoires, an overview of this exciting field. *Immunol Lett* (2020) **221**:49–55. doi:10.1016/j.imlet.2020.02.013
15. Chaplin DD. Overview of the immune response. *J Allergy Clin Immunol* (2010) **125**:S3-23. doi:10.1016/j.jaci.2009.12.980
16. *Immunobiology: The immune system in health and disease*. New York: Garland Publishing (2001). 732 p.
17. Sproul TW, Cheng PC, Dykstra ML, Pierce SK. A role for MHC class II antigen processing in B cell development. *Int Rev Immunol* (2000) **19**:139–55. doi:10.3109/08830180009088502
18. Tarlinton D, Radbruch A, Hiepe F, Dörner T. Plasma cell differentiation and survival. *Curr Opin Immunol* (2008) **20**:162–9. doi:10.1016/j.coi.2008.03.016
19. Chiu ML, Goulet DR, Teplyakov A, Gilliland GL. Antibody Structure and Function: The Basis for Engineering Therapeutics. *Antibodies (Basel)* (2019) **8**. doi:10.3390/antib8040055
20. Poljak RJ, Amzel LM, Avey HP, Chen BL, Phizackerley RP, Saul F. Three-dimensional structure of the Fab' fragment of a human immunoglobulin at 2,8-Å resolution. *Proc Natl Acad Sci U S A* (1973) **70**:3305–10. doi:10.1073/pnas.70.12.3305

21. Damelang T, Brinkhaus M, van Osch TL, Schuurman J, Labrijn AF, Rispens T, et al. Impact of structural modifications of IgG antibodies on effector functions. *Front Immunol* (2023) **14**:1304365. doi:10.3389/fimmu.2023.1304365
22. Vidarsson G, Dekkers G, Rispens T. IgG subclasses and allotypes: from structure to effector functions. *Front Immunol* (2014) **5**:520. doi:10.3389/fimmu.2014.00520
23. Arnold JN, Wormald MR, Sim RB, Rudd PM, Dwek RA. The impact of glycosylation on the biological function and structure of human immunoglobulins. *Annu Rev Immunol* (2007) **25**:21–50. doi:10.1146/annurev.immunol.25.022106.141702
24. Amzel LM, Poljak RJ. Three-dimensional structure of immunoglobulins. *Annu Rev Biochem* (1979) **48**:961–97. doi:10.1146/annurev.bi.48.070179.004525
25. Davies DR, Metzger H. Structural basis of antibody function. *Annu Rev Immunol* (1983) **1**:87–117. doi:10.1146/annurev.iy.01.040183.000511
26. Daëron M. Fc receptor biology. *Annu Rev Immunol* (1997) **15**:203–34. doi:10.1146/annurev.immunol.15.1.203
27. van der Poel CE, Spaapen RM, van de Winkel JG, Leusen JH. Functional characteristics of the high affinity IgG receptor, FcγRI. *J Immunol* (2011) **186**:2699–704. doi:10.4049/jimmunol.1003526
28. Alevy YG, Tucker J, Naziruddin B, Mohanakumar T. CD32C (Fc gamma RIIC) mRNA expression and regulation. *Mol Immunol* (1993) **30**:775–82. doi:10.1016/0161-5890(93)90149-6
29. Gómez Román VR, Murray JC, Weiner LM. “Antibody-Dependent Cellular Cytotoxicity (ADCC),”. In: *Antibody Fc*. Elsevier (2014). p. 1–27.
30. Zahavi D, AlDeghaither D, O'Connell A, Weiner LM. Enhancing antibody-dependent cell-mediated cytotoxicity: a strategy for improving antibody-based immunotherapy. *Antib Ther* (2018) **1**:7–12. doi:10.1093/abt/tby002
31. Wang W, Erbe AK, Hank JA, Morris ZS, Sondel PM. NK Cell-Mediated Antibody-Dependent Cellular Cytotoxicity in Cancer Immunotherapy. *Front Immunol* (2015) **6**:368. doi:10.3389/fimmu.2015.00368
32. Ricklin D, Hajishengallis G, Yang K, Lambris JD. Complement: a key system for immune surveillance and homeostasis. *Nat Immunol* (2010) **11**:785–97. doi:10.1038/ni.1923
33. Wang B, Yang C, Jin X, Du Q, Wu H, Dall'Acqua W, et al. Regulation of antibody-mediated complement-dependent cytotoxicity by modulating the intrinsic affinity and binding valency of IgG for target antigen. *MAbs* (2020) **12**:1690959. doi:10.1080/19420862.2019.1690959
34. Kamen L, Myneni S, Langsdorf C, Kho E, Ordonia B, Thakurta T, et al. A novel method for determining antibody-dependent cellular phagocytosis. *J Immunol Methods* (2019) **468**:55–60. doi:10.1016/j.jim.2019.03.001
35. Roopenian DC, Akilesh S. FcRn: the neonatal Fc receptor comes of age. *Nat Rev Immunol* (2007) **7**:715–25. doi:10.1038/nri2155
36. Pyzik M, Rath T, Lencer WI, Baker K, Blumberg RS. FcRn: The Architect Behind the Immune and Nonimmune Functions of IgG and Albumin. *J Immunol* (2015) **194**:4595–603. doi:10.4049/jimmunol.1403014
37. Roth DB. V(D)J Recombination: Mechanism, Errors, and Fidelity. *Microbiol Spectr* (2014) **2**. doi:10.1128/microbiolspec.MDNA3-0041-2014
38. Rees AR. Understanding the human antibody repertoire. *MAbs* (2020) **12**:1729683. doi:10.1080/19420862.2020.1729683
39. Schatz DG, Swanson PC. V(D)J recombination: mechanisms of initiation. *Annu Rev Genet* (2011) **45**:167–202. doi:10.1146/annurev-genet-110410-132552



- 
40. *Molecular biology of the cell*. New York: Garland Science (2002).
  41. Di Noia JM, Neuberger MS. Molecular mechanisms of antibody somatic hypermutation. *Annu Rev Biochem* (2007) **76**:1–22. doi:10.1146/annurev.biochem.76.061705.090740
  42. Maul RW, Gearhart PJ. AID and somatic hypermutation. *Adv Immunol* (2010) **105**:159–91. doi:10.1016/S0065-2776(10)05006-6
  43. Maity PC, Datta M, Nicolò A, Jumaa H. Isotype Specific Assembly of B Cell Antigen Receptors and Synergism With Chemokine Receptor CXCR4. *Front Immunol* (2018) **9**:2988. doi:10.3389/fimmu.2018.02988
  44. Stavnezer J, Guikema JE, Schrader CE. Mechanism and regulation of class switch recombination. *Annu Rev Immunol* (2008) **26**:261–92. doi:10.1146/annurev.immunol.26.021607.090248
  45. Winau F, Winau R. Emil von Behring and serum therapy. *Microbes Infect* (2002) **4**:185–8. doi:10.1016/S1286-4579(01)01526-X
  46. Stabsarzt B von, Kutasati. Ueber das zustandekommen der diphtherie-immunität und der tetanus-immunität bei thieren. *Mol Immunol* (1991) **28**:1319–20. doi:10.1016/0161-5890(91)90033-g
  47. Stockwin LH, Holmes S. Antibodies as therapeutic agents: vive la renaissance! *Expert Opin Biol Ther* (2003) **3**:1133–52. doi:10.1517/14712598.3.7.1133
  48. Dhar C, Sasmal A, Varki A. From "Serum Sickness" to "Xenosialitis": Past, Present, and Future Significance of the Non-human Sialic Acid Neu5Gc. *Front Immunol* (2019) **10**:807. doi:10.3389/fimmu.2019.00807
  49. Leavy O. The birth of monoclonal antibodies. *Nat Immunol* (2016) **17**:S13-S13. doi:10.1038/ni.3608
  50. Zaroff S, Tan G. Hybridoma technology: the preferred method for monoclonal antibody generation for in vivo applications. *Biotechniques* (2019) **67**:90–2. doi:10.2144/btn-2019-0054
  51. Quinteros DA, Bermúdez JM, Ravetti S, Cid A, Allemandi DA, Palma SD. "Therapeutic use of monoclonal antibodies: general aspects and challenges for drug delivery,". In: *Nanostructures for drug delivery*. Elsevier (uuuu-uuuu). p. 807–33.
  52. Legouffe E, Liautard J, Gaillard JP, Rossi JF, Wijdenes J, Bataille R, et al. Human anti-mouse antibody response to the injection of murine monoclonal antibodies against IL-6. *Clin Exp Immunol* (1994) **98**:323–9. doi:10.1111/j.1365-2249.1994.tb06145.x
  53. Meeker TC, Lowder J, Maloney DG, Miller RA, Thielemans K, Warnke R, et al. A clinical trial of anti-idiotypic therapy for B cell malignancy. *Blood* (1985) **65**:1349–63. doi:10.1182/blood.V65.6.1349.bloodjournal6561349
  54. Richards JM, Vogelzang NJ, Bluestone JA. Neurotoxicity after treatment with muromonab-CD3. *N Engl J Med* (1990) **323**:487–8. doi:10.1056/NEJM199008163230715
  55. van der Horst HJ, Nijhof IS, Mutis T, Chamuleau ME. Fc-Engineered Antibodies with Enhanced Fc-Effector Function for the Treatment of B-Cell Malignancies. *Cancers (Basel)* (2020) **12**. doi:10.3390/cancers12103041
  56. Morrison SL, Johnson MJ, Herzenberg LA, Oi VT. Chimeric human antibody molecules: mouse antigen-binding domains with human constant region domains. *Proc Natl Acad Sci U S A* (1984) **81**:6851–5. doi:10.1073/pnas.81.21.6851
  57. Faulds D, Sorkin EM. Abciximab (c7E3 Fab). A review of its pharmacology and therapeutic potential in ischaemic heart disease. *Drugs* (1994) **48**:583–98. doi:10.2165/00003495-199448040-00007
  58. Hwang WY, Foote J. Immunogenicity of engineered antibodies. *Methods* (2005) **36**:3–10. doi:10.1016/j.ymeth.2005.01.001

- 
59. Jones PT, Dear PH, Foote J, Neuberger MS, Winter G. Replacing the complementarity-determining regions in a human antibody with those from a mouse. *Nature* (1986) **321**:522–5. doi:10.1038/321522a0
  60. Roguska MA, Pedersen JT, Keddy CA, Henry AH, Searle SJ, Lambert JM, et al. Humanization of murine monoclonal antibodies through variable domain resurfacing. *Proc Natl Acad Sci U S A* (1994) **91**:969–73. doi:10.1073/pnas.91.3.969
  61. Tan P, Mitchell DA, Buss TN, Holmes MA, Anasetti C, Foote J. "Superhumanized" antibodies: reduction of immunogenic potential by complementarity-determining region grafting with human germline sequences: application to an anti-CD28. *J Immunol* (2002) **169**:1119–25. doi:10.4049/jimmunol.169.2.1119
  62. Lazar GA, Desjarlais JR, Jacinto J, Karki S, Hammond PW. A molecular immunology approach to antibody humanization and functional optimization. *Mol Immunol* (2007) **44**:1986–98. doi:10.1016/j.molimm.2006.09.029
  63. Padlan EA. A possible procedure for reducing the immunogenicity of antibody variable domains while preserving their ligand-binding properties. *Mol Immunol* (1991) **28**:489–98. doi:10.1016/0161-5890(91)90163-E
  64. Bell J, Colaneri J. Zenapax: transplant's first humanized monoclonal antibody. *ANNA J* (1998) **25**:429–30.
  65. Lonberg N. Fully human antibodies from transgenic mouse and phage display platforms. *Curr Opin Immunol* (2008) **20**:450–9. doi:10.1016/j.coi.2008.06.004
  66. Hoogenboom HR. Selecting and screening recombinant antibody libraries. *Nat Biotechnol* (2005) **23**:1105–16. doi:10.1038/nbt1126
  67. Frenzel A, Schirrmann T, Hust M. Phage display-derived human antibodies in clinical development and therapy. *MAbs* (2016) **8**:1177–94. doi:10.1080/19420862.2016.1212149
  68. Harding FA, Stickler MM, Razo J, DuBridge RB. The immunogenicity of humanized and fully human antibodies: residual immunogenicity resides in the CDR regions. *MAbs* (2010) **2**:256–65. doi:10.4161/mabs.2.3.11641
  69. Crescioli S, Kaplon H, Chenoweth A, Wang L, Visweswarajah J, Reichert JM. Antibodies to watch in 2024. *MAbs* (2024) **16**:2297450. doi:10.1080/19420862.2023.2297450
  70. Kaplon H, Chenoweth A, Crescioli S, Reichert JM. Antibodies to watch in 2022. *MAbs* (2022) **14**:2014296. doi:10.1080/19420862.2021.2014296
  71. Kholodenko RV, Kalinovsky DV, Doronin II, Ponomarev ED, Kholodenko IV. Antibody Fragments as Potential Biopharmaceuticals for Cancer Therapy: Success and Limitations. *Curr Med Chem* (2019) **26**:396–426. doi:10.2174/0929867324666170817152554
  72. Nelson AL. Antibody fragments: hope and hype. *MAbs* (2010) **2**:77–83. doi:10.4161/mabs.2.1.10786
  73. Bever CS, Dong J-X, Vasylieva N, Barnych B, Cui Y, Xu Z-L, et al. VHH antibodies: emerging reagents for the analysis of environmental chemicals. *Anal Bioanal Chem* (2016) **408**:5985–6002. doi:10.1007/s00216-016-9585-x
  74. Usta C, Turgut NT, Bedel A. How abciximab might be clinically useful. *Int J Cardiol* (2016) **222**:1074–8. doi:10.1016/j.ijcard.2016.07.213
  75. Ferlay J, Colombet M, Soerjomataram I, Parkin DM, Piñeros M, Znaor A, et al. Cancer statistics for the year 2020: An overview. *Int J Cancer* (2021). doi:10.1002/ijc.33588
  76. Zahavi D, Weiner L. Monoclonal Antibodies in Cancer Therapy. *Antibodies (Basel)* (2020) **9**. doi:10.3390/antib9030034

77. Padma VV. An overview of targeted cancer therapy. *Biomedicine (Taipei)* (2015) **5**:19. doi:10.7603/s40681-015-0019-4
78. Maloney DG, Grillo-López AJ, White CA, Bodkin D, Schilder RJ, Neidhart JA, et al. IDEC-C2B8 (Rituximab) Anti-CD20 Monoclonal Antibody Therapy in Patients With Relapsed Low-Grade Non-Hodgkin's Lymphoma. *Blood* (1997) **90**:2188–95. doi:10.1182/blood.V90.6.2188
79. Scott AM, Wolchok JD, Old LJ. Antibody therapy of cancer. *Nat Rev Cancer* (2012) **12**:278–87. doi:10.1038/nrc3236
80. Wykosky J, Fenton T, Furnari F, Cavenee WK. Therapeutic targeting of epidermal growth factor receptor in human cancer: successes and limitations. *Chin J Cancer* (2011) **30**:5–12. doi:10.5732/cjc.010.10542
81. Da Santos ES, Nogueira KA, Fernandes LC, Martins JR, Reis AV, Neto Jd, et al. EGFR targeting for cancer therapy: Pharmacology and immunoconjugates with drugs and nanoparticles. *Int J Pharm* (2021) **592**:120082. doi:10.1016/j.ijpharm.2020.120082
82. Tai W, Mahato R, Cheng K. The role of HER2 in cancer therapy and targeted drug delivery. *J Control Release* (2010) **146**:264–75. doi:10.1016/j.jconrel.2010.04.009
83. Cai W-Q, Zeng L-S, Wang L-F, Wang Y-Y, Cheng J-T, Zhang Y, et al. The Latest Battles Between EGFR Monoclonal Antibodies and Resistant Tumor Cells. *Front Oncol* (2020) **10**:1249. doi:10.3389/fonc.2020.01249
84. Swain SM, Shastry M, Hamilton E. Targeting HER2-positive breast cancer: advances and future directions. *Nat Rev Drug Discov* (2023) **22**:101–26. doi:10.1038/s41573-022-00579-0
85. Martinelli E, Palma R de, Orditura M, Vita F de, Ciardiello F. Anti-epidermal growth factor receptor monoclonal antibodies in cancer therapy. *Clin Exp Immunol* (2009) **158**:1–9. doi:10.1111/j.1365-2249.2009.03992.x
86. Pardoll DM. The blockade of immune checkpoints in cancer immunotherapy. *Nat Rev Cancer* (2012) **12**:252–64. doi:10.1038/nrc3239
87. Shiravand Y, Khodadadi F, Kashani SM, Hosseini-Fard SR, Hosseini S, Sadeghirad H, et al. Immune Checkpoint Inhibitors in Cancer Therapy. *Curr Oncol* (2022) **29**:3044–60. doi:10.3390/curroncol29050247
88. Sadeghi Rad H, Monkman J, Warkiani ME, Ladwa R, O'Byrne K, Rezaei N, et al. Understanding the tumor microenvironment for effective immunotherapy. *Med Res Rev* (2021) **41**:1474–98. doi:10.1002/med.21765
89. Seidel JA, Otsuka A, Kabashima K. Anti-PD-1 and Anti-CTLA-4 Therapies in Cancer: Mechanisms of Action, Efficacy, and Limitations. *Front Oncol* (2018) **8**:86. doi:10.3389/fonc.2018.00086
90. Hodi FS, O'Day SJ, McDermott DF, Weber RW, Sosman JA, Haanen JB, et al. Improved survival with ipilimumab in patients with metastatic melanoma. *N Engl J Med* (2010) **363**:711–23. doi:10.1056/NEJMoa1003466
91. Park UB, Jeong TJ, Gu N, Lee HT, Heo Y-S. Molecular basis of PD-1 blockade by dostarlimab, the FDA-approved antibody for cancer immunotherapy. *Biochem Biophys Res Commun* (2022) **599**:31–7. doi:10.1016/j.bbrc.2022.02.026
92. Kang C. Retifanlimab: First Approval. *Drugs* (2023) **83**:731–7. doi:10.1007/s40265-023-01884-7
93. Keam SJ. Toripalimab: First Global Approval. *Drugs* (2019) **79**:573–8. doi:10.1007/s40265-019-01076-2
94. Sunshine J, Taube JM. PD-1/PD-L1 inhibitors. *Curr Opin Pharmacol* (2015) **23**:32–8. doi:10.1016/j.coph.2015.05.011

95. Han Y, Liu D, Li L. PD-1/PD-L1 pathway: current researches in cancer. *Am J Cancer Res* (2020) **10**:727–42.
96. Shi X, Li C-W, Tan L-C, Wen S-S, Liao T, Zhang Y, et al. Immune Co-inhibitory Receptors PD-1, CTLA-4, TIM-3, LAG-3, and TIGIT in Medullary Thyroid Cancers: A Large Cohort Study. *J Clin Endocrinol Metab* (2021) **106**:120–32. doi:10.1210/clinem/dgaa701
97. Zhang W, Huang Q, Xiao W, Zhao Y, Pi J, Xu H, et al. Advances in Anti-Tumor Treatments Targeting the CD47/SIRP $\alpha$  Axis. *Front Immunol* (2020) **11**:18. doi:10.3389/fimmu.2020.00018
98. Yang H, Xun Y, You H. The landscape overview of CD47-based immunotherapy for hematological malignancies. *Biomark Res* (2023) **11**:15. doi:10.1186/s40364-023-00456-x
99. Lu R-M, Hwang Y-C, Liu I-J, Lee C-C, Tsai H-Z, Li H-J, et al. Development of therapeutic antibodies for the treatment of diseases. *J Biomed Sci* (2020) **27**:1. doi:10.1186/s12929-019-0592-z
100. Valldorf B, Hinz SC, Russo G, Pekar L, Mohr L, Klemm J, et al. Antibody display technologies: selecting the cream of the crop. *Biol Chem* (2022) **403**:455–77. doi:10.1515/hsz-2020-0377
101. Zielonka S, Krahl S. *Genotype Phenotype Coupling*. New York, NY: Springer US (2023).
102. Ponsel D, Neugebauer J, Ladetzki-Baehs K, Tissot K. High affinity, developability and functional size: the holy grail of combinatorial antibody library generation. *Molecules* (2011) **16**:3675–700. doi:10.3390/molecules16053675
103. Braunagel M, Little M. Construction of a semisynthetic antibody library using trinucleotide oligos. *Nucleic Acids Res* (1997) **25**:4690–1. doi:10.1093/nar/25.22.4690
104. Rader C, Ritter G, Nathan S, Elia M, Gout I, Jungbluth AA, et al. The rabbit antibody repertoire as a novel source for the generation of therapeutic human antibodies. *J Biol Chem* (2000) **275**:13668–76. doi:10.1074/jbc.275.18.13668
105. Brüggemann M, Osborn MJ, Ma B, Hayre J, Avis S, Lundstrom B, et al. Human antibody production in transgenic animals. *Arch Immunol Ther Exp (Warsz)* (2015) **63**:101–8. doi:10.1007/s00005-014-0322-x
106. Green LL, Hardy MC, Maynard-Currie CE, Tsuda H, Louie DM, Mendez MJ, et al. Antigen-specific human monoclonal antibodies from mice engineered with human Ig heavy and light chain YACs. *Nat Genet* (1994) **7**:13–21. doi:10.1038/ng0594-13
107. Lerner RA. Combinatorial antibody libraries: new advances, new immunological insights. *Nat Rev Immunol* (2016) **16**:498–508. doi:10.1038/nri.2016.67
108. Moon SA, Ki MK, Lee S, Hong M-L, Kim M, Kim S, et al. Antibodies against non-immunizing antigens derived from a large immune scFv library. *Mol Cells* (2011) **31**:509–13. doi:10.1007/s10059-011-2268-8
109. Nelson B, Sidhu SS. Synthetic antibody libraries. *Methods Mol Biol* (2012) **899**:27–41. doi:10.1007/978-1-61779-921-1\_2
110. Lipovsek D, Plückthun A. In-vitro protein evolution by ribosome display and mRNA display. *J Immunol Methods* (2004) **290**:51–67. doi:10.1016/j.jim.2004.04.008
111. Kunamneni A, Ogaugwu C, Bradfute S, Durvasula R. Ribosome Display Technology: Applications in Disease Diagnosis and Control. *Antibodies (Basel)* (2020) **9**. doi:10.3390/antib9030028
112. Smith GP. Filamentous fusion phage: novel expression vectors that display cloned antigens on the virion surface. *Science* (1985) **228**:1315–7. doi:10.1126/science.4001944
113. McCafferty J, Griffiths AD, Winter G, Chiswell DJ. Phage antibodies: filamentous phage displaying antibody variable domains. *Nature* (1990) **348**:552–4. doi:10.1038/348552a0

114. Francisco JA, Campbell R, Iverson BL, Georgiou G. Production and fluorescence-activated cell sorting of Escherichia coli expressing a functional antibody fragment on the external surface. *Proc Natl Acad Sci U S A* (1993) **90**:10444–8. doi:10.1073/pnas.90.22.10444
115. Ho M, Nagata S, Pastan I. Isolation of anti-CD22 Fv with high affinity by Fv display on human cells. *Proc Natl Acad Sci U S A* (2006) **103**:9637–42. doi:10.1073/pnas.0603653103
116. Beerli RR, Bauer M, Buser RB, Gwerder M, Muntwiler S, Maurer P, et al. Isolation of human monoclonal antibodies by mammalian cell display. *Proc Natl Acad Sci U S A* (2008) **105**:14336–41. doi:10.1073/pnas.0805942105
117. Boder ET, Wittrup KD. Yeast surface display for screening combinatorial polypeptide libraries. *Nat Biotechnol* (1997) **15**:553–7. doi:10.1038/nbt0697-553
118. Winter G, Milstein C. Man-made antibodies. *Nature* (1991) **349**:293–9. doi:10.1038/349293a0
119. Kehoe JW, Kay BK. Filamentous phage display in the new millennium. *Chem Rev* (2005) **105**:4056–72. doi:10.1021/cr000261r
120. Huang JX, Bishop-Hurley SL, Cooper MA. Development of anti-infectives using phage display: biological agents against bacteria, viruses, and parasites. *Antimicrob Agents Chemother* (2012) **56**:4569–82. doi:10.1128/AAC.00567-12
121. Alfaleh MA, Alsaab HO, Mahmoud AB, Alkayyal AA, Jones ML, Mahler SM, et al. Phage Display Derived Monoclonal Antibodies: From Bench to Bedside. *Front Immunol* (2020) **11**:1986. doi:10.3389/fimmu.2020.01986
122. Wilson DR, Finlay BB. Phage display: applications, innovations, and issues in phage and host biology. *Can J Microbiol* (1998) **44**:313–29.
123. Teymennet-Ramírez KV, Martínez-Morales F, Trejo-Hernández MR. Yeast Surface Display System: Strategies for Improvement and Biotechnological Applications. *Front Bioeng Biotechnol* (2021) **9**:794742. doi:10.3389/fbioe.2021.794742
124. Cherf GM, Cochran JR. Applications of Yeast Surface Display for Protein Engineering. *Methods Mol Biol* (2015) **1319**:155–75. doi:10.1007/978-1-4939-2748-7\_8
125. Könning D, Kolmar H. Beyond antibody engineering: directed evolution of alternative binding scaffolds and enzymes using yeast surface display. *Microb Cell Fact* (2018) **17**:32. doi:10.1186/s12934-018-0881-3
126. Zhao H, Shen ZM, Kahn PC, Lipke PN. Interaction of alpha-agglutinin and a-agglutinin, Saccharomyces cerevisiae sexual cell adhesion molecules. *J Bacteriol* (2001) **183**:2874–80. doi:10.1128/JB.183.9.2874-2880.2001
127. Kapteyn JC, van den Ende H, Klis FM. The contribution of cell wall proteins to the organization of the yeast cell wall. *Biochim Biophys Acta* (1999) **1426**:373–83. doi:10.1016/s0304-4165(98)00137-8
128. Roy A, Lu CF, Marykwas DL, Lipke PN, Kurjan J. The AGA1 product is involved in cell surface attachment of the Saccharomyces cerevisiae cell adhesion glycoprotein a-agglutinin. *Mol Cell Biol* (1991) **11**:4196–206. doi:10.1128/mcb.11.8.4196-4206.1991
129. Boder ET, Raeszadeh-Sarmazdeh M, Price JV. Engineering antibodies by yeast display. *Arch Biochem Biophys* (2012) **526**:99–106. doi:10.1016/j.abb.2012.03.009
130. Blaise L, Wehnert A, Steukers MP, van den Beucken T, Hoogenboom HR, Hufton SE. Construction and diversification of yeast cell surface displayed libraries by yeast mating: application to the affinity maturation of Fab antibody fragments. *Gene* (2004) **342**:211–8. doi:10.1016/j.gene.2004.08.014

131. Weaver-Feldhaus JM, Lou J, Coleman JR, Siegel RW, Marks JD, Feldhaus MJ. Yeast mating for combinatorial Fab library generation and surface display. *FEBS Lett* (2004) **564**:24–34. doi:10.1016/S0014-5793(04)00309-6
132. Doerner A, Rhiel L, Zielonka S, Kolmar H. Therapeutic antibody engineering by high efficiency cell screening. *FEBS Lett* (2014) **588**:278–87. doi:10.1016/j.febslet.2013.11.025
133. VanAntwerp JJ, Wittrup KD. Fine affinity discrimination by yeast surface display and flow cytometry. *Biotechnol Prog* (2000) **16**:31–7. doi:10.1021/bp990133s
134. Lee W, Syed Atif A, Tan SC, Leow CH. Insights into the chicken IgY with emphasis on the generation and applications of chicken recombinant monoclonal antibodies. *J Immunol Methods* (2017) **447**:71–85. doi:10.1016/j.jim.2017.05.001
135. Larsson A, Bålów RM, Lindahl TL, Forsberg PO. Chicken antibodies: taking advantage of evolution--a review. *Poult Sci* (1993) **72**:1807–12. doi:10.3382/ps.0721807
136. Andris-Widhopf J, Rader C, Steinberger P, Fuller R, Barbas CF. Methods for the generation of chicken monoclonal antibody fragments by phage display. *J Immunol Methods* (2000) **242**:159–81. doi:10.1016/s0022-1759(00)00221-0
137. Finlay WJ, deVore NC, Dobrovolskaia EN, Gam A, Goodyear CS, Slater JE. Exploiting the avian immunoglobulin system to simplify the generation of recombinant antibodies to allergenic proteins. *Clin Exp Allergy* (2005) **35**:1040–8. doi:10.1111/j.1365-2222.2005.02307.x
138. Sequence and comparative analysis of the chicken genome provide unique perspectives on vertebrate evolution. *Nature* (2004) **432**:695–716. doi:10.1038/nature03154
139. Gibbs RA, Weinstock GM, Metzker ML, Muzny DM, Sodergren EJ, Scherer S, et al. Genome sequence of the Brown Norway rat yields insights into mammalian evolution. *Nature* (2004) **428**:493–521. doi:10.1038/nature02426
140. Banik SS, Kushnir N, Doranz BJ, Chambers R. Breaking barriers in antibody discovery: harnessing divergent species for accessing difficult and conserved drug targets. *MAbs* (2023) **15**:2273018. doi:10.1080/19420862.2023.2273018
141. Zhang X, Calvert RA, Sutton BJ, Doré KA. IgY: a key isotype in antibody evolution. *Biol Rev Camb Philos Soc* (2017) **92**:2144–56. doi:10.1111/brv.12325
142. Leslie GA, Clem LW. Phylogen of immunoglobulin structure and function. 3. Immunoglobulins of the chicken. *J Exp Med* (1969) **130**:1337–52. doi:10.1084/jem.130.6.1337
143. Taylor AI, Gould HJ, Sutton BJ, Calvert RA. Avian IgY binds to a monocyte receptor with IgG-like kinetics despite an IgE-like structure. *J Biol Chem* (2008) **283**:16384–90. doi:10.1074/jbc.M801321200
144. Müller S, Schubert A, Zajac J, Dyck T, Oelkrug C. IgY antibodies in human nutrition for disease prevention. *Nutr J* (2015) **14**:109. doi:10.1186/s12937-015-0067-3
145. Taylor AI, Fabiane SM, Sutton BJ, Calvert RA. The crystal structure of an avian IgY-Fc fragment reveals conservation with both mammalian IgG and IgE. *Biochemistry* (2009) **48**:558–62. doi:10.1021/bi8019993
146. Dou L, Zhang Y, Bai Y, Li Y, Liu M, Shao S, et al. Advances in Chicken IgY-Based Immunoassays for the Detection of Chemical and Biological Hazards in Food Samples. *J Agric Food Chem* (2022) **70**:976–91. doi:10.1021/acs.jafc.1c06750
147. Wu L, Oficjalska K, Lambert M, Fennell BJ, Darmanin-Sheehan A, Ní Shúilleabháin D, et al. Fundamental characteristics of the immunoglobulin VH repertoire of chickens in comparison with those of humans, mice, and camelids. *J Immunol* (2012) **188**:322–33. doi:10.4049/jimmunol.1102466

148. Mallaby J, Ng J, Stewart A, Sinclair E, Dunn-Walters D, Hershberg U. Chickens, more than humans, focus the diversity of their immunoglobulin genes on the complementarity-determining region but utilise amino acids, indicative of a more cross-reactive antibody repertoire. *Front Immunol* (2022) **13**:837246. doi:10.3389/fimmu.2022.837246
149. Reynaud CA, Dahan A, Weill JC. Complete sequence of a chicken lambda light chain immunoglobulin derived from the nucleotide sequence of its mRNA. *Proc Natl Acad Sci U S A* (1983) **80**:4099–103. doi:10.1073/pnas.80.13.4099
150. Conroy PJ, Law RH, Gilgunn S, Hearty S, Caradoc-Davies TT, Lloyd G, et al. Reconciling the structural attributes of avian antibodies. *J Biol Chem* (2014) **289**:15384–92. doi:10.1074/jbc.M114.562470
151. Guo Y, Gao M, Wang J. A novel gene encoding goose immunoglobulin  $\lambda$  light chain. *Acta Biochim Biophys Sin (Shanghai)* (2012) **44**:805–6. doi:10.1093/abbs/gms063
152. McCormack WT, Tjoelker LW, Thompson CB. Avian B-cell development: generation of an immunoglobulin repertoire by gene conversion. *Annu Rev Immunol* (1991) **9**:219–41. doi:10.1146/annurev.iy.09.040191.001251
153. Bogen JP, Grzeschik J, Krah S, Zielonka S, Kolmar H. Rapid Generation of Chicken Immune Libraries for Yeast Surface Display. *Methods Mol Biol* (2020) **2070**:289–302. doi:10.1007/978-1-4939-9853-1\_16
154. Ratcliffe MJ. Antibodies, immunoglobulin genes and the bursa of Fabricius in chicken B cell development. *Dev Comp Immunol* (2006) **30**:101–18. doi:10.1016/j.dci.2005.06.018
155. Ratcliffe MJ, Jacobsen KA. Rearrangement of immunoglobulin genes in chicken B cell development. *Semin Immunol* (1994) **6**:175–84. doi:10.1006/smim.1994.1023
156. *Avian Immunology*. Elsevier (2008).
157. Gjetting T, Gad M, Fröhlich C, Lindsted T, Melander MC, Bhatia VK, et al. Sym021, a promising anti-PD1 clinical candidate antibody derived from a new chicken antibody discovery platform. *MAbs* (2019) **11**:666–80. doi:10.1080/19420862.2019.1596514
158. Stack E, McMurray S, McMurray G, Wade J, Clark M, Young G, et al. In vitro affinity optimization of an anti-BDNF monoclonal antibody translates to improved potency in targeting chronic pain states in vivo. *MAbs* (2020) **12**:1755000. doi:10.1080/19420862.2020.1755000
159. Bednenko J, Harriman R, Mariën L, Nguyen HM, Agrawal A, Papoyan A, et al. A multiplatform strategy for the discovery of conventional monoclonal antibodies that inhibit the voltage-gated potassium channel Kv1.3. *MAbs* (2018) **10**:636–50. doi:10.1080/19420862.2018.1445451
160. Kandari D, Bhatnagar R. Antibody engineering and its therapeutic applications. *Int Rev Immunol* (2023) **42**:156–83. doi:10.1080/08830185.2021.1960986
161. Tabasinezhad M, Talebkhan Y, Wenzel W, Rahimi H, Omidinia E, Mahboudi F. Trends in therapeutic antibody affinity maturation: From in-vitro towards next-generation sequencing approaches. *Immunol Lett* (2019) **212**:106–13. doi:10.1016/j.imlet.2019.06.009.
162. Ducancel F, Muller BH. Molecular engineering of antibodies for therapeutic and diagnostic purposes. *MAbs* (2012) **4**:445–57. doi:10.4161/mabs.20776
163. Fujii I. Antibody affinity maturation by random mutagenesis. *Methods Mol Biol* (2004) **248**:345–59. doi:10.1385/1-59259-666-5:345.
164. Weng W-K, Levy R. Two immunoglobulin G fragment C receptor polymorphisms independently predict response to rituximab in patients with follicular lymphoma. *J Clin Oncol* (2003) **21**:3940–7. doi:10.1200/JCO.2003.05.013

165. Liu R, Oldham RJ, Teal E, Beers SA, Cragg MS. Fc-Engineering for Modulated Effector Functions-Improving Antibodies for Cancer Treatment. *Antibodies (Basel)* (2020) **9**. doi:10.3390/antib9040064
166. Mimoto F, Kuramochi T, Katada H, Igawa T, Hattori K. Fc Engineering to Improve the Function of Therapeutic Antibodies. *Curr Pharm Biotechnol* (2016) **17**:1298–314. doi:10.2174/1389201017666160824161854
167. Shields RL, Namenuk AK, Hong K, Meng YG, Rae J, Briggs J, et al. High resolution mapping of the binding site on human IgG1 for Fc gamma RI, Fc gamma RII, Fc gamma RIII, and FcRn and design of IgG1 variants with improved binding to the Fc gamma R. *J Biol Chem* (2001) **276**:6591–604. doi:10.1074/jbc.M009483200
168. Lazar GA, Dang W, Karki S, Vafa O, Peng JS, Hyun L, et al. Engineered antibody Fc variants with enhanced effector function. *Proc Natl Acad Sci U S A* (2006) **103**:4005–10. doi:10.1073/pnas.0508123103
169. Yamane-Ohnuki N, Kinoshita S, Inoue-Urakubo M, Kusunoki M, Iida S, Nakano R, et al. Establishment of FUT8 knockout Chinese hamster ovary cells: an ideal host cell line for producing completely defucosylated antibodies with enhanced antibody-dependent cellular cytotoxicity. *Biotechnol Bioeng* (2004) **87**:614–22. doi:10.1002/bit.20151
170. Subedi GP, Barb AW. The Structural Role of Antibody N-Glycosylation in Receptor Interactions. *Structure* (2015) **23**:1573–83. doi:10.1016/j.str.2015.06.015
171. Almagro JC, Daniels-Wells TR, Perez-Tapia SM, Penichet ML. Progress and Challenges in the Design and Clinical Development of Antibodies for Cancer Therapy. *Front Immunol* (2017) **8**:1751. doi:10.3389/fimmu.2017.01751
172. Epp A, Sullivan KC, Herr AB, Strait RT. Immunoglobulin Glycosylation Effects in Allergy and Immunity. *Curr Allergy Asthma Rep* (2016) **16**:79. doi:10.1007/s11882-016-0658-x
173. Marcus R, Davies A, Ando K, Klapper W, Opat S, Owen C, et al. Obinutuzumab for the First-Line Treatment of Follicular Lymphoma. *N Engl J Med* (2017) **377**:1331–44. doi:10.1056/NEJMoa1614598
174. Wang X, Mathieu M, Brezski RJ. IgG Fc engineering to modulate antibody effector functions. *Protein Cell* (2018) **9**:63–73. doi:10.1007/s13238-017-0473-8
175. Xu D, Alegre ML, Varga SS, Rothermel AL, Collins AM, Pulito VL, et al. In vitro characterization of five humanized OKT3 effector function variant antibodies. *Cell Immunol* (2000) **200**:16–26. doi:10.1006/cimm.2000.1617
176. Schlothauer T, Herter S, Koller CF, Grau-Richards S, Steinhart V, Spick C, et al. Novel human IgG1 and IgG4 Fc-engineered antibodies with completely abolished immune effector functions. *Protein Eng Des Sel* (2016) **29**:457–66. doi:10.1093/protein/gzw040
177. Sazinsky SL, Ott RG, Silver NW, Tidor B, Ravetch JV, Wittrup KD. Aglycosylated immunoglobulin G1 variants productively engage activating Fc receptors. *Proc Natl Acad Sci U S A* (2008) **105**:20167–72. doi:10.1073/pnas.0809257105
178. Jo M, Kwon HS, Lee K-H, Lee JC, Jung ST. Engineered aglycosylated full-length IgG Fc variants exhibiting improved FcγRIIIa binding and tumor cell clearance. *MAbs* (2018) **10**:278–89. doi:10.1080/19420862.2017.1402995
179. Bolt S, Routledge E, Lloyd I, Chatenoud L, Pope H, Gorman SD, et al. The generation of a humanized, non-mitogenic CD3 monoclonal antibody which retains in vitro immunosuppressive properties. *Eur J Immunol* (1993) **23**:403–11. doi:10.1002/eji.1830230216
180. Igawa T, Tsunoda H, Kuramochi T, Sampei Z, Ishii S, Hattori K. Engineering the variable region of therapeutic IgG antibodies. *MAbs* (2011) **3**:243–52. doi:10.4161/mabs.3.3.15234.



- 
181. *Novel Approaches and Strategies for Biologics, Vaccines and Cancer Therapies*. Elsevier (2015).
  182. Persson H, Kirik U, Thörnqvist L, Greiff L, Levander F, Ohlin M. In Vitro Evolution of Antibodies Inspired by In Vivo Evolution. *Front Immunol* (2018) **9**:1391. doi:10.3389/fimmu.2018.01391
  183. Chan DT, Groves MA. Affinity maturation: highlights in the application of in vitro strategies for the directed evolution of antibodies. *Emerg Top Life Sci* (2021) **5**:601–8. doi:10.1042/ETLS20200331
  184. Lamdan H, Gavilondo JV, Muñoz Y, Pupo A, Huerta V, Musacchio A, et al. Affinity maturation and fine functional mapping of an antibody fragment against a novel neutralizing epitope on human vascular endothelial growth factor. *Mol Biosyst* (2013) **9**:2097–106. doi:10.1039/c3mb70136k
  185. Colley CS, Popovic B, Sridharan S, Debreczeni JE, Hargeaves D, Fung M, et al. Structure and characterization of a high affinity C5a monoclonal antibody that blocks binding to C5aR1 and C5aR2 receptors. *MAbs* (2018) **10**:104–17. doi:10.1080/19420862.2017.1384892
  186. Chowdhury PS, Pastan I. Improving antibody affinity by mimicking somatic hypermutation in vitro. *Nat Biotechnol* (1999) **17**:568–72. doi:10.1038/9872
  187. Rajpal A, Beyaz N, Haber L, Cappuccilli G, Yee H, Bhatt RR, et al. A general method for greatly improving the affinity of antibodies by using combinatorial libraries. *Proc Natl Acad Sci U S A* (2005) **102**:8466–71. doi:10.1073/pnas.0503543102
  188. Laffly E, Pelat T, Cédronne F, Blésa S, Bedouelle H, Thullier P. Improvement of an antibody neutralizing the anthrax toxin by simultaneous mutagenesis of its six hypervariable loops. *J Mol Biol* (2008) **378**:1094–103. doi:10.1016/j.jmb.2008.03.045
  189. Li B, Zhao L, Wang C, Guo H, Wu L, Zhang X, et al. The protein-protein interface evolution acts in a similar way to antibody affinity maturation. *J Biol Chem* (2010) **285**:3865–71. doi:10.1074/jbc.M109.076547
  190. Hameduh T, Haddad Y, Adam V, Heger Z. Homology modeling in the time of collective and artificial intelligence. *Comput Struct Biotechnol J* (2020) **18**:3494–506. doi:10.1016/j.csbj.2020.11.007
  191. Sun Y, Jiao Y, Shi C, Zhang Y. Deep learning-based molecular dynamics simulation for structure-based drug design against SARS-CoV-2. *Comput Struct Biotechnol J* (2022) **20**:5014–27. doi:10.1016/j.csbj.2022.09.002
  192. Guest JD, Vreven T, Zhou J, Moal I, Jeliazkov J, Gray JJ, et al. An Expanded Benchmark for Antibody-Antigen Docking and Affinity Prediction Reveals Insights into Antibody Recognition Determinants. *SSRN Journal* (2020). doi:10.2139/ssrn.3564997
  193. He T, Nie Y, Yan T, Zhu J, He X, Li Y, et al. Enhancing the detection sensitivity of nanobody against aflatoxin B1 through structure-guided modification. *Int J Biol Macromol* (2022) **194**:188–97. doi:10.1016/j.ijbiomac.2021.11.182
  194. Yoshida K, Kuroda D, Kiyoshi M, Nakakido M, Nagatoishi S, Soga S, et al. Exploring designability of electrostatic complementarity at an antigen-antibody interface directed by mutagenesis, biophysical analysis, and molecular dynamics simulations. *Sci Rep* (2019) **9**:4482. doi:10.1038/s41598-019-40461-5
  195. Li J, Kang G, Wang J, Yuan H, Wu Y, Meng S, et al. Affinity maturation of antibody fragments: A review encompassing the development from random approaches to computational rational optimization. *Int J Biol Macromol* (2023) **247**:125733. doi:10.1016/j.ijbiomac.2023.125733
  196. Clark LA, Boriack-Sjodin PA, Eldredge J, Fitch C, Friedman B, Hanf KJ, et al. Affinity enhancement of an in vivo matured therapeutic antibody using structure-based computational design. *Protein Sci* (2006) **15**:949–60. doi:10.1110/ps.052030506

197. Labrijn AF, Janmaat ML, Reichert JM, Parren PW. Bispecific antibodies: a mechanistic review of the pipeline. *Nat Rev Drug Discov* (2019) **18**:585–608. doi:10.1038/s41573-019-0028-1
198. Dahlén E, Veitonmäki N, Norlén P. Bispecific antibodies in cancer immunotherapy. *Ther Adv Vaccines Immunother* (2018) **6**:3–17. doi:10.1177/2515135518763280
199. Zhao Q. Bispecific Antibodies for Autoimmune and Inflammatory Diseases: Clinical Progress to Date. *BioDrugs* (2020) **34**:111–9. doi:10.1007/s40259-019-00400-2
200. Segaliny AI, Jayaraman J, Chen X, Chong J, Luxon R, Fung A, et al. A high throughput bispecific antibody discovery pipeline. *Commun Biol* (2023) **6**:380. doi:10.1038/s42003-023-04746-w
201. Kontermann RE, Brinkmann U. Bispecific antibodies. *Drug Discov Today* (2015) **20**:838–47. doi:10.1016/j.drudis.2015.02.008
202. Wang S, Chen K, Lei Q, Ma P, Yuan AQ, Zhao Y, et al. The state of the art of bispecific antibodies for treating human malignancies. *EMBO Mol Med* (2021) **13**:e14291. doi:10.15252/emmm.202114291
203. NISONOFF A, WISSELER FC, LIPMAN LN. Properties of the major component of a peptic digest of rabbit antibody. *Science* (1960) **132**:1770–1. doi:10.1126/science.132.3441.1770
204. NISONOFF A, RIVERS MM. Recombination of a mixture of univalent antibody fragments of different specificity. *Arch Biochem Biophys* (1961) **93**:460–2. doi:10.1016/0003-9861(61)90296-x
205. Milstein C, Cuello AC. Hybrid hybridomas and their use in immunohistochemistry. *Nature* (1983) **305**:537–40. doi:10.1038/305537a0
206. Klein C, Brinkmann U, Reichert JM, Kontermann RE. The present and future of bispecific antibodies for cancer therapy. *Nat Rev Drug Discov* (2024). doi:10.1038/s41573-024-00896-6
207. Sun Y, Yu X, Wang X, Yuan K, Wang G, Hu L, et al. Bispecific antibodies in cancer therapy: Target selection and regulatory requirements. *Acta Pharm Sin B* (2023) **13**:3583–97. doi:10.1016/j.apsb.2023.05.023
208. Surowka M, Klein C. A pivotal decade for bispecific antibodies? *MAbs* (2024) **16**:2321635. doi:10.1080/19420862.2024.2321635
209. Wang Q, Chen Y, Park J, Liu X, Hu Y, Wang T, et al. Design and Production of Bispecific Antibodies. *Antibodies (Basel)* (2019) **8**. doi:10.3390/antib8030043
210. Krah S, Kolmar H, Becker S, Zielonka S. Engineering IgG-Like Bispecific Antibodies-An Overview. *Antibodies (Basel)* (2018) **7**. doi:10.3390/antib7030028
211. Ridgway JB, Presta LG, Carter P. 'Knobs-into-holes' engineering of antibody CH3 domains for heavy chain heterodimerization. *Protein Eng* (1996) **9**:617–21. doi:10.1093/protein/9.7.617
212. Ma J, Mo Y, Tang M, Shen J, Qi Y, Zhao W, et al. Bispecific Antibodies: From Research to Clinical Application. *Front Immunol* (2021) **12**:626616. doi:10.3389/fimmu.2021.626616
213. Atwell S, Ridgway JB, Wells JA, Carter P. Stable heterodimers from remodeling the domain interface of a homodimer using a phage display library. *J Mol Biol* (1997) **270**:26–35. doi:10.1006/jmbi.1997.1116
214. Liu H, Saxena A, Sidhu SS, Wu D. Fc Engineering for Developing Therapeutic Bispecific Antibodies and Novel Scaffolds. *Front Immunol* (2017) **8**:38. doi:10.3389/fimmu.2017.00038
215. Gunasekaran K, Pentony M, Shen M, Garrett L, Forte C, Woodward A, et al. Enhancing antibody Fc heterodimer formation through electrostatic steering effects: applications to bispecific molecules and monovalent IgG. *J Biol Chem* (2010) **285**:19637–46. doi:10.1074/jbc.M110.117382
216. Brinkmann U, Kontermann RE. The making of bispecific antibodies. *MAbs* (2017) **9**:182–212. doi:10.1080/19420862.2016.1268307

- 
217. Nardis C de, Hendriks LJ, Poirier E, Arvinte T, Gros P, Bakker AB, et al. A new approach for generating bispecific antibodies based on a common light chain format and the stable architecture of human immunoglobulin G1. *J Biol Chem* (2017) **292**:14706–17. doi:10.1074/jbc.M117.793497
218. Davis JH, Aperlo C, Li Y, Kurosawa E, Lan Y, Lo K-M, et al. SEEDbodies: fusion proteins based on strand-exchange engineered domain (SEED) CH3 heterodimers in an Fc analogue platform for asymmetric binders or immunofusions and bispecific antibodies. *Protein Eng Des Sel* (2010) **23**:195–202. doi:10.1093/protein/gzp094
219. Merchant AM, Zhu Z, Yuan JQ, Goddard A, Adams CW, Presta LG, et al. An efficient route to human bispecific IgG. *Nat Biotechnol* (1998) **16**:677–81. doi:10.1038/nbt0798-677
220. Xu JL, Davis MM. Diversity in the CDR3 region of V(H) is sufficient for most antibody specificities. *Immunity* (2000) **13**:37–45. doi:10.1016/s1074-7613(00)00006-6
221. Schaefer W, Regula JT, Böhner M, Schanzer J, Croasdale R, Dürr H, et al. Immunoglobulin domain crossover as a generic approach for the production of bispecific IgG antibodies. *Proc Natl Acad Sci U S A* (2011) **108**:11187–92. doi:10.1073/pnas.1019002108
222. Lewis SM, Wu X, Pustilnik A, Sereno A, Huang F, Rick HL, et al. Generation of bispecific IgG antibodies by structure-based design of an orthogonal Fab interface. *Nat Biotechnol* (2014) **32**:191–8. doi:10.1038/nbt.2797
223. Eigenbrot C, Fuh G. Two-in-One antibodies with dual action Fabs. *Curr Opin Chem Biol* (2013) **17**:400–5. doi:10.1016/j.cbpa.2013.04.015
224. Bostrom J, Yu S-F, Kan D, Appleton BA, Lee CV, Billeci K, et al. Variants of the antibody herceptin that interact with HER2 and VEGF at the antigen binding site. *Science* (2009) **323**:1610–4. doi:10.1126/science.1165480
225. Bostrom J, Haber L, Koenig P, Kelley RF, Fuh G. High affinity antigen recognition of the dual specific variants of herceptin is entropy-driven in spite of structural plasticity. *PLoS One* (2011) **6**:e17887. doi:10.1371/journal.pone.0017887
226. Kelley RF, O'Connell MP. Thermodynamic analysis of an antibody functional epitope. *Biochemistry* (1993) **32**:6828–35. doi:10.1021/bi00078a005
227. Schaefer G, Haber L, Crocker LM, Shia S, Shao L, Dowbenko D, et al. A two-in-one antibody against HER3 and EGFR has superior inhibitory activity compared with monospecific antibodies. *Cancer Cell* (2011) **20**:472–86. doi:10.1016/j.ccr.2011.09.003
228. Huang S, Li C, Armstrong EA, Peet CR, Saker J, Amler LC, et al. Dual targeting of EGFR and HER3 with MEHD7945A overcomes acquired resistance to EGFR inhibitors and radiation. *Cancer Res* (2013) **73**:824–33. doi:10.1158/0008-5472.CAN-12-1611
229. Hill AG, Findlay MP, Burge ME, Jackson C, Alfonso PG, Samuel L, et al. Phase II Study of the Dual EGFR/HER3 Inhibitor Duligotuzumab (MEHD7945A) versus Cetuximab in Combination with FOLFIRI in Second-Line RAS Wild-Type Metastatic Colorectal Cancer. *Clin Cancer Res* (2018) **24**:2276–84. doi:10.1158/1078-0432.CCR-17-0646
230. Beckmann R, Jensen K, Fenn S, Speck J, Krause K, Meier A, et al. DutaFabs are engineered therapeutic Fab fragments that can bind two targets simultaneously. *Nat Commun* (2021) **12**:708. doi:10.1038/s41467-021-20949-3
231. Huang S, van Duijnhoven SM, Sijts AJ, van Elsas A. Bispecific antibodies targeting dual tumor-associated antigens in cancer therapy. *J Cancer Res Clin Oncol* (2020) **146**:3111–22. doi:10.1007/s00432-020-03404-6
232. Schubert I, Stein C, Fey GH. Dual-Targeting for the Elimination of Cancer Cells with Increased Selectivity. *Antibodies* (2012) **1**:2–18. doi:10.3390/antib1010002

- 
233. Buatois V, Johnson Z, Salgado-Pires S, Papaioannou A, Hatterer E, Chauchet X, et al. Preclinical Development of a Bispecific Antibody that Safely and Effectively Targets CD19 and CD47 for the Treatment of B-Cell Lymphoma and Leukemia. *Mol Cancer Ther* (2018) **17**:1739–51. doi:10.1158/1535-7163.MCT-17-1095
234. Mazor Y, Sachsenmeier KF, Yang C, Hansen A, Filderman J, Mulgrew K, et al. Enhanced tumor-targeting selectivity by modulating bispecific antibody binding affinity and format valence. *Sci Rep* (2017) **7**:40098. doi:10.1038/srep40098
235. Moores SL, Chiu ML, Bushey BS, Chevalier K, Luistro L, Dorn K, et al. A Novel Bispecific Antibody Targeting EGFR and cMet Is Effective against EGFR Inhibitor-Resistant Lung Tumors. *Cancer Res* (2016) **76**:3942–53. doi:10.1158/0008-5472.CAN-15-2833
236. Syed YY. Amivantamab: First Approval. *Drugs* (2021) **81**:1349–53. doi:10.1007/s40265-021-01561-7
237. Koopmans I, Hendriks D, Samplonius DF, van Ginkel RJ, Heskamp S, Wierstra PJ, et al. A novel bispecific antibody for EGFR-directed blockade of the PD-1/PD-L1 immune checkpoint. *Oncoimmunology* (2018) **7**:e1466016. doi:10.1080/2162402X.2018.1466016
238. Rubio-Pérez L, Lázaro-Gorines R, Harwood SL, Compte M, Navarro R, Tapia-Galisteo A, et al. A PD-L1/EGFR bispecific antibody combines immune checkpoint blockade and direct anti-cancer action for an enhanced anti-tumor response. *Oncoimmunology* (2023) **12**:2205336. doi:10.1080/2162402X.2023.2205336
239. Grakoui A, Bromley SK, Sumen C, Davis MM, Shaw AS, Allen PM, et al. The immunological synapse: a molecular machine controlling T cell activation. *Science* (1999) **285**:221–7. doi:10.1126/science.285.5425.221
240. Shin HG, Yang HR, Yoon A, Lee S. Bispecific Antibody-Based Immune-Cell Engagers and Their Emerging Therapeutic Targets in Cancer Immunotherapy. *Int J Mol Sci* (2022) **23**. doi:10.3390/ijms23105686
241. Offner S, Hofmeister R, Romaniuk A, Kufer P, Baeuerle PA. Induction of regular cytolytic T cell synapses by bispecific single-chain antibody constructs on MHC class I-negative tumor cells. *Molecular Immunology* (2006) **43**:763–71. doi:10.1016/j.molimm.2005.03.007
242. Fucà G, Spagnoletti A, Ambrosini M, Braud F de, Di Nicola M. Immune cell engagers in solid tumors: promises and challenges of the next generation immunotherapy. *ESMO Open* (2021) **6**:100046. doi:10.1016/j.esmoop.2020.100046
243. Abbs IC, Clark M, Waldmann H, Chatenoud L, Koffman CG, Sacks SH. Sparing of first dose effect of monovalent anti-CD3 antibody used in allograft rejection is associated with diminished release of pro-inflammatory cytokines. *Ther Immunol* (1994) **1**:325–31.
244. Tapia-Galisteo A, Álvarez-Vallina L, Sanz L. Bi- and trispecific immune cell engagers for immunotherapy of hematological malignancies. *J Hematol Oncol* (2023) **16**:83. doi:10.1186/s13045-023-01482-w
245. Goulet DR, Atkins WM. Considerations for the Design of Antibody-Based Therapeutics. *J Pharm Sci* (2020) **109**:74–103. doi:10.1016/j.xphs.2019.05.031
246. Renz M, Dorigo O. “Immunotherapy in gynecologic malignancies,”. In: *DiSaia and Creasman Clinical Gynecologic Oncology*. Elsevier (2023). 506-520.e7.
247. Linke R, Klein A, Seimetz D. Catumaxomab: clinical development and future directions. *MAbs* (2010) **2**:129–36. doi:10.4161/mabs.2.2.11221
248. Newman MJ, Benani DJ. A review of blinatumomab, a novel immunotherapy. *J Oncol Pharm Pract* (2016) **22**:639–45. doi:10.1177/1078155215618770

- 
249. Kang J, Sun T, Zhang Y. Immunotherapeutic progress and application of bispecific antibody in cancer. *Front Immunol* (2022) **13**:1020003. doi:10.3389/fimmu.2022.1020003
250. Middleton MR, McAlpine C, Woodcock VK, Corrie P, Infante JR, Steven NM, et al. Tebentafusp, A TCR/Anti-CD3 Bispecific Fusion Protein Targeting gp100, Potently Activated Antitumor Immune Responses in Patients with Metastatic Melanoma. *Clin Cancer Res* (2020) **26**:5869–78. doi:10.1158/1078-0432.CCR-20-1247
251. Dhillon S. Tebentafusp: First Approval. *Drugs* (2022) **82**:703–10. doi:10.1007/s40265-022-01704-4
252. Guo Y, Quijano Cardé NA, Kang L, Verona R, Banerjee A, Kobos R, et al. Teclistamab: Mechanism of action, clinical, and translational science. *Clin Transl Sci* (2024) **17**:e13717. doi:10.1111/cts.13717
253. Pillarisetti K, Powers G, Luistro L, Babich A, Baldwin E, Li Y, et al. Teclistamab is an active T cell-redirecting bispecific antibody against B-cell maturation antigen for multiple myeloma. *Blood Adv* (2020) **4**:4538–49. doi:10.1182/bloodadvances.2020002393
254. Kang C. Mosunetuzumab: First Approval. *Drugs* (2022) **82**:1229–34. doi:10.1007/s40265-022-01749-5
255. Engelberts PJ, Hiemstra IH, Jong B de, Schuurhuis DH, Meesters J, Beltran Hernandez I, et al. DuoBody-CD3xCD20 induces potent T-cell-mediated killing of malignant B cells in preclinical models and provides opportunities for subcutaneous dosing. *EBioMedicine* (2020) **52**:102625. doi:10.1016/j.ebiom.2019.102625
256. Frampton JE. Epcoritamab: First Approval. *Drugs* (2023) **83**:1331–40. doi:10.1007/s40265-023-01930-4
257. Hutchings M, Morschhauser F, Iacoboni G, Carlo-Stella C, Offner FC, Sureda A, et al. Glofitamab, a Novel, Bivalent CD20-Targeting T-Cell-Engaging Bispecific Antibody, Induces Durable Complete Remissions in Relapsed or Refractory B-Cell Lymphoma: A Phase I Trial. *J Clin Oncol* (2021) **39**:1959–70. doi:10.1200/JCO.20.03175
258. Shirley M. Glofitamab: First Approval. *Drugs* (2023) **83**:935–41. doi:10.1007/s40265-023-01894-5
259. Dhillon S. Elranatamab: First Approval. *Drugs* (2023) **83**:1621–7. doi:10.1007/s40265-023-01954-w
260. Chari A, Minnema MC, Berdeja JG, Oriol A, van de Donk NW, Rodríguez-Otero P, et al. Talquetamab, a T-Cell-Redirecting GPRC5D Bispecific Antibody for Multiple Myeloma. *N Engl J Med* (2022) **387**:2232–44. doi:10.1056/NEJMoa2204591
261. Shanshal M, Caimi PF, Adjei AA, Ma WW. T-Cell Engagers in Solid Cancers-Current Landscape and Future Directions. *Cancers (Basel)* (2023) **15**. doi:10.3390/cancers15102824
262. Sheridan C. Industry appetite for natural killer cells intensifies. *Nat Biotechnol* (2023) **41**:159–61. doi:10.1038/s41587-023-01671-5
263. Pinto S, Pahl J, Schottelius A, Carter PJ, Koch J. Reimagining antibody-dependent cellular cytotoxicity in cancer: the potential of natural killer cell engagers. *Trends Immunol* (2022) **43**:932–46. doi:10.1016/j.it.2022.09.007
264. Whalen KA, Rakhra K, Mehta NK, Steinle A, Michaelson JS, Baeuerle PA. Engaging natural killer cells for cancer therapy via NKG2D, CD16A and other receptors. *MAbs* (2023) **15**:2208697. doi:10.1080/19420862.2023.2208697
265. Ellwanger K, Reusch U, Fucek I, Wingert S, Ross T, Müller T, et al. Redirected optimized cell killing (ROCK®): A highly versatile multispecific fit-for-purpose antibody platform for engaging innate immunity. *MAbs* (2019) **11**:899–918. doi:10.1080/19420862.2019.1616506

266. Reusch U, Burkhardt C, Fucek I, Le Gall F, Le Gall M, Hoffmann K, et al. A novel tetravalent bispecific TandAb (CD30/CD16A) efficiently recruits NK cells for the lysis of CD30+ tumor cells. *MAbs* (2014) **6**:728–39. doi:10.4161/mabs.28591
267. Kerbauy LN, Marin ND, Kaplan M, Banerjee PP, Berrien-Elliott MM, Becker-Hapak M, et al. Combining AFM13, a Bispecific CD30/CD16 Antibody, with Cytokine-Activated Blood and Cord Blood-Derived NK Cells Facilitates CAR-like Responses Against CD30+ Malignancies. *Clin Cancer Res* (2021) **27**:3744–56. doi:10.1158/1078-0432.CCR-21-0164
268. Jung G, Freimann U, Marschall Z von, Reisfeld RA, Wilmanns W. Target cell-induced T cell activation with bi- and trispecific antibody fragments. *Eur J Immunol* (1991) **21**:2431–5. doi:10.1002/eji.1830211020
269. Hudson PJ, Kortt AA. High avidity scFv multimers; diabodies and triabodies. *J Immunol Methods* (1999) **231**:177–89. doi:10.1016/s0022-1759(99)00157-x
270. Somasundaram C, Sundarapandiyam K, Keler T, Deo YM, Graziano RF. Development of a trispecific antibody conjugate that directs two distinct tumor-associated antigens to CD64 on myeloid effector cells. *Hum Antibodies* (1999) **9**:47–54.
271. Yao Y, Hu Y, Wang F. Trispecific antibodies for cancer immunotherapy. *Immunology* (2023) **169**:389–99. doi:10.1111/imm.13636
272. Tapia-Galisteo A, Sánchez Rodríguez Í, Aguilar-Sopeña O, Harwood SL, Narbona J, Ferreras Gutierrez M, et al. Trispecific T-cell engagers for dual tumor-targeting of colorectal cancer. *Oncoimmunology* (2022) **11**:2034355. doi:10.1080/2162402X.2022.2034355
273. Chen L, Qian W, Pan F, Li D, Yu W, Tong L, et al. A trispecific antibody induces potent tumor-directed T-cell activation and antitumor activity by CD3/CD28 co-engagement. *Immunotherapy* (2024) **16**:143–59. doi:10.2217/imt-2023-0256
274. Steinmetz A, Vallée F, Beil C, Lange C, Baurin N, Beninga J, et al. CODV-Ig, a universal bispecific tetravalent and multifunctional immunoglobulin format for medical applications. *MAbs* (2016) **8**:867–78. doi:10.1080/19420862.2016.1162932
275. Wu L, Seung E, Xu L, Rao E, Lord DM, Wei RR, et al. Trispecific antibodies enhance the therapeutic efficacy of tumor-directed T cells through T cell receptor co-stimulation. *Nat Cancer* (2020) **1**:86–98. doi:10.1038/s43018-019-0004-z
276. Seung E, Xing Z, Wu L, Rao E, Cortez-Retamozo V, Ospina B, et al. A trispecific antibody targeting HER2 and T cells inhibits breast cancer growth via CD4 cells. *Nature* (2022) **603**:328–34. doi:10.1038/s41586-022-04439-0
277. Tapia-Galisteo A, Compte M, Álvarez-Vallina L, Sanz L. When three is not a crowd: trispecific antibodies for enhanced cancer immunotherapy. *Theranostics* (2023) **13**:1028–41. doi:10.7150/thno.81494
278. Dicara DM, Bhakta S, Go MA, Ziai J, Firestein R, Forrest B, et al. Development of T-cell engagers selective for cells co-expressing two antigens. *MAbs* (2022) **14**:2115213. doi:10.1080/19420862.2022.2115213
279. Kuchnio A, Yang D, Vloemans N, Lowenstein C, Cornelissen I, Amorim R, et al. Characterization of JNJ-80948543, a Novel CD79bxCD20xCD3 Trispecific T-Cell Redirecting Antibody for the Treatment of B-Cell Non-Hodgkin Lymphoma. *Blood* (2022) **140**:3105–6. doi:10.1182/blood-2022-168739
280. Pihlgren M, Hall O, Carretero L, Estoppey C, Drake A, Pais D, et al. ISB 2001, a First-in-Class Trispecific BCMA and CD38 T Cell Engager Designed to Overcome Mechanisms of Escape from Treatments for Multiple Myeloma By Targeting Two Antigens. *Blood* (2022) **140**:858–9. doi:10.1182/blood-2022-159353

- 
281. Kügler M, Stein C, Kellner C, Mentz K, Saul D, Schwenkert M, et al. A recombinant trispecific single-chain Fv derivative directed against CD123 and CD33 mediates effective elimination of acute myeloid leukaemia cells by dual targeting. *Br J Haematol* (2010) **150**:574–86. doi:10.1111/j.1365-2141.2010.08300.x
282. Braciak TA, Roskopf CC, Wildenhain S, Fenn NC, Schiller CB, Schubert IA, et al. Dual-targeting triplebody 33-16-123 (SPM-2) mediates effective redirected lysis of primary blasts from patients with a broad range of AML subtypes in combination with natural killer cells. *Oncoimmunology* (2018) **7**:e1472195. doi:10.1080/2162402X.2018.1472195
283. Gantke T, Weichel M, Herbrecht C, Reusch U, Ellwanger K, Fucek I, et al. Trispecific antibodies for CD16A-directed NK cell engagement and dual-targeting of tumor cells. *Protein Eng Des Sel* (2017) **30**:673–84. doi:10.1093/protein/gzx043
284. Bogen JP, Carrara SC, Fiebig D, Grzeschik J, Hock B, Kolmar H. Design of a Trispecific Checkpoint Inhibitor and Natural Killer Cell Engager Based on a 2 + 1 Common Light Chain Antibody Architecture. *Front Immunol* (2021) **12**:669496. doi:10.3389/fimmu.2021.669496
285. Gauthier L, Morel A, Anceriz N, Rossi B, Blanchard-Alvarez A, Grondin G, et al. Multifunctional Natural Killer Cell Engagers Targeting Nkp46 Trigger Protective Tumor Immunity. *Cell* (2019) **177**:1701-1713.e16. doi:10.1016/j.cell.2019.04.041
286. Tang A, Gauthier L, Beninga J, Rossi B, Gourdin N, Blanchard-Alvarez A, et al. The Novel Trifunctional Anti-BCMA NK Cell Engager SAR'514 Has Potent in-Vitro and in-Vivo Anti-Myeloma Effect through Dual NK Cell Engagement. *Blood* (2022) **140**:9985–6. doi:10.1182/blood-2022-166187
287. Safran H, Cassier PA, Vicier C, Forget F, Gomez-Roca CA, Penel N, et al. Phase 1/2 Study of DF1001, a novel tri-specific, NK cell engager therapy targeting HER2, in patients with advanced solid tumors: Phase 1 DF1001 monotherapy dose-escalation results. *J Clin Oncol* (2023) **41**:2508. doi:10.1200/JCO.2023.41.16\_suppl.2508

---

## 4. Cumulative Section

---

### 4.1. A Generic Strategy to Generate Bifunctional Two-in-One Antibodies by Chicken Immunization

Titel:

A Generic Strategy to Generate Bifunctional Two-in-One Antibodies by Chicken Immunization

Authors:

Julia Harwardt\*, Jan Patrick Bogen\*, Stefania Candela Carrara, Michael Ullitzka, Julius Grzeschik, Björn Hock and Harald Kolmar

(\*shared first authorship)

Bibliographic data:

Journal – Frontiers in Immunology

Volume 13 – 2022

Article published online: 11 April 2022

DOI: 10.3389/fimmu.2022.888838

Copyright © 2022 Harwardt, Bogen, Carrara, Ullitzka, Grzeschik, Hock and Kolmar. This is an open-access article distributed under the terms of the Creative Commons Attribution License (CC BY).

Contributions by J. Harwardt:

- Design and planning of experiments with J.P. Bogen
- Generation and screening of the library
- Reformatting and characterization of isolated antibodies
- Design and generation of all figures
- Writing of manuscript together with J.P. Bogen and H. Kolmar





# A Generic Strategy to Generate Bifunctional Two-in-One Antibodies by Chicken Immunization

Julia Harwardt<sup>1†</sup>, Jan P. Bogen<sup>1,2†</sup>, Stefania C. Carrara<sup>1,2</sup>, Michael Ulitzka<sup>1,2</sup>, Julius Grzeschik<sup>3</sup>, Björn Hock<sup>3</sup> and Harald Kolmar<sup>1,4\*</sup>

<sup>1</sup>Institute for Organic Chemistry and Biochemistry, Technical University of Darmstadt, Darmstadt, Germany, <sup>2</sup>Ferring Darmstadt Laboratory, Biologics Technology and Development, Darmstadt, Germany, <sup>3</sup>Ferring Biologics Innovation Centre, Biologics Technology and Development, Epalinges, Switzerland, <sup>4</sup>Centre for Synthetic Biology, Technical University of Darmstadt, Darmstadt, Germany

## OPEN ACCESS

### Edited by:

Christian Klein,  
Roche Innovation Center Zurich,  
Switzerland

### Reviewed by:

Ulrich Brinkmann,  
Roche, United Kingdom  
Chang-Han Lee,  
Seoul National University, South Korea

### \*Correspondence:

Harald Kolmar  
Harald.Kolmar@TU-Darmstadt.de

<sup>†</sup>These authors contributed  
equally to this work

### Specialty section:

This article was submitted to  
Cancer Immunity  
and Immunotherapy,  
a section of the journal  
Frontiers in Immunology

Received: 03 March 2022

Accepted: 18 March 2022

Published: 11 April 2022

### Citation:

Harwardt J, Bogen JP, Carrara SC,  
Ulitzka M, Grzeschik J, Hock B and  
Kolmar H (2022) A Generic Strategy to  
Generate Bifunctional Two-in-One  
Antibodies by Chicken Immunization.  
*Front. Immunol.* 13:888838.  
doi: 10.3389/fimmu.2022.888838

Various formats of bispecific antibodies exist, among them Two-in-One antibodies in which each Fab arm can bind to two different antigens. Their IgG-like architecture accounts for low immunogenicity and also circumvents laborious engineering and purification steps to facilitate correct chain pairing. Here we report for the first time the identification of a Two-in-One antibody by yeast surface display (YSD) screening of chicken-derived immune libraries. The resulting antibody simultaneously targets the epidermal growth factor receptor (EGFR) and programmed death-ligand 1 (PD-L1) at the same Fv fragment with two non-overlapping paratopes. The dual action Fab is capable of inhibiting EGFR signaling by binding to dimerization domain II as well as blocking the PD-1/PD-L1 interaction. Furthermore, the Two-in-One antibody demonstrates specific cellular binding properties on EGFR/PD-L1 double positive tumor cells. The presented strategy relies solely on screening of combinational immune-libraries and obviates the need for any additional CDR engineering as described in previous reports. Therefore, this study paves the way for further development of therapeutic antibodies derived from avian immunization with novel and tailor-made binding properties.

**Keywords:** bispecific antibody, two-in-one antibody, dual action fab, yeast display, chicken-derived

## INTRODUCTION

In recent years, an increasing number of bispecific antibody (bsAb) approaches have been developed (1, 2). BsAbs, which can simultaneously target two distinct antigens, enabled new therapeutic mechanisms of action that can neither be addressed by conventional monoclonal antibodies (mAbs) nor by their combination (3–5). A subclass of bsAbs are Two-in-One antibodies with dual action Fabs (DAFs), in which each Fab arm addresses two distinct antigens, resulting in a bispecific, tetravalent IgG-like molecule (6, 7). The classical IgG like bispecific antibody setting requires correct heavy chain heterodimerization as well as correct light chain pairing, which statistically results in only 12.5% of correctly assembled molecules (**Supplementary Figure 1**) (8). Two-in-One antibodies, in contrast, consist of two identical heavy and light chains and can be produced

without additional engineering of constant chains (9). Therefore, the need to include unnaturally occurring amino acid sequences as found in knob-into-hole antibodies (10) or orthogonal Fab interfaces (11) is circumvented.

The first Two-in-One antibody was generated by Bostrom et al. based on mutagenesis of the light chain complementarity-determining regions (CDRs) of the HER2 specific antibody trastuzumab resulting in HER2 and VEGF binding (12). Subsequently, mutagenesis approaches were used towards the generation of Two-in-One antibodies targeting HER3 and EGFR (13), IL-4 and IL-5 (14), or VEGF and angiopoietin 2 (15). The Two-in-One antibody duligotuzumab, which targets HER3 and EGFR (13), has been tested in clinical trials for treating epithelial-derived cancer (16, 17), highlighting the importance of this class of therapeutics. However, these antibodies all exhibit partially overlapping CDR residues leading to antigen 1 blocking the binding of antigen 2, consequently allowing binding of only one antigen at the same time.

DutaFabs, in contrast, comprise two independent binding sites within the CDR loops. The H-side paratope consists of CDR H1, H3 and L2, while the L-side paratope comprises CDR L1, L3 and H2. Therefore, these Fabs are able to target two antigens simultaneously with the same Fv region, however the design of DutaFabs is comparatively complex (18). Furthermore, tetravalent IgG-like bispecific constructs were described that do not consist of regular Fab arms but rather of engineered arms in which one VH domain is attached to each of the constant CH<sub>1</sub> and CL domains (19). Here, one VH is placed at its usual position and the second VH replaces the VL domain in a conventional IgG. It was found that the tetra-VH IgGs can simultaneously bind two antigens on each arm of the IgG molecule (19).

Due to their ability to cross-link receptors, mediate proximity between immune effector cells and tumor cells, or block two disease-related signaling pathways, bsAbs are exceptional therapeutic entities for cancer treatment (20–22). Tumor-specificity of bsAbs can be elevated by simultaneous targeting of two cancer-specific antigens on the same malignant cell (23). Two therapeutic targets being upregulated in many solid tumors are the programmed death ligand 1 (PD-L1) and human epidermal growth factor receptor (EGFR) (24, 25). Overexpression of PD-L1 is observed in a variety of malignancies and represents a mechanism by which cancer evades immune surveillance (24, 26). EGFR, which is natively expressed on epithelial cells in the skin and lung, is overexpressed in a wide range of cancers including bladder cancer, lung cancer, colorectal cancer, and breast cancer, where it is involved in tumor progression and metastasis (25, 27–29). Koopmans and coworkers demonstrated that tumor-specificity can be increased by EGFR directed PD-L1 blockade, resulting in a potentially favorable safety profile of the described bsAb (30).

Most approved therapeutic mAbs were generated by immunization of rodents, including mice, rabbits, or other mammalian species (31). However, due to their close phylogenetic relationship to humans, targeting epitopes which are broadly conserved in mammalian species is challenging.

Chicken immunization, in contrast, may result in antibodies targeting epitopes that are not accessible by immunization of mammals (32, 33). Additionally, library generation can be done with a single set of primers because of the gene diversification in birds, significantly reducing the hands-on time and costs compared to rodents (34). Recently, our group described the isolation of highly affine chicken-derived antibodies using yeast surface display (YSD) in combination with fluorescence-activated cell sorting (FACS) (34–36).

In this study, we describe the isolation and characterization of the first Two-in-One antibody that simultaneously targets PD-L1 and EGFR with two independent paratopes on a single Fab. It is derived from immunized chickens by combining the heavy chain of a common light chain antibody with an immune light chain library without engineering the antibodies' CDR regions (**Figure 1**). The Two-in-One antibody demonstrated specific cellular binding properties on EGFR- and PD-L1-expressing tumor cells, as well as inhibition of EGFR-dependent signal transduction and blockage of the PD-1/PD-L1 interaction.

## RESULTS

### Two-in-One Library Generation and Screening

In order to generate a Two-in-One antibody, we sought to combine the heavy chain of a chicken-derived antibody with a chicken-derived immune YSD light chain library followed by subsequent screening for binding properties towards two antigens. As model targets, the extracellular domains of PD-L1 (PD-L1-ECD) and EGFR (EGFR-ECD) were chosen. Currently, various monoclonal antibodies targeting either EGFR, including the therapeutic antibodies panitumumab (37), necitumumab (38), nimotuzumab (39) and cetuximab (40), or PD-L1, among them durvalumab (41), avelumab (42) and atezolizumab (43) are approved for tumor treatment in multiple countries. Recently, our group isolated a chicken-derived anti-PD-L1 antibody called ICI2 (44). Since ICI2 exhibited a common light chain as it was utilized in a multispecific setup, we assumed that the heavy chain CDRs were mainly responsible for antigen recognition and could tolerate various light chains, as reported for other antibodies (45, 46). In order to isolate a Two-in-One antibody targeting both PD-L1 and EGFR, the ICI2 heavy chain was paired with a diversity of anti-EGFR light chains (**Figure 1**). The light chain library was generated by amplification of VL genes from cDNA derived from a chicken immunized with EGFR-ECD and subsequent insertion into a pYD<sub>1</sub>-derived vector encoding a human lambda CL by homologous recombination in BJ5464 yeast as previously described (44). The light chain diversity of  $2.9 \times 10^8$  transformants was combined with EBY100 yeast cells encoding the ICI2 VH-CH<sub>1</sub> fragment by yeast mating (**Figure 1**), resulting in adequate oversampling of the estimated light chain diversity, which was estimated to be about  $5 \times 10^8$  unique variants.

This diploid common heavy chain yeast library was screened by FACS over three consecutive sorting rounds with 250 nM EGFR-Fc (**Supplementary Figure 2A**). This resulted in the

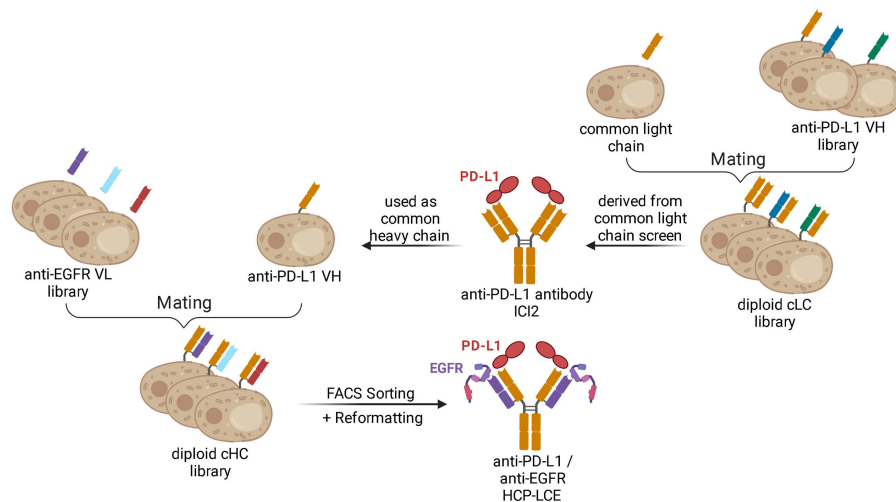


**FIGURE 1** | Schematic representation demonstrating the generation of the Two-in-One antibody HCP-LCE. The anti-PD-L1 antibody ICI2 is derived from a common light chain YSD library. The VH fragment of the anti-PD-L1 antibody ICI2 was paired with an anti-EGFR VL library by yeast mating. FACS screening and subsequent reformatting into the full-length antibody format enabled the isolation and production of a Two-in-One antibody targeting PD-L1 and EGFR. Created with BioRender.com.

enrichment of a yeast population carrying the genes for Fab fragments recognizing both EGFR-Fc and PD-L1-Fc with 250 nM of the respective antigen. Fc binding could be excluded based on binding analysis to an unrelated Fc fusion protein (**Supplementary Figure 2B**). Sequence analysis of ten randomly chosen clones revealed one distinct VL sequence, which was enriched in the sorting process.

## EGFR Epitope Mapping on the Subdomain Level

Expi293F cells were co-transfected using the isolated VL sequence reformatted into a pTT5-derived vector encoding a lambda CL sequence and a pTT5 vector encoding the ICI2 heavy chain as described before (44, 47). Purification of the Two-in-One antibody, hereafter referred to as HCP-LCE (heavy chain PD-L1 – light chain EGFR), was performed using Protein A affinity chromatography.

The extracellular region of EGFR consists of two homologous ligand-binding domains (domains I and III) and two cysteine-rich domains (domains II and IV) (48). The binding of EGF to the EGFR monomers at domains I and III promotes domain rearrangement to expose the dimerization arm in domain II finally resulting in the generation of EGFR homodimers (49, 50). For full EGFR activation, ligand binding and EGFR dimerization are crucial (27).

To analyze which of the four extracellular EGFR domains HCP-LCE targeted, flow cytometric analysis was performed using yeast cells displaying truncated fragments of the EGFR-ECD, as described previously (51, 52) (**Figure 2A**). Since HCP-LCE exclusively targets EGFR fragment 1-294 but neither 1-124 nor 1-176, it was mapped to EGFR domain II, which is involved in receptor dimerization (**Figure 2B**). Cetuximab is known to target domain III inhibiting EGF-binding to EGFR, while

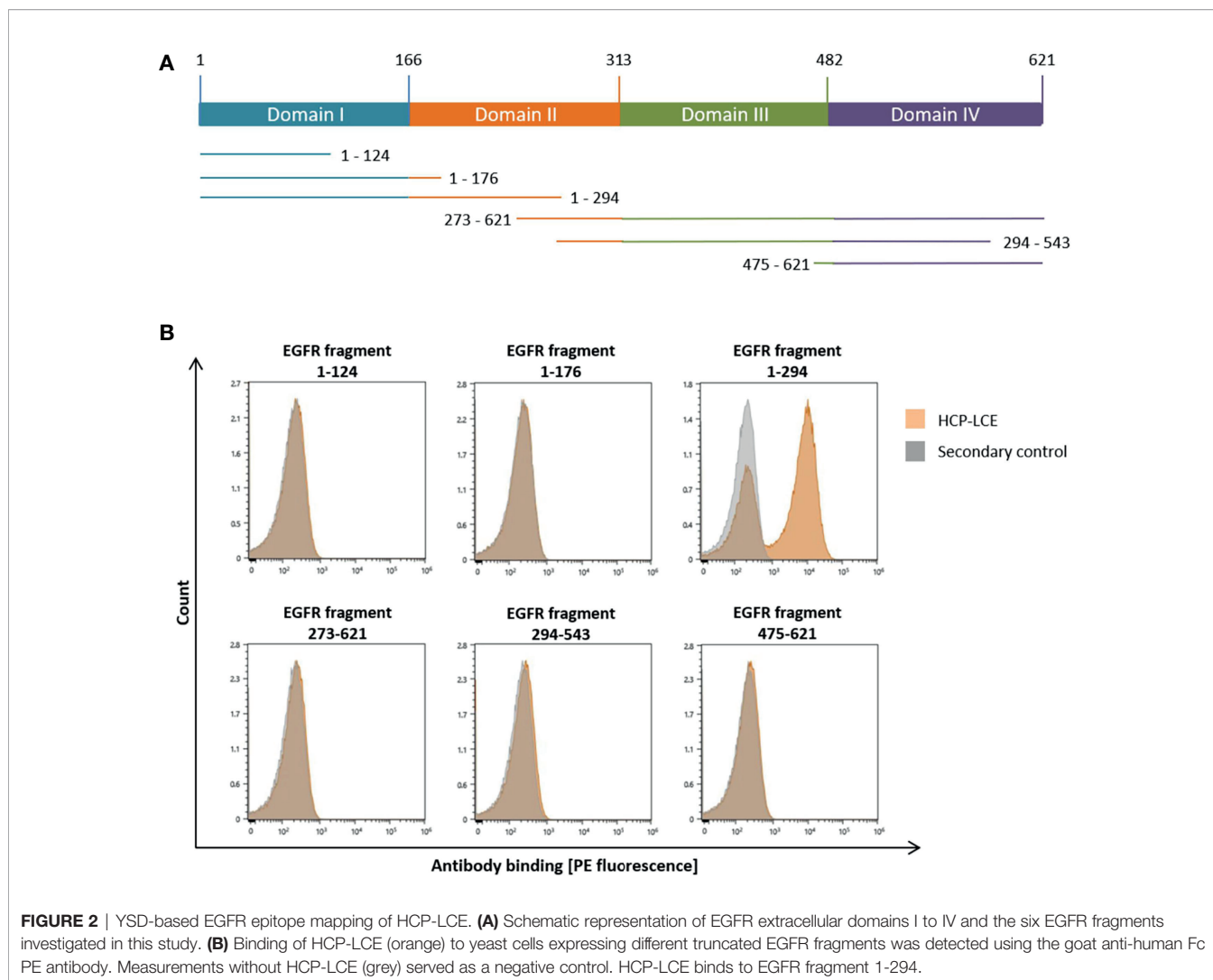
matuzumab blocks the receptor activation by sterically preventing the domain rearrangement (53). Binding of HCP-LCE to EGFR domain II may suggest inhibition of receptor dimerization and subsequent activation.

## Affinity Measurement

Bi-layer interferometry (BLI) measurements were performed in order to determine the affinity of HCP-LCE to both PD-L1 and EGFR. In order to confirm that non-overlapping paratopes were present and binding to both antigens was possible with a single Fab, an additional one-armed HCP-LCE variant was produced using Knob-into-Hole (KiH) technology, as previously described (10). Furthermore, affinity measurements of the HCP-LCE heavy chain combined with an unrelated light chain (ICI2\_H2) and that of the HCP-LCE light chain together with an unrelated heavy chain (LCE) to the two proteins of interest were performed.

HCP-LCE was able to bind both antigens with a  $K_D$  of 78.3 nM and 236 nM for PD-L1 and EGFR binding, respectively, exhibiting a high off-rate (**Figure 3A, Table 1**). The one-armed variant showed slightly lower affinities to both antigens which might presumably be caused by the lower avidity (**Supplementary Figure 3**). Variant ICI2\_H2 exclusively targeted PD-L1 with an affinity in the double digit nanomolar range, whereas variant LCE showed no binding to either PD-L1 or EGFR (**Figure 3A, Table 1**). This suggests that only the three HCP-LCE heavy chain CDRs are responsible for PD-L1 binding, contrary to EGFR binding involving overlapping heavy and light chain CDRs.

Since EGFR and PD-L1 are widely expressed on healthy cells (30, 54), simultaneous binding of both proteins is essential to increase tumor-specificity. To analyze the binding behaviour of HCP-LCE and to verify whether both antigens can be targeted



simultaneously with a single Fab, oaHCP-LCE was loaded onto AHC biosensors and sequentially incubated with both target proteins of interest. Here it was essential to use the one-armed variant, since the symmetric HCP-LCE antibody could target one antigen with each Fab arm. Binding to PD-L1 first and EGFR second as well as reverse binding was considered. The oaHCP-LCE variant was able to bind both antigens simultaneously, regardless of the order of target protein incubation (**Figure 3B**). These findings indicate that the paratopes do not overlap.

### Biophysical Characterization

Size-exclusion chromatography (SEC) profiles demonstrated that HCP-LCE exhibited favorable properties with almost no measurable aggregation (**Table 1, Supplementary Figure 5**). Monospecific antibodies ICI2\_H2 and LCE showed an excellent aggregation profile, while the bispecific EGFR- and PD-L1-binding antibody SEB7xICI2\_H2 and the oaHCP-LCE variant exhibited aggregation of 10.8% and 11.20%, respectively (**Table 1**). SEB7 has already been characterized previously (52).

Retention times were as expected (**Table 1, Supplementary Figure 5**), indicating the accurate size of the antibodies produced, which is in accordance with SDS-PAGE analysis (**Supplementary Figure 4**). In the case of both antibodies with KiH, oaHCP-LCE and SEB7xICI2\_H2, SDS-PAGE demonstrated the expression of similar amounts of both heavy chains, with the TwinStrep-tagged Fc having a significantly higher molecular weight than the His-tagged Fc (**Supplementary Figure 4**).

Thermal stability was analyzed using NanoDSF, yielding  $T_M$  values between 58.9°C and 67.3°C, indicating high thermal stability of all variants (**Table 1, Supplementary Figure 5**). For full-length antibodies, two to three  $T_M$  values are expected based on unfolding of the Fab fragment and CH<sub>2</sub>/CH<sub>3</sub> domains (55). The lowest  $T_M$  value was utilized to compare the stability of all antibodies generated.

### EGF and PD-1 Competition

To investigate antibody-mediated ligand receptor blockade, a competition assay was performed by aid of biolayer interferometry. For analysis of EGF competition, anti-human

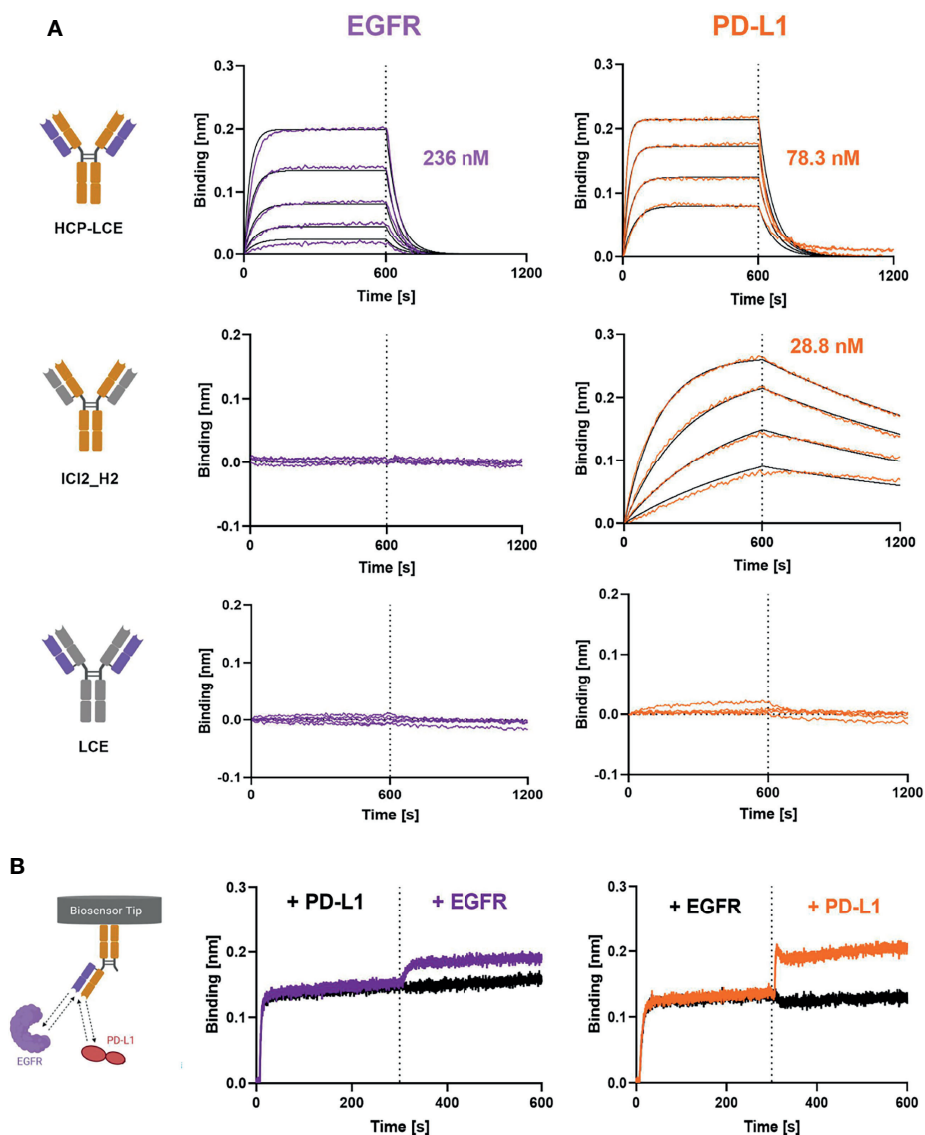


**FIGURE 3** | Characterization of antigen binding of the Two-in-One antibody HCP-LCE by BLI-measurements. **(A)** BLI-measurements of HCP-LCE, ICI2\_H2 and LCE against EGFR and PD-L1. HCP-LCE binds both antigens, whereas ICI2\_H2 exclusively targets PD-L1. LCE shows no binding to either antigen. **(B)** BLI-assisted simultaneous binding assay. The one-armed HCP-LCE variant was loaded onto biosensors and antigens are added step-wise, revealing simultaneous EGFR and PD-L1 binding. Created with BioRender.com.

IgG Fc Capture (AHC) biosensors were loaded with HCP-LCE and subsequently associated to 250 nM EGFR pre-incubated with 250 nM or 1000 nM EGF. Due to the binding of EGFR to EGF, the complex exhibits a larger molecular size compared to EGFR alone. Binding of HCP-LCE to this complex, therefore, results in a higher increase in layer thickness compared to binding of EGFR alone (**Figure 4A**), indicating that the antibody does not target the interaction site of EGF and EGFR, which is consistent with the YSD-based epitope mapping experiment (**Figure 2B**). EGF binds simultaneously to EGFR domains I and III, whereas HCP-LCE targets EGFR domain II, which is involved in receptor dimerization (48).

For total EGFR activation, ligand binding and EGFR dimerization are essential. EGF binding to EGFR promotes domain rearrangement to expose the dimerization arm in domain II (49). Since HCP-LCE targets domain II, it was investigated whether the Two-in-One antibody is able to inhibit EGF-induced EGFR dimerization by measuring the downstream phosphorylation of AKT in EGFR-positive A549 cells. In the presence of HCP-LCE (100  $\mu\text{g}/\text{mL}$ ), AKT phosphorylation is significantly reduced compared to the EGF stimulated control (20 ng/mL) (**Figure 4B**). Anti-EGFR antibody SEB7 and SEB7xICI2\_H2, which also target EGFR domain II (52), showed comparable inhibition of AKT

**TABLE 1** | Biophysical properties of HCP-LCE, LCE, ICI2\_H2 and SEB7xICI2\_H2 including affinity, kinetic binding rates, melting temperature and aggregation.

Antibody	K <sub>D</sub> [nM]		k <sub>on</sub> [M <sup>-1</sup> s <sup>-1</sup> ]		k <sub>dis</sub> [s <sup>-1</sup> ]		T <sub>m</sub> [°C]	Aggregation [%]
	EGFR	PD-L1	EGFR	PD-L1	EGFR	PD-L1		
HCP-LCE	236 ± 10.7	78.3 ± 1.36	4.15 × 10 <sup>5</sup> ± 1.58 × 10 <sup>4</sup>	9.73 × 10 <sup>5</sup> ± 1.37 × 10 <sup>4</sup>	9.81 × 10 <sup>-2</sup> ± 2.41 × 10 <sup>-3</sup>	7.62 × 10 <sup>-2</sup> ± 7.78 × 10 <sup>-4</sup>	58.9	2.22
oaHCP-LCE	295 ± 17.1	117 ± 4.15	3.88 × 10 <sup>5</sup> ± 1.92 × 10 <sup>4</sup>	9.29 × 10 <sup>5</sup> ± 2.62 × 10 <sup>4</sup>	1.14 × 10 <sup>-1</sup> ± 3.52 × 10 <sup>-3</sup>	1.09 × 10 <sup>-1</sup> ± 2.32 × 10 <sup>-3</sup>	59.6	12.44
LCE	—	—	—	—	—	—	61.1	1.27
ICI2_H2	—	28.8 ± 0.236	—	1.22 × 10 <sup>5</sup> ± 5.46 × 10 <sup>2</sup>	—	3.5 × 10 <sup>-3</sup> ± 2.40 × 10 <sup>-5</sup>	63.0	0
SEB7xICI2_H2	7.85 ± 0.173	29.9 ± 0.556	2.34 × 10 <sup>5</sup> ± 1.56 × 10 <sup>3</sup>	1.30 × 10 <sup>5</sup> ± 1.41 × 10 <sup>3</sup>	1.84 × 10 <sup>-3</sup> ± 3.87 × 10 <sup>-5</sup>	3.90 × 10 <sup>-3</sup> ± 5.90 × 10 <sup>-5</sup>	65.8	10.8

phosphorylation as HCP-LCE. The EGFR domain III binder Cetuximab (56) completely inhibited EGF-induced phosphorylation of AKT (**Figure 4B**) since binding of domain III blocked EGF binding (52). To conclude, EGFR signaling is significantly inhibited by HCP-LCE binding to dimerization domain II without interfering EGF-binding to its receptor.

To investigate HCP-LCE-mediated PD-1/PD-L1 competition, HCP-LCE was loaded onto FAB2G biosensors and was associated to 250 nM PD-L1 pre-incubated with either 250 nM or 1000 nM of PD-1. HCP-LCE exhibited significantly impaired binding to PD-L1 in the presence of PD-1, indicating that the antibody targets and blocks the PD-1/PD-L1 interaction site (57) (**Figure 5A**). This antibody-mediated PD-1/PD-L1 blockade was expected, as the heavy chain of HCP-LCE is derived from the anti-PD-L1 antibody ICI2 described by Bogen and coworkers, which demonstrated blockage of the PD-1/PD-L1 axis (44).

Verification of the PD-L1 blockage activity of HCP-LCE was performed in a cell-based context using the Promega PD-L1 blockade assay kit. HCP-LCE showed notable PD-L1 blockade, although with a less dominant effect compared with ICI2\_H2 (**Figure 5B**). This diminished EC<sub>50</sub> value most probably originates from the lower affinity towards PD-L1 binding. However, in combination with the original common light chain dFEB4-1, the ICI2 heavy chain exhibited a blockage of the PD-1/PD-L1 interaction comparable to durvalumab, as well as a significantly higher affinity PD-L1 binding (44). SEB7xICI2\_H2 exhibited comparable PD-L1 blockade as HCP-LCE, despite monovalent target binding of the bispecific antibody. The anti-EGFR antibody SEB7 did not interfere with PD-1/PD-L1 interaction even at high concentrations (**Figure 5B**). Conclusively, the binding of PD-1 to PD-L1 is significantly inhibited by HCP-LCE, indicating its function as a checkpoint inhibitor.

## Cell Titration on A431 Cells

Since HCP-LCE is expected to provide increased tumor-specificity compared to the bispecific antibody SEB7xICI2\_H2 and the corresponding monospecific antibodies due to simultaneous binding of EGFR and PD-L1 at each Fab arm, cell binding experiments were performed on EGFR/PD-L1 double-positive A431 cells by flow cytometry. Cells were stained with the respective antibody at a concentration ranging from 0.12 pM to 500 nM utilizing a four-fold dilution series and binding was verified using an anti-human Fc PE detection antibody. HCP-LCE exhibited cellular binding with an EC<sub>50</sub> value of 1.37 nM, while the EC<sub>50</sub> value of the bsAb SEB7xICI2\_H2 was comparable (**Figure 6**). EGFR overexpression on cancer cells typically exceeds that of PD-L1 (44), as demonstrated by A431 binding of the monospecific antibodies (**Figure 6; Supplementary Figure 6A**). The antibodies did not show binding to EGFR/PD-L1 double-negative HEK cells, excluding non-specific cell binding (**Supplementary Figure 6**). These data indicate that simultaneous binding of EGFR and PD-L1 at both Fab arms

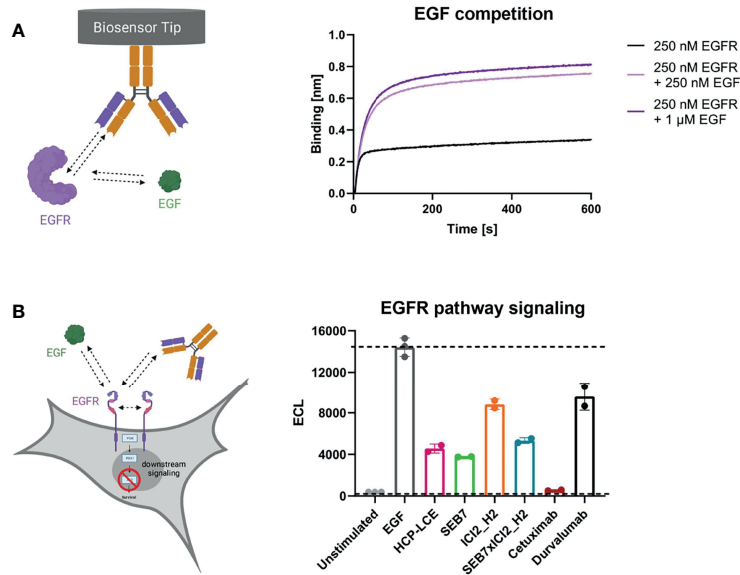


**FIGURE 4 |** EGF competition and EGFR signaling assays. **(A)** BLI-assisted EGF competition assay. HCP-LCE was loaded onto AHC biosensors and subsequently associated to EGFR pre-incubated with varying EGF concentrations. HCP-LCE binds to EGFR despite EGF binding. **(B)** Cell-based EGFR signaling assay. EGF-induced AKT phosphorylation was analysed in EGFR-positive A549 cells. SEB7 (green), ICI2\_H2 (orange), the bispecific construct SEB7xICI2\_H2 (blue), cetuximab (red) and durvalumab (black) were tested in comparison to the Two-in-One antibody HCP-LCE (pink). All measurements were performed in triplicates. Created with BioRender.com.

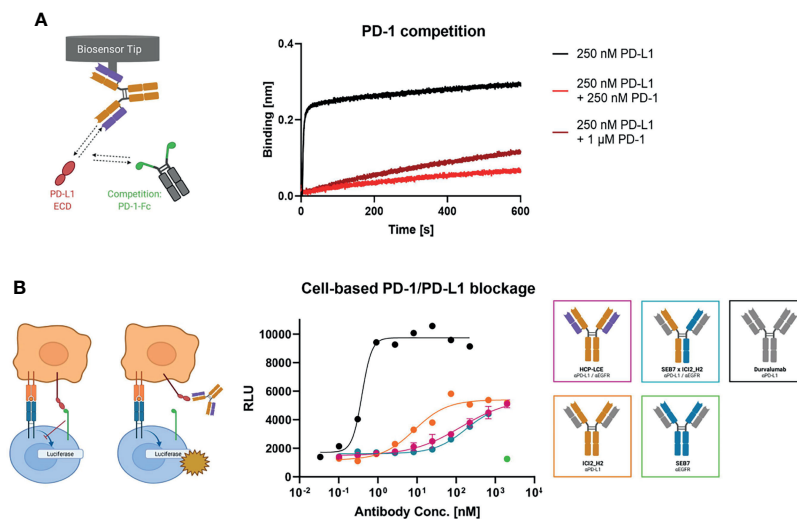


**FIGURE 5 |** PD-1 competition and PD-1/PD-L1 blockage assays. **(A)** BLI-assisted PD-1 competition assay. HCP-LCE was loaded onto FAB2G biosensors and subsequently associated to PD-L1 pre-incubated with varying PD-1 concentrations. The binding of HCP-LCE to PD-L1 at different PD-1 concentrations reveals dose-dependent binding. **(B)** Cell-based PD-1/PD-L1 blockage assay. SEB7 (green), ICI2\_H2 (orange), the bispecific construct SEB7xICI2\_H2 (blue) and durvalumab (black) were tested in comparison to the Two-in-One antibody HCP-LCE (pink). EC<sub>50</sub> values: durvalumab, 0.39 nM; ICI2\_H2, 8.60 nM; SEB7xICI2\_H2, 179 nM; HCP-LCE, 214 nM. Luciferase activity is plotted against the logarithmic antibody concentration. All measurements were performed in duplicates, and the experiments were repeated at least three times, yielding similar results. Created with BioRender.com.

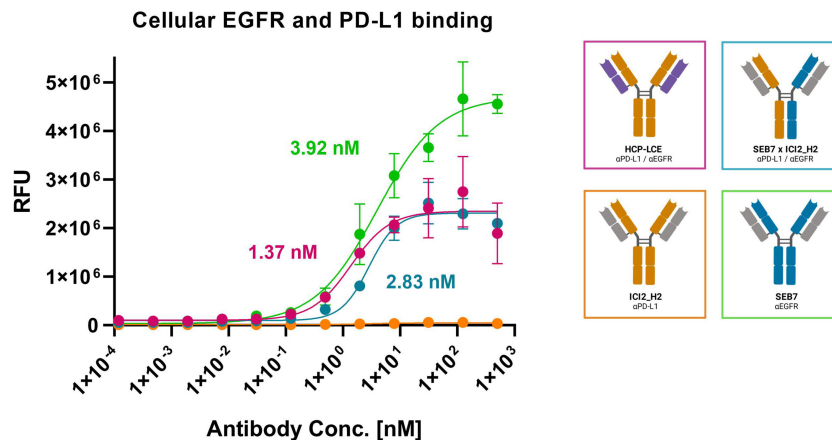


**FIGURE 6** | Cell binding of EGFR and PD-L1 on A431 cells. Cell titration of HCP-LCE (pink), ICI2\_H2 (orange), SEB7 (green) and the bispecific construct (blue) on EGFR/PD-L1 double positive A431 cells. A variable slope four-parameter fit was utilized to fit the resulting curves.  $EC_{50}$  values: HCP-LCE, 1.37 nM; SEB7, 3.92 nM; SEB7xICI2\_H2, 2.83 nM. All measurements were performed in triplicates, and the experiments were repeated at least three times, yielding similar results.

enhances A431 cell binding, compared to monovalent or bivalent target protein binding.

## DISCUSSION

Most antibodies utilize the heavy chain CDRs as the dominant moiety in antigen binding and can tolerate some mutations at the light chain CDRs (45, 46). This property was exploited to isolate the first Two-in-One antibody from a phage display library by mutating the light chain CDR fragments (12, 58). Subsequently, further engineering approaches were used for the generation of Two-in-One antibodies involving computational-based design, structural-guided design or random mutagenesis (13–15, 18, 19).

In this study, we generated the first chicken-derived Two-in-One antibody without CDR engineering that simultaneously targets EGFR and PD-L1 within the same Fv region. To this end, we paired the heavy chain of the chicken-derived anti-PD-L1 antibody ICI2 (44) with a chicken-derived anti-EGFR light chain immune library by yeast mating. Isolation of the Two-in-One antibody HCP-LCE was performed by three rounds of FACS-based selection using YSD. HCP-LCE showed binding affinities in the double- to triple-digit nanomolar range, favorable aggregation behaviour and remarkable thermostability, consistent with previously published results (44, 52). This approach of library generation enables the generation of Two-in-One antibodies targeting two unrelated proteins without additional engineering of the CDRs. In contrast to bispecific antibodies, which target one antigen with each Fab arm, HCP-LCE is capable of simultaneous binding two antigens with a single Fab, resulting in increased avidity.

An antibody subgroup that is also based on a common heavy chain are kappa-lambda ( $\kappa\lambda$ ) bodies. The  $\kappa\lambda$  body platform uses a fixed heavy chain that is combined with a lambda or kappa light chain naïve or synthetic antibody repertoire and subsequently selected for target binding by phage display (59).

HCP-LCE was generated according to a similar approach, with the difference that the Two-in-One antibody is not synthetic, but rather derived from immune libraries.

The conventional, symmetric IgG architecture of HCP-LCE reduces the need for multi-step purification and allows for straight-forward manufacturing since the main challenge in producing bispecific antibodies arises from their heterogeneous structure (60). Like DutaFabs (18), HCP-LCE is able to simultaneously bind two target molecules with one Fab arm. The co-binding of two targets or epitopes on the same Fv fragment might enable unique mechanisms of action based on receptor clustering or on positioning proteins in functional distance. However, it is important to note that HCP-LCE does not contain two independent paratopes. BLI measurements indicated that exclusively the HCP-LCE heavy chain is responsible for PD-L1 binding, in contrast to EGFR binding involving overlapping heavy and light chain CDR residues. Binding to PD-L1 is not disrupted by the use of an unrelated light chain, suggesting that PD-L1 is targeted exclusively by the three heavy chain CDRs. However, both the heavy and light chains of HCP-LCE are required for EGFR binding, indicating that CDR residues of both antibody chains are responsible for binding. Nevertheless, the heavy chain CDR residues required for EGFR binding do not appear to overlap with the residues involved in PD-L1 binding, otherwise simultaneous binding would not be possible. To investigate the arrangement of both paratopes, co-crystallographic analysis would be of great interest.

Flow cytometric measurements demonstrated that HCP-LCE targets an epitope on domain II of EGFR, which is involved in receptor dimerization (48). Cetuximab and matuzumab, two EGFR-binding antibodies, are known to bind EGFR domain III, which together with domain I mediates EGF binding (53, 61). Although biolayer interferometric measurements confirmed that the EGFR domain II binder HCP-LCE does not block EGF binding, the Two-in-One antibody significantly inhibited EGFR downstream signaling, as demonstrated by analyzing AKT



phosphorylation. Furthermore, HCP-LCE disrupted the PD-1/PD-L1 interaction by binding to an overlapping epitope with the therapeutic antibody durvalumab (44). Since the PD-1:PD-L1 axis is an immune checkpoint for NK cells and T cells, PD-L1 blockage may contribute to NK cell- and T cell-mediated killing (62–65).

Monoclonal antibody therapy is a treatment option for patients suffering from EGFR-related tumor burden (66). Since EGFR is natively expressed on epithelial cells in the skin and lung, the major side effect associated with treatment using EGFR targeting mAbs is skin toxicity, including skin rash, dry skin, hair growth disorders, and nail changes (67, 68). Koopmans and coworkers demonstrated an elevated tumor-specificity and tumor uptake by an EGFRxPD-L1 bispecific antibody (30). By simultaneous binding of EGFR and PD-L1, HCP-LCE might exhibit elevated tumor-selectivity, which could reduce side effects. This requires maximum discrimination between single-positive healthy cells and double-positive malignant cells. Moreover, due to the comparatively low affinity of HCP-LCE to EGFR (236 nM), increased EGFR cell expression, which is predominantly found on tumor cells (69), is required for targeting of the antibody. This could result in reduced on-target/off-tumor binding. In addition, the low binding affinity conceivably causes EGFR binding exclusively on cells that additionally express PD-L1 due to spatial proximity and local concentration. This concept has been described for bsAbs targeting tumor-specific receptors with high affinity on one arm and CD47 with lower affinity on the other arm (70–72). CD47 is ubiquitously expressed in human cells and has been found to be overexpressed in many tumors (73). The low-affinity binding to CD47 and the associated increased tumor selectivity results in a higher safety profile of the described bsAbs. Currently, four of these antibodies are in clinical or preclinical study (74). In the case of HCP-LCE, the antibody would inhibit PD-L1 in an EGFR-dependent manner, which could significantly reduce side effects.

HCP-LCE is a chimeric antibody consisting of chicken-derived VH and VL domains, grafted onto a human IgG1 scaffold. Starting from a heavy chain binder that was obtained by VH library screening likely facilitates the discovery of binders to a different target using a VL library of an immunized chicken. Unlike in mice, the light chain repertoire of chicken antibodies is generated *via* gene conversion (75). This might be one reason for chicken-derived antibodies being suitable for the generation of light chain binders. In regard to immunogenicity, humanization of the Two-in-One antibody is essential for potential therapeutic applications. Our group recently demonstrated an effective approach to humanize avian-derived antibodies based on Vernier residue randomization and high throughput screening (76) that could be applied for this purpose but is beyond the scope of this proof-of-concept study.

Taken together, we present a straightforward method for the isolation of chicken-derived Two-in-One antibodies without CDR engineering by combining the heavy chain of an anti-PD-L1 common light chain antibody with an anti-EGFR immune light chain library and YSD screening. The resulting

antibody HCP-LCE simultaneously targets EGFR and PD-L1 at the same Fv fragment while exhibiting favorable biophysical properties and aggregation behaviour. The Two-in-One antibody is able to inhibit EGFR signaling by binding to dimerization domain II and can also block the PD-1/PD-L1 interaction. Furthermore, HCP-LCE demonstrated specific cellular binding properties on EGFR/PD-L1 double-positive tumor cells. To our knowledge, this represents the first Two-in-One antibody without CDR engineering that simultaneously targets two antigens with one Fab fragment.

## MATERIAL AND METHODS

### Plasmids and Yeast Strains

For yeast surface display, pYD<sub>1</sub>-derived vectors (Yeast Display Vector Kit, version D, #V835-01, Thermo Fisher Scientific) were used. The heavy chain encoding plasmid contained the AGA2 signal peptide, followed by the ICI2 (44) VH-CH<sub>1</sub> sequence and the AGA2 gene, a tryptophan auxotrophic marker as well as an ampicillin resistance. The light chain plasmid encoded an  $\alpha$ MFpp8 signal sequence, followed by the VL-CL $\lambda$  sequences, a leucine auxotrophic marker and a kanamycin resistance gene. Gene expression of either plasmid was controlled *via* the galactose-inducible promoter (*GAL*<sub>1</sub>). For soluble expression of full-length chimeric antibodies, pTT5-derived vectors (47) were used, encoding either the heavy or light chain constant domains. Bispecific variants were expressed using pTT5-derived vectors encoding the full-length chimeric antibody with either a knob or hole mutation (10) within the CH<sub>3</sub> sequence, and a C-terminal His- or Twin-StrepII-Tag, respectively. For the one-armed variant, a pTT5-derived vector encoding the Hinge-CH<sub>2</sub>-CH<sub>3</sub> domain with the hole mutation and a C-terminal Twin-StrepII-Tag was utilized.

The *Saccharomyces cerevisiae* strains EBY100 [MAT $\alpha$  URA3-52 trp1 leu2 $\Delta$ 1 his3 $\Delta$ 200 pep4::HIS3 prb1 $\Delta$ 1.6R can1 GAL (pIU211:URA3)] (Thermo Fisher Scientific) and BJ5464 (MAT $\alpha$  URA3-52 trp1 leu2 $\Delta$ 1his3 $\Delta$ 200 pep4::HIS3 prb1 $\Delta$ 1.6R can1 GAL) (American Type Culture Collection) were transformed with the plasmids harbouring the heavy chain and light chain genes for Fab display, respectively. Yeast strains were cultivated in YPD medium composed of 20 g/L peptone/casein, 20 g/L glucose and 10 g/L yeast extract. Cultivation of haploid and diploid yeasts in SD-CAA and SG-CAA media was performed as described previously (77).

### Library Generation and Sorting

For yeast library generation, the VH-CH<sub>1</sub> fragment of the anti-PD-L1 antibody ICI2 (44) was combined with an anti-EGFR VL-CL $\lambda$  library (44). The ICI2 VH gene was amplified by PCR using Q5 polymerase (NEB) and the heavy chain pYD<sub>1</sub> vector was linearized utilizing NheI HF and BamHI-HF (NEB) according to the manufacturer's protocol. Homologous recombination of ICI2 VH gene into pYD<sub>1</sub> was conducted in EBY100 yeast cells according to the protocol described by Benatuil et al. (78).

Generation of the utilized anti-EGFR VL-CL $\lambda$  yeast library was described by Grzeschik et al. (35). To combine the light chain diversity with the common ICI2 heavy chain for subsequent Fab display, yeast mating was performed as described before (77).

For library sorting, cells of the diploid yeast library were grown overnight in SD-Trp-Leu medium at 30°C and 120 rpm. The next day, cells were harvested by centrifugation and used to inoculate SG-Trp-Leu medium at an OD<sub>600</sub> of 1.0 and incubated overnight at 30°C and 120 rpm. Cells were harvested by centrifugation, washed once with PBS-B [PBS + 0.1% (w/v) BSA] and incubated with 250 nM EGFR-ECD-Fc chimera (R&D Systems) for 30 min on ice. After washing once with PBS-B, cells were incubated with a goat anti-human-Lambda Alexa Fluor 647 F(ab')<sub>2</sub> antibody (SouthernBiotech, diluted 1:75) to detect Fab surface presentation, and a goat anti-human IgG-Fc-PE conjugate (Fisher Scientific, diluted 1:50) to detect target binding for 15 min on ice. Following another washing step, cells were screened by FACS using a Sony SH800S.

## Reformatting, Expression and Purification of Full-Length, One-Armed and Bispecific Antibodies

Plasmid isolation from yeast cells was performed using the Zymoprep Yeast Plasmid Miniprep Kit (Zymo Research) according to the manufacturer's protocol. Isolated plasmids were transformed into *E. coli* XL1-Blue and sequenced at Microsynth Seqlab (Göttingen). The resulting VL gene was amplified by PCR using Q5 polymerase (NEB) according to the manufacturer's protocol, incorporating *SapI* sites to enable subsequent Golden Gate cloning into pTT5-derived vectors as described previously (47). For soluble expression, Expi293F (Thermo Fisher, A14527) cells were transiently transfected following the manufacturer's protocol. Cells were cultivated in Expi293 Expression Medium (Thermo Fisher) at 37°C and 8.0% CO<sub>2</sub> at 110 rpm. For purification of full-length antibodies, sterile-filtered cell culture supernatant was applied to a Protein A HP column (GE Healthcare) five days after transfection using an ÄKTA pure system (GE Healthcare). One-armed and bispecific molecules were captured by IMAC (HisTrap HP, GE Healthcare), followed by Strep-Tactin XT affinity chromatography according to the manufacturer's protocol. Buffer exchange against PBS was performed using a HiTrap Desalting column (GE Healthcare).

## Epitope Mapping on the Subdomain Level via YSD

YSD-based epitope mapping was performed using yeast cells displaying six different truncated versions of EGFR-ECD (amino acids 1-124, 1-176, 1-294, 273-621, 294-543 and 475-621), as described previously (51, 52). Cells were harvested by centrifugation, washed once with PBS-B and incubated with 200 nM HCP-LCE for 30 min on ice. Surface presentation was verified using a biotinylated anti-c-myc antibody (Miltenyi Biotech, diluted 1:75) and Streptavidin APC (Thermo Fisher, diluted 1:75). Separately, antibody binding was verified by an anti-human IgG Fc PE-conjugated antibody (Fisher Scientific,

diluted 1:50). Cells were analyzed by flow cytometry using a SH800S (Sony Biotechnology).

## Affinity Determination, Receptor-Ligand Competition and Simultaneous Binding Assay via Biolayer Interferometry

For affinity determination of chimeric antibodies, anti-human IgG-Fc capture (AHC) biosensors were equilibrated in PBS pH 7.4 for 10 min and subsequently loaded with 10 µg/ml of the antibody of interest until a layer thickness of 1 nm was reached. All following steps were performed using kinetics buffer (KB, Sartorius). Association was measured for 600 s using varying concentrations of EGFR-ECD or PD-L1-ECD (produced in-house) ranging from 7.8 nM to 500 nM followed by dissociation for 600 s. KB was used as a negative control. Binding kinetics were determined based on Savitzky-Golay filtering and a 1:1 Langmuir binding model.

For the EGF competition assay, AHC biosensors were loaded with 10 µg/ml of HCP-LCE until a layer thickness of 1 nm was reached. Subsequently, 250 nM EGFR-ECD pre-incubated with either 0 nM, 250 nM or 1000 nM EGF was applied for 600 s.

For the PD-1 competition assay, anti-human Fab-CH<sub>1</sub> 2nd Generation (FAB2G) biosensors were loaded with 10 µg/ml of HCP-LCE until a layer thickness of 1 nm was reached. Subsequently, 250 nM PD-L1-ECD pre-incubated with either 0 nM, 250 nM or 1000 nM PD-1 was applied for 600 s.

For the simultaneous binding assay, AHC biosensors were loaded with 10 µg/ml of oaHCP-LCE until a layer thickness of 1 nm was reached. After measurement of the association to 250 nM antigen 1 for 300 s, association to 250 nM antigen 2 was determined for 300 s. As controls, oaHCP-LCE was incubated with antigen 1 or PBS only. EGFR-ECD and PD-L1-ECD were used as antigens and the order of association was analyzed in both settings.

All measurements were performed using the Octet RED96 system (FortéBio, Molecular Devices) at 30°C and 1000 rpm.

## NanoDSF and Size Exclusion Chromatography

Thermal stability of produced antibodies was characterized by nano differential scanning fluorimetry (NanoDSF) using the Prometheus NT.48 Protein Stability Instrument (NanoTemper Technologies). Tryptophan fluorescence of a 0.5 mg/mL protein solution was measured at 350 and 330 nm applying a temperature gradient from 20°C to 95°C with a temperature slope of 1°C/min. T<sub>M</sub> values were defined as the first maxima of the ratios of the first derivative of fluorescence at 330 nm and 350 nm.

Size exclusion chromatography (SEC) using TSKgel SuperSW3000 column (Tosoh Bioscience) together with 1260 Infinity chromatography system (Agilent Technologies) was utilized to analyze the aggregation behaviour of antibodies. Chromatography was performed at a flow rate of 0.35 mL/min for 20 min, and protein elution was detected by measuring absorbance at 280 nm.

## Cultivation of A431 and A549 Cells

A431 human epidermoid carcinoma cells (ATCC<sup>®</sup> CRL-1555<sup>™</sup>) and A549 human epithelial lung carcinoma cells (DSMZ ACC 107) were cultured in Dulbecco's Modified Eagle Medium (DMEM, Thermo Fisher), supplemented with 10% fetal bovine serum (FBS) superior (Merck Millipore) and 1% Penicillin-Streptomycin (Sigma Aldrich). Cells were cultured in T75 cell culture flasks at 37°C in a humidified atmosphere with 5% CO<sub>2</sub> and passaged every three to four days after reaching 80% confluence.

## EC50 Determination

Cellular binding of the produced antibodies was determined by affinity titration using EGFR/PD-L1 double positive A431 cells. EGFR/PD-L1 double negative HEK cells were used to analyze unspecific cell binding. To this end, 10<sup>5</sup> cells/well were seeded in 96-well plates, washed with PBS-F [PBS + 2% (w/v) FBS] and subsequently incubated with the respective antibody in varying concentrations (500 nM to 0.24 nM in a two-fold serial dilution) for 30 min on ice. Following another washing step, anti-human IgG-Fc PE-conjugated antibody was applied for 20 min. After washing, mean fluorescence was determined by flow cytometry using a CytoFLEX S (Beckman Coulter) and plotted against logarithmic antibody concentration. The resulting curves were fitted with a variable slope four-parameter fit using GraphPad Prism. All measurements were performed in triplicates, and the experiments were repeated at least three times, yielding comparable results.

## AKT Pathway Signaling Assay

Two days prior to the assay, A549 cells were seeded onto sterile 48-well cell culture plates at a cell density of 10<sup>5</sup> cells/well. The following day, cells were serum-starved in DMEM medium overnight. Subsequently, cells were pre-incubated with the desired antibody concentration for 1 h, followed by stimulation with 20 ng/mL rhEGF for 10 min at 37°C. Following stimulation, cells were quickly rinsed with pre-chilled PBS and lysed using Complete Lysis Buffer. For AKT phosphorylation analysis, the cell lysates were analysed using the AKT Signaling Whole Cell Lysate Kit (MesoScale Discovery) according to the manufacturer's protocol. The electrochemiluminescence (ECL) values were plotted using GraphPad Prism.

## Cell-Based PD-1/PD-L1 Blockage Reporter Assay

For the cell-based PD-1/PD-L1 blockade assay, the Promega PD-1/PD-L1 Blockade Bioassay (J1250) was used according to the manufacturer's instructions. Antibodies of interest were tested at a 3-fold dilution series, ranging from 2 μM to 0.3 nM for HCP-LCE, ICI2\_H2 and SEB7xICI2\_H2 and from 222.2 nM to 0.1 nM for Durvalumab. SEB7 was used as a control at a concentration of 2 μM. After incubation at 37°C and 5% CO<sub>2</sub> for six hours, luciferase activity was measured and plotted against

logarithmic antibody concentration. The resulting curves were fitted utilizing a variable slope four-parameter fit.

## DATA AVAILABILITY STATEMENT

The original contributions presented in the study are included in the article/**Supplementary Material**. Further inquiries can be directed to the corresponding author.

## AUTHOR CONTRIBUTIONS

JH, JB and HK conceived and designed the majority of experiments. JH and SC performed experiments. JH, JB, SC and HK analyzed the data. MU, BH and JG gave scientific advice. JH, JB and HK wrote the manuscript. All authors contributed to the article and approved the manuscript.

## FUNDING

This work was supported by the Ferring Darmstadt Laboratories at Technical University of Darmstadt and by the department of GPRD at Ferring Holding S.A., Saint-Prex. The funders had no role in study design, data collection and analysis, interpretation of data, decision to publish, or preparation of the manuscript. All authors declare no other competing interests.

## ACKNOWLEDGMENTS

We would like to thank the department of GPRD at Ferring Holding S.A., Saint-Prex for funding and instruments. We also would like to thank Janine Becker for technical assistance and Prof. Dr. Fessner for the possibility of performing NanoDSF measurements in his laboratory. We acknowledge support by the Deutsche Forschungsgemeinschaft (DFG-German Research Foundation) and the Open Access Publishing Fund of the Technical University of Darmstadt. Figures were created with BioRender.com.

## SUPPLEMENTARY MATERIAL

The Supplementary Material for this article can be found online at: <https://www.frontiersin.org/articles/10.3389/fimmu.2022.888838/full#supplementary-material>

## REFERENCES

- Husain B, Ellerman D. Expanding the Boundaries of Biotherapeutics With Bispecific Antibodies. *BioDrugs* (2018) 32:441–64. doi: 10.1007/s40259-018-0299-9
- Nie S, Wang Z, Moscoso-Castro M, D'Souza P, Lei C, Xu J, et al. Biology Drives the Discovery of Bispecific Antibodies as Innovative Therapeutics. *Antib Ther* (2020) 3:18–62. doi: 10.1093/abt/tbaa003
- Fischer N, Léger O. Bispecific Antibodies: Molecules That Enable Novel Therapeutic Strategies. *Pathobiology* (2007) 74:3–14. doi: 10.1159/000101046
- Thakur A, Huang M, Lum LG. Bispecific Antibody Based Therapeutics: Strengths and Challenges. *Blood Rev* (2018) 32:339–47. doi: 10.1016/j.blre.2018.02.004
- Rader C. Bispecific Antibodies in Cancer Immunotherapy. *Curr Opin Biotechnol* (2020) 65:9–16. doi: 10.1016/j.copbio.2019.11.020
- Eigenbrot C, Fuh G. Two-In-One Antibodies With Dual Action Fabs. *Curr Opin Chem Biol* (2013) 17:400–5. doi: 10.1016/j.cbpa.2013.04.015
- Lee HY, Schaefer G, Lesaca I, Lee CV, Wong PY, Jiang G. “Two-In-One” Approach for Bioassay Selection for Dual Specificity Antibodies. *J Immunol Methods* (2017) 448:74–9. doi: 10.1016/j.jim.2017.05.011
- Krah S, Kolmar H, Becker S, Zielonka S. Engineering IgG-Like Bispecific Antibodies-An Overview. *Antibodies (Basel)* (2018) 7:28. doi: 10.3390/antib7030028
- Beck A, Wurch T, Bailly C, Corvaia N. Strategies and Challenges for the Next Generation of Therapeutic Antibodies. *Nat Rev Immunol* (2010) 10:345–52. doi: 10.1038/nri2747
- Ridgway JB, Presta LG, Carter P. ‘Knobs-Into-Holes’ Engineering of Antibody CH3 Domains for Heavy Chain Heterodimerization. *Protein Eng* (1996) 9:617–21. doi: 10.1093/protein/9.7.617
- Lewis SM, Wu X, Pustilnik A, Sereno A, Huang F, Rick HL, et al. Generation of Bispecific IgG Antibodies by Structure-Based Design of an Orthogonal Fab Interface. *Nat Biotechnol* (2014) 32:191–8. doi: 10.1038/nbt.2797
- Bostrom J, Yu S-F, Kan D, Appleton BA, Lee CV, Billeci K, et al. Variants of the Antibody Herceptin That Interact With HER2 and VEGF at the Antigen Binding Site. *Science* (2009) 323:1610–4. doi: 10.1126/science.1165480
- Schaefer G, Haber L, Crocker LM, Shia S, Shao L, Dowbenko D, et al. A Two-in-One Antibody Against HER3 and EGFR has Superior Inhibitory Activity Compared With Monospecific Antibodies. *Cancer Cell* (2011) 20:472–86. doi: 10.1016/j.ccr.2011.09.003
- Lee CV, Koenig P, Fuh G. A Two-in-One Antibody Engineered From a Humanized Interleukin 4 Antibody Through Mutation in Heavy Chain Complementarity-Determining Regions. *MAbs* (2014) 6:622–7. doi: 10.4161/mabs.28483
- Koenig P, Lee CV, Sanowar S, Wu P, Stinson J, Harris SF, et al. Deep Sequencing-Guided Design of a High Affinity Dual Specificity Antibody to Target Two Angiogenic Factors in Neovascular Age-Related Macular Degeneration. *J Biol Chem* (2015) 290:21773–86. doi: 10.1074/jbc.M115.662783
- Fayette J, Wirth L, Oprean C, Udrea A, Jimeno A, Rischin D, et al. Randomized Phase II Study of Duligotuzumab (MEHD7945A) vs. Cetuximab in Squamous Cell Carcinoma of the Head and Neck (MEHGAN Study). *Front Oncol* (2016) 6:232. doi: 10.3389/fonc.2016.00232
- Hill AG, Findlay MP, Burge ME, Jackson C, Alfonso PG, Samuel L, et al. Phase II Study of the Dual EGFR/HER3 Inhibitor Duligotuzumab (MEHD7945A) Versus Cetuximab in Combination With FOLFIRI in Second-Line RAS Wild-Type Metastatic Colorectal Cancer. *Clin Cancer Res* (2018) 24:2276–84. doi: 10.1158/1078-0432.CCR-17-0646
- Beckmann R, Jensen K, Fenn S, Speck J, Krause K, Meier A, et al. DutaFabs Are Engineered Therapeutic Fab Fragments That can Bind Two Targets Simultaneously. *Nat Commun* (2021) 12:708. doi: 10.1038/s41467-021-20949-3
- Ljungars A, Schiött T, Mattson U, Steppa J, Hambe B, Semmrich M, et al. A Bispecific IgG Format Containing Four Independent Antigen Binding Sites. *Sci Rep* (2020) 10:1546. doi: 10.1038/s41598-020-58150-z
- Chen S, Li J, Li Q, Wang Z. Bispecific Antibodies in Cancer Immunotherapy. *Hum Vaccin Immunother* (2016) 12:2491–500. doi: 10.1080/21645515.2016.1187802
- Sheridan C. Bispecific Antibodies Poised to Deliver Wave of Cancer Therapies. *Nat Biotechnol* (2021) 39:251–4. doi: 10.1038/s41587-021-00850-6
- Krishnamurthy A, Jimeno A. Bispecific Antibodies for Cancer Therapy: A Review. *Pharmacol Ther* (2018) 185:122–34. doi: 10.1016/j.pharmthera.2017.12.002
- Suurs FV, Lub-de Hooge MN, de Vries EG, de Groot DJ. A Review of Bispecific Antibodies and Antibody Constructs in Oncology and Clinical Challenges. *Pharmacol Ther* (2019) 201:103–19. doi: 10.1016/j.pharmthera.2019.04.006
- Ju X, Zhang H, Zhou Z, Wang Q. Regulation of PD-L1 Expression in Cancer and Clinical Implications in Immunotherapy. *Am J Cancer Res* (2020) 10:1–11.
- Sigismund S, Avanzato D, Lanzetti L. Emerging Functions of the EGFR in Cancer. *Mol Oncol* (2018) 12:3–20. doi: 10.1002/1878-0261.12155
- Brunner-Weinzierl MC, Rudd CE. CTLA-4 and PD-1 Control of T-Cell Motility and Migration: Implications for Tumor Immunotherapy. *Front Immunol* (2018) 9:2737. doi: 10.3389/fimmu.2018.02737
- Wee P, Wang Z. Epidermal Growth Factor Receptor Cell Proliferation Signaling Pathways. *Cancers (Basel)* (2017) 9(5):52. doi: 10.3390/cancers9050052
- Pastore S, Mascia F, Mariani V, Girolomoni G. The Epidermal Growth Factor Receptor System in Skin Repair and Inflammation. *J Invest Dermatol* (2008) 128:1365–74. doi: 10.1038/sj.jid.5701184
- Bogen JP, Grzeschik J, Jakobsen J, Bähre A, Hock B, Kolmar H. Treating Bladder Cancer: Engineering of Current and Next Generation Antibody-, Fusion Protein-, mRNA-, Cell- and Viral-Based Therapeutics. *Front Oncol* (2021) 11:672262. doi: 10.3389/fonc.2021.672262
- Koopmans I, Hendriks D, Samplonius DF, van Ginkel RJ, Heskamp S, Wierstra PJ, et al. A Novel Bispecific Antibody for EGFR-Directed Blockade of the PD-1/PD-L1 Immune Checkpoint. *Oncoimmunology* (2018) 7:e1466016. doi: 10.1080/2162402X.2018.1466016
- Lu R-M, Hwang Y-C, Liu I-J, Lee C-C, Tsai H-Z, Li H-J, et al. Development of Therapeutic Antibodies for the Treatment of Diseases. *J Biomed Sci* (2020) 27:1. doi: 10.1186/s12929-019-0592-z
- Ching KH, Collarini EJ, Abdiche YN, Bedinger D, Pedersen D, Izquierdo S, et al. Chickens With Humanized Immunoglobulin Genes Generate Antibodies With High Affinity and Broad Epitope Coverage to Conserved Targets. *MAbs* (2018) 10:71–80. doi: 10.1080/19420862.2017.1386825
- Larsson A, Bälöw RM, Lindahl TL, Forsberg PO. Chicken Antibodies: Taking Advantage of Evolution—a Review. *Poult Sci* (1993) 72:1807–12. doi: 10.3382/ps.0721807
- Bogen JP, Grzeschik J, Krah S, Zielonka S, Kolmar H. Rapid Generation of Chicken Immune Libraries for Yeast Surface Display. *Methods Mol Biol* (2020) 2070:289–302. doi: 10.1007/978-1-4939-9853-1\_16
- Grzeschik J, Yanakieva D, Roth L, Krah S, Hinz SC, Elter A, et al. Yeast Surface Display in Combination With Fluorescence-Activated Cell Sorting Enables the Rapid Isolation of Antibody Fragments Derived From Immunized Chickens. *Biotechnol J* (2019) 14:e1800466. doi: 10.1002/biot.201800466
- Roth L, Grzeschik J, Hinz SC, Becker S, Toleikis L, Busch M, et al. Facile Generation of Antibody Heavy and Light Chain Diversities for Yeast Surface Display by Golden Gate Cloning. *Biol Chem* (2019) 400:383–93. doi: 10.1515/hsz-2018-0347
- Chua YJ, Cunningham D. Panitumumab. *Drugs Today (Barc)* (2006) 42:711–9. doi: 10.1358/dot.2006.42.11.1032061
- Dienstmann R, Tabernero J. Necitumumab, a Fully Human IgG1 mAb Directed Against the EGFR for the Potential Treatment of Cancer. *Curr Opin Investig Drugs* (2010) 11:1434–41.
- Mazorra Z, Chao L, Lavastida A, Sanchez B, Ramos M, Iznaga N, et al. Nimotuzumab: Beyond the EGFR Signaling Cascade Inhibition. *Semin Oncol* (2018) 45:18–26. doi: 10.1053/j.seminoncol.2018.04.008
- Graham J, Muhsin M, Kirkpatrick P. Cetuximab. *Nat Rev Drug Discovery* (2004) 3:549–50. doi: 10.1038/nrd1445
- Faena I, Cummings AL, Crosetti AM, Pantuck AJ, Chamie K, Drakaki A. Durvalumab: An Investigational Anti-PD-L1 Monoclonal Antibody for the Treatment of Urothelial Carcinoma. *Drug Des Devel Ther* (2018) 12:209–15. doi: 10.2147/DDDT.S141491
- Collins JM, Gulley JL. Product Review: Avelumab, an Anti-PD-L1 Antibody. *Hum Vaccin Immunother* (2019) 15:891–908. doi: 10.1080/21645515.2018.1551671

43. Shah NJ, Kelly WJ, Liu SV, Choquette K, Spira A. Product Review on the Anti-PD-L1 Antibody Atezolizumab. *Hum Vaccin Immunother* (2018) 14:269–76. doi: 10.1080/21645515.2017.1403694
44. Bogen JP, Carrara SC, Fiebig D, Grzeschik J, Hock B, Kolmar H. Design of a Trispecific Checkpoint Inhibitor and Natural Killer Cell Engager Based on a 2 + 1 Common Light Chain Antibody Architecture. *Front Immunol* (2021) 12:669496:669496. doi: 10.3389/fimmu.2021.669496
45. Xu JL, Davis MM. Diversity in the CDR3 Region of VH Is Sufficient for Most Antibody Specificities. *Immunity* (2000) 13:37–45. doi: 10.1016/s1074-7613(00)00006-6
46. Krah S, Schröter C, Eller C, Rhiel L, Rasche N, Beck J, et al. Generation of Human Bispecific Common Light Chain Antibodies by Combining Animal Immunization and Yeast Display. *Protein Eng Des Sel* (2017) 30:291–301. doi: 10.1093/protein/gzw077
47. Bogen JP, Storka J, Yanakieva D, Fiebig D, Grzeschik J, Hock B, et al. Isolation of Common Light Chain Antibodies From Immunized Chickens Using Yeast Biopanning and Fluorescence-Activated Cell Sorting. *Biotechnol J* (2021) 16:e2000240. doi: 10.1002/biot.202000240
48. Ferguson KM. Structure-Based View of Epidermal Growth Factor Receptor Regulation. *Annu Rev Biophys* (2008) 37:353–73. doi: 10.1146/annurev.biophys.37.032807.125829
49. Ferguson KM, Berger MB, Mendrola JM, Cho H-S, Leahy DJ, Lemmon MA. EGF Activates Its Receptor by Removing Interactions That Autoinhibit Ectodomain Dimerization. *Mol Cell* (2003) 11:507–17. doi: 10.1016/S1097-2765(03)00047-9
50. Burgess AW, Cho H-S, Eigenbrot C, Ferguson KM, Garrett TPJ, Leahy DJ, et al. An Open-And-Shut Case? Recent Insights Into the Activation of EGF/ ErbB Receptors. *Mol Cell* (2003) 12:541–52. doi: 10.1016/s1097-2765(03)00350-2
51. Cochran JR, Kim Y-S, Olsen MJ, Bhandari R, Wittrup KD. Domain-Level Antibody Epitope Mapping Through Yeast Surface Display of Epidermal Growth Factor Receptor Fragments. *J Immunol Methods* (2004) 287:147–58. doi: 10.1016/j.jim.2004.01.024
52. Bogen JP, Carrara SC, Fiebig D, Grzeschik J, Hock B, Kolmar H. Expedient Generation of Biparatopic Common Light Chain Antibodies via Chicken Immunization and Yeast Display Screening. *Front Immunol* (2020) 11:606878:606878. doi: 10.3389/fimmu.2020.606878
53. Schmiedel J, Blaukat A, Li S, Knöchel T, Ferguson KM. Matuzumab Binding to EGFR Prevents the Conformational Rearrangement Required for Dimerization. *Cancer Cell* (2008) 13:365–73. doi: 10.1016/j.ccr.2008.02.019
54. Ocvirk J, Cencelj S. Management of Cutaneous Side-Effects of Cetuximab Therapy in Patients With Metastatic Colorectal Cancer. *J Eur Acad Dermatol Venerol* (2010) 24:453–9. doi: 10.1111/j.1468-3083.2009.03446.x
55. Ionescu RM, Vlasak J, Price C, Kirchmeier M. Contribution of Variable Domains to the Stability of Humanized IgG1 Monoclonal Antibodies. *J Pharm Sci* (2008) 97:1414–26. doi: 10.1002/jps.21104
56. Makabe K, Yokoyama T, Uehara S, Uchikubo-Kamo T, Shirouzu M, Kimura K, et al. Anti-EGFR Antibody 528 Binds to Domain III of EGFR at a Site Shifted From the Cetuximab Epitope. *Sci Rep* (2021) 11:5790. doi: 10.1038/s41598-021-84171-3
57. Zak KM, Grudnik P, Magiera K, Dömling A, Dubin G, Holak TA. Structural Biology of the Immune Checkpoint Receptor PD-1 and Its Ligands PD-L1/PD-L2. *Structure* (2017) 25:1163–74. doi: 10.1016/j.str.2017.06.011
58. Bostrom J, Haber L, Koenig P, Kelley RF, Fuh G. High Affinity Antigen Recognition of the Dual Specific Variants of Herceptin is Entropy-Driven in Spite of Structural Plasticity. *PLoS One* (2011) 6:e17887. doi: 10.1371/journal.pone.0017887
59. Fischer N, Elson G, Magistrelli G, Dheilly E, Fouque N, Laurendon A, et al. Exploiting Light Chains for the Scalable Generation and Platform Purification of Native Human Bispecific IgG. *Nat Commun* (2015) 6:6113. doi: 10.1038/ncomms7113
60. Brinkmann U, Kontermann RE. The Making of Bispecific Antibodies. *MAbs* (2017) 9:182–212. doi: 10.1080/19420862.2016.1268307
61. Li S, Schmitz KR, Jeffrey PD, Wiltzius JJ, Kussie P, Ferguson KM. Structural Basis for Inhibition of the Epidermal Growth Factor Receptor by Cetuximab. *Cancer Cell* (2005) 7:301–11. doi: 10.1016/j.ccr.2005.03.003
62. Sun C, Mezzadra R, Schumacher TN. Regulation and Function of the PD-L1 Checkpoint. *Immunity* (2018) 48:434–52. doi: 10.1016/j.immuni.2018.03.014
63. Chen Y, Pei Y, Luo J, Huang Z, Yu J, Meng X. Looking for the Optimal PD-1/PD-L1 Inhibitor in Cancer Treatment: A Comparison in Basic Structure, Function, and Clinical Practice. *Front Immunol* (2020) 11:1088. doi: 10.3389/fimmu.2020.01088
64. Juliá EP, Amante A, Pampena MB, Mordoh J, Levy EM. Avelumab, an IgG1 Anti-PD-L1 Immune Checkpoint Inhibitor, Triggers NK Cell-Mediated Cytotoxicity and Cytokine Production Against Triple Negative Breast Cancer Cells. *Front Immunol* (2018) 9:2140. doi: 10.3389/fimmu.2018.02140
65. Pesce S, Greppi M, Grossi F, Del Zotto G, Moretta L, Sivori S, et al. PD-1/PD-Ls Checkpoint: Insight on the Potential Role of NK Cells. *Front Immunol* (2019) 10:1242. doi: 10.3389/fimmu.2019.01242
66. Fakih M, Wong R. Efficacy of the Monoclonal Antibody EGFR Inhibitors for the Treatment of Metastatic Colorectal Cancer. *Curr Oncol* (2010) 17 Suppl 1:S3–17. doi: 10.3747/CO.V17IS1.616
67. Segaeert S, van Cutsem E. Clinical Signs, Pathophysiology and Management of Skin Toxicity During Therapy With Epidermal Growth Factor Receptor Inhibitors. *Ann Oncol* (2005) 16:1425–33. doi: 10.1093/annonc/mdi279
68. Lacouture ME. Mechanisms of Cutaneous Toxicities to EGFR Inhibitors. *Nat Rev Cancer* (2006) 6:803–12. doi: 10.1038/nrc1970
69. Nicholson RI, Gee JM, Harper ME. EGFR and Cancer Prognosis. *Eur J Cancer* (2001) 37:9–15. doi: 10.1016/S0959-8049(01)00231-3
70. Zhang H, Deng M, Lin P, Liu J, Liu C, Strohl WR, et al. Frontiers and Opportunities: Highlights of the 2nd Annual Conference of the Chinese Antibody Society. *Antib Ther* (2018) 1:65–74. doi: 10.1093/abt/tby009
71. Dheilly E, Moine V, Broyer L, Salgado-Pires S, Johnson Z, Papaioannou A, et al. Selective Blockade of the Ubiquitous Checkpoint Receptor CD47 Is Enabled by Dual-Targeting Bispecific Antibodies. *Mol Ther* (2017) 25:523–33. doi: 10.1016/j.ythm.2016.11.006
72. Piccione EC, Juarez S, Liu J, Tseng S, Ryan CE, Narayanan C, et al. A Bispecific Antibody Targeting CD47 and CD20 Selectively Binds and Eliminates Dual Antigen Expressing Lymphoma Cells. *MAbs* (2015) 7:946–56. doi: 10.1080/19420862.2015.1062192
73. Hayat SM, Bianconi V, Pirro M, Jaafari MR, Hatampour M, Sahebkar A. CD47: Role in the Immune System and Application to Cancer Therapy. *Clin Oncol (Dordr)* (2020) 43:19–30. doi: 10.1007/s13402-019-00469-5
74. Yang Y, Yang Z, Yang Y. Potential Role of CD47-Directed Bispecific Antibodies in Cancer Immunotherapy. *Front Immunol* (2021) 12:686031. doi: 10.3389/fimmu.2021.686031
75. Kurosawa K, Ohta K. Genetic Diversification by Somatic Gene Conversion. *Genes (Basel)* (2011) 2:48–58. doi: 10.3390/genes2010048
76. Elter A, Bogen JP, Hinz SC, Fiebig D, Macarrón Palacios A, Grzeschik J, et al. Humanization of Chicken-Derived scFv Using Yeast Surface Display and NGS Data Mining. *Biotechnol J* (2021) 16:e2000231. doi: 10.1002/biot.202000231
77. Bogen JP, Hinz SC, Grzeschik J, Ebenig A, Krah S, Zielonka S, et al. Dual Function pH Responsive Bispecific Antibodies for Tumor Targeting and Antigen Depletion in Plasma. *Front Immunol* (2019) 10:1892. doi: 10.3389/fimmu.2019.01892
78. Benatuil L, Perez JM, Belk J, Hsieh C-M. An Improved Yeast Transformation Method for the Generation of Very Large Human Antibody Libraries. *Protein Eng Des Sel* (2010) 23:155–9. doi: 10.1093/protein/gzq002

**Conflict of Interest:** BH and JG are employees of Ferring Pharmaceuticals. JB, SC and MU were employed by TU Darmstadt in frame of a collaboration project with Ferring Pharmaceuticals. HK, JH, JB, SC and MU are inventors of a patent related to the Two-in-One antibody HCP-LCE (EP22159491.4).

The remaining authors declare that the research was conducted in the absence of any commercial or financial relationship that could be construed as a potential conflict of interest.

**Publisher's Note:** All claims expressed in this article are solely those of the authors and do not necessarily represent those of their affiliated organizations, or those of the publisher, the editors and the reviewers. Any product that may be evaluated in

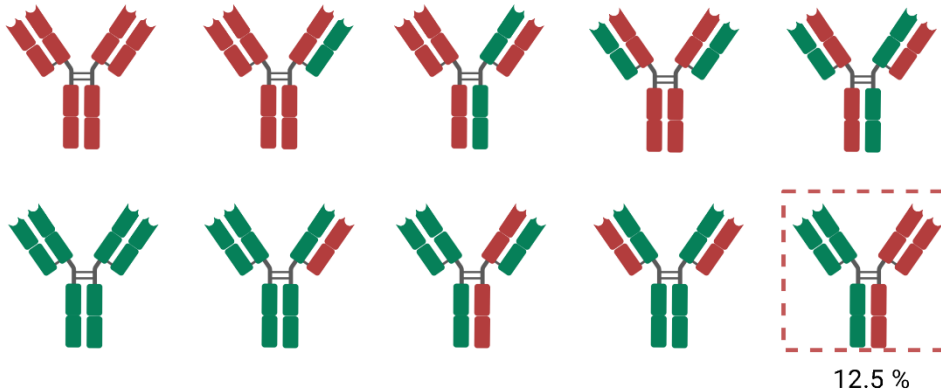
this article, or claim that may be made by its manufacturer, is not guaranteed or endorsed by the publisher.

Copyright © 2022 Harwardt, Bogen, Carrara, Ulitzka, Grzeschik, Hock and Kolmar. This is an open-access article distributed under the terms of the Creative Commons

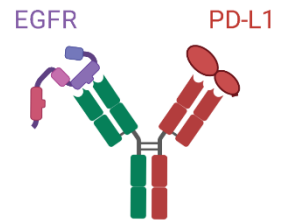
*Attribution License (CC BY). The use, distribution or reproduction in other forums is permitted, provided the original author(s) and the copyright owner(s) are credited and that the original publication in this journal is cited, in accordance with accepted academic practice. No use, distribution or reproduction is permitted which does not comply with these terms.*

*Supplementary Material*

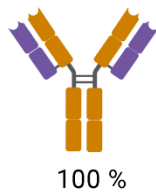
**A** Chain association problem of bispecific antibodies



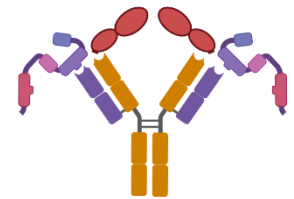
**C** Bispecific Antibody



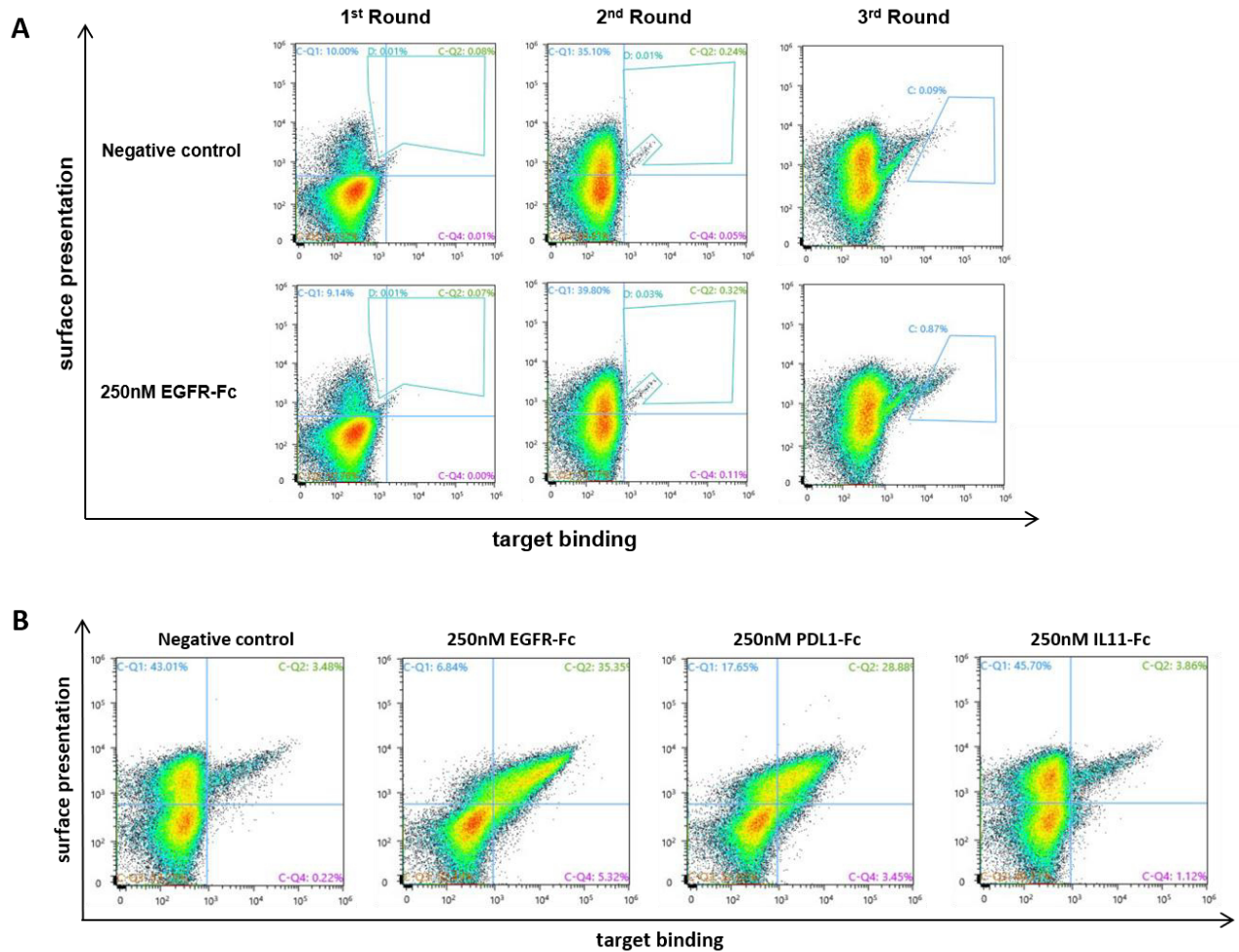
**B** Chain assembly of Two-in-One antibodies



**D** Two-in-One Antibody

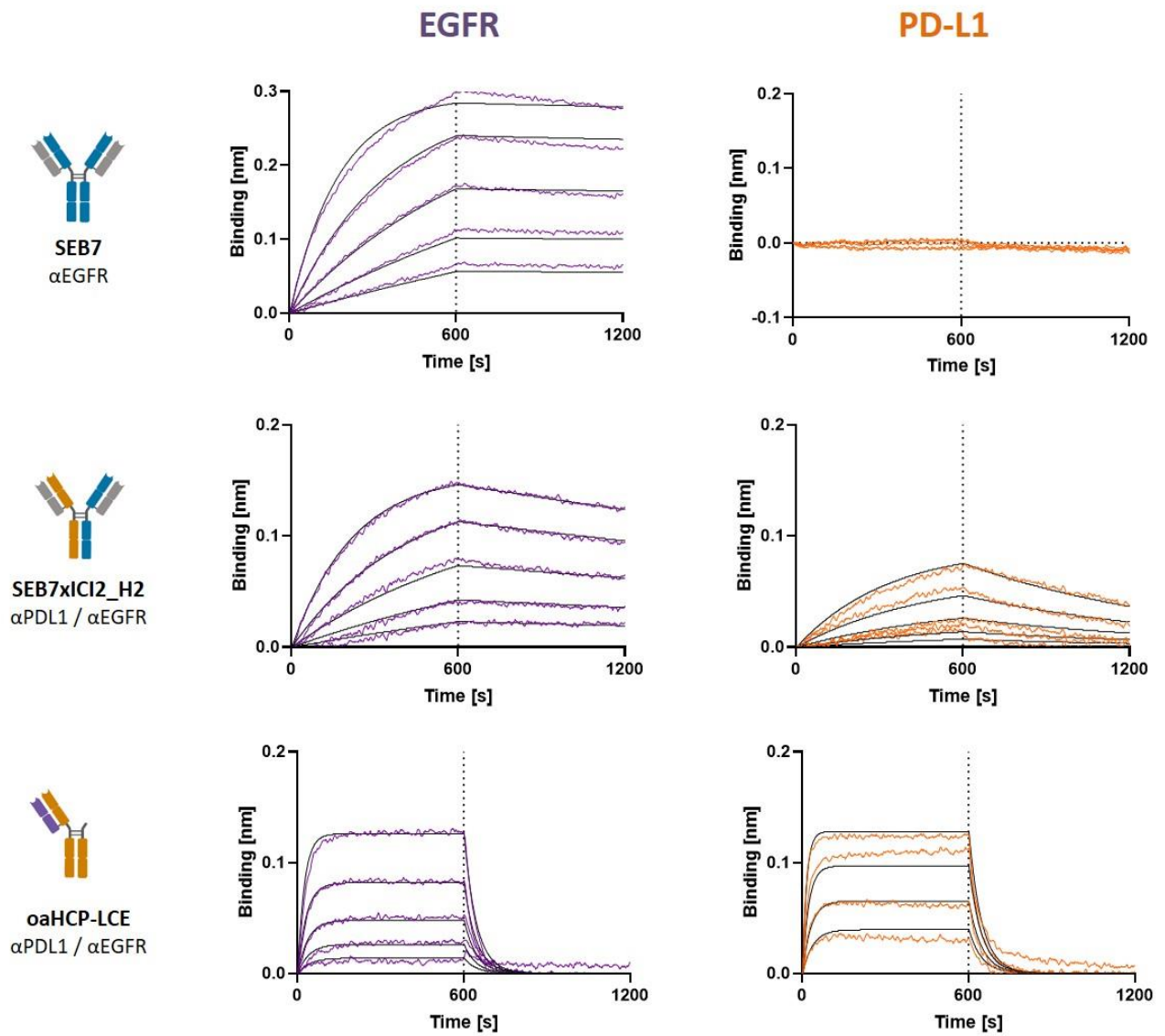


**Supplementary Figure 1.** Chain assembly of bispecific antibodies. A) Possible heavy and light chain pairing combinations of bispecific antibodies. The correctly paired variant is marked in red. B) For Two-in-One antibodies, there is only one possibility of chain assembly. C) A bispecific antibody binds one antigen with each Fab fragment. D) Two-in-One antibodies target two antigens with each Fab arm.

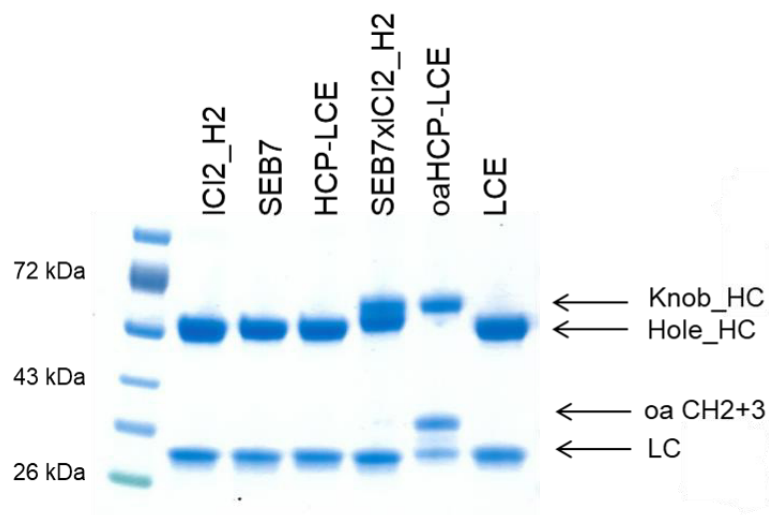


**Supplementary Figure 2.** Isolation of HCP-LCE. A) Sorting of the diploid common heavy chain yeast library. Surface presentation is depicted on the y-axis utilizing the anti-human lambda chain antibody AF647 labelled, while EGFR-Fc binding is shown on the x-axis using the anti-human Fc-PE antibody. B) Flow cytometric analysis of the isolated yeast population after three consecutive rounds of FACS screening. Surface presentation is depicted on the y-axis utilizing the anti-human lambda chain antibody AF647 labelled, while EGFR-Fc, PD-L1-Fc and IL11-Fc binding is shown on the x-axis using the anti-human Fc-PE antibody.

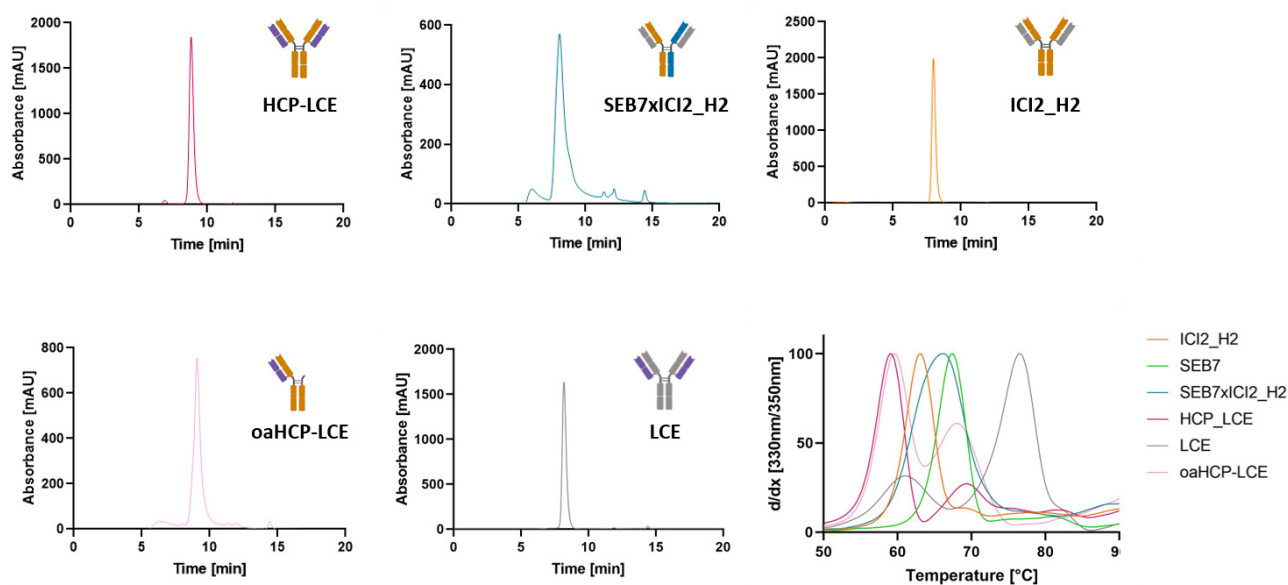




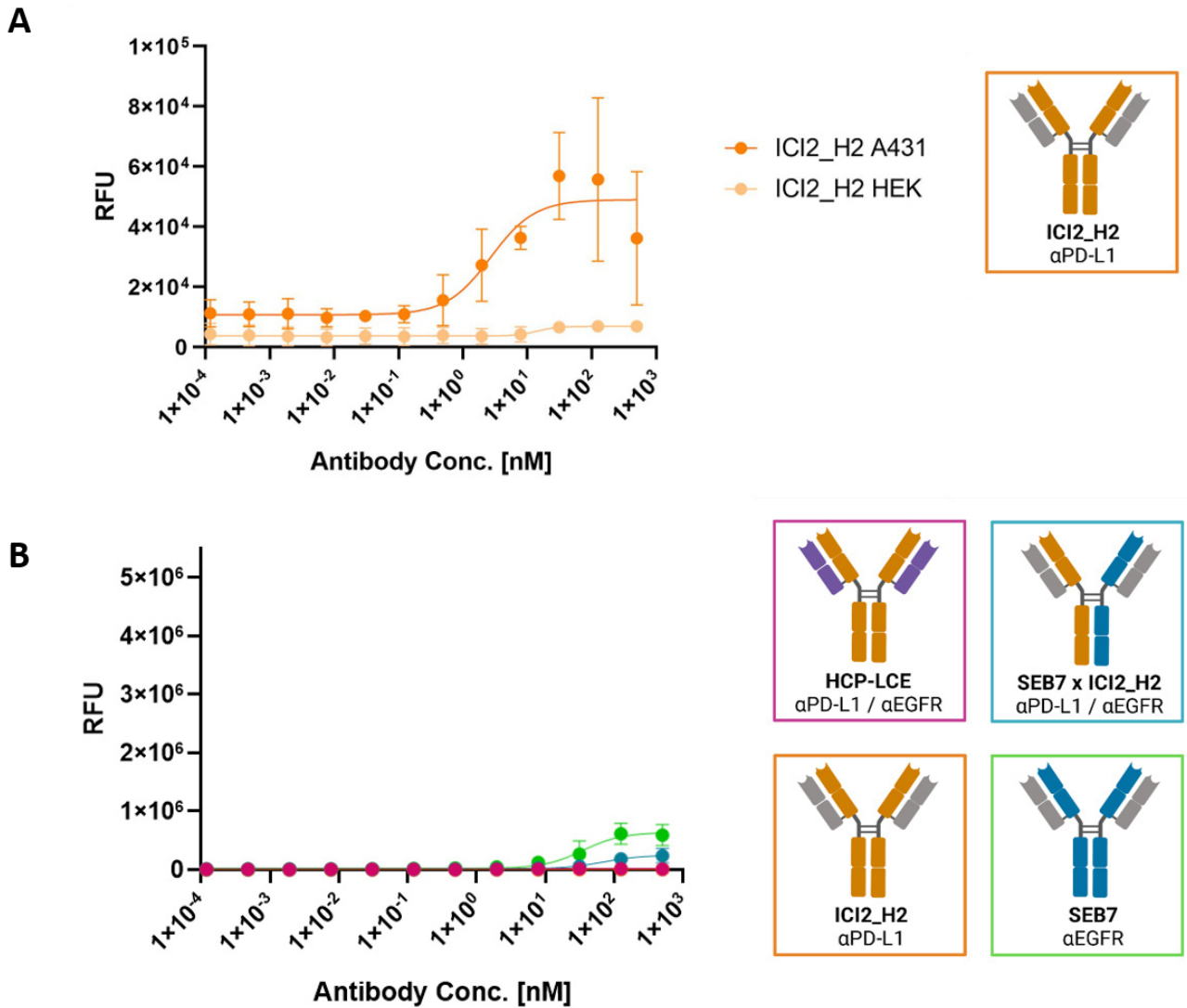
**Supplementary Figure 3.** Affinity measurements. Binding kinetics of SEB7, SEB7xICI2\_H2 and oaHCP-LCE to EGFR and PD-L1.



**Supplementary Figure 4.** SDS-PAGE analysis of ICI2\_H2, SEB7, HCP-LCE, SEB7xICI2\_H2, oaHCP-LCE and LCE under reducing conditions revealed high purity and the expected molecular weights.



**Supplementary Figure 5.** Characterization of HCP-LCE (pink), SEB7xICI2\_H2 (blue), ICI2\_H2 (orange), oaHCP-LCE (light pink) and LCE (grey). SEC profiles and NanoDSF measured melting temperatures.



**Supplementary Figure 6.** Cellular binding on A431 cells and HEK cells. A) Cell titration of ICI2\_H2 on EGFR/PD-L1 double positive A431 cells (orange) and on EGFR/PD-L1 double negative HEK cells (light orange). A variable slope four-parameter fit was utilized to fit the resulting curves. B) Cell titration of HCP-LCE, SEB7xICI2\_H2, ICI2\_H2 and SEB7 on EGFR/PD-L1 double negative HEK cells. The y-axis is chosen as in figure 6 for comparability of the graphs. A variable slope four-parameter fit was utilized to fit the resulting curves. The assay was repeated twice, yielding comparable results.

---

## 4.2. Generation of a symmetrical trispecific NK cell engager based on a two-in-one antibody

### Titel:

Generation of a symmetrical trispecific NK cell engager based on a two-in-one antibody

### Authors:

Julia Harwardt, Stefania Candela Carrara, Jan Patrick Bogen, Katrin Schoenfeld, Julius Grzeschik, Björn Hock and Harald Kolmar

### Bibliographic data:

Journal – Frontiers in Immunology

Volume 14 – 2023

Article published online: 04 April 2023

DOI: 10.3389/fimmu.2023.1170042

Copyright © 2023 Harwardt, Carrara, Bogen, Schoenfeld, Grzeschik, Hock and Kolmar. This is an open-access article distributed under the terms of the Creative Commons Attribution License (CC BY).

### Contributions by J. Harwardt:

- Literature search and conceptual design
- Design and planning of experiments
- Generation and screening of the library
- Reformatting and characterization of trispecific antibody variants
- Design and generation of all figures
- Writing of manuscript together with H. Kolmar



## OPEN ACCESS

## EDITED BY

Gabriella Palmieri,  
Sapienza University of Rome, Italy

## REVIEWED BY

Peter R. Lowe,  
Merus N.V., Netherlands  
Maite Alvarez,  
University of Navarra, Spain  
Brigitte Kerfelec,  
U1068 Centre de Recherche en  
Cancérologie de Marseille (CRCM)  
(INSERM), France  
Longlong Luo,  
Beijing Institute of Pharmacology and  
Toxicology, China

## \*CORRESPONDENCE

Harald Kolmar  
✉ harald.kolmar@tu-darmstadt.de

## SPECIALTY SECTION

This article was submitted to  
Cancer Immunity  
and Immunotherapy,  
a section of the journal  
Frontiers in Immunology

RECEIVED 20 February 2023

ACCEPTED 21 March 2023

PUBLISHED 04 April 2023

## CITATION

Harwardt J, Carrara SC, Bogen JP,  
Schoenfeld K, Grzeschik J, Hock B and  
Kolmar H (2023) Generation of a  
symmetrical trispecific NK cell engager  
based on a two-in-one antibody.  
*Front. Immunol.* 14:1170042.  
doi: 10.3389/fimmu.2023.1170042

## COPYRIGHT

© 2023 Harwardt, Carrara, Bogen,  
Schoenfeld, Grzeschik, Hock and Kolmar.  
This is an open-access article distributed  
under the terms of the [Creative Commons  
Attribution License \(CC BY\)](https://creativecommons.org/licenses/by/4.0/). The use,  
distribution or reproduction in other  
forums is permitted, provided the original  
author(s) and the copyright owner(s) are  
credited and that the original publication in  
this journal is cited, in accordance with  
accepted academic practice. No use,  
distribution or reproduction is permitted  
which does not comply with these terms.

# Generation of a symmetrical trispecific NK cell engager based on a two-in-one antibody

Julia Harwardt<sup>1</sup>, Stefania C. Carrara<sup>1,2</sup>, Jan P. Bogen<sup>1,2</sup>,  
Katrin Schoenfeld<sup>1</sup>, Julius Grzeschik<sup>3</sup>, Björn Hock<sup>1</sup>  
and Harald Kolmar<sup>1,4\*</sup>

<sup>1</sup>Institute for Organic Chemistry and Biochemistry, Technical University of Darmstadt, Darmstadt, Germany, <sup>2</sup>Biologics Technology and Development, Ferring Darmstadt Laboratory, Darmstadt, Germany, <sup>3</sup>Biologics Technology and Development, Ferring Biologics Innovation Centre, Epalinges, Switzerland, <sup>4</sup>Centre for Synthetic Biology, Technical University of Darmstadt, Darmstadt, Germany

To construct a trispecific IgG-like antibody at least three different binding moieties need to be combined, which results in a complex architecture and challenging production of these molecules. Here we report for the first time the construction of trispecific natural killer cell engagers based on a previously reported two-in-one antibody combined with a novel anti-CD16a common light chain module identified by yeast surface display (YSD) screening of chicken-derived immune libraries. The resulting antibodies simultaneously target epidermal growth factor receptor (EGFR), programmed death-ligand 1 (PD-L1) and CD16a with two Fab fragments, resulting in specific cellular binding properties on EGFR/PD-L1 double positive tumor cells and a potent ADCC effect. This study paves the way for further development of multispecific therapeutic antibodies derived from avian immunization with desired target combinations, valencies, molecular symmetries and architectures.

## KEYWORDS

trispecific antibody, two-in-one antibody, NK cell engager, common light chain, yeast surface display

## Introduction

While monoclonal antibodies (mAbs) have tremendous potential for treating a variety of diseases, certain modes of action require two different cells to be positioned in close proximity to achieve the desired therapeutic effect. Due to their monospecificity, this is not possible with a mAb or combination therapy, but can be achieved by combining antibody-like fragments in one molecule (1, 2). Since the first proposition of bispecific antibodies (bsAbs) targeting two independent epitopes in the 1960s (3), they have been extensively explored in translational and clinical studies (4, 5).

One possible mode of action for bsAbs, which are referred to as NK cell engager (NKCE), is the recruitment of natural killer (NK) cells by simultaneously binding to a

tumor-associated antigen (TAA) and a specific marker on the surface of NK cells to harness the immune function of NK cells in tumor therapy (6).

Among many other proteins, NK cells express CD16a, also known as Fc $\gamma$ RIIIa, which is targeted with low affinity by the Fc region of TAA-bound IgG antibodies (7). These IgG molecules can thus mediate antibody-dependent cellular cytotoxicity (ADCC), an effective mechanism for tumor cell killing by NK cells (8). The anti-CD20 antibody rituximab was the first cytotoxic ADCC-capable mAb to be approved for the treatment of non-Hodgkin's lymphoma in 1997 (9). Since then, more than 30 cytotoxic antibodies have been developed (10) and considerable efforts have been made to increase the efficacy of these therapeutic antibodies by Fc engineering (11). Preclinical models and clinical outcome of patients have shown that ADCC is one of the most important mechanisms contributing to the therapeutic effect of many approved antibodies, including rituximab, cetuximab and trastuzumab (12). Thereby, binding affinity to CD16a seems to be an important component. The 158V isoform of CD16a, which mediates a stronger binding to IgG1 Fcs compared to its 158F counterpart, has been shown to be positively associated with clinical outcome in patients (13, 14).

To further increase affinity and cytotoxicity, antibody-like molecules have been developed that target CD16a with higher affinity than the wild-type Fc of an IgG1 antibody (15). An example of this are bispecific killer cell engagers (BiKEs) targeting CD16a with one binding arm and a TAA with the other e.g. Epithelial Cell Adhesion Molecule (EpCAM) (16) or CD133 (17), respectively. Trispecific killer engagers (TriKEs) are an improved version of BiKEs with CD16a and TAA targeting single chain variable fragments (scFvs) cross-linked with a human IL-15 moiety, having an additional stimulatory effect on NK cell proliferation and activation (18). Innate Pharma is developing trifunctional NKCEs consisting of antibody fragments targeting two NK cell-activating receptors, CD16a and NKp46, and one TAA including CD19, CD20 and EGFR (19). Some approaches utilize two CD16a engaging binding moieties. The company Affimed has introduced its bispecific ROCK<sup>®</sup> (Redirected Optimized Cell Killing) antibody platform into the clinic. This platform is based on a tetravalent bispecific antibody consisting of altogether four diabodies with two fragment variable (Fv) domains against CD16a and a TAA (20).

One TAA that has already shown impressive outcomes *in vitro* and *in vivo* in combination with CD16a as an NKCE (19) and has even been clinically validated in phase 1/2a clinical trials (AFM24, NCT 04259450) as part of the bispecific ROCK<sup>®</sup> platform (20) is epidermal growth factor receptor (EGFR). Overexpression of EGFR has been reported in a variety of cancers, where it is involved in tumor progression and metastasis (21–23).

Furthermore, AFM24 is also being investigated in phase 1/2a clinical trials in combination with atezolizumab, an anti-programmed death-ligand 1 (PD-L1) antibody (NCT05109442). PD-L1 is overexpressed in many malignancies and represents a mechanism by which cancer evades immune surveillance (24, 25). Moreover, NK cell activity can be negatively affected by immune checkpoints such as PD-1/PD-L1 axis (26). Therefore, the combination of targeting CD16a,

EGFR and PD-L1 could provide significant clinical benefit also in view of the recently reported finding that tumor-specificity can be elevated by simultaneous targeting EGFR and PD-L1 by a bispecific antibody (27).

Recently, we reported the isolation of a chicken-derived two-in-one antibody (HCP-LCE) targeting EGFR and PD-L1 with two independent paratopes on a single Fab (28). Unlike classical IgG-like bispecific antibodies that require heterodimerization of the heavy chains and correct light chain pairing (29), two-in-one antibodies are symmetrical molecules consisting of two identical heavy and light chains (30). Consequently, they can be produced without engineering of constant chains, eliminating the need to incorporate unnaturally occurring amino acids as found in knob-into-hole antibodies (31) or orthogonal Fab interfaces (32). This chicken-derived two-in-one antibody inhibits EGFR signaling by binding to dimerization domain II and blocks the PD-1/PD-L1 interaction (28). Notably, while individual affinities to EGFR and PD-L1 are moderate with  $K_D$  values in the triple and double digit nanomolar range, the two-in-one combined antibody displays high affinity binding to cells expressing both targets (28).

Although most approved therapeutic antibodies have been generated using rodent immunization (33), immunization of chickens has gained interest in the scientific community. Due to the wider phylogenetic distance from humans, chicken immunization may result in antibodies targeting epitopes not accessible upon immunization of rodents (34, 35). In addition, gene diversification in birds allows library generation with a single set of primers, significantly reducing hands-on time and costs compared to rodents (36). Subsequently, chicken-derived antibodies with high affinity can be isolated using yeast surface display (YSD) in combination with fluorescence-activated cell sorting (FACS) (36–38).

In this study, we describe the construction and characterization of a symmetric trispecific common light chain antibody based on a previously identified two-in-one antibody targeting EGFR and PD-L1. By utilization of the light chain of this two-in-one antibody as a common light chain (cLC) in a chicken-derived anti-CD16a immune heavy chain library, a novel CD16a engaging cLC antibody was identified and subsequently fused in a head-to-tail setup with the parental two-in-one antibody. The resulting trispecific antibody (HC16-HCP) has the ability to simultaneously bind PD-L1, EGFR and CD16a with six independent paratopes on four single Fabs, without additional engineering of the CDR regions and in a generic, symmetrical architecture. Comparable to the two-in-one antibody HCP-LCE, it exhibits specific cellular binding on EGFR and PD-L1 double positive tumor cells, blocks the PD-1/PD-L1 axis and mediates a potent ADCC effect as an NKCE. This work paves the way for the generation of chicken-derived trispecific common light chain immune cell engager molecules in a straightforward manner and facilitates subsequent process development through its symmetrical architecture.

## Results

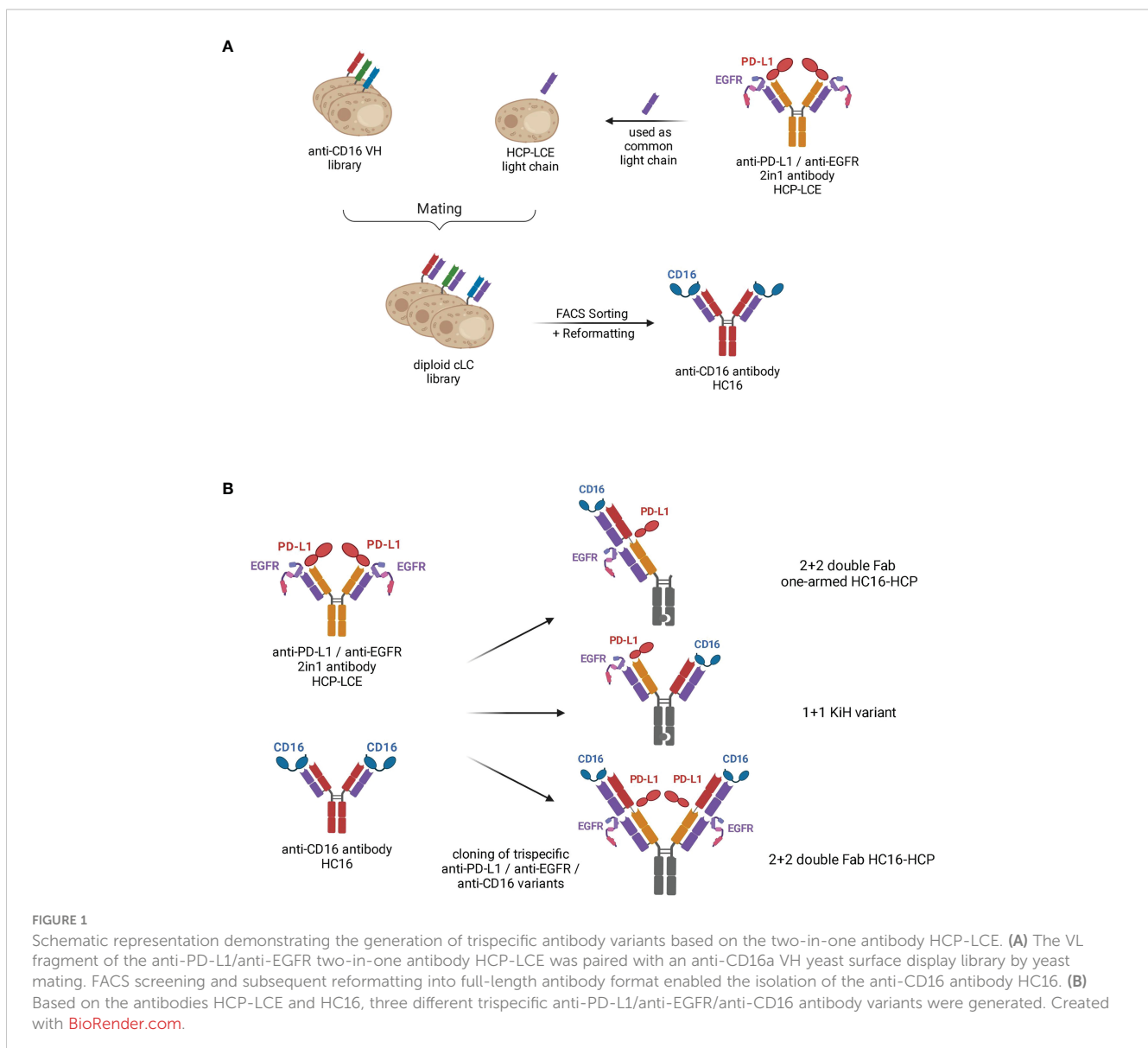
### Library generation and screening

Recently, we isolated a chicken-derived two-in-one antibody (HCP-LCE) that simultaneously targets EGFR and PD-L1 with the

same Fv region (28). Notably, additional studies revealed that the two-in-one antibody targets keratinocytes and fibroblasts with a lower on-cell affinity than cetuximab (Supplementary Figures 1A, B). Therefore, HCP-LCE may be expected to cause milder side effects compared to EGFR high affinity binding antibodies such as cetuximab, for which the main side effect is skin toxicity, including rash, dry skin, hair growth disturbances and nail changes (39, 40). Based on its ability to inhibit EGFR signaling by binding to dimerization domain II, block the PD-1/PD-L1 interaction and mediate specific cellular recognition to EGFR/PD-L1 double-positive tumor cells, HCP-LCE was chosen as a starting molecule to introduce a NK cell engaging module. Since the most straightforward approach to circumvent light chain pairing problems in multispecific antibodies is the use of a common light chain that pairs with all VH moieties (41, 42), the HCP-LCE light chain was combined with a VH library from chickens immunized with the CD16a extracellular domain aimed at screening for high affinity binders (Figure 1). To this end, the heavy chain yeast surface display library was generated

by amplification of VH genes from cDNA derived from a chicken immunized with CD16a-Fc and boosted with monomeric CD16a and subsequently inserted into a pYD<sub>1</sub>-derived vector encoding a human CH<sub>1</sub> domain by homologous recombination in EBY100 yeast, as previously described (43). The heavy chain diversity was combined with BJ5464 yeast cells encoding the HCP-LCE VL-CL $\lambda$  fragment by yeast mating (Figure 1), resulting in an estimated library size of  $4 \times 10^8$  variants.

The diploid common light chain yeast library was screened by FACS over four consecutive sorting rounds using His<sub>6</sub>-tagged monomeric CD16a, resulting in an enrichment of a binding population (Supplementary Figure 2A). Sequence analysis of eight randomly chosen clones revealed one distinct VH sequence, which was enriched during the sorting process. The isolated anti-CD16a antibody is referred to as HC16. Binding to the His<sub>6</sub>-Tag of the protein could be excluded by binding analysis of a yeast single clone to an unrelated His<sub>6</sub>-tagged protein (Supplementary Figure 2B).



## Cloning and biophysical characterization of trispecific antibodies

For the generation of EGFR, PD-L1 and CD16a targeting antibody variants, Fab fragments of the two-in-one antibody HCP-LCE and the anti-CD16a antibody HC16 were fused in a head-to-tail setup into a 2 + 2 double Fab format (termed HC16-HCP) and an 1 + 1 IgG-like format (termed KiH variant) *via* Golden Gate Cloning. For the symmetrical 2 + 2 variant HC16-HCP, similar to a Fabs-in-tandem immunoglobulin (FIT-Ig) (44), two Fabs were located on each heavy chain, connected by a flexible linker. Contrary to the crisscross orientation of the FIT-Igs (44), the VH of the inner Fab was connected to the CH<sub>1</sub> domain of the outer Fab. Since the light chains were identical for each binding moiety of the 2 + 2 variant HC16-HCP, the possibility of mismatch between heavy and light chains was eliminated. The Fc exhibited the LALA mutation to circumvent Fc : CD16a-interactions (45, 46). Following production in Expi293F cells, HC16-HCP was purified like a conventional IgG *via* Protein A affinity chromatography due to its symmetrical architecture, circumventing the need to include unnaturally occurring amino acid sequences in constant chains as found in knob-into-hole antibodies or orthogonal Fab interfaces (31). In addition, a trispecific 1 + 1 variant (KiH variant; Figure 1) and a one-armed double Fab HC16-HCP variant (termed oaHC16-HCP) were generated in which the Fc fragments exhibited the knob-into-hole mutations to force heterodimerization of the heavy chains (31). To ensure the isolation of heterodimers only, a TwinStrepII-Tag was fused to the C-terminus of the Knob heavy chain (HC), whereas a His<sub>6</sub>-Tag was placed C-terminally to the Hole-HC, enabling two-step purification *via* IMAC followed by StrepTactin purification as previously described (28).

SDS-PAGE analysis revealed the presence of all expected heavy and light chains under reducing conditions, as well as the expected molecular size under non-reducing conditions without degradation products (Supplementary Figure 3A). For the KiH variant, the two heavy chains run higher than the unmodified two-in-one HCP-LCE heavy chains, due to the additional Twin-StrepII- and His<sub>6</sub>-tag used for purification. The significantly higher molecular weight of the 2 + 2 variant HC16-HCP compared to a full-length antibody was

confirmed during size-exclusion chromatography (SEC) by the lower retention time. SEC profiles demonstrated that HC16-HCP exhibited favorable properties with almost no measurable aggregation (Supplementary Figure 3B). Thermostability investigated by SYPRO Orange revealed melting temperatures between 64.0°C and 66.0°C, with the parental antibodies HCP-LCE and HC16 exhibiting 58.9°C and 61.5°C respectively, indicating no reduction in thermal stability (Table 1).

## Affinity measurement

BLI measurements were performed to determine the affinity of the different trispecific variants to all three targets of interest. All three antibody variants were able to target CD16a as well as EGFR and PD-L1 (Figure 2A). The binding affinities to EGFR and PD-L1 were in similar ranges to those previously published for the two-in-one antibody HCP-LCE (28). This suggests that the outer CD16a targeting Fab arm does not significantly interfere with EGFR and PD-L1 binding of the inner two-in-one Fab arm of the 2 + 2 variant HC16-HCP and the oaHC16-HCP variant. The parental antibody HC16 exclusively targeted CD16a with a K<sub>D</sub> value of 18 nM and exhibited no binding to EGFR (Supplementary Figure 4). The binding affinities of the trispecific variants to CD16a were in similar ranges to that of the parental antibody (Figure 2). This supports the notion that EGFR binding of the HCP-LCE light chain is supported by the presence of the anti-PD-L1 heavy chain (28).

In order to maintain tumor selectivity of the two-in-one antibody and additionally obtain effector cell recruitment, simultaneous binding to all three targets is essential. To analyze whether CD16a, EGFR and PD-L1 can be targeted simultaneously with two Fab arms, the KiH variant and the double Fab oaHC16-HCP variant were loaded onto anti-human IgG Fc Capture (AHC) biosensors and incubated sequentially with the target proteins of interest. Here, it was important to use the one-armed variant, since the symmetrical 2 + 2 HC16-HCP is hexavalent. Binding to PD-L1 first, EGFR second and CD16a third was considered (Figure 2B). Both variants were able to bind all three targets simultaneously with two Fab fragments, supporting the suggestion that the outer Fab arms does not disrupt the EGFR and PD-L1 binding properties of the two-in-one Fab.

TABLE 1 Biophysical properties of HCP-LCE, HC16-HCP, oaHC16-HCP, KiH including affinity, kinetic binding rates and melting temperatures.

Antibody	K <sub>D</sub> [nM]			k <sub>on</sub> [M <sup>-1</sup> s <sup>-1</sup> ]			k <sub>dis</sub> [s <sup>-1</sup> ]			T <sub>M</sub> [°C]
	EGFR	PD-L1	CD16a	EGFR	PD-L1	CD16a	EGFR	PD-L1	CD16a	
HC16-HCP	331 ± 29.9	68.0 ± 1.82	17 ± 0.21	5.06 × 10 <sup>5</sup> ± 3.39 × 10 <sup>4</sup>	7.75 × 10 <sup>5</sup> ± 1.58 × 10 <sup>4</sup>	1.37 × 10 <sup>5</sup> ± 1.14 × 10 <sup>3</sup>	1.68 × 10 <sup>-1</sup> ±	5.26 × 10 <sup>-2</sup> ± 9.16 × 10 <sup>-4</sup>	2.33 × 10 <sup>-3</sup> ± 2.14 × 10 <sup>-5</sup>	66.0°C
oaHC16-HCP	463 ± 51.2	64.8 ± 1.84	19.9 ± 2.01	4.22 × 10 <sup>5</sup> ± 3.5 × 10 <sup>4</sup>	8.83 × 10 <sup>5</sup> ± 1.90 × 10 <sup>4</sup>	1.36 × 10 <sup>5</sup> ± 9.76 × 10 <sup>2</sup>	1.96 × 10 <sup>-1</sup> ± 1.43 × 10 <sup>-2</sup>	5.73 × 10 <sup>-2</sup> ± 1.06 × 10 <sup>-3</sup>	2.70 × 10 <sup>-3</sup> ± 1.91 × 10 <sup>-5</sup>	64.0°C
KiH	320 ± 26.8	57.7 ± 4.10	21.9 ± 0.23	5.63 × 10 <sup>5</sup> ± 3.50 × 10 <sup>4</sup>	1.17 × 10 <sup>6</sup> ± 6.24 × 10 <sup>4</sup>	1.14 × 10 <sup>5</sup> ± 1.07 × 10 <sup>3</sup>	1.80 × 10 <sup>-1</sup> ± 1.01 × 10 <sup>-2</sup>	6.76 × 10 <sup>-2</sup> ± 3.17 × 10 <sup>-3</sup>	3.09 × 10 <sup>-3</sup> ± 2.10 × 10 <sup>-5</sup>	64.5°C
HC16	-	-	18.3 ± 0.20	-	-	1.55 × 10 <sup>5</sup> ± 1.23 × 10 <sup>3</sup>	-	-	2.83 × 10 <sup>-3</sup> ± 2.14 × 10 <sup>-5</sup>	61.5°C
HCP-LCE	236 ± 10.7	78.3 ± 1.36	-	4.15 × 10 <sup>5</sup> ± 1.58 × 10 <sup>4</sup>	9.73 × 10 <sup>5</sup> ± 1.37 × 10 <sup>4</sup>	-	9.81 × 10 <sup>-2</sup> ± 2.41 × 10 <sup>-3</sup>	7.62 × 10 <sup>-2</sup> ± 7.78 × 10 <sup>-4</sup>	-	58.9°C



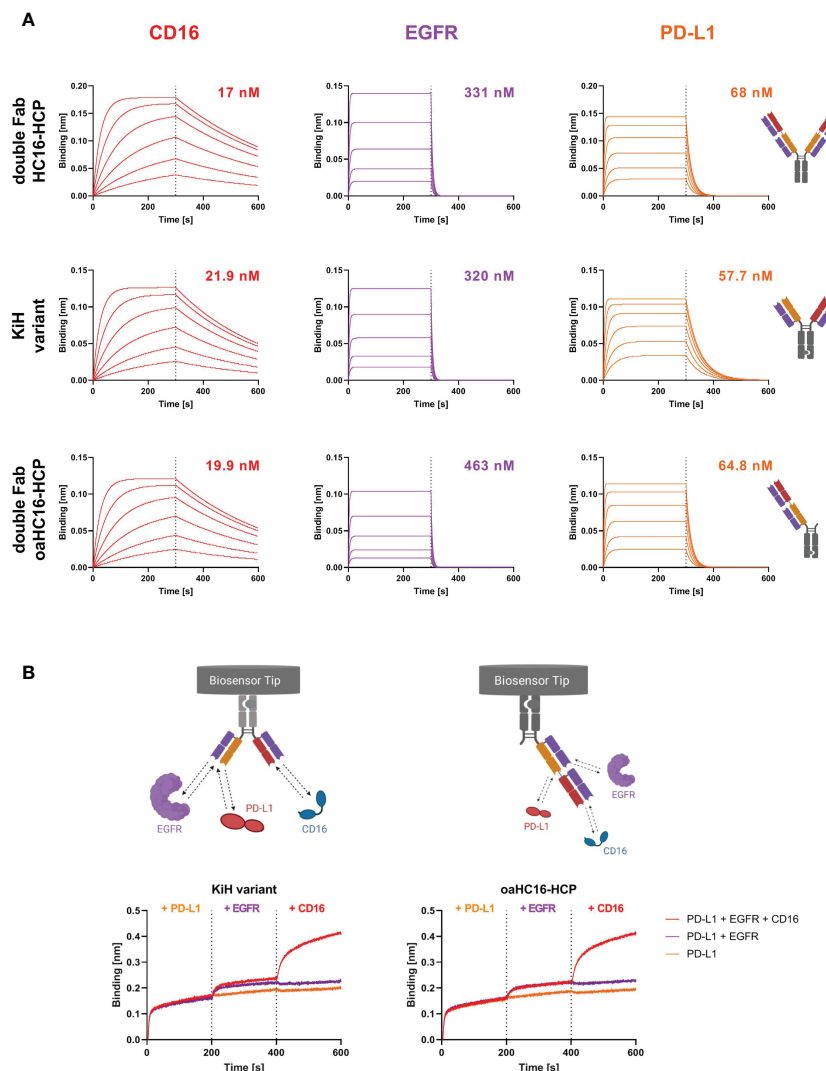


FIGURE 2

Characterization of antigen binding of the trispecific antibody variants by BLI-measurements. **(A)** BLI-measurements of the double Fab variant HC16-HCP, the knob-into-hole (KiH) variant and the one-armed (oa) double Fab variant oaHC16-HCP against CD16a, EGFR and PD-L1. All antibody variants target the three respective antigens with comparable  $K_D$  values. **(B)** BLI-assisted simultaneous binding assay. The KiH variant and the oa double Fab variant were loaded onto AHC biosensors and antigens were added stepwise, demonstrating simultaneous PD-L1, EGFR and CD16a binding. Created with [BioRender.com](https://www.biorender.com).

## EGF and PD-1 competition

To study whether not only the binding kinetics of the two-in-one antibody were preserved but also the antibody-mediated ligand receptor blocking properties, BLI-assisted competition assays were performed. To investigate PD-1/PD-L1 competition, the respective antibodies were loaded onto FAB2G biosensors and associated with 250 nM PD-L1 preincubated with either 250 nM or 1000 nM PD-1-Fc. Binding of both trispecific antibody variants to PD-L1 was significantly impaired in the presence of PD-1 (Figure 3A), suggesting that the ability of the two-in-one antibody to target and block the PD-1/PD-L1 interaction site is preserved.

HCP-LCE targets EGFR domain II, which is involved in receptor dimerization (28, 47). Since EGF binds simultaneously to EGFR domains I and III, the antibody does not block the EGF/

EGFR interaction. Ligand binding and EGFR dimerization are essential for full EGFR activation, so HCP-LCE inhibits EGFR signaling by inhibiting dimerization of EGFR. For analysis of EGF competition, AHC biosensors were loaded with the respective antibody and associated with 250 nM EGFR preincubated with 250 nM or 1000 nM monomeric EGF. Binding of the antibodies to the EGFR/EGF complex resulted in an increase in layer thickness compared with binding to EGFR alone (Figure 3B), indicating that both trispecific antibodies, like the two-in-one antibody, do not target the interaction site of EGF and EGFR.

## Cellular EGFR and PD-L1 binding

To ensure that the 2 + 2 HC16-HCP variant shows comparable tumor-targeting to the two-in-one antibody HCP-LCE, cellular binding

experiments were performed on EGFR/PD-L1 double positive A431 and A549 cells by flow cytometry. Cells were stained with the respective antibodies at a concentration ranging from 0.1 pM to 80 nM for A431 cells and from 5.12 pM to 80 nM for A549 cells utilizing a five-fold dilution series. Binding was verified using an anti-human Fc PE detection antibody. As a control, the cells were stained with the KiH variants at a concentration ranging from 0.1 pM to 400 nM for A431 cells and from 5.12 pM to 400 nM for A549 cells. The 2 + 2 antibody HC16-HCP exhibited cellular binding with an  $EC_{50}$  value of 0.68 nM on A431 cells and 1.49 nM on A549 cells, which was within the range of the two-in-one antibody (Figure 4). The  $EC_{50}$  values of the 1 + 1 KiH variant and the oaHC16-HCP were also in a similar range for both cell lines. However, the antibody variants consisting of only one two-in-one Fab exhibited a higher  $EC_{50}$  value by a factor of approximately 6 on A431 cells and about 30 on A549 cells (Figure 4). Since EGFR

expression on A431 cells is significantly higher than that on A549 cells (48), lower  $EC_{50}$  values were expected on A431 cells. The similar  $EC_{50}$  values of the antibodies HCP-LCE and HC16-HCP, as well as of the 1 + 1 KiH variant and oaHC16-HCP, were also in line with expectations, as they each consist of the same number of EGFR/PD-L1 binding Fab fragments. The different valency of EGFR/PD-L1 binding likely contributes to the lower  $EC_{50}$  value of the double Fab HC16-HCP variant, which, contrary to the KiH variants, targets the antigens bivalently instead of monovalently. Similarly, the lower binding maximum observed for the monovalent constructs was to be expected due to the lack of avidity effects. The antibodies did not show binding to EGFR/PD-L1 double negative Daudi cells, excluding non-specific cellular binding (Supplementary Figure 5). These data indicate that the tumor-targeting ability of the two-in-one Fab fragment remains functional even when another antibody fragment is fused to it. In

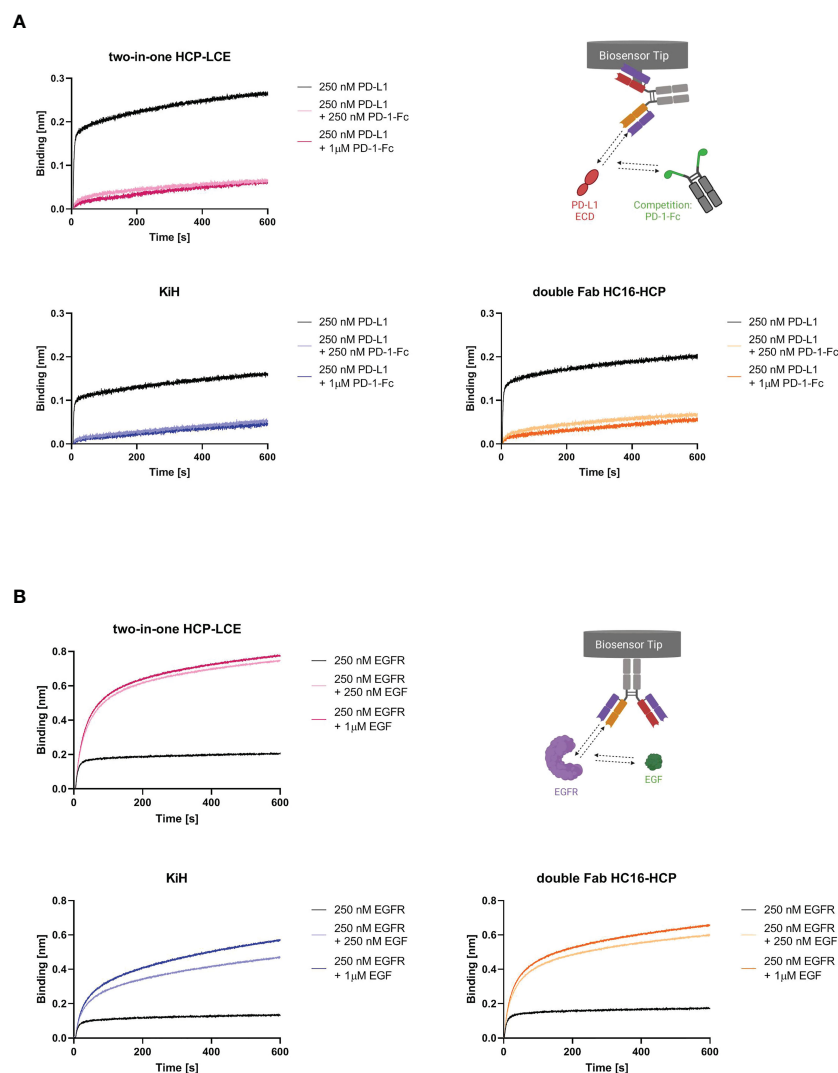


FIGURE 3

EGF and PD-1 competition assay by BLI. **(A)** BLI-assisted PD-1 competition assay. The two-in-one antibody HCP-LCE (pink), the KiH variant (blue) and the double Fab variant HC16-HCP (orange) were loaded onto FAB2G biosensors and subsequently associated to PD-L1 preincubated with varying PD-1 concentrations. Binding of the antibody variants to PD-L1 at different PD-1 concentrations reveal dose-dependent binding. **(B)** BLI-assisted EGF competition assay. The two-in-one antibody HCP-LCE (pink), the KiH variant (blue) and the double Fab variant HC16-HCP (orange) were loaded onto AHC biosensors and subsequently associated to EGFR preincubated with varying EGF concentrations. The trispesic antibody variants bind to EGFR despite EGF binding. Created with [BioRender.com](https://www.biorender.com).

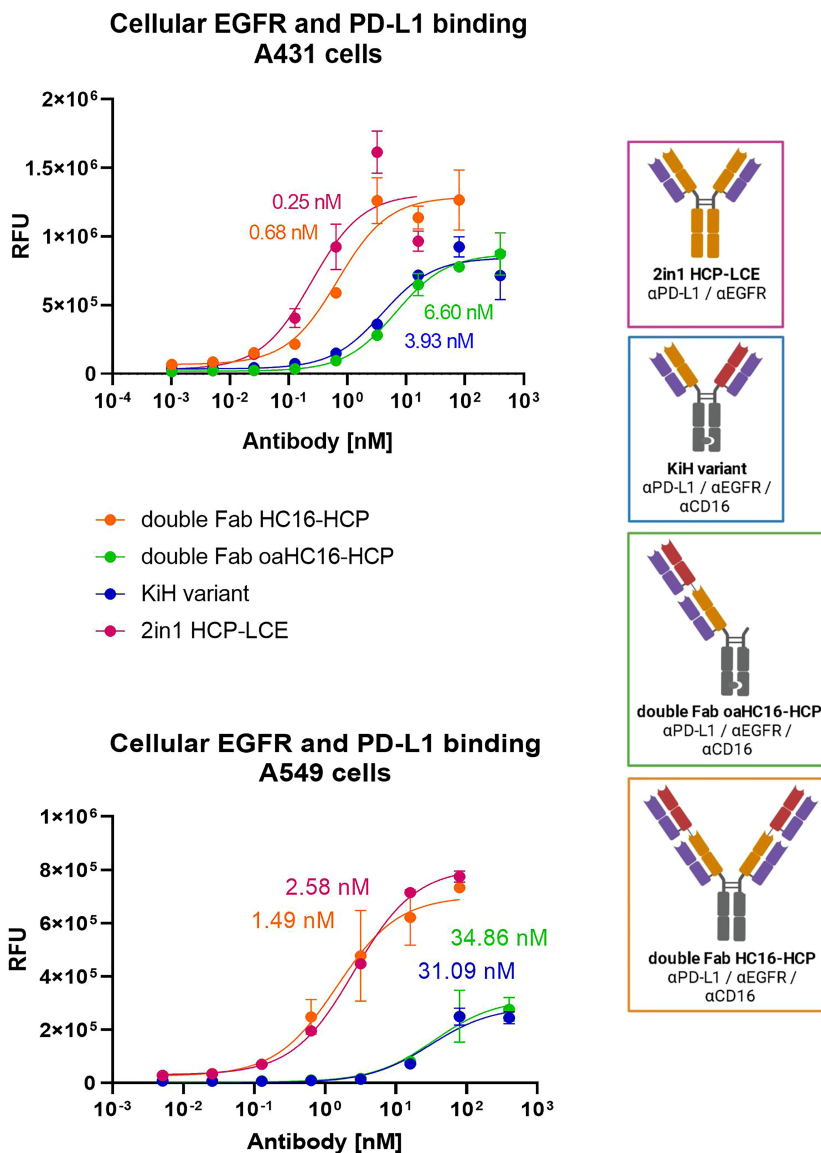


FIGURE 4

Cellular binding of trispecific variants on EGFR and PD-L1 double positive cells. Cell titration of double Fab HC16-HCP (orange), double Fab oaHC16-HCP (green), KiH variant (blue) and HCP-LCE (pink) on EGFR/PD-L1 double positive A431 and A549 cells. A variable slope three-parameter fit was used to fit the resulting curves. EC50 values of A431 cellular binding: HCP-LCE, 0.25 nM; HC16-HCP, 0.68 nM; KiH, 3.93 nM; oaHC16-HCP, 6.60 nM. EC50 values of A549 cellular binding: HCP-LCE, 2.58 nM; HC16-HCP, 1.49 nM; KiH, 31.09 nM; oaHC16-HCP, 34.86 nM. All measurements were performed in duplicates and the experiments were repeated at least three times, yielding similar results. Created with [BioRender.com](https://www.biorender.com).

addition, tumor selectivity is assumed to be maintained as demonstrated by cellular MRC-5 binding ([Supplementary Figure 1C](#)).

## Antibody-dependent cell-mediated cytotoxicity reporter assay

Fundamental aspects of an NK-cell engager are immune cell stimulation and cell killing. To compare the ADCC effect of the trispecific variants, the Promega ADCC luminescent reporter assay was used with EGFR/PD-L1 double-positive A431 cells as target cells. All variants contained the LALA mutation, except for

HCP-LCE were, additional to a LALA variant, an antibody with wild-type Fc was tested. As expected, HCP-LCE exhibiting the LALA mutation failed to mediate an ADCC effect even at high antibody concentrations. The 1 + 1 trispecific KiH variant mediated an ADCC effect that showed a two-fold higher induction than the bivalent EGFR and PD-L1 binding HCP-LCE exhibiting a wild-type IgG1 Fc. The 2 + 2 HC16-HCP trispecific showed the most potent ADCC effect, indicating the effector cell engaging properties of the anti-CD16a Fab fragment ([Figure 5](#)). No signal was detected in the absence of tumor cells, suggesting that HC16-HCP does not activate NK cells *via* CD16a cross-linking ([Supplementary Figure 6](#)).

In summary, the generated trispecific antibody of symmetric architecture (HC16-HCP) is able to simultaneously target PD-L1, EGFR and CD16a with six independent paratopes on four individual Fab fragments. Comparable to the two-in-one antibody HCP-LCE, it exhibits specific cellular binding to EGFR and PD-L1 double positive tumor cells, blocks the PD-1/PD-L1 axis and mediates a potent ADCC effect as an NKCE.

## Discussion

Trispecific antibodies are considered promising molecules since, compared to bispecific antibodies, the additional specificity expands the repertoire of targets and provides flexibility in designing the antigen binding valence. Consequently, trispecific antibodies are available in many different formats and target combinations (49–51).

In this study, we generated the first chicken-derived trispecific antibody based on a two-in-one antibody simultaneously targeting EGFR, PD-L1 and CD16a with two Fab fragments. To this end, the light chain of the chicken-derived EGFR and PD-L1 targeting two-in-one antibody HCP-LCE (28) was paired with a chicken-derived anti-CD16a heavy chain immune library by yeast mating. Isolation of the anti-CD16a antibody HC16 tolerating the common light chain was performed by four rounds of FACS-based selection using YSD. Based on the antibodies HCP-LCE and HC16, two different trispecific common light chain antibodies were generated, which differ in their structure and antigen binding valency. One of the two variants consists of a 2 + 2 format (HC16-HCP), while the KiH variant is constructed like a conventional 1 + 1 IgG-like antibody. The tumor-targeting ability of the two-in-one Fab fragment remained intact and the trispecific antibody variants additionally showed a potent ADCC effect.

Most trispecific antibodies consist of three independent monomeric antigen binding units (49, 50). Another trispecific antibody that resembles the structure of the 1 + 1 trispecific variant is the CD38×CD3×CD28 crossover variable domain (COVD) antibody SAR442257. Here, CD38 is targeted by a conventional Fab and the other arm consists of two linked Fv

fragments targeting CD3 and CD28 (52). SAR442257 is currently investigated in a phase I clinical trial (NCT04401020). The same molecular architecture was used by Xu et al. to generate an antibody that targets three different epitopes of HIV envelope (53). Nevertheless, the structure of the 1 + 1 trispecific variant resembles that of a natural IgG more closely, since it consists of two conventional Fab fragments. One advantage of a mAb-like structure is that immunogenicity is expected to be like that of a conventional mAb.

A class of antibodies close to the 2 + 2 trispecific HC16-HCP variant include FIT-Ig molecules (44). FIT-Igs are symmetrical and tetravalent IgG-like bispecific molecules, where two Fabs are fused directly in a crisscross orientation leading to correct VH/VL pairing. A similar structure results in similar advantages which include simple purification of homodimers using standard procedures without extensive optimization. FIT-Ig molecules demonstrate favorable drug-like properties, *in vitro* and *in vivo* functions, and efficient manufacturing for commercial development (44, 54), which is also expected for the 2 + 2 trispecific variant.

Remarkably, the inner HCP-LCE arm of the 2 + 2 variant exhibits binding kinetics comparable to the parental two-in-one antibody. Previous studies using 2 + 2 bispecific antibodies found that the affinity of some mAbs at the inner position decreased slightly, whereas no major effects on affinity were observed for other antibodies, which most likely depends on the shape of the paratope of the inner Fab (44, 54–56). This highlights the suitability of two-in-one antibodies for use in a 2 + 2 architecture. Interestingly, the newly isolated antibody HC16 carrying the two-in-one light chain exclusively targets CD16a, corroborating the notion that EGFR binding of the light chain is supported by the presence of the PD-L1 heavy chain (28), while no contribution to binding or even adverse effects are provided by the CD16a binding VH domain.

By utilizing the HCP-LCE Fab arm as tumor targeting fragment, the trispecific molecules of this study might have increased tumor selectivity. Koopmans and coworkers demonstrated elevated tumor specificity by an EGFR×PD-L1 antibody (27). Because of the comparatively low affinity of HCP-LCE to EGFR, increased target expression, which is predominantly found on tumor cells (57), is required for targeting of the antibody. The low binding affinity

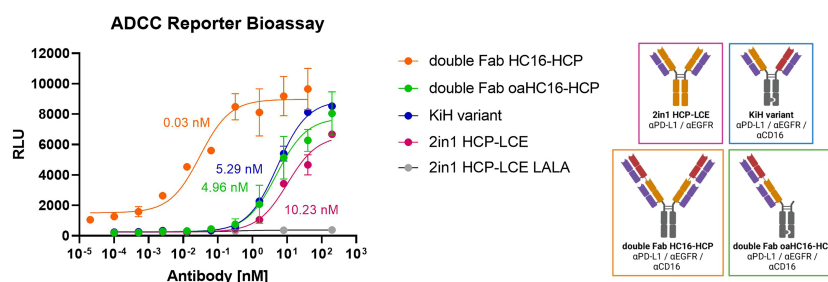


FIGURE 5

ADCC cell-based reporter assay. The trispecific constructs KiH (blue), HC16-HCP (orange), oaHC16-HCP (green) and HCP-LCE (grey) with the LALA mutation were tested in comparison to HCP-LCE with a wildtype IgG1 Fc (pink). EC<sub>50</sub> values: HC16-HCP, 0.03 nM; oaHC16-HCP, 4.96 nM; KiH, 5.29 nM; HCP-LCE, 10.23 nM. Luciferase activity is plotted against the logarithmic antibody concentration. A variable slope three-parameter fit was used to fit the resulting curves. All measurements were performed in duplicates and the experiment was repeated at least three times, yielding similar results. Created with [BioRender.com](https://www.biorender.com).

could cause EGFR binding exclusively on cells that additionally express PD-L1 due to spatial proximity and local concentration, based on the same concept described for bispecific antibodies targeting CD47 (58–60). This notion is supported by the lower on-cell affinity to MRC-5 and NHEK cells compared to cetuximab. The associated increased tumor selectivity would lead to a more favorable safety profile of the trispecific antibodies.

The design of the two reported trispecific antibody variants varies mainly in their valency towards EGFR, PD-L1 and CD16a, with 2 + 2 HC16-HCP binding bivalently and 1 + 1 variant only monovalently. The effect of bivalent target binding was primarily seen in the cellular binding assay on EGFR and PD-L1 double positive cells, which resulted in lower EC<sub>50</sub> values. In addition, a significant more potent ADCC effect was observed with bivalent CD16a binding.

Bivalent targeting of CD16a by the 2 + 2 variant HC16-HCP might result in NK cell fratricide after crosslinking two NK cells. Preclinical studies with NKCEs and TriKEs have reported low/no NK cell-mediated fratricide in *in vitro* cytotoxicity assays despite the potential co-engagement of CD16a or NKP46/CD16a on separate NK cells (19, 20). Moreover, the use of an effector-competent Fc could induce even stronger NK cell activation. However, NK cell activity also depends on the distance between target and effector cell (61–63). Therefore, an anti-CD16a Fab adjacent to the tumor arm targeting NK cells might mediate a more favorable distance between target and effector cells than an Fc.

In summary, the trifunctional antibodies exhibit the following properties: i) dual tumor-targeting by EGFR and PD-L1 binding to increase tumor selectivity, ii) immune checkpoint inhibition by blocking the PD-1/PD-L1 axis, and iii) potent NK cell-mediated cytotoxicity by CD16a targeting (Figure 6). As a result, the symmetrical 2 + 2 antibody mediates tetravalent TAA binding and bivalent NK cell binding. To our knowledge, this is the first hexavalent antibody of this format. The advantages of the symmetrical 2 + 2 and the IgG-like 1 + 1 trispecific constructs may pave the way to generate more trispecific molecules based on a two-in-one antibody. In this context, different target combinations and modes of action are possible.

## Material and methods

### Plasmids and yeast strains

For yeast surface display, pYD<sub>1</sub>-derived vectors (Yeast Display Vector Kit, version D, #V835-01, Thermo Fisher Scientific) were used. The heavy chain encoding plasmid contained the AGA2 signal peptide, followed by the VH-CH<sub>1</sub> sequences and the AGA2 gene, a tryptophan auxotrophic marker and an ampicillin resistance. The light chain plasmid encoded an αMFPp8 signal sequence, followed by the HCP-LCE (28) VL-CLλ sequence, a leucine auxotrophic marker as well as a kanamycin resistance gene. Plasmid gene expression was controlled by the galactose-inducible promoter (GAL<sub>1</sub>). For soluble expression of full-length and double Fab chimeric antibodies, pTT5-derived vectors (64) encoding either the heavy or light chain constant domain were utilized. The KiH

variant was expressed using pTT5-derived vectors encoding the full-length chimeric antibody with either a knob or hole mutation (31) within the CH<sub>3</sub> sequence and a C-terminal His<sub>6</sub>- or Twin-StrepII-Tag, respectively. For the one-armed double Fab variant, a pTT5-derived vector encoding the Hinge CH<sub>2</sub>-CH<sub>3</sub> domain with a hole mutation and a C-terminal Twin-StrepII-Tag was used.

For Fab display, *Saccharomyces cerevisiae* strains EBY100 [MATa URA3-52 trp1 leu2Δ1 his3Δ200 pep4::HIS3 prb1Δ1.6R can1 GAL (pIU211:URA3)] (Thermo Fisher Scientific) and BJ5464 (MATα URA3-52 trp1 leu2Δ1his3Δ200 pep4::HIS3 prb1Δ1.6R can1 GAL) (American Type Culture Collection) were transformed with the plasmids containing the heavy and light chain genes, respectively. Cultivation of haploid and diploid yeasts in YPD, SD-CAA and SG-CAA media was performed as previously described (65).

### Library generation and sorting

For yeast library generation, the VL-CLλ fragment of the two-in-one antibody HCP-LCE (28) was combined with a chicken-derived anti-CD16a VH-CH<sub>1</sub> library (43). The HCP-LCE VL gene was amplified by PCR using Q5 polymerase (NEB) and the light chain pYD<sub>1</sub> vector was linearized utilizing BamHI-HF (NEB) and NheI-HF (NEB) according to the manufacturer's protocol. Homologous recombination of HCP-LCE VL gene in pYD<sub>1</sub> was performed in BJ5464 yeast cells according to the protocol described by Bernatuil et al. (65). In order to combine the anti-CD16a heavy chain diversity with the common HCP-LCE light chain for subsequent Fab display, yeast mating was performed as described previously (66).

For library sorting, the diploid yeast library was grown overnight in SD-Trp-Leu medium at 30°C and 120 rpm. The next day, cells were harvested by centrifugation and used to inoculate SG-Trp-Leu medium at an OD<sub>600</sub> of 1.0. After incubation at 30°C and 120 rpm overnight, cells were harvested by centrifugation, washed once with PBS-B [PBS + 0.1% (w/v) BSA], and incubated on ice with 1 μM or 200 nM biotinylated CD16a-His<sub>6</sub> (produced in-house) or CD16a-His<sub>6</sub> (produced in house) for 30 minutes. Following a PBS-B wash, cells were incubated with a goat anti-human-Lambda Alexa Fluor 647 F(ab')<sub>2</sub> antibody (SouthernBiotech, diluted 1:75) to detect Fab surface presentation and Streptavidin-APC conjugate (Thermo Fisher Scientific, diluted 1:75) or a 6x-His Tag antibody (Fisher Scientific, diluted 1:75) to detect target binding for 15 minutes on ice. An additional PBS-B wash step was followed by FACS screening of the cells using a Sony SH800S.

### Reformatting, expression and purification of full-length, one-armed and trispecific antibodies

Plasmid isolation from yeast cells was performed using the Zymoprep Yeast Plasmid Miniprep Kit (Zymo Research) according to the manufacturer's protocol. The isolated plasmids were transformed into *E. coli* XL1-Blue and sequenced at

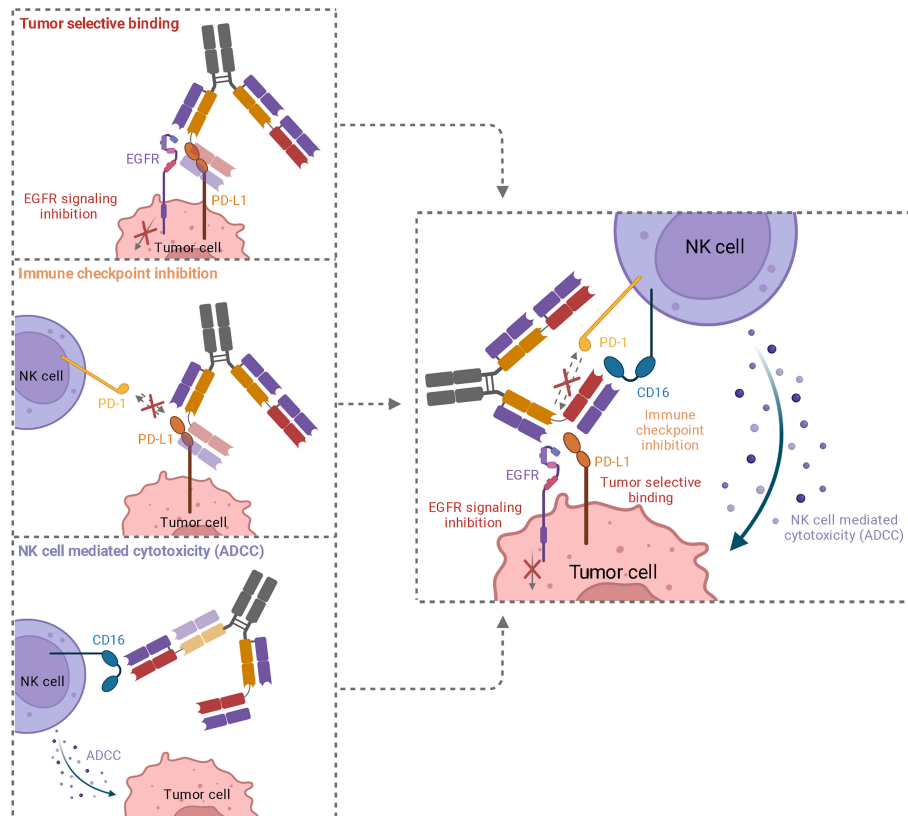


FIGURE 6

Schematic representation of the three functionalities of trispecific 2 + 2 antibody variant HC16-HCP. While simultaneous binding of EGFR and PD-L1 mediated an elevated tumor specificity, EGFR downstream signaling is inhibited and PD-L1 is blocked, inhibiting interaction with PD-1 on NK cells. The recruitment of cytotoxic NK cells *via* CD16a engagement leads to an effective ADCC.

Microsynth Seqlab (Göttingen). The resulting VH gene was amplified by PCR using Q5 polymerase (NEB) according to the manufacturer's protocol, incorporating *SapI* sites for subsequent Golden Gate cloning into pTT5-derived vectors as previously described (43). Expi293F cells (Thermo Fisher Scientific, A14527) were transiently transfected with Expifectamine293 (Thermo Fisher Scientific) for soluble expression following the manufacturer's instructions. The cells were cultured in Expi293 Expression medium (Thermo Fisher Scientific) at 37°C and 8.0% CO<sub>2</sub> at 110 rpm. For purification of full-length and double Fab antibodies, sterile-filtered cell culture supernatant was applied to a Protein A HP column (GE Healthcare) five days after transfection using an ÄKTA pure system (GE Healthcare). The KiH and one-armed variant were captured by IMAC (HisTrap HP, GE Healthcare), followed by Strep-Tactin XT affinity chromatography according to the manufacturer's protocol. Buffer exchange against PBS was performed using a HiTrap Desalting column (GE Healthcare).

### Affinity determination, receptor-ligand competition and simultaneous binding assay *via* biolayer interferometry

For affinity determination, anti-human IgG-Fc capture (AHC) biosensors were loaded with 10 µg/ml of the antibody of interest

until a layer thickness of 1 nm was reached. For the following steps kinetics buffer (KB, Sartorius) was used. Association was measured for 300 s using varying concentrations of EGFR-ECD, PD-L1-ECD or CD16a-ECD (produced in-house) ranging from 7.8 nM to 500 nM followed by dissociation for 300 s. Binding kinetics were determined based on Savitzky-Golay filtering and a 1:1 Langmuir binding model.

For the EGF competition assay, AHC biosensors were loaded with 10 µg/ml of the antibody of interest until a layer thickness of 1 nm was reached. Subsequently, 250 nM EGFR-ECD pre-incubated with either 0 nM, 250 nM or 1000 nM monomeric EGF was applied for 600 s.

For the PD-1 competition assay, anti-human Fab-CH1 2nd Generation (FAB2G) biosensors were loaded with 10 µg/ml of the antibody of interest until a layer thickness of 1 nm was reached. Subsequently, 250 nM PD-L1-ECD pre-incubated with either 0 nM, 250 nM or 1000 nM PD-1-Fc was applied for 600 s.

For the simultaneous binding assay, anti-human IgG-Fc capture (AHC) biosensors were loaded with 2 µg of the KiH variant or the one-armed variant until a layer thickness of 1 nm was reached. After measuring association to 250 nM PD-L1-ECD for 200 s, 250 nM EGFR-ECD followed by 250 nM CD16a-ECD were added stepwise, each for a period of 200 s.

All measurements were performed using the Octet RED96 system (FortéBio, Molecular Devices) at 30°C and 1000 rpm.

## Thermal stability, SDS-PAGE and size exclusion chromatography

To determine thermal stability, antibodies were incubated with SYPRO Orange (Thermo Fisher Scientific) and a thermal shift assay was performed using a CFX Connect Real-Time PCR System (BioRad). The temperature gradient was set from 10°C to 95°C with an increment of 0.5°C/10s. The derivatives of the melting curves were determined using the CFX Maestro software to calculate the melting temperature ( $T_M$ ).

SDS-PAGE analysis was performed to characterize the produced antibodies. For this purpose, 3 µg of purified antibody were loaded onto a Mini-PROTEAN TGX 4-15% gel (BioRad) with either reducing or non-reducing Laemmli buffer and subsequently stained with Coomassie.

Size exclusion chromatography (SEC) using a Superdex 200 increase 10/300 GL column (Cytiva) together with an ÄKTA pure system (GE Healthcare) was performed at a flow rate of 0.15 mL/min for 20 min.

## Cultivation of A431, A549, MRC-5 and Daudi cells

A431 (DSMZ ACC 91), A549 (DSMZ ACC 107) and MRC-5 (ATCC CCL-171) cells were cultured in Dulbecco's Eagle Medium (DMEM, Thermo Fisher), supplemented with 10% fetal bovine serum (FBS) superior (Merck Millipore) and 1x penicillin/streptomycin (Sigma Aldrich). Cells were cultured in T75 cell culture flasks at 37°C in a humidified atmosphere with 5% CO<sub>2</sub> and passaged every 3-4 days after reaching 80% confluence. Daudi cells were maintained in RPMI 1640 supplemented with 20% FBS and 1x penicillin/streptomycin. Cells were subcultured every 2-3 days and incubated at 37°C and 5% CO<sub>2</sub>. Ready-to-use NHEK cells (PromoCell) were utilized for cellular binding studies.

## Cellular binding assay

Cellular binding of the produced antibodies was determined by affinity titration using EGFR/PD-L1 double positive A431 and A549 cells as well as EGFR positive MRC-5 and NHEK cells. To this end, 10<sup>5</sup> cells/well were seeded in 96-well plates, washed with PBS-F [PBS + 2% (w/v) FBS] and subsequently incubated with the respective antibody in varying concentrations for 30 min on ice. Following another washing step, anti-human IgG-Fc PE-conjugated antibody was applied for 15 min. After washing, mean fluorescence was determined by flow cytometry using a CytoFLEX S (Beckman Coulter) and plotted against logarithmic antibody concentration. The resulting curves were fitted with a variable slope three-parameter fit using GraphPad Prism. All measurements were performed in duplicates, and the experiments were repeated at least three times, yielding comparable results. EGFR/PD-L1/CD16a triple negative Daudi cells were used to analyze nonspecific cellular binding.

## Antibody-dependent cell-mediated cytotoxicity (ADCC) reporter assay

The ADCC assay was performed using the Promega ADCC Reporter Bioassay Kit (G7010) according to the manufacturer's protocol. The day before the assay, 10,000 A431 cells were seeded into a 96-well plate. A five-fold serial dilution of the antibodies of interest was tested (0.1 pM – 200 nM). The double Fab variant was analyzed in the range of 0.02 pM – 40nM. The assay was performed at 37°C and 5% CO<sub>2</sub> for six hours. Luciferase activity was plotted against logarithmic antibody concentration and a variable slope four-parameter fit was used for fitting of the resulting curves.

## Data availability statement

The original contributions presented in the study are included in the article/[Supplementary Material](#). Further inquiries can be directed to the corresponding author.

## Author contributions

JH and HK conceived and designed the majority of experiments. JH and SC performed the experiments. JH, SC, JB, KS, and HK analyzed the data. JG and BH gave scientific advice. JH and HK wrote the manuscript. All authors contributed to the article and approved the submitted version.

## Funding

This work was supported by the Ferring Darmstadt Laboratories at Technical University of Darmstadt and by the department of GPRD at Ferring Holding S.A., Saint-Prex. The funders had no role in study design, data collection and analysis, interpretation of data, decision to publish, or preparation of the manuscript.

## Acknowledgments

We would like to thank the department of GPRD at Ferring Holding S.A., Saint-Prex for funding and instruments. We would also like to thank Michael Ullitzka and Janine Becker for technical assistance. We acknowledge support by the Deutsche Forschungsgemeinschaft (DFG-German Research Found) and the Open Access Publishing Fund of the Technical University of Darmstadt. Figures were created with BioRender.com.

## Conflict of interest

JG is an employee of Ferring Pharmaceuticals. JB and SC were employed by TU Darmstadt in frame of a collaboration project with

Ferring Pharmaceuticals. HK, JH, JB, and SC are inventors of a patent application related to the Two-in-One antibody HCP-LCE EP22159491.4.

The remaining authors declare that the research was conducted in the absence of any commercial or financial relationships that could be construed as a potential conflict of interest.

## Publisher's note

All claims expressed in this article are solely those of the authors and do not necessarily represent those of their affiliated

organizations, or those of the publisher, the editors and the reviewers. Any product that may be evaluated in this article, or claim that may be made by its manufacturer, is not guaranteed or endorsed by the publisher.

## Supplementary material

The Supplementary Material for this article can be found online at: <https://www.frontiersin.org/articles/10.3389/fimmu.2023.1170042/full#supplementary-material>

## References

- Fischer N, Léger O. Bispecific antibodies: Molecules that enable novel therapeutic strategies. *Pathobiology* (2007) 74(1):3–14. doi: 10.1159/000101046
- Thakur A, Huang M, Lum LG. Bispecific antibody based therapeutics: Strengths and challenges. *Blood Rev* (2018) 32(4):339–47. doi: 10.1016/j.blre.2018.02.004
- Nisonoff A, Wissler FC, Lipman LN. Properties of the major component of a peptic digest of rabbit antibody. *Science* (1960) 132(3441):1770–1. doi: 10.1126/science.132.3441.1770
- Wang S, Chen K, Lei Q, Ma P, Yuan AQ, Zhao Y, et al. The state of the art of bispecific antibodies for treating human malignancies. *EMBO Mol Med* (2021) 13(9):e14291. doi: 10.15252/emmm.202114291
- Rader C. Bispecific antibodies in cancer immunotherapy. *Curr Opin Biotechnol* (2020) 65:9–16. doi: 10.1016/j.copbio.2019.11.020
- Demaria O, Gauthier L, Debroas G, Vivier E. Natural killer cell engagers in cancer immunotherapy: Next generation of immuno-oncology treatments. *Eur J Immunol* (2021) 51(8):1934–42. doi: 10.1002/eji.202048953
- Khan M, Arooj S, Wang H. NK cell-based immune checkpoint inhibition. *Front Immunol* (2020) 11. doi: 10.3389/fimmu.2020.00167
- Yeap WH, Wong KL, Shimasaki N, Teo ECY, Quek JKS, Yong HX, et al. CD16 is indispensable for antibody-dependent cellular cytotoxicity by human monocytes. *Sci Rep* (2016) 6(1):34310. doi: 10.1038/srep34310
- Molina A. A decade of rituximab: Improving survival outcomes in non-hodgkin's lymphoma. *Annu Rev Med* (2008) 59(1):237–50. doi: 10.1146/annurev.med.59.060906.220345
- Kaplan H, Muralidharan M, Schneider Z, Reichert JM. Antibodies to watch in 2020. *MAbs* (2020) 12:1. doi: 10.1080/19420862.2019.1703531
- Abès R, Teillaud J-L. Impact of glycosylation on effector functions of therapeutic IgG. *Pharmaceuticals* (2010) 3(1):146–57. doi: 10.3390/ph3010146
- Weng W-K, Levy R. Two immunoglobulin G fragment c receptor polymorphisms independently predict response to rituximab in patients with follicular lymphoma. *J Clin Oncol* (2003) 21(21):3940–7. doi: 10.1200/JCO.2003.05.013
- Felices M, Lenvik TR, Davis ZB, Miller JS, Vallera DA. Generation of BiKEs and TriKEs to improve NK cell-mediated targeting of tumor cells. In: S., Somanchi. (eds) *Natural Killer Cells. Methods in Molecular Biology*. New York, NY: Humana Press. (2016), 1441:333–46. doi: 10.1007/978-1-4939-3684-7\_28
- Congy-Jolivet N, Bolzec A, Ternant D, Ohresser M, Watier H, Thibault G. FcγRIIIa expression is not increased on natural killer cells expressing the FcγRIIIa-158V allotype. *Cancer Res* (2008) 68(4):976–80. doi: 10.1158/0008-5472.CAN-07-6523
- Moore GL, Bautista C, Pong E, Nguyen D-HT, Jacinto J, Eivazi A, et al. A novel bispecific antibody format enables simultaneous bivalent and monovalent co-engagement of distinct target antigens. *MAbs* (2011) 3(6):546–57. doi: 10.4161/mabs.3.6.18123
- Vallera DA, Zhang B, Gleason MK, Oh S, Weiner LM, Kaufman DS, et al. Heterodimeric bispecific single-chain variable-fragment antibodies against EpCAM and CD16 induce effective antibody-dependent cellular cytotoxicity against human carcinoma cells. *Cancer Biother Radiopharm* (2013) 28(4):274–82. doi: 10.1089/cbr.2012.1329
- Schmohl JU, Gleason MK, Dougherty PR, Miller JS, Vallera DA. Heterodimeric bispecific single chain variable fragments (scFv) killer engagers (BiKEs) enhance NK-cell activity against CD133+ colorectal cancer cells. *Target Oncol* (2016) 11(3):353–61. doi: 10.1007/s11523-015-0391-8
- Schmohl JU, Felices M, Oh F, Lenvik AJ, Lebeau AM, Panyam J, et al. Engineering of anti-CD133 trispecific molecule capable of inducing NK expansion and driving antibody-dependent cell-mediated cytotoxicity. *Cancer Res Treat* (2017) 49(4):1140–52. doi: 10.4143/crt.2016.491
- Gauthier L, Morel A, Anceriz N, Rossi B, Blanchard-Alvarez A, Grondin G, et al. Multifunctional natural killer cell engagers targeting NKp46 trigger protective tumor immunity. *Cell* (2019) 177(7):1701–1713.e16. doi: 10.1016/j.cell.2019.04.041
- Ellwanger K, Reusch U, Fucek I, Wingert S, Ross T, Müller T, et al. Redirected optimized cell killing (ROCK®): A highly versatile multispecific fit-for-purpose antibody platform for engaging innate immunity. *MABs* (2019) 11(5):899–918. doi: 10.1080/19420862.2019.1616506
- Sigmund S, Avanzato D, Lanzetti L. Emerging functions of the EGFR in cancer. *Mol Oncol* (2018) 12(1):3–20. doi: 10.1002/1878-0261.12155
- Wee P, Wang Z. Epidermal growth factor receptor cell proliferation signaling pathways. *Cancers (Basel)* (2017) 9(5):52. doi: 10.3390/cancers9050052
- Pastore S, Mascia F, Mariani V, Girolomoni G. The epidermal growth factor receptor system in skin repair and inflammation. *J Invest Dermatol* (2008) 128(6):1365–74. doi: 10.1038/sj.jid.5701184
- Brunner-Weinzierl MC, Rudd CE. CTLA-4 and PD-1 control of T-cell motility and migration: Implications for tumor immunotherapy. *Front Immunol* (2018) 9. doi: 10.3389/fimmu.2018.02737
- Ju X, Zhang H, Zhou Z, Wang Q. Regulation of PD-L1 expression in cancer and clinical implications in immunotherapy. *Am J Cancer Res* (2020) 10(1):1–11.
- Hsu J, Hodgins JJ, Marathe M, Nicolai CJ, Bourgeois-Daigneault M-C, Trevino TN, et al. Contribution of NK cells to immunotherapy mediated by PD-1/PD-L1 blockade. *J Clin Invest* (2018) 128(10):4654–68. doi: 10.1172/JCI99317
- Koopmans I, Hendriks D, Samplonius DF, van Ginkel RJ, Heskamp S, Wierstra PJ, et al. A novel bispecific antibody for EGFR-directed blockade of the PD-1/PD-L1 immune checkpoint. *Oncoimmunology* (2018) 7(8):e1466016. doi: 10.1080/2162402X.2018.1466016
- Harwardt J, Bogen JP, Carrara SC, Ulitzka M, Grzeschik J, Hock B, et al. A generic strategy to generate bifunctional two-in-One antibodies by chicken immunization. *Front Immunol* (2022) 13. doi: 10.3389/fimmu.2022.888838
- Krah S, Kolmar H, Becker S, Zielonka S. Engineering IgG-like bispecific antibodies—an overview. *Antibodies* (2018) 7(3):28. doi: 10.3390/antib7030028
- Beck A, Wurch T, Bailly C, Corvaia N. Strategies and challenges for the next generation of therapeutic antibodies. *Nat Rev Immunol* (2010) 10(5):345–52. doi: 10.1038/nri2747
- Ridgway JBB, Presta LG, Carter P. 'Knobs-into-holes' engineering of antibody c<sub>H</sub>3 domains for heavy chain heterodimerization. *Protein Eng Des Sel* (1996) 9(7):617–21. doi: 10.1093/protein/9.7.617
- Lewis SM, Wu X, Pustilnik A, Sereno A, Huang F, Rick HL, et al. Generation of bispecific IgG antibodies by structure-based design of an orthogonal fab interface. *Nat Biotechnol* (2014) 32(2):191–8. doi: 10.1038/nbt.2797
- Lu R-M, Hwang Y-C, Liu I-J, Lee C-C, Tsai H-Z, Li H-J, et al. Development of therapeutic antibodies for the treatment of diseases. *J BioMed Sci* (2020) 27(1):1. doi: 10.1186/s12929-019-0592-z
- Ching KH, Collarini EJ, Abdiche YN, Bedinger D, Pedersen D, Izquierdo S, et al. Chickens with humanized immunoglobulin genes generate antibodies with high affinity and broad epitope coverage to conserved targets. *MABs* (2018) 10(1):71–80. doi: 10.1080/19420862.2017.1386825
- Larsson A, Bälöw R-M, Lindahl TL, Forsberg P-O. Chicken antibodies: Taking advantage of evolution—a review. *Poult Sci* (1993) 72(10):1807–12. doi: 10.3382/ps.0721807
- Bogen JP, Grzeschik J, Krah S, Zielonka S, Kolmar H. Rapid generation of chicken immune libraries for yeast surface display. In: S., Zielonka, S., Krah, (eds) *Genotype Phenotype Coupling. Methods in Molecular Biology*. New York, NY: Humana Press. (2020) 2070:289–302. doi: 10.1007/978-1-4939-9853-1\_16
- Grzeschik J, Yanakieva D, Roth L, Krah S, Hinz SC, Elter A, et al. Yeast surface display in combination with fluorescence-activated cell sorting enables the rapid isolation of antibody fragments derived from immunized chickens. *Biotechnol J* (2019) 14(4):1800466. doi: 10.1002/biot.201800466



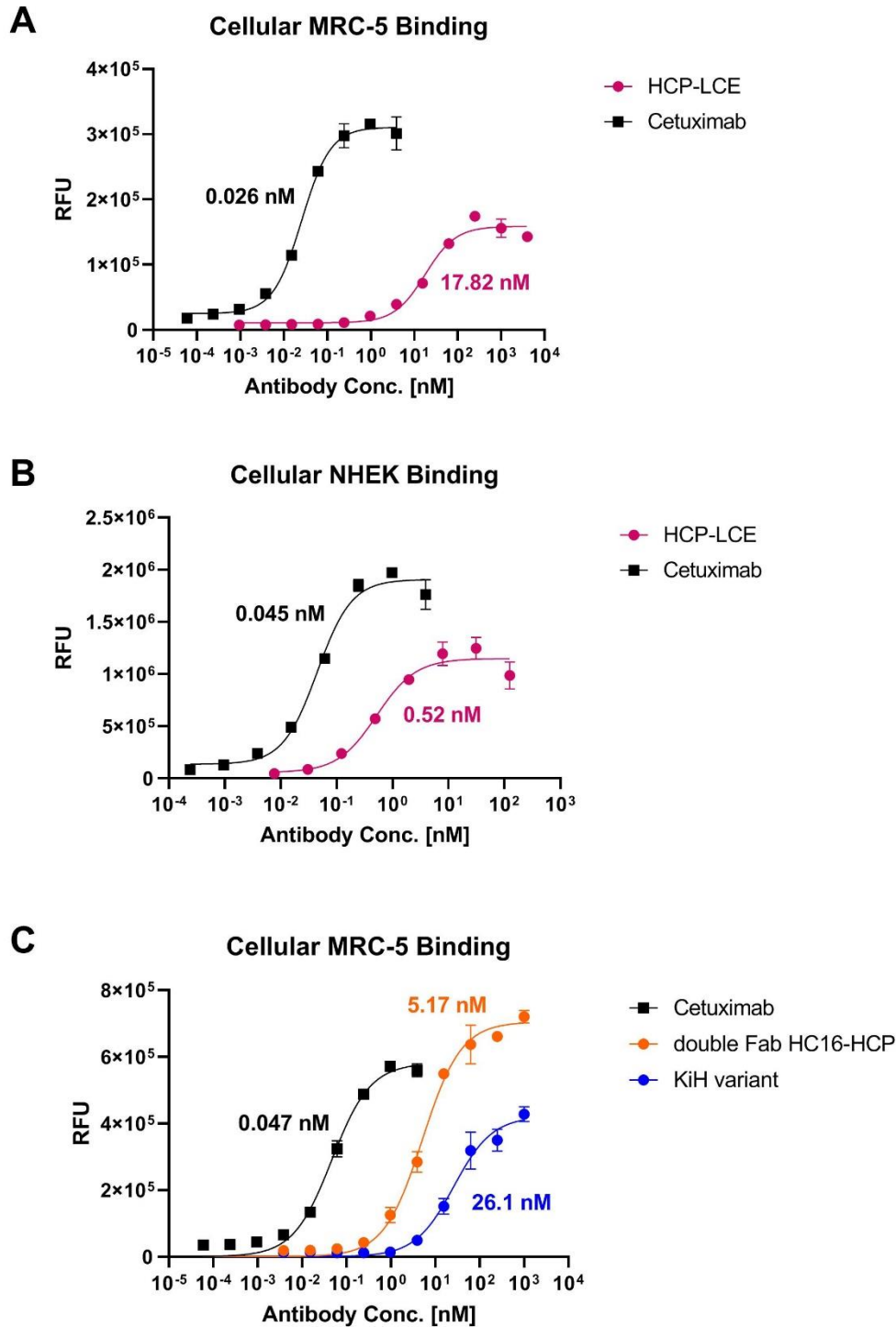
38. Roth L, Grzeschik J, Hinz SC, Becker S, Toleikis L, Busch M, et al. Facile generation of antibody heavy and light chain diversities for yeast surface display by golden gate cloning. *Biol Chem* (2019) 400(3):383–93. doi: 10.1515/hsz-2018-0347
39. Segaert S, Van Cutsem E. Clinical signs, pathophysiology and management of skin toxicity during therapy with epidermal growth factor receptor inhibitors. *Ann Oncol* (2005) 16(9):1425–33. doi: 10.1093/annonc/mdt279
40. Lacouture ME. Mechanisms of cutaneous toxicities to EGFR inhibitors. *Nat Rev Cancer* (2006) 6(10):803–12. doi: 10.1038/nrc1970
41. De Nardis C, Hendriks LJA, Poirier E, Arvinte T, Gros P, Bakker ABH, et al. A new approach for generating bispecific antibodies based on a common light chain format and the stable architecture of human immunoglobulin G1. *J Biol Chem* (2017) 292(35):14706–17. doi: 10.1074/jbc.M117.793497
42. Krah S, Schröter C, Eller C, Rhiel L, Rasche N, Beck J, et al. Generation of human bispecific common light chain antibodies by combining animal immunization and yeast display. *Protein Eng Des Sel* (2017) 30(4):291–301. doi: 10.1093/protein/gzw077
43. Bogen JP, Carrara SC, Fiebig D, Grzeschik J, Hock B, Kolmar H. Design of a trispecific checkpoint inhibitor and natural killer cell engager based on a 2 + 1 common light chain antibody architecture. *Front Immunol* (2021) 12. doi: 10.3389/fimmu.2021.669496
44. Gong S, Ren F, Wu D, Wu X, Wu C. Fabs-in-tandem immunoglobulin is a novel and versatile bispecific design for engaging multiple therapeutic targets. *MAbs* (2017) 9(7):1118–28. doi: 10.1080/19420862.2017.1345401
45. Schlothauer T, Herter S, Koller CF, Grau-Richards S, Steinhart V, Spick C, et al. Novel human IgG1 and IgG4 fc-engineered antibodies with completely abolished immune effector functions. *Protein Eng Des Sel* (2016) 29(10):457–66. doi: 10.1093/protein/gzw040
46. Cambay F, Raymond C, Brochu D, Gilbert M, Tu TM, Cantin C, et al. Impact of IgG1 n-glycosylation on their interaction with fc gamma receptors. *Curr Res Immunol* (2020) 1:23–37. doi: 10.1016/j.crimmu.2020.06.001
47. Ferguson KM. Structure-based view of epidermal growth factor receptor regulation. *Annu Rev Biophys* (2008) 37(1):353–73. doi: 10.1146/annurev.biophys.37.032807.125829
48. Zhang F, Wang S, Yin L, Yang Y, Guan Y, Wang W, et al. Quantification of epidermal growth factor receptor expression level and binding kinetics on cell surfaces by surface plasmon resonance imaging. *Anal Chem* (2015) 87(19):9960–5. doi: 10.1021/acs.analchem.5b02572
49. Elshiaty M, Schindler H, Christopoulos P. Principles and current clinical landscape of multispecific antibodies against cancer. *Int J Mol Sci* (2021) 22(11):5632. doi: 10.3390/ijms22115632
50. Wu X, Demarest SJ. Building blocks for bispecific and trispecific antibodies. *Methods* (2019) 154:3–9. doi: 10.1016/j.ymeth.2018.08.010
51. Guo ZS, Lotze MT, Zhu Z, Storkus WJ, Song X-T. Biomedicines bi-and trispecific T cell engager-armed oncolytic viruses: Next-generation cancer immunotherapy. (2020) 8(7):204. doi: 10.3390/biomedicines8070204
52. Wu L, Seung E, Xu L, Rao E, Lord DM, Wei RR, et al. Trispecific antibodies enhance the therapeutic efficacy of tumor-directed T cells through T cell receptor co-stimulation. *Nat Cancer* (2020) 1(1):86–98. doi: 10.1038/s43018-019-0004-z
53. Xu L, Pegu A, Rao E, Doria-Rose N, Beninga J, McKee K, et al. Trispecific broadly neutralizing HIV antibodies mediate potent SHIV protection in macaques. *Science* (2017) 358(6359):85–90. doi: 10.1126/science.aan8630
54. Gong S, Wu C. Generation of fabs-in-tandem immunoglobulin molecules for dual-specific targeting. *Methods* (2019) 154:87–92. doi: 10.1016/j.ymeth.2018.07.014
55. Golay J, Choblet S, Iwaszkiewicz J, Cérutti P, Ozil A, Loisel S, et al. Design and validation of a novel generic platform for the production of tetraivalent IgG1-like bispecific antibodies. *J Immunol* (2016) 196(7):3199–211. doi: 10.4049/jimmunol.1501592
56. Klein C, Sustmann C, Thomas M, Stubenrauch K, Croasdale R, Schanzer J, et al. Progress in overcoming the chain association issue in bispecific heterodimeric IgG antibodies. *MAbs* (2012) 4(6):653–63. doi: 10.4161/mabs.21379
57. Nicholson R, Gee JM, Harper M. EGFR and cancer prognosis. *Eur J Cancer* (2001) 37(SUPPLEMENT 4):9–15. doi: 10.1016/S0959-8049(01)00231-3
58. Zhang H, Deng M, Lin P, Liu J, Liu C, Strohl WR, et al. Frontiers and opportunities: Highlights of the 2nd annual conference of the Chinese antibody society. *Antib Ther* (2018) 1(2):27–36. doi: 10.1093/abt/tby009
59. Piccione EC, Juarez S, Liu J, Tseng S, Ryan CE, Narayanan C, et al. A bispecific antibody targeting CD47 and CD20 selectively binds and eliminates dual antigen expressing lymphoma cells. *MAbs* (2015) 7(5):946–56. doi: 10.1080/19420862.2015.1062192
60. Dheilly E, Moine V, Broyer L, Salgado-Pires S, Johnson Z, Papaioannou A, et al. Selective blockade of the ubiquitous checkpoint receptor CD47 is enabled by dual-targeting bispecific antibodies. *Mol Ther* (2017) 25(2):523–33. doi: 10.1016/j.jymthe.2016.11.006
61. Cleary KLS, Chan HTC, James S, Glennie MJ, Cragg MS. Antibody distance from the cell membrane regulates antibody effector mechanisms. *J Immunol* (2017) 198(10):3999–4011. doi: 10.4049/jimmunol.1601473
62. Orange JS. Formation and function of the lytic NK-cell immunological synapse. *Nat Rev Immunol* (2008) 8(9):713–25. doi: 10.1038/nri2381
63. Murin CD. Considerations of antibody geometric constraints on NK cell antibody dependent cellular cytotoxicity. *Front Immunol* (2020) 11. doi: 10.3389/fimmu.2020.01635
64. Bogen JP, Storka J, Yanakieva D, Fiebig D, Grzeschik J, Hock B, et al. Isolation of common light chain antibodies from immunized chickens using yeast biopanning and fluorescence-activated cell sorting. *Biotechnol J* (2021) 16(3):2000240. doi: 10.1002/biot.202000240
65. Benatuil L, Perez JM, Belk J, Hsieh C-M. An improved yeast transformation method for the generation of very large human antibody libraries. *Protein Eng Des Sel* (2010) 23(4):155–9. doi: 10.1093/protein/gzq002
66. Bogen JP, Hinz SC, Grzeschik J, Ebenig A, Krah S, Zielonka S, et al. Dual function pH responsive bispecific antibodies for tumor targeting and antigen depletion in plasma. *Front Immunol* (2019) 10. doi: 10.3389/fimmu.2019.01892

*Supplementary Material*

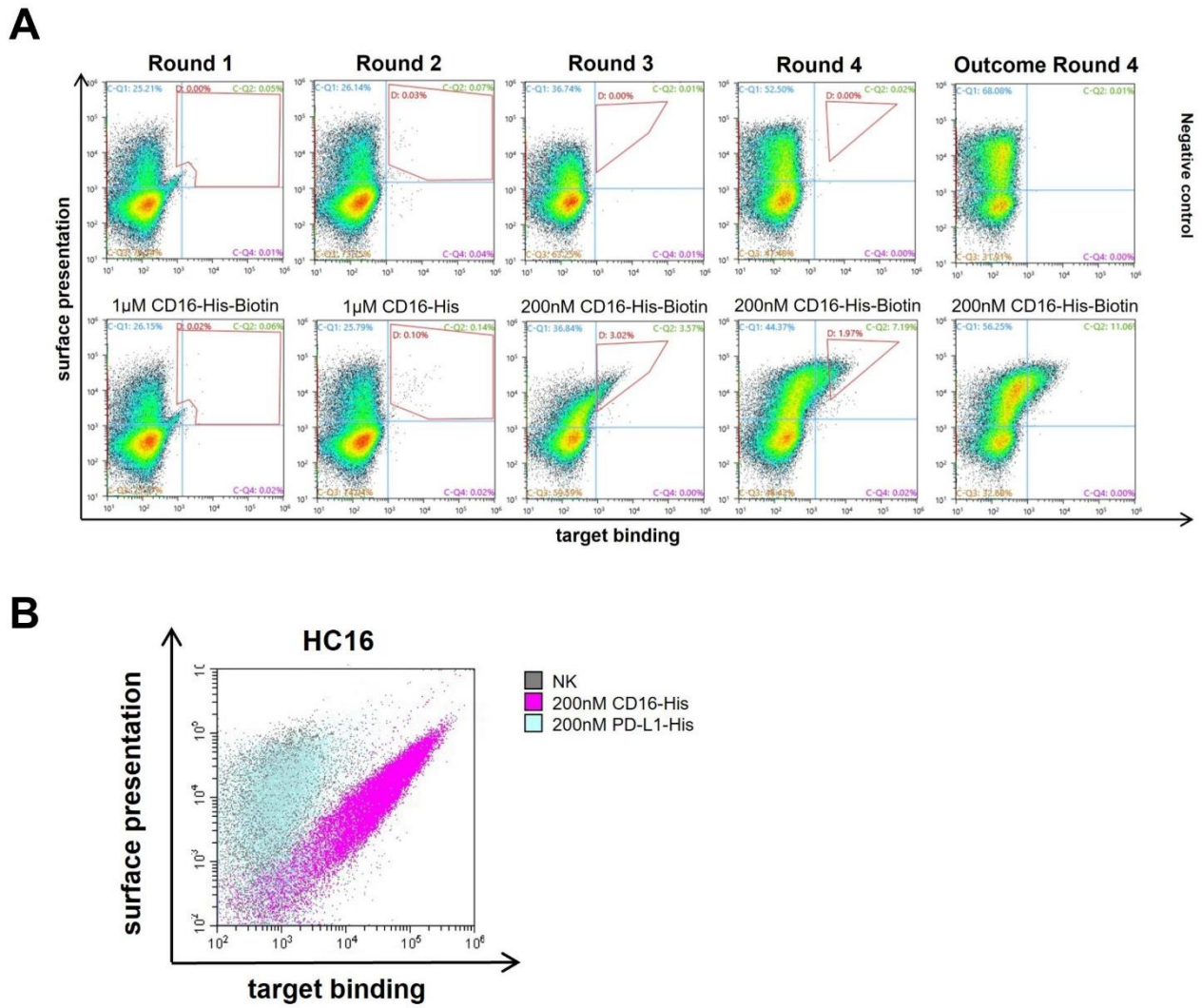
**Generation of a symmetrical trispecific NK cell engager based on a two-in-one antibody**

**Julia Harwardt, Stefania C. Carrara, Jan P. Bogen, Katrin Schoenfeld, Julius Grzeschik, Björn Hock and Harald Kolmar\***

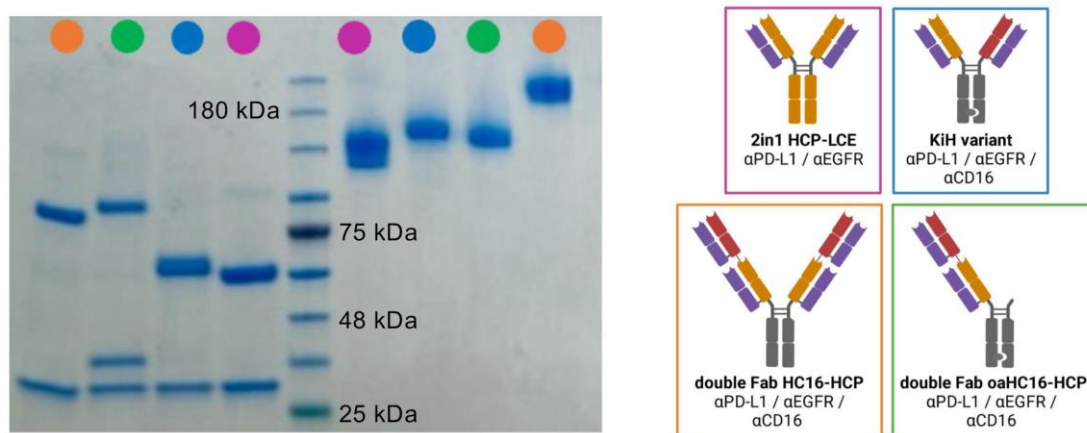
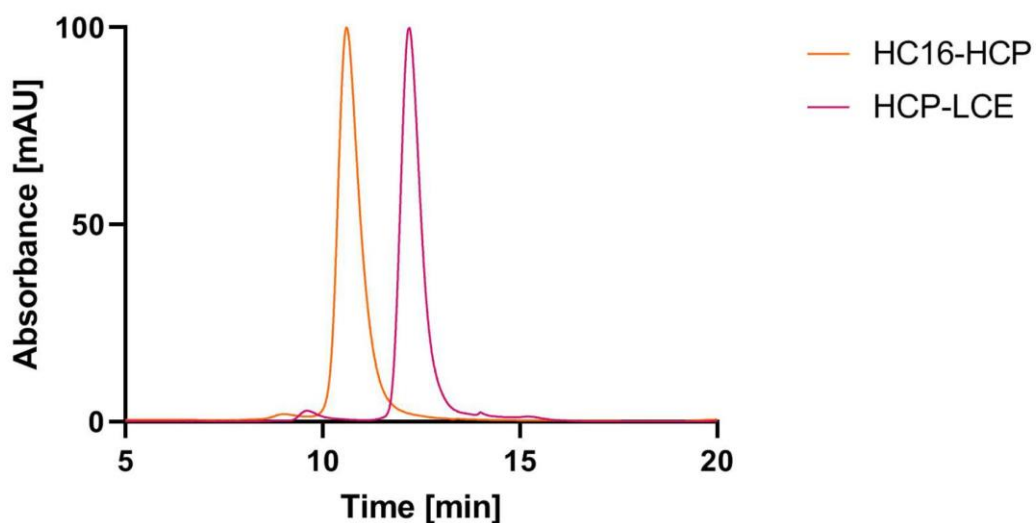
\*Correspondence: Harald Kolmar: [harald.kolmar@tu-darmstadt.de](mailto:harald.kolmar@tu-darmstadt.de)



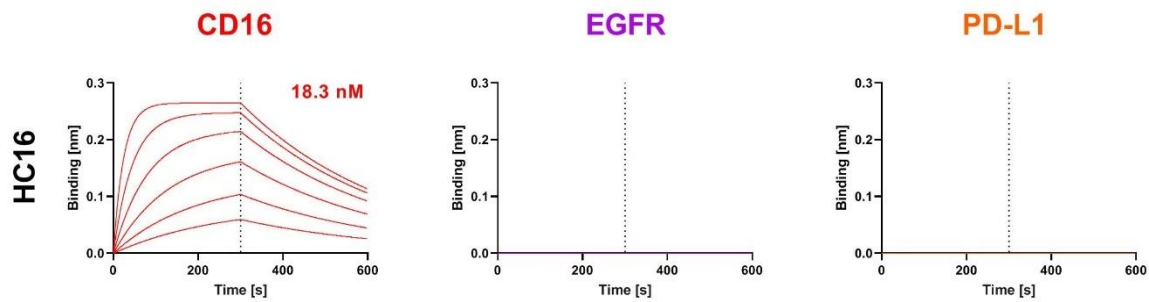
**Supplementary Figure 1.** Cellular binding on MRC-5 and NHEK cells. Cell titration of Cetuximab (black), HCP-LCE (pink), HC16-HCP (orange) and KiH variant (blue) on EGFR positive MRC-5 and NHEK cells. A variable slope three-parameter fit was utilized to for the resulting curves.



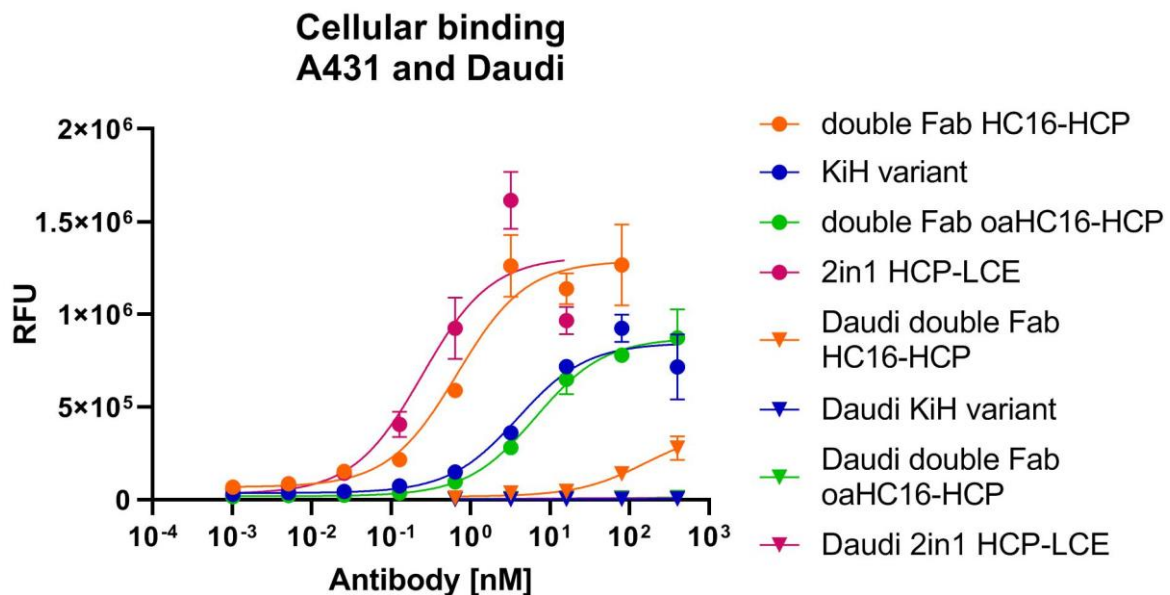
**Supplementary Figure 2.** Isolation of HC16. A) Sorting of the diploid common light chain yeast library. Surface presentation is depicted on the y-axis utilizing the anti-human lambda chain antibody PE labelled, while CD16-His-Biotin or CD16-His binding is shown on the x-axis using Streptavidin APC conjugated or the anti-6xHis AF647 antibody. B) Flow cytometric analysis of the isolated single clone after four consecutive rounds of FACS screening. Surface presentation is depicted on the y-axis utilizing the anti-human lambda chain antibody PE labelled, while CD16-His (pink) and PD-L1-His (blue) binding is shown on the x-axis using the anti-6xHis AF647 antibody.

**A****B**

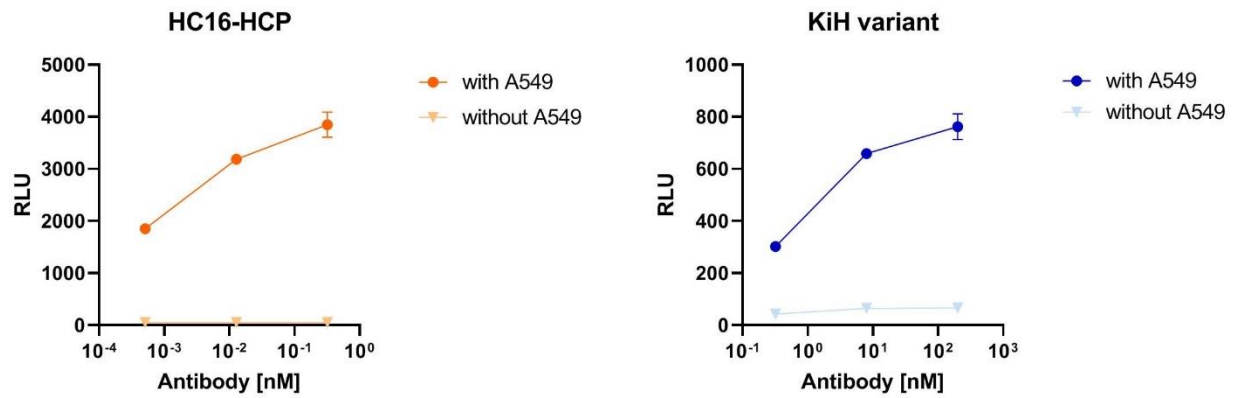
**Supplementary Figure 3.** SDS-PAGE analysis and SEC profiles. A) SDS-PAGE analysis of HC16-HCP (orange), oaHC16-HCP (green), KiH variant (blue) and HCP-LCE (pink) under reducing conditions (left) and under non-reducing conditions (right) revealing high purity and the expected molecular weights. B) SEC profiles of HCP-LCE (pink) and HC16-HCP (orange) revealing high purity and the expected molecular weights.



**Supplementary Figure 4.** Binding kinetics of HC16 by BLI-assisted measurements. BLI-measurement of the anti-CD16 antibody HC16 against CD16a, EGFR and PD-L1. The antibody targets CD16a exclusively.



**Supplementary Figure 5.** Cellular binding on A431 cells and Daudi cells. Cell titration of HC16-HCP (orange), KiH variant (blue), oaHC16-HCP (green) and HCP-LCE (pink) on EGFR/PD-L1 double positive A431 cells (circles) and on EGFR/PD-L1 double negative Daudi cells (triangles). A variable slope three-parameter fit was utilized to fit the resulting curves. The assay was repeated twice, yielding comparable results.



**Supplementary Figure 6.** ADCC cell-based reporter assay. The trispecific constructs HC16-HCP (orange) and KiH variant (blue) were tested in an ADCC reporter assay in the presence of EGFR/PD-L1 double-positive A549 cells (dots) and in the absence of A549 cells (triangles). Luciferase activity is plotted against the logarithmic antibody concentration. All measurements were performed in duplicates.

---

### 4.3. Balancing the Affinity and Tumor Cell Binding of a Two-in-One Antibody Simultaneously Targeting EGFR and PD-L1

Titel:

Balancing the Affinity and Tumor Cell Binding of a Two-in-One Antibody Simultaneously Targeting EGFR and PD-L1

Authors:

Julia Harwardt, Felix Klaus Geyer, Katrin Schoenfeld, David Baumstark, Vera Molkenthin and Harald Kolmar

Bibliographic data:

Journal – Antibodies

Volume 13, Issue 2

Section: Antibody Discovery and Engineering

Article published online: 02 May 2024

DOI: 10.3390/antib13020036

Copyright © 2024 by the authors. Licensee MDPI, Basel, Switzerland. This article is an open access article distributed under the terms and conditions of the Creative Commons Attribution (CC BY) license.


Contributions by J. Harwardt:

- Literature search and conceptual design
- Design and planning of 70% of the described experiments
- Generation and screening of the library
- Reformatting and characterization of antibody variants by BLI measurements and cellular binding assays
- Design and generation of 70% of illustrated figures
- Writing of manuscript together with V. Molkenthin and H. Kolmar



## Article

# Balancing the Affinity and Tumor Cell Binding of a Two-in-One Antibody Simultaneously Targeting EGFR and PD-L1

Julia Harwardt <sup>1</sup>, Felix Klaus Geyer <sup>1</sup>, Katrin Schoenfeld <sup>1</sup>, David Baumstark <sup>2</sup>, Vera Molkenhain <sup>2</sup>  
and Harald Kolmar <sup>1,3,\*</sup> 

<sup>1</sup> Institute for Organic Chemistry and Biochemistry, Technical University of Darmstadt, Peter-Grünberg-Strasse 4, 64287 Darmstadt, Germany

<sup>2</sup> 2bind GmbH, Im Gewerbepark D19a, 93059 Regensburg, Germany

<sup>3</sup> Centre for Synthetic Biology, Technical University of Darmstadt, 64287 Darmstadt, Germany

\* Correspondence: harald.kolmar@tu-darmstadt.de

**Abstract:** The optimization of the affinity of monoclonal antibodies is crucial for the development of drug candidates, as it can impact the efficacy of the drug and, thus, the dose and dosing regimen, limit adverse effects, and reduce therapy costs. Here, we present the affinity maturation of an EGFR×PD-L1 Two-in-One antibody for EGFR binding utilizing site-directed mutagenesis and yeast surface display. The isolated antibody variants target EGFR with a 60-fold-improved affinity due to the replacement of a single amino acid in the CDR3 region of the light chain. The binding properties of the Two-in-One variants were confirmed using various methods, including BLI measurements, real-time antigen binding measurements on surfaces with a mixture of both recombinant proteins and cellular binding experiments using flow cytometry as well as real-time interaction cytometry. An AlphaFold-based model predicted that the amino acid exchange of tyrosine to glutamic acid enables the formation of a salt bridge to an arginine at EGFR position 165. This easily adaptable approach provides a strategy for the affinity maturation of bispecific antibodies with respect to the binding of one of the two antigens.

**Keywords:** antibody affinity maturation; bispecific antibody; Two-in-One antibody; yeast display; EGFR binding; PD-L1 binding



**Citation:** Harwardt, J.; Geyer, F.K.; Schoenfeld, K.; Baumstark, D.; Molkenhain, V.; Kolmar, H. Balancing the Affinity and Tumor Cell Binding of a Two-in-One Antibody Simultaneously Targeting EGFR and PD-L1. *Antibodies* **2024**, *13*, 36. <https://doi.org/10.3390/antib13020036>

Academic Editor: Qi Zhao

Received: 9 February 2024

Revised: 27 March 2024

Accepted: 25 April 2024

Published: 2 May 2024



**Copyright:** © 2024 by the authors. Licensee MDPI, Basel, Switzerland. This article is an open access article distributed under the terms and conditions of the Creative Commons Attribution (CC BY) license (<https://creativecommons.org/licenses/by/4.0/>).

## 1. Introduction

Over the last few decades, monoclonal antibodies (mAbs) have become an important class of therapeutics for the treatment of various diseases. To increase efficacy and reduce side effects, high affinity and specificity of an antibody to its antigen is essential [1]. An antigen-binding paratope consists of six complementarity-determining regions (CDRs), three of the heavy chain and three of the light chain [2]. During antibody affinity maturation, CDRs undergo a high degree of somatic mutation. In mammals, the generation of high-affinity antibodies occurs in activated B cells by the mutagenic diversification of the variable regions of immunoglobulin (Ig) genes, a process called somatic hypermutation (SHM) [3,4]. As a result of an alternating process between the stochastic SHM of Ig genes and the selection and clonal expansion of B cells that contain affinity-enhanced mutations, the affinity of antibodies increases massively during an immune response [5].

Therapeutic antibodies can be derived from a variety of sources, such as mice, rats, rabbits, chickens, or non-human primates [6,7]. The advantage of animal immunization is that the antibodies have already undergone *in vivo* affinity maturation through several rounds of SHM [8]. However, even an *in vivo*-derived antibody may not have the desired affinity for the antigen, which, subsequently, can be optimized by *in vitro* affinity maturation [9]. For this, random or targeted mutagenesis can be applied [8]. Using the random mutagenesis method, a wide range of mutants can be generated from native antibodies by error-prone PCR, with the mutations occurring randomly rather than selectively [8,10].

The targeted mutagenesis method uses site-directed mutagenesis to produce a library of antibody variants, where the mutations can be designed to occur exclusively in the CDR regions [8,11]. The best matured antibody variant can be isolated by an affinity screening process using a display panning technology such as phage display [12], yeast surface display [13], or ribosome display [14,15]. However, for an antibody library including all possible combinations of single and multiple mutations at all CDRs of a usual variable domain, a library size exceeding  $10^{30}$  variants would be required, making it infeasible to screen using a common display technology [8]. Hot-spot mutagenesis [16], look-through mutagenesis [17], and simultaneous mutagenesis [18] are strategies for improving CDR diversification efficiency and reducing library size.

Mutagenesis approaches have been used in several studies to improve the binding affinity of mAbs. Tillotson et al. used the random mutagenesis approach via error-prone PCR followed by yeast surface display screening to isolate single-chain variable fragment (scFv) mutants that target the transferrin receptor (TfR) with a 3-7-fold-improved binding affinity [19]. A panel of Fab antibody fragments with up to a 10-fold improvement in affinity to the tetravalent antigen streptavidin were obtained by Beucken et al. after the selection of a yeast-displayed library diversified by error-prone PCR [20]. Hu et al. utilized the targeted diversification of multiple CDR regions of a humanized anti-receptor tyrosine kinase 2 (ErbB2) antibody together with phage display to identify a mutant with a 158-fold-increased affinity [21].

Optimizing the affinity of monospecific antibodies can impact the efficacy of a drug and, therefore, the dose and dosing regimen, limit adverse effects, and significantly reduce therapy costs, making optimal affinity a critical factor of drug discovery [10,22,23]. In the case of bispecific antibodies (bsAbs), the affinity of the drug needs to be optimized with respect to two targets [24]. BsAbs are remarkable therapeutic entities for cancer treatment as they are able to cross-link receptors or block two disease-related signaling pathways [25–27]. By simultaneously targeting two cancer-specific antigens on the same malignant cell, the tumor specificity of bsAbs can be enhanced [28]. Two therapeutic targets that are upregulated in many solid tumors are programmed death-ligand 1 (PD-L1) and epidermal growth factor receptor (EGFR) [29,30]. We recently reported the isolation of a chicken-derived Two-in-One antibody (HCP-LCE) that simultaneously targets PD-L1 and EGFR with two independent paratopes on a single Fab fragment [31]. Two-in-One antibodies are symmetrical molecules consisting of two identical heavy and light chains, meaning that additional engineering of constant chains is not required [32]. This antibody was the first Two-in-One antibody to be isolated by the separate immunization of two chickens with the EGFR and PD-L1 extracellular domains, followed by combining the respective heavy and light chain modules into a Fab format to isolate antibody variants that bind both targets simultaneously. HCP-LCE inhibits EGFR signaling by binding to dimerization domain II and blocks the PD-1/PD-L1 interaction, exhibiting moderate individual affinity for each antigen [31].

In this study, we investigated whether a Two-in-One antibody could have its affinity optimized for the binding of one target molecule (EGFR) without losing the binding of the second functionality (PD-L1). To our knowledge, the affinity maturation of a Two-in-One antibody obtained by animal immunization and combinatorial screening is described for the first time herein. We optimized the affinity of HCP-LCE regarding EGFR binding via site-directed mutagenesis and yeast surface display (YSD) in combination with fluorescence-activated cell sorting (FACS). By randomizing individual amino acids of the light chain CDR1 (LCDR1) and CDR3 (LCDR3), Two-in-One variants that exhibit a 60-fold improvement in EGFR binding affinity due to the replacement of a single amino acid at LCDR3 position three were isolated, while PD-L1 binding was not impaired. AlphaFold-based modeling predicted that the increased affinity is caused by the formation of an additional salt bridge.

## 2. Materials and Methods

### 2.1. Yeast Library Construction and Screening

For yeast library construction, primers degenerated via NNS coding at one of the nine amino acids of LCDR1 or at one of the 12 amino acids of LCDR3 were designed. For each mutated position, two PCR reactions each containing 200  $\mu$ M dNTPs (New England Biolabs, Ipswich, MA, USA), 0.5  $\mu$ M forward primer, 0.5  $\mu$ M reverse primer, 10 ng LCE template DNA, and 10 U Q5<sup>®</sup> High-Fidelity DNA Polymerase (New England Biolabs) in Q5 Reaction Buffer (New England Biolabs) were performed. The PCR mixture was subjected to an initial denaturation step of 98 °C (30 s) followed by 30 cycles of 98 °C (10 s), 68 °C (20 s), and 72 °C (30 s). This was followed by a final elongation at 72 °C for 300 s. Both PCR fragments were ligated during a second PCR under the same conditions, resulting in a full-length VL sequence. Subsequently, VL genes were transferred into a pYD<sub>1</sub>-derived vector via homologous recombination in yeast (*Saccharomyces cerevisiae* strain BJ5461) as described previously [31]. Library generation in BJ5464 cells was conducted according to Benatuil and colleagues [33]. To combine the light chain diversity with the heavy chain of HCP-LCE for subsequent Fab display, yeast mating was performed as described before [34].

The induction of gene expression and Fab surface presentation was achieved by the inoculation of yeast cells in Synthetic Galactose minimal medium with Casein Amino Acids (SG-CAA) at an OD<sub>600</sub> of 1.0 and incubation overnight at 30 °C and 180 rpm. For library sorting, the cells were harvested by centrifugation, washed with PBS + 0.1% (*w/v*) BSA (PBS-B) and incubated with 500 nM EGFR-Fc (round 1), 100 nM EGFR-His<sub>6</sub> + 500 nM HCP-LCE (round 2) or 50 nM EGFR-His<sub>6</sub> (round 3) for 30 min on ice. Following a PBS-B wash, the cells were incubated with a goat anti-human-Lambda AF647-conjugated F(ab')<sub>2</sub> antibody (SouthernBiotech, Birmingham, AL, USA, diluted 1:75) to detect Fab surface presentation and an anti-human IgG Fc PE-conjugated antibody (Thermo Fisher Scientific, Waltham, MA, USA, diluted 1:50) to detect target binding or with a goat anti-human-Lambda PE-conjugated F(ab')<sub>2</sub> antibody (SouthernBiotech, diluted 1:75) and a 6xHis-Tag AF647-conjugated antibody (Thermo Fisher Scientific, diluted 1:75) for 15 min on ice. An additional PBS-B washing step was followed by FACS screening using a Sony SH800S device.

### 2.2. Expression and Purification of Two-in-One Variants

The reformatting, expression, and purification of full-length antibodies was performed as described previously [31,35]. Isolated yeast vectors were sequenced, and the VL fragment was reformatted into pTT5-derived vectors by golden gate assembly. For the soluble expression of full-length chimeric antibodies, Expi293F<sup>™</sup> cells (Thermo Fisher Scientific) were transiently transfected using the ExpiFectamine<sup>™</sup> 293 Transfection Kit (Thermo Fisher Scientific) following the manufacturer's protocol. For purification, cell culture supernatants were collected five days post transfection, sterile-filtered, and applied to a MabSelect<sup>™</sup> PrismA HP column (GE Healthcare, Piscataway, NJ, USA) using an ÄKTA pure<sup>™</sup> chromatography system (GE Healthcare). One-armed molecules were captured by IMAC (HisTrap HP, GE Healthcare), followed by Strep-Tactin XT affinity chromatography according to the manufacturer's protocol. Buffer exchange against PBS was performed using a HiTrap<sup>™</sup> Desalting column (GE Healthcare).

### 2.3. Cell Lines

Expi293F<sup>™</sup> cells were cultured in Expi293<sup>™</sup> Expression Medium (Thermo Fisher Scientific), sub-cultured every 3–4 days, and incubated at 37 °C and 8% CO<sub>2</sub>. A431 and A549 cells were cultured in Dulbecco's Eagle Medium (DMEM, Thermo Fisher Scientific) supplemented with 10% FBS (Merck Millipore, Burlington, MA, USA) and 1% Penicillin–Streptomycin (Sigma Aldrich, St. Louis, MI, USA) in T75 cell culture flasks at 37 °C and 5% CO<sub>2</sub> and sub-cultured every 3–4 days. Jurkat cells were maintained in RPMI-1640 supplemented with 10% FBS and 1% Penicillin–Streptomycin, sub-cultured every 3–4 days, and incubated at 37 °C and 5% CO<sub>2</sub>.

#### 2.4. Thermal Shift Assay

Experiments to determine the thermal stability of the antibody variants were performed using a CFX Connect Real-Time PCR Detection System (BioRad, Hercules, CA, USA) with a temperature gradient from 20 °C to 95 °C and 0.5 °C/10 s. The derivatives of the melting curves were calculated using the corresponding BioRad CFX Maestro 3.0 software to determine the melting temperature ( $T_M$ ). All reactions were performed in PBS in the presence of 1 mg/mL protein and SYPRO Orange (Thermo Fisher Scientific, diluted 1:100).

#### 2.5. YSD-Based Epitope Mapping

EGFR epitope mapping on the subdomain level was performed using yeast cells displaying truncated versions of EGFR-ECD (amino acids 1–124, 1–176, 1–294, 273–621, 294–543, and 475–621), as previously described [36,37]. The cells were harvested by centrifugation, washed once with PBS-B, and incubated with 250 nM of the respective antibody for 30 min on ice. Surface presentation was verified using an FITC conjugated anti-c-myc antibody (Miltenyi Biotec, Bergisch Gladbach, Germany, diluted 1:75). Separately, antibody binding was verified using an anti-human IgG Fc PE-conjugated antibody (Thermo Fisher Scientific, diluted 1:50). The cells were analyzed by flow cytometry using the CytoFLEX S System (Beckman Coulter, Brea, CA, USA).

#### 2.6. Biolayer Interferometry

For affinity determination via biolayer interferometric measurements, the Octet RED96 system (ForteBio, Sartorius, Göttingen, Germany) was used. Anti-human IgG-Fc capture (AHC, Sartorius, Göttingen, Germany) biosensors were soaked in PBS pH 7.4 for at least 10 min before the start of the assay and subsequently used for the immobilization of the HCP-LCE variants. A quenching step in kinetics buffer (KB, Sartorius, Göttingen, Germany) was followed by an association step using EGFR-ECD or PD-L1-ECD at concentrations ranging from 250 nM to 7.81 nM or 500 nM to 7.81 nM, respectively, followed by a dissociation step in KB. Data analysis was performed using ForteBio data analysis software 9.0.0.14. Binding kinetics, including the equilibrium constant  $K_D$ , were determined using Savitzky–Golay filtering and a 1:1 Langmuir binding model.

For the PD-1 competition assay, HCP-LCE and LCE-E were immobilized on anti-human Fab-CH1 2nd-Generation (FAB2G, Sartorius, Göttingen, Germany) biosensors. Subsequently, 250 nM PD-L1-ECD pre-incubated with either 0 nM, 250 nM, or 500 nM PD-1 was applied for 600 s.

For the simultaneous binding assay, AHC biosensors were loaded with one-armed (oa) versions of HCP-LCE or LCE-E. After the measurement of the association to 250 nM PD-L1 for 300 s, the association to 250 nM EGFR was determined for 300 s. As controls, oaHCP-LCE and oaLCE-E were incubated with PD-L1 only.

#### 2.7. switchSENSE<sup>®</sup> Measurements

switchSENSE<sup>®</sup> measurements were performed in a helix<sup>+</sup> instrument (Dynamic Biosensors, Munich, Germany) using standard adapter chips (ADP-48-2-0, Dynamic Biosensors) in the static fluorescence proximity sensing (FPS) mode. In preparation of the measurement, the target proteins were conjugated to the ligand strand using the heliX<sup>®</sup> Amine Coupling Kit 1 (HK-NHS-1, Dynamic Biosensors) according to the user manual. Protein–DNA conjugates were purified in the proFIRE<sup>®</sup> (Dynamic Biosensors). Two Protein–DNA conjugates were separated for both proteins. The earlier eluting conjugate (conjugate 1) was used for the experiments. PD-L1-ligand strand conjugates were hybridized with adapter strand 1 with red dye Ra (AS1-Ra, Dynamic Biosensors) and EGFR–ligand strand conjugates were hybridized with adapter strand 1 with green dye Ga (AS1-Ga, Dynamic Biosensors,) for 20 min at 25 °C. For the single-protein surface experiments, 20% PD-L1-LS/AS1-Ra or 20% EGFR-LS/AS1-Ga was mixed with 80% complementary anchor strand 1 (c-Anchor 1, DC-0, Dynamic Biosensors). For the dual-protein surface experiments, the functionalization mix for electrode 1 contained 10% PD-L1-LS/AS1-Ra, 10% EGFR-LS/AS1-Ga, and 80%

complementary anchor strand 1 (c-Anchor 1, DC-0, Dynamic Biosensors). The functionalization mix for electrode 2 contained a ligand-free strand (LFS-0, Dynamic Biosensors) hybridized with adapter strand 2 with the respective dyes (AS-2-Ra and AS-2-Ga, Dynamic Biosensors) and mixed with c-Anchor 2 (DC-0, Dynamic Biosensors) in corresponding ratios. The workflow was set up in heliOS software v2024.1.0. The surface was functionalized for 200 s. The analytes were diluted to 1E-8 M, 1E-9 M, and 1E-10 M in 1x PE140, diluted from the 10-fold-concentrated buffer stock (BU-PE-140-10, Dynamic Biosensors), which was used as a running buffer. Association was measured for 180 s with a flow rate of 200  $\mu\text{L}/\text{min}$ . Dissociation was measured for 1800 s with a flow rate of 500  $\mu\text{L}/\text{min}$ . In the PD-L1-only experiments, the red LED power was set to 2%, and the green LED power was set to 0%. In the EGFR-only experiments, the green LED power was set to 2%, and the red LED power was set to 0%. In the dual-protein/dual-color experiments, both LEDs were used with 2% power. The measurement was performed at 25 °C. The measured binding curves were evaluated with the heliOS software v2024.1.0. The binding curves obtained in the target-containing electrode were referenced against the target-free electrode. A binding curve with 0 nM analyte was subtracted as a blank. The resulting double-referenced data points were fitted by applying the monophasic association–biphasic dissociation model with continuous amplitudes. The resulting fit curves were plotted using the R package ggplot2.

### 2.8. Cellular Binding

The cellular binding of the HCP-LCE variants was determined by affinity titration using EGFR and PD-L1 double-positive A549 cells. The cells ( $10^5$  cells/well) were washed with PBS-B and subsequently incubated with the corresponding antibody construct in varying concentrations (2.56 pM–200 nM, serial dilution) for 30 min on ice. Followed by another PBS-B washing step, anti-human IgG Fc PE-conjugated antibody (Thermo Fisher Scientific, diluted 1:50) was applied for 20 min on ice. After final washing with PBS-B, flow cytometry was performed using the CytoFLEX S System (Beckman Coulter). The relative fluorescence units (RFUs) were plotted against the respective logarithmic antibody concentration. The resulting curves were fitted with a variable slope four-parameter fit using GraphPad Prism.

### 2.9. Real-Time Interaction Cytometry (RT-IC)

The real-time kinetics on the cells were measured in a heliX<sup>cyto</sup> device (Dynamic Biosensors) with chip type M5 (CY-M5-1, Dynamic Biosensors). Antibodies were labeled with the red dye using the heliX<sup>cyto</sup> labeling kit red dye 1 (CY-LK-R1-1, Dynamic Biosensors) according to the instructions in the manual. The degree of labeling (DOL) was determined by photometric measurements. The determined DOLs were 2.5 and 4 for HCP-LCE and LCE-E, respectively. The cells were resuspended in PBS and strained through a 30  $\mu\text{m}$  cell strainer (FIL-30-20, Dynamic Biosensors). Except for one measurement of LCE-E on A431 cells, all interactions were measured with cells that had been treated with 2% PFA for 15 min at room temperature. The cells were used at a concentration of  $2 \times 10^6$  cells/mL for capturing. The antibodies HCP-LCE and LCE-E were diluted to 60/20/6.67 nM and 100/50/25 nM, respectively. We used 1xPPBS, diluted from a 10-fold stock (BU-RB-10-1, Dynamic Biosensors), for antibody dilution and as a running buffer. The workflow was set up in the heliOS software v2024.1.0. Signals were normalized with normalization solution for the red dyes (NOR-0, Dynamic Biosensors) at the respective concentration. Red LED power was set to 0.11–0.13%. The measurement was carried out at 25 °C, and the autosampler was cooled to 4 °C. Each association was measured for 300 s, and dissociation was measured for 1800 s. The measured binding curves were evaluated using heliOS software v2024.1.0. The binding curves in electrode 1 and electrode 2 were normalized according to the signal obtained with the normalization solution. The signals obtained in the cell trap-containing electrode were referenced against the trap-free electrode. The resulting referenced data points were fitted by applying the monophasic association–

biphasic dissociation model with discontinuous amplitudes and with the end of dissociation set to zero. The data points, fit curves, and calculated parameters of the fit model were plotted using the R package ggplot2. Half-lives were approximated by applying the Newton–Raphson method provided in the R package animation.

### 2.10. AlphaFold-Based Modeling

AlphaFold2 modeling was performed with ColabFold version 1.5.5 [38–41]. Multiple sequence alignments (MSAs) were generated by MMseq2 [42,43] using the databases of UniRef100 [44]. The final model was relaxed by the AMBER force field [45]. Binding energies were calculated using PRODIGY [46,47], and the dissociation constant calculated for a temperature of 25 °C. Therefore, the top-ranked structure of the trimeric VH:VL and antigen domain complex was selected based on residue confidence scores (pIDDT) and error plots (PAE). The tetrameric complex was generated by modeling VH:VL with EGFR (P00533; L25-S645) using AlphaFold2 and the subsequent docking of PD-L1 (Q9NZQ7; N17-P227) utilizing HDOCK [48,49].

## 3. Results

### 3.1. Yeast Surface Display Library Generation and Screening

The EGFR-binding module of the Two-in-One antibody HCP-LCE (Figure 1A) was identified via the screening of a chicken-derived yeast surface display library, which was generated by combining the heavy chain of an anti-PD-L1 antibody with an immune anti-EGFR light chain library. Since HCP-LCE targets EGFR and PD-L1 simultaneously with the same Fv region and PD-L1 binding is primarily performed by the heavy chain CDRs, we assume that the light-chain CDRs are mainly involved in EGFR binding [31]. Consequently, in order to mature the EGFR binding affinity of the Two-in-One antibody HCP-LCE, a YSD library was generated by randomizing single amino acids of L1CDR1 and L1CDR3 (Figure 1B). To minimize the number of mutations, L1CDR2 was not modified. Consequently, the YSD library was designed in a way to contain one mutation in any of the nine amino acids of L1CDR1 and one mutation in any of the 12 amino acids of L1CDR3, resulting in a maximum mutation rate of two mutations per light chain (LC). For this, site-saturation mutagenesis [50] was applied by simultaneously substituting a single L1CDR1 and L1CDR3 codon with a codon encoding one of the twenty naturally occurring amino acids. To minimize stop codons, degenerated NNS codons were used (Figure 1B). The combination of all possible mutation pairs results in a maximum theoretical library size of  $4.3 \times 10^4$  light chain mutants on the protein level and  $1.1 \times 10^5$  mutants on the DNA level. For NNS YSD library cloning, amplified VL fragments were inserted into a pYD<sub>1</sub>-derived vector encoding a human lambda CL by homologous recombination in BJ5464 yeast as described previously [51]. The LC diversity was combined with EBY100 yeast cells encoding the wildtype Two-in-One VH-CH1 fragment by yeast mating (Figure 1B), resulting in adequate oversampling of the calculated light chain diversity.

The diploid Two-in-One LC NNS library was screened for high-affinity EGFR binders by FACS over three consecutive sorting rounds starting with 500 nM EGFR-Fc (Figure 1C). In order to isolate mutants that target EGFR with higher affinity than the wildtype Two-in-One antibody, a competition screen was performed during the second sorting round. For this purpose, the enriched library was stained with 100 nM His-tagged EGFR pre-incubated with 500 nM wildtype Two-in-One antibody (Figure 1C). Double-positive yeast cells are indicative of surface-displayed Fabs that target EGFR with higher affinity than HCP-LCE. After a third round of sorting using 50 nM His-tagged EGFR, six yeast clones were screened individually for EGFR and PD-L1 binding (Figure S1). Since all analyzed clones target both 50 nM EGFR and 250 nM PD-L1, the VL fragment of twelve randomly selected clones of the enriched library after three rounds of sorting was sequenced.

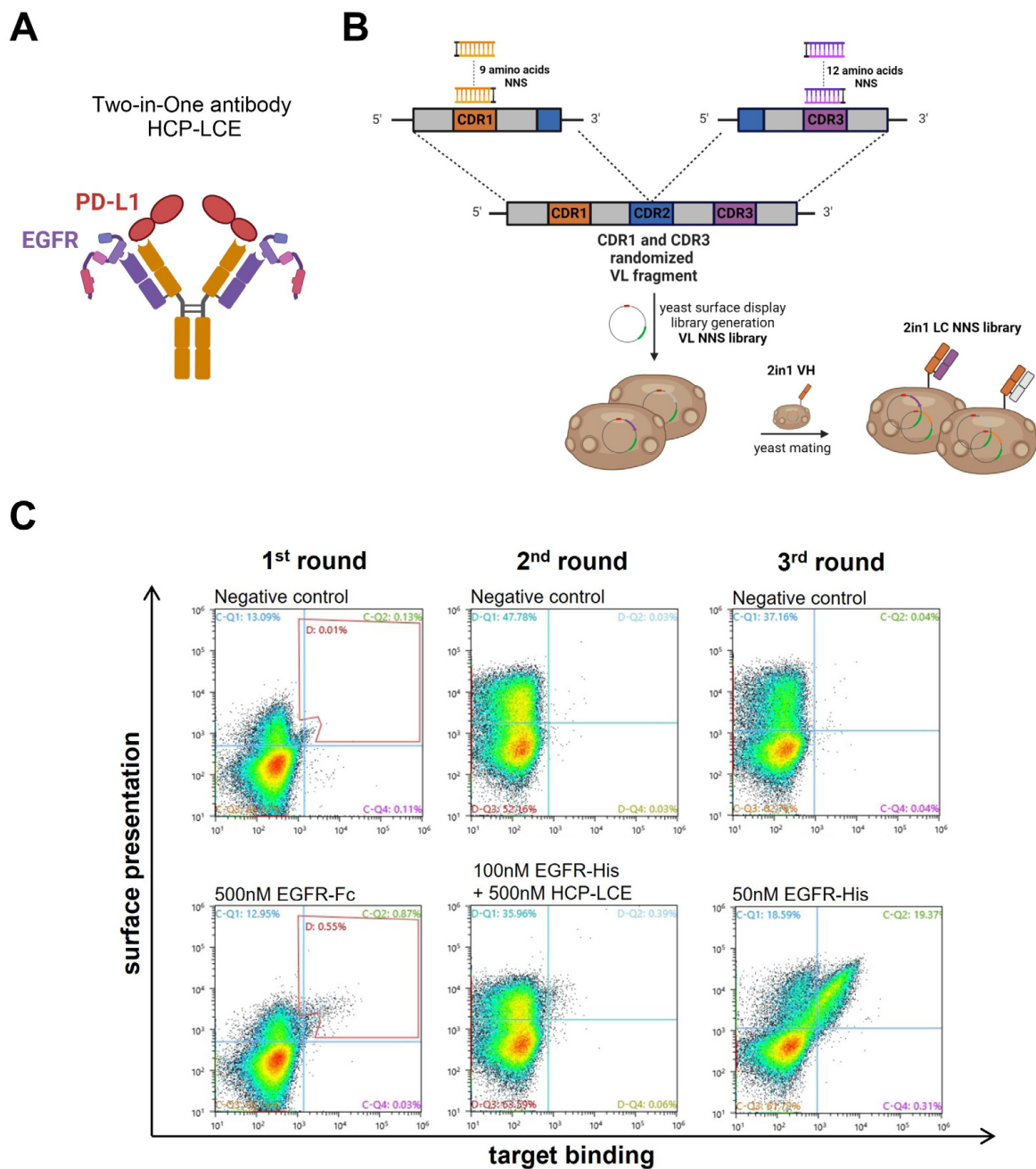


**Figure 1.** HCP-LCE light chain NNS yeast surface display library generation and sorting. (A) Schematic representation of the EGFR and PD-L1 binding Two-in-One antibody HCP-LCE. (B) Schematic representation of the cloning procedure for YSD library generation. Single amino acids of LCDR1 and LCDR3 were substituted with a codon encoding for the 20 naturally occurring amino acids. The light chain diversity was combined with the wildtype HCP-LCE heavy chain by yeast mating. Created with BioRender.com (accessed on 11 January 2024) (C) Sorting of the diploid HCP-LCE light chain mutant YSD library via FACS. Surface presentation is depicted on the y-axis utilizing the anti-human lambda chain antibody AF647- or PE-labeled, while EGFR-Fc or EGFR-His binding is shown on the x-axis using the anti-human Fc PE antibody or the anti-6xHis AF647 antibody, respectively.

### 3.2. Cloning and Biophysical Characterization of Full-Length Two-in-One Antibody Variants

Of the twelve Two-in-One LC mutants analyzed, the majority contained a wildtype LCDR1 region, suggesting that the light chain CDR1 is not predominantly involved in EGFR binding. Interestingly, all variants showed a mutation at the same position in LCDR3, indicating that this position (amino acid three of LCDR3) has a major impact on EGFR binding. Eleven of the twelve variants had a tyrosine to glutamic acid mutation (Y → E) at position three of LCDR3, and one variant harbored a tyrosine to aspartic acid mutation (Y → D) at this position, which implies the exchange of a polar, neutral amino acid to an acidic amino acid. To investigate the impact of a basic amino acid at position three of LCDR3, a variant carrying a tyrosine to lysine (Y → K) mutation was generated in addition to the variants isolated from the YSD library.

To produce full-length Two-in-One antibody mutants, Expi293F™ cells were co-transfected with the respective VL sequence reformatted into a pTT5-derived vector encoding a lambda CL sequence and a pTT5 vector encoding the Two-in-One heavy chain as previously described [52]. The purification of the HCP-LCE antibody variants, hereafter referred to as LCE-E, LCE-D, and LCE-K depending on the mutation at the LCE light chain, was performed by Protein A affinity chromatography.

SDS-PAGE analysis demonstrated the presence of all expected heavy and light chains under reducing conditions as well as the expected molecular size under non-reducing conditions without degradation products (Figure S2). Thermostability investigated by SYPRO Orange revealed that the melting temperatures of the HCP-LCE variants were between 60.5 °C and 66.5 °C, with the wildtype antibody exhibiting 58.9 °C, indicating no reduction in thermal stability (Table 1).

**Table 1.** Biophysical properties of HCP-LCE, LCE-E, LCE-D, and LCE-K, including BLI measured affinity and kinetic binding rates, flow cytometry-measured EC<sub>50</sub> values, PRODIGY web server predicted affinity values, and melting temperatures.

Antibody	K <sub>D</sub> [nM]		k <sub>on</sub> [M <sup>-1</sup> s <sup>-1</sup> ]		K <sub>dis</sub> [s <sup>-1</sup> ]		R <sup>2</sup>		EC <sub>50</sub> A549 [nM]	Predicted K <sub>D</sub> [nM]	T <sub>M</sub> [°C]
	EGFR	PD-L1	EGFR	PD-L1	EGFR	PD-L1	EGFR	PD-L1			
HCP-LCE	286	70.7	6.13 × 10 <sup>5</sup>	1.42 × 10 <sup>5</sup>	1.75 × 10 <sup>-1</sup>	1.01 × 10 <sup>-2</sup>	0.85	0.89	2.3	110	58.9
LCE-E	4.7	52.2	2.25 × 10 <sup>5</sup>	1.54 × 10 <sup>5</sup>	1.06 × 10 <sup>-3</sup>	8.02 × 10 <sup>-3</sup>	0.96	0.84	1.2	6.2	60.5
LCE-D	7.2	25.6	1.66 × 10 <sup>5</sup>	5.63 × 10 <sup>5</sup>	1.19 × 10 <sup>-3</sup>	1.44 × 10 <sup>-2</sup>	0.97	0.96	1.0	not determined	61.0
LCE-K	-	23.8	-	5.30 × 10 <sup>5</sup>	-	1.26 × 10 <sup>-2</sup>	-	0.98	28.6	not determined	66.5

### 3.3. Characterization of Antigen Binding via Biolayer Interferometry

Biolayer interferometry (BLI) measurements were performed to determine the affinity of the HCP-LCE variants to both EGFR (Figure 2) and PD-L1 (Figure S3). Compared to the HCP-LCE wildtype, the mutants LCE-D and LCE-E exhibit an affinity for EGFR that is increased by a factor of approximately 60. Both LCE-D and LCE-E bind EGFR with a K<sub>D</sub> value in the single-digit nanomolar range (Figure 2, Table 1). The significant increase in affinity is mainly caused by an improvement in the dissociation rate, which was recorded during the second part of the measurement (300–600 s). The LCE-K mutant does not target EGFR (Figure 2). This indicates that position three in LCDR3 has a strong impact on EGFR binding. A negatively charged amino acid such as aspartic acid (D) or glutamic acid (E) improves binding, whereas a positively charged amino acid like lysine (K) eliminates binding. The antibodies did not show binding to a negative control protein, excluding non-specific binding (Figure S4).

Flow cytometric analysis using yeast cells displaying truncated fragments of the EGFR-ECD confirmed that LCE-D and LCE-E target EGFR at the same domain as described for HCP-LCE [31], suggesting that the LCDR3 mutation does not modify the targeted EGFR



epitope (Figure S5). The three antibody variants exclusively target EGFR fragment 1–294 but neither 1–124 nor 1–176, which is why they are mapped to the EGFR dimerization domain II.

All four HCP-LCE variants analyzed target PD-L1 with comparable binding kinetics, indicating that the mutation in L3CDR3 does not have a major impact on PD-L1 binding. The PD-L1 binding kinetics are characterized by a fast association rate and a fast dissociation rate, which results in  $K_D$  values in the double-digit nanomolar range (Figure S3, Table 1). As demonstrated by BLI measurements, the ability to target and block the PD-1/PD-L1 interaction is preserved for variant LCE-E, as the antibody is unable to bind the PD-1/PD-L1 complex (Figure S6). In addition, LCE-E, like the parental antibody HCP-LCE, targets both antigens simultaneously with a single Fab fragment. This was investigated by the immobilization of the one-armed variants of the respective antibodies on BLI biosensors and the subsequent sequential incubation of PD-L1 first and EGFR second (Figure S7).

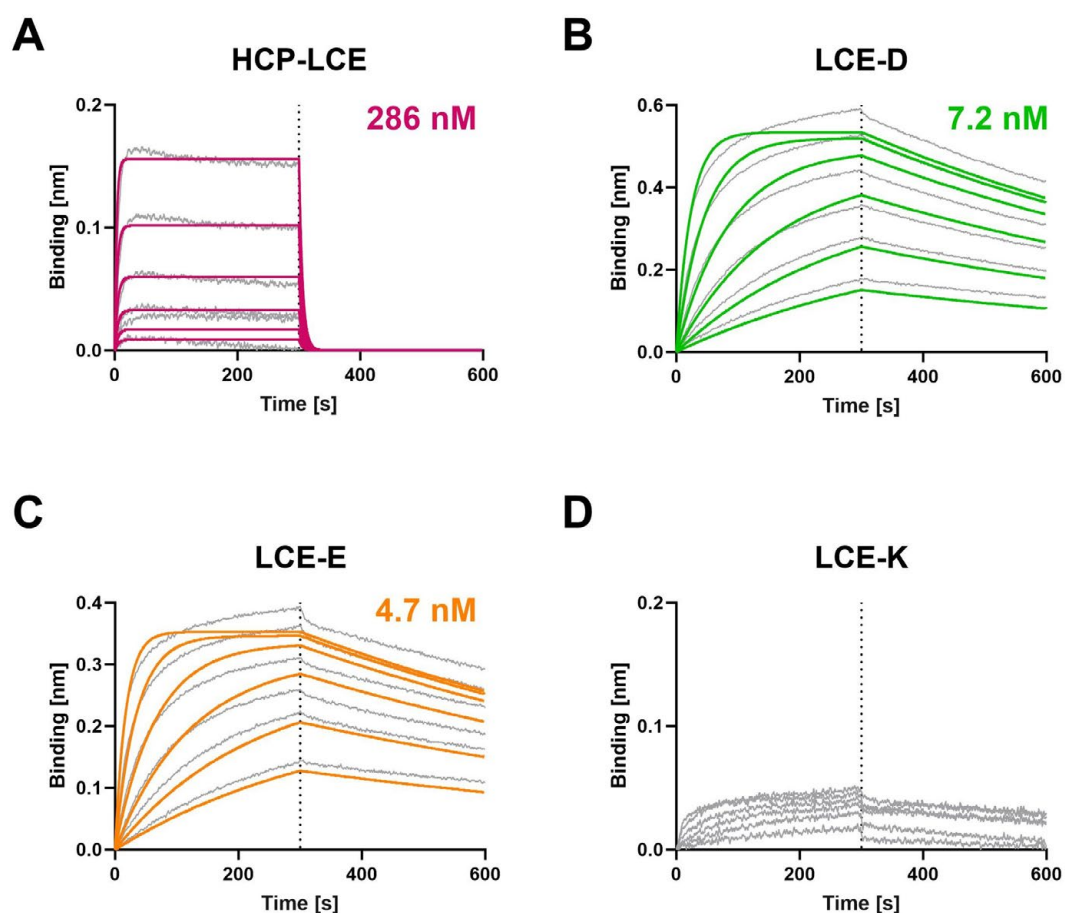


**Figure 2.** Characterization of the EGFR binding of the HCP-LCE variants by BLI measurements. BLI measurements of (A) HCP-LCE, (B) LCE-D, (C) LCE-E, and (D) LCE-K against EGFR. LCE-D and LCE-E target EGFR with a higher affinity than HCP-LCE, whereas the mutant LCE-K is not able to bind EGFR. The fit is depicted by the colored curves.

### 3.4. Real-Time Antigen Binding Measured on Single-Protein and Dual-Protein Surfaces in switchSENSE®

The binding kinetics of HCP-LCE and LCE-E to both targets were characterized in a helix® biosensor instrument using switchSENSE® technology. DNA-conjugated targets are hybridized with fluorophore-tagged adapter strands, which hybridize to anchor strands on the chip surface. The binding of the analyte is sensed by the fluorophore, which is sensitive to changes in its local environment. In this case, analyte binding resulted in a quenching effect, visualized as a signal decrease (Figure 3A–D). The technology offers the

possibility of using different fluorophores to tag different antigens which can be analyzed in parallel on the same surface in a dual-color experiment. The binding kinetics of the two antibody variants to EGFR and PD-L1, either on surfaces with one immobilized protein or on surfaces where both target proteins were immobilized, were compared. The observed interactions showed biphasic dissociations with a fast and slow dissociation rate (Figure 3). The glutamic acid introduced in LCE-E variant reduces the impact of the fast dissociation rate and stabilizes the binding of the antibody to EGFR (Figure 3C). The results obtained on surfaces with one of the target proteins and on surfaces with both target proteins are highly comparable (Table S1). A comparison of the one-armed HCP-LCE and IgG-like HCP-LCE revealed differences in the binding to PD-L1 immobilized on a surface in corresponding density. This indicates that the HCP-LCE kinetic includes the avidity effect caused by bivalent binding to PD-L1. In the given set-up, the presence of EGFR did not stabilize the binding of HCP-LCE or LCE-E to PD-L1.

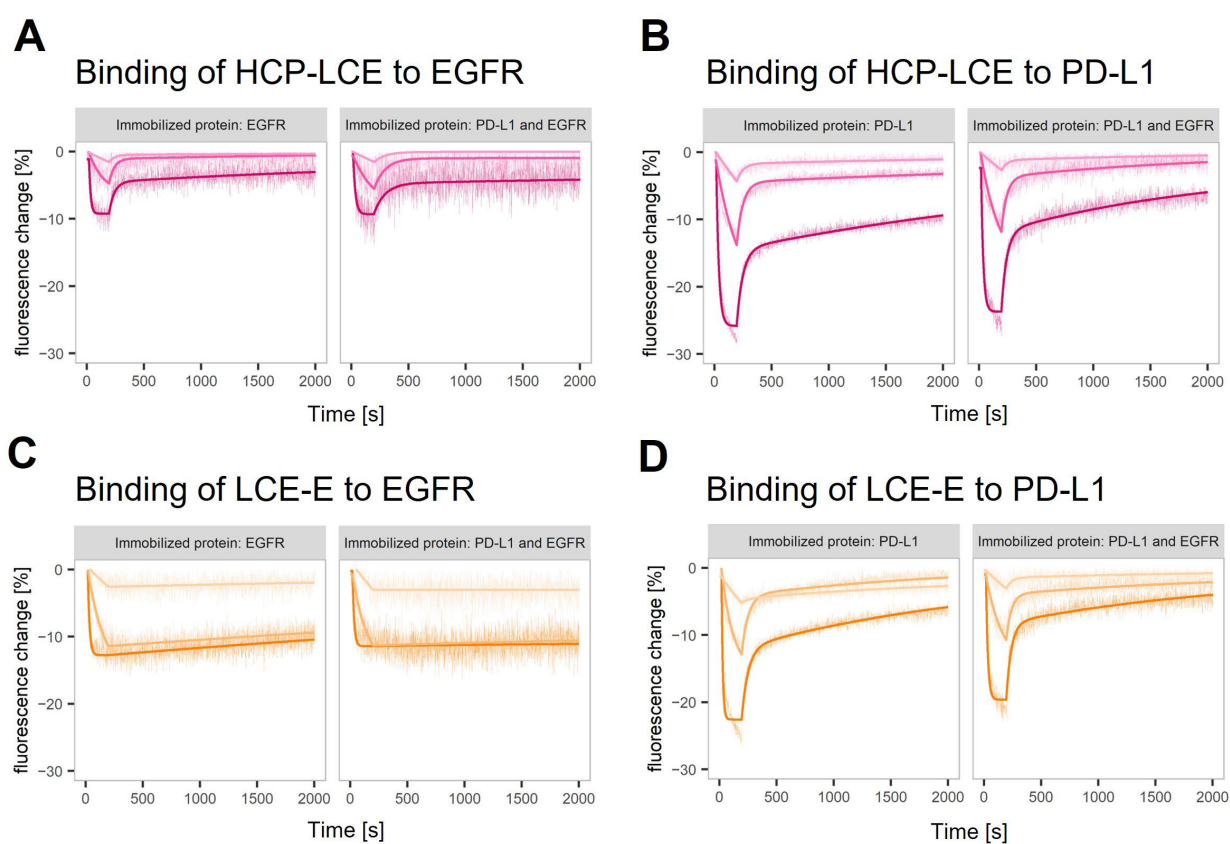


**Figure 3.** Real-time antigen binding measured on single-protein and dual-protein surfaces. Characterization of (A,C) EGFR and (B,D) PD-L1 binding of (A,B) HCP-LCE and (C,D) LCE-E on surfaces with EGFR or PD-L1 and on surfaces with both proteins (left and right panel in each plot). The fitting model assumes biphasic dissociation for all observed interactions. The interaction between LCE-E and EGFR shows the lowest contribution of the fast dissociation phase.

### 3.5. On-Cell Binding of Affinity-Matured Two-in-One Variants Measured by Flow Cytometry

To ensure that the HCP-LCE mutants LCE-E and LCE-D also showed more affine binding to target-positive tumor cells than the wildtype Two-in-One antibody, cellular binding experiments were performed on EGFR and PD-L1 double-positive A549 cells by flow cytometry. The cells were stained with the respective antibody at a concentration ranging from 2.56 pM to 200 nM utilizing a 5-fold dilution series, and binding was verified using an anti-human Fc PE detection antibody. As expected, LCE-E and LCE-D show specific cellular binding, with comparable  $EC_{50}$  values of about 1 nM and a similar binding maximum (Figure 4A). The wildtype antibody HCP-LCE targets the tumor cells with

lower affinity ( $EC_{50} = 2.3$  nM) and with a significantly reduced maximum binding. The deletion of the EGFR binding property of the mutant LCE-K is also reflected in cellular binding (Figure 4A,B). The overexpression of EGFR on cancer cells usually exceeds that of PD-L1 [51], which is why LCE-K demonstrates a lower  $EC_{50}$  value (28.6 nM) and significantly reduced maximum binding. This is also illustrated by the A549 cellular binding of monospecific anti-EGFR and anti-PD-L1 antibodies (Figure S8). The antibodies did not show binding to EGFR and PD-L1 double-negative Jurkat cells, excluding non-specific cellular binding (Figure S9). These data indicate that the amino acid exchange at position three in LCDR3 from tyrosine to glutamic acid (E) or aspartic acid (D) also results in significantly improved tumor cell binding, as expected.

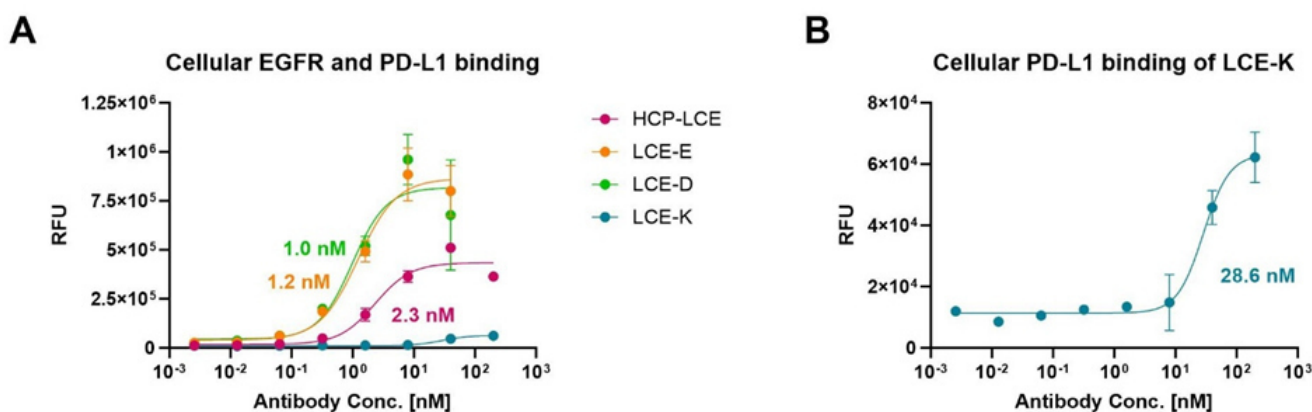


**Figure 4.** Cellular binding of the HCP-LCE variants on EGFR/PD-L1 double-positive A549 cells. (A) Cell titration of HCP-LCE (pink), LCE-E (orange), LCE-D (green), and LCE-K (blue) on A549 cells. (B) Cell titration of LCE-K on A549 cells; zoomed-in view of the graph shown in A. A variable slope four-parameter fit was utilized to fit the resulting curves.  $EC_{50}$  values: HCP-LCE, 2.3 nM; LCE-E, 1.2 nM; LCE-D, 1.0 nM; LCE-K, 28.6 nM. All measurements were performed in duplicates, and the experiments were repeated at least three times, yielding similar results.

### 3.6. Real-Time Binding Kinetics on Target-Positive Cells Detected with Real-Time Interaction Cytometry

A real-time interaction cytometry (RT-IC) experiment using heliX<sup>cyto</sup> biosensor was designed to reveal the impact of the improved EGFR binding kinetics on the binding kinetics of the antibody variant LCE-E and target-positive tumor cells compared to the wildtype HCP-LCE. Binding kinetics were measured using two different EGFR and PD-L1 double-positive tumor cell lines, A431 and A549. On A431 cells, expression levels for EGFR and PD-L1 are higher compared to A549 cells, with EGFR expression being higher than the expression of PD-L1 on both cell lines [51]. The cells were loaded into the cell traps on the chip of the heliX<sup>cyto</sup> biosensor, and fluorescently labeled antibody variants were injected in three injection steps at increasing antibody concentrations. The association of the antibodies was visibly reflected by an increase in the fluorescence signal; the dissociation was visibly reflected by a decrease in the signal after switching to buffer flow. The binding of both antibodies (HCP-LCE and LCE-E) was detectable on A431 cells and A549 cells (Figure 5A–D).

In most cases, the dissociation rate was biphasic and dominated by the slower dissociation rate (Figure 6). The  $K_D$  values calculated with the slower dissociation rate ( $KD_2$ ) are in the range of 0.1–0.7 nM for HCP-LCE on A431 cells and 1–2 nM for all other measured interactions (Table S2). The lower  $KD_2$  values determined for HCP-LCE on A431 were caused by a faster association rate (Figure 6A,B).

On both cell lines, LCE-E shows a slower second dissociation rate ( $kd_2$ ) (Figure 6C,D) and a weaker contribution of the second dissociation phase to the total dissociation amplitude (Figure 6C). This results in an increase in the length of time for which the affinity-matured antibody is retained on the cell surface (Figure 6D).

### 3.7. Characterization of Antigen Binding via AlphaFold-Based Modeling

In order to investigate the protein–protein interaction of the LCE-E mutant and the wildtype HCP-LCE with its antigens EGFR and PD-L1 in more detail, AlphaFold Multimer was used [38,39]. As experimentally predicted for HCP-LCE [31], PD-L1 binding occurs mainly via the heavy chain CDRs (Figure 7A), whereas heavy and light chain CDRs are involved in EGFR binding (Figure 7B). The AlphaFold-based model predicts that HCDR3 and LCDR3 mainly target the EGFR epitope. This is consistent with the experimentally obtained data showing an impact of LCDR3 on EGFR binding. Remarkably, the predicted EGFR epitope, EGFR dimerization domain II, is consistent with the epitope experimentally determined by YSD-based epitope mapping. To predict the affinity of the protein–protein complexes, the PRODIGY web server was utilized [46]. For HCP-LCE binding to EGFR, a  $K_D$  value of 110 nM was predicted, and for LCE-E binding to EGFR, a  $K_D$  value of 6.2 nM was predicted (Table 1). Thus, the affinity prediction also implies a significant increase in affinity as a result of the amino acid exchange at LCDR3 position three. Structural insights indicate that the increased affinity is caused by the formation of a salt bridge between the glutamic acid at LCDR3 position three (E87) and an arginine at EGFR position 165 (R165) (Figure 7C). The binding of the parental antibody HCP-LCE involves the formation of a salt bridge between EGFR R165 and D27, which is also observed for the interaction of EGFR and LCE-E.

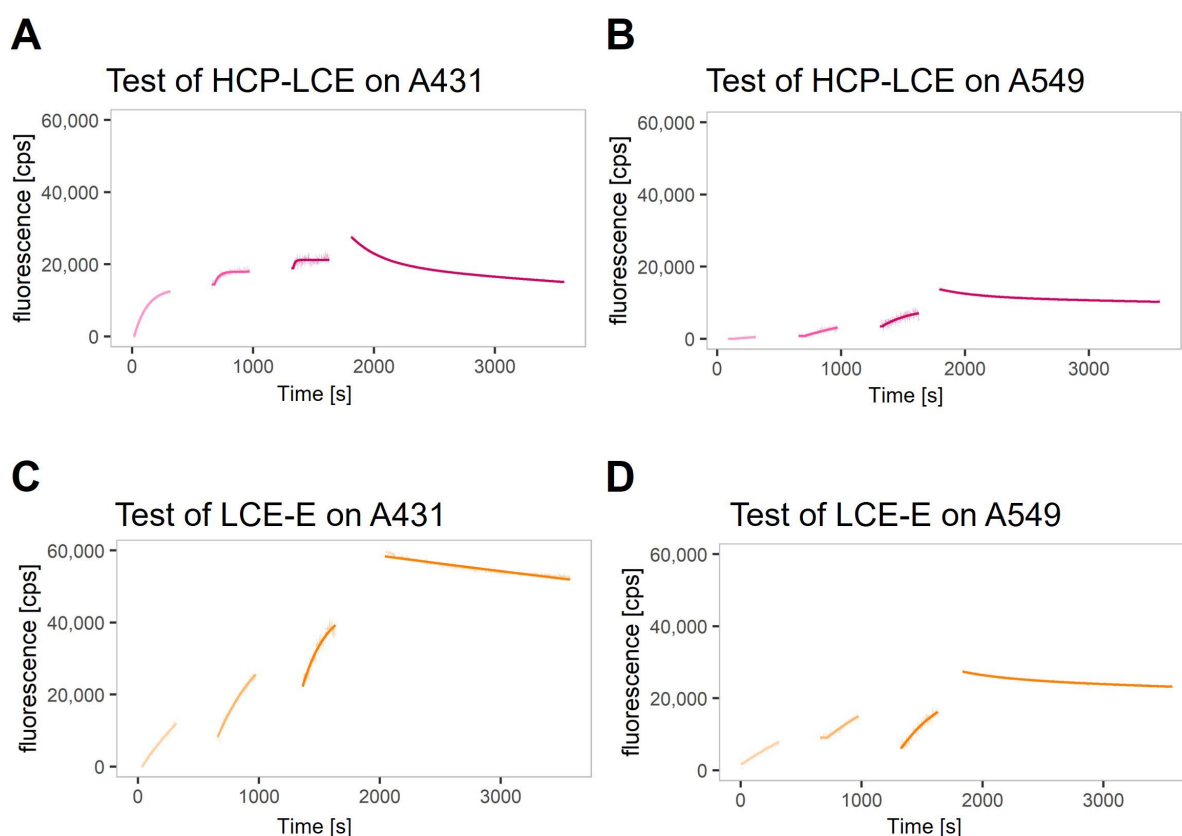


**Figure 5.** Real-time binding kinetics on EGFR and PD-L1 double-positive A431 and A549 cells. Real-time binding curves of (A,B) HCP-LCE and (C,D) LCE-E measured on (A,C) A431 and (B,D) A549 via real-time interaction cytometry (RT-IC) in a heliX<sup>cyto</sup> biosensor. The cells were fixed with PFA and loaded into the five individual cell traps on the chip. Fluorescently labeled analytes were injected in increasing concentrations in three subsequent injection steps. The association of the analytes was visibly reflected by an increase in the fluorescent signal. After the third injection, the system switches to buffer flow to monitor the dissociation of the analytes, which visibly manifests as a decrease in signal. Data points were fitted with a kinetic model that assumes monophasic association and biphasic dissociation.

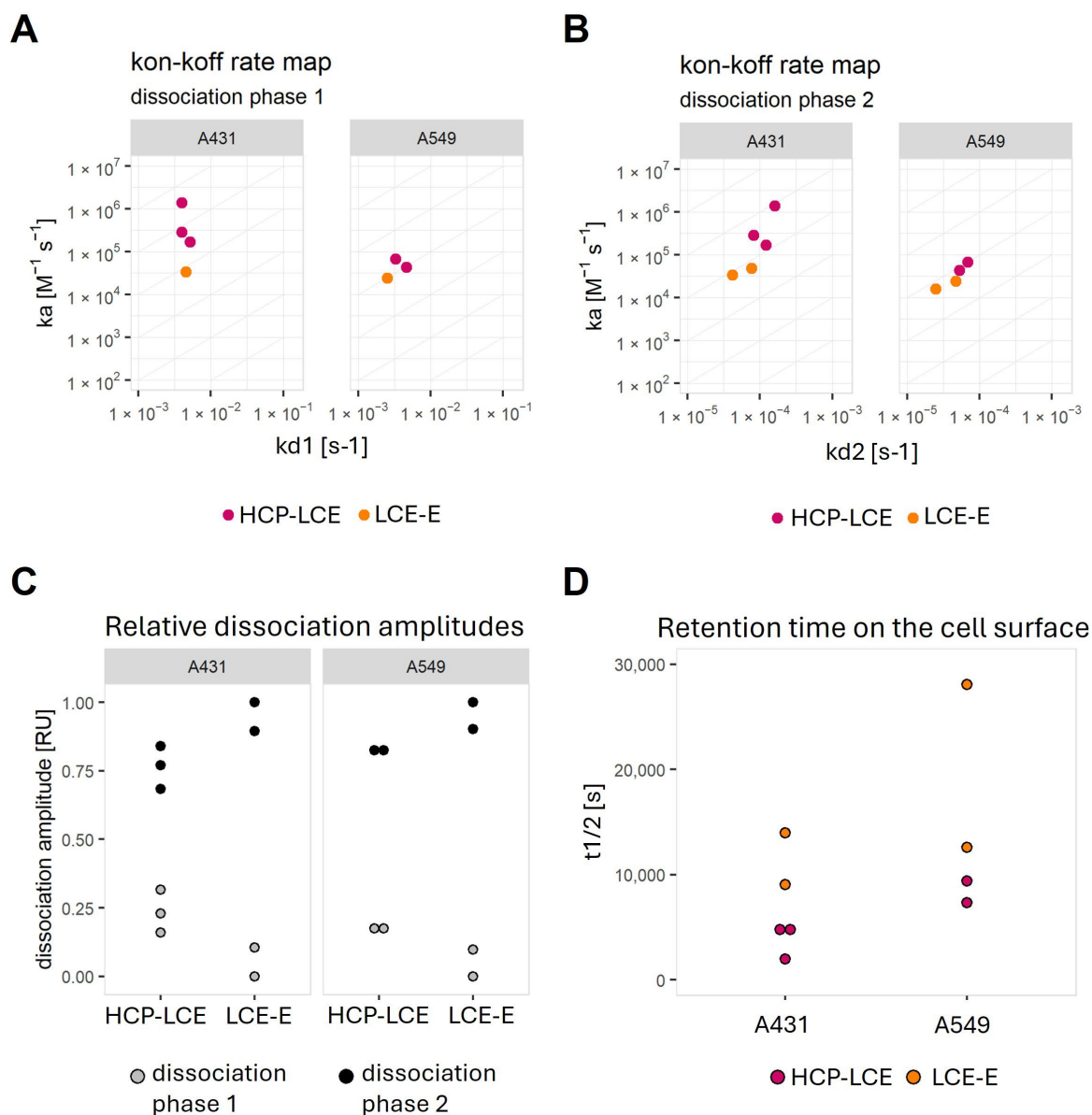


**Figure 6.** Graphical representation of calculated kinetic values after fitting the binding curves with a kinetic model that assumes the monophasic association and biphasic dissociation, as well as the complete dissociation, of the analyte. On-off-rate maps plotting (A) the association rate versus dissociation rate 1 or (B) versus dissociation rate 2. (C) Plot demonstrating the relative contribution of the faster dissociation rate (dissociation phase 1) and the slower dissociation rate (dissociation phase 2). (D) Plot of half-life values calculated from the fit model for each interaction.

To demonstrate that the Two-in-One VH:VL dimer can target EGFR and PD-L1 simultaneously, a protein docking method was applied [48,53]. PD-L1 was docked to the EGFR:VH:VL complex, resulting in a tetrameric protein complex in which both antigens can bind simultaneously without steric hindrance (Figure 7D). PAE and pLDDT plots generated using AlphaFold Multimer are shown in Figure S10. The computer-based data are very consistent with the experimentally determined data.

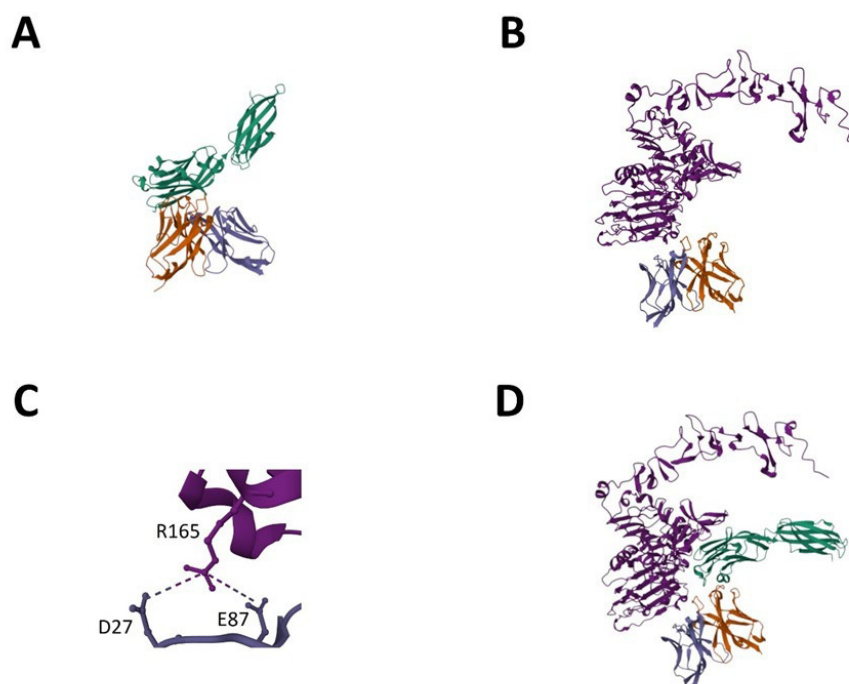


**Figure 7.** AlphaFold-based model for EGFR and PD-L1 binding of LCE-E. (A) PD-L1-ECD (green) binding of LCE-E. (B) EGFR-ECD (light purple) binding of LCE-E. (C) Salt bridge between the glutamic acid at LCDR3 of LCE-E (E87) and an arginine at EGFR-ECD position 165 (R165). (D) Tetrameric protein complex of PD-L1 docked to the EGFR:VH:VL complex. The VH fragment is shown in orange, and the VL fragment is shown in dark purple. Created with AlphaFold Multimer.

#### 4. Discussion

Affinity maturation is the process in which antibodies obtain increased affinity and functionality. It is the result of the somatic hypermutation of immunoglobulin genes in B cells, coupled with selection for antigen binding, a process that occurs over weeks after an acute infection or vaccination [54]. The resulting antibodies can be highly mutated compared to their germline-encoded counterparts, with the affinity for antigens being significantly increased compared to the corresponding naïve B cell receptors [55,56]. This makes affinity maturation a key technique in protein engineering to improve affinity and binding interactions *in vitro* in order to optimize the therapeutic potential of antibodies [57]. Adler et al. observed that *in vivo* affinity-matured antibodies predominantly accumulate mutations within the CDR3 regions, with a total of 6–7 amino acid changes in the heavy and light chain [58]. However, during *in vitro* affinity maturation, libraries with a mutation rate of 1–2 are sufficient for isolating high-affinity binders [59].

In this study, we generated affinity-matured variants of a chicken-derived EGFR×PD-L1 Two-in-One antibody that are enhanced in terms of their EGFR binding properties. To this end, site-saturation mutagenesis was performed by simultaneously substituting a single LCDR1 and LCDR3 codon with degenerated NNS codons. FACS screening of the randomized YSD library resulted in the isolation of a Two-in-One variant (LCE-E) that exhibited a 60-fold improvement in EGFR binding affinity due to the exchange of a single amino acid at LCDR3 position three (Y → E). An AlphaFold-based model showed that the improved EGFR affinity is likely caused by the formation of a salt bridge between the positively charged glutamic acid at LCDR3 position three and a negatively charged arginine at EGFR position 165. A salt bridge is the strongest type of non-covalent interaction in nature, and salt bridges are known to be involved in protein–protein interactions and molecular recognition. A salt bridge combines an electrostatic attraction between oppositely charged chemical groups and a hydrogen bond, which is why its strength exceeds that of a simple hydrogen bond [60–62]. The LCE-D variant, which contains the amino acid

aspartic acid at LCDR3 position three (Y → D), also shows significantly improved EGFR binding comparable to LCE-E. This indicates that the positive charge at this position has a major impact on EGFR binding. A negative charge at LCDR3 position three, as found in the LCE-K mutant (Y → K), eliminates EGFR binding, further supporting this hypothesis.

The improved EGFR binding affinity of the Two-in-One variant LCE-E was confirmed using various methods. The BLI measurements, as well as real-time antigen binding measurements on mixed surfaces and cellular binding experiments on tumor cells, showed significantly improved EGFR binding compared to the wildtype HCP-LCE. In particular, the dissociation rate of LCE-E was reduced, resulting in a stabilized binding and a longer retention time on the cell surface.

However, a higher affinity does not guarantee an improved clinical efficacy. One example for this is a variant of palivizumab with 44-fold-improved potency which only demonstrated a modest improvement in efficacy in subsequent *in vivo* studies and a poor pharmacokinetic profile due to non-specific binding [23].

HCP-LCE is a chimeric antibody consisting of chicken-derived VH and VL domains grafted onto a human IgG1 scaffold [31]. Unlike in mammals, the rearrangement of the variable (V), diverse (D), and connecting (J) gene segments in chickens occurs simultaneously in the heavy and light chains [63,64]. In avian species, however, there is only a small selection of immunoglobulin genes during V(D)J gene rearrangement. Therefore, somatic gene conversion and somatic hypermutation are utilized to further diversify the variable gene [65,66]. The generation of the heavy and light chain repertoire of a chicken thus differs considerably from that of rodents such as mice or rats, which are commonly used for antigen immunization. This could be one reason for the success of affinity maturation based on the targeted mutation of the variable CDR regions of the chicken-derived antibody.

One advantage of antibody generation after animal immunization is that the antibodies have already undergone *in vivo* affinity maturation [8]. Since two chickens were immunized for the generation of HCP-LCE [31] and the heavy chain of an anti-PD-L1 antibody was paired with an anti-EGFR light chain diversity, the heavy and light chain of the Two-in-One antibody were never present in the same chicken. Therefore, no *in vivo* affinity maturation occurred for this heavy and light chain combination, demonstrating the potential for *in vitro* affinity optimization.

HCP-LCE simultaneously targets EGFR and PD-L1 at the same Fv fragment, inhibiting EGFR signaling by binding to dimerization domain II and blocking the PD-1/PD-L1 interaction [31]. The advantageous combination of the antigens EGFR and PD-L1 has also been described in other studies. Koopmans et al. constructed a bispecific PD-L1 × EGFR antibody to direct PD-L1 blockade to EGFR-expressing cancer cells [67]. By fusing a dual-targeting tandem trimmer body with the human IgG1 hinge and Fc region, Rubio-Pérez et al. generated a symmetric bispecific PD-L1 × EGFR antibody that combines an immune checkpoint blockade with a direct action on cancer cells [68]. It is assumed that this target combination improves the efficacy of current immunotherapies.

Overall, we have presented a straightforward method for the affinity maturation of chicken-derived Two-in-One antibodies, optimizing the affinity of only one of the two targets addressed simultaneously with a single Fab fragment. The mutation of individual amino acids of the LCDR3 region followed by YSD library generation and FACS screening resulted in the isolation of a variant that targets EGFR with a 60-fold-increased affinity. BLI measurements demonstrated that the increase in affinity is mainly caused by an improvement in the dissociation rate. LCE-E and LCE-D demonstrated specific cellular binding properties on EGFR/PD-L1 double-positive tumor cells with higher affinity and improved maximum binding compared to the wildtype HCP-LCE. AlphaFold-based models predict that the glutamic acid in LCDR3 forms a salt bridge to EGFR, which causes the increase in affinity. The exchange of glutamic acid to lysine (LCE-K) completely deletes the EGFR binding property. To our knowledge, this represents the first affinity-matured Two-in-One antibody with optimized binding for one of its two targets.

**Supplementary Materials:** The following supporting information can be downloaded at: <https://www.mdpi.com/article/10.3390/antib13020036/s1> Figure S1: Flow cytometric analysis of six isolated yeast single clones after three consecutive rounds of FACS screening; Figure S2: SDS-PAGE analysis of the wildtype Two-in-One antibody HCP-LCE and mutants LCE-E, LCE-D, and LCE-K under reducing (left) and non-reducing conditions (right); Figure S3: Characterization of PD-L1 binding of the HCP-LCE variants by BLI measurements; Figure S4: Characterization of (A) HCP-LCE, (B) LCE-D, (C) LCE-E, and (D) LCE-K binding to a negative control protein by BLI measurements; Figure S5: YSD-based EGFR epitope mapping; Figure S6: BLI-assisted PD-1 competition assay; Figure S7: BLI-assisted simultaneous binding assay; Figure S8: Cellular binding of a monospecific anti-EGFR (grey) and anti-PD-L1 antibody (blue) compared to LCE-E (orange) on EGFR/PD-L1 double-positive A549 cells; Figure S9: Cellular binding of the HCP-LCE variants on EGFR/PD-L1 double-negative Jurkat cells; Figure S10: pLDDT and PAE plots generated by AlphaFold Multimer; Table S1: Kinetic values calculated from switchSENSE<sup>®</sup> measurements; Table S2: Kinetic values calculated from RT-IC measurements.

**Author Contributions:** Conceptualization, J.H., V.M. and H.K.; software, F.K.G.; validation, J.H. and V.M.; investigation, J.H., K.S., D.B. and V.M.; writing—original draft preparation, J.H., V.M. and H.K.; writing—review and editing, F.K.G., K.S. and D.B.; visualization, J.H. and V.M.; supervision, H.K. All authors have read and agreed to the published version of the manuscript.

**Funding:** This research received no external funding.

**Institutional Review Board Statement:** Not applicable.

**Informed Consent Statement:** Not applicable.

**Data Availability Statement:** The data pertaining to this study are available in the manuscript.

**Acknowledgments:** We thank the Customer Support team of Dynamic Biosensors for training, problem solving, and on-site support. We acknowledge the support we received from the Open Access Publishing Fund of Technical University of Darmstadt.

**Conflicts of Interest:** J.H. and H.K. are the inventors of a patent related to the Two-in-One antibody HCP-LCE (EP4238992). David Baumstark and Vera Molkenthin are employed by the company 2bind GmbH. The remaining authors declare no conflicts of interest.

## References

1. Hansel, T.T.; Kropshofer, H.; Singer, T.; Mitchell, J.A.; George, A.J.T. The safety and side effects of monoclonal antibodies. *Nat. Rev. Drug Discov.* **2010**, *9*, 325–338. [[CrossRef](#)] [[PubMed](#)]
2. Stanfield, R.L.; Wilson, I.A. Antibody Structure. *Microbiol. Spectr.* **2014**, *2*. [[CrossRef](#)] [[PubMed](#)]
3. Tsuji, I.; Vang, F.; Dominguez, D.; Karwal, L.; Sanjali, A.; Livengood, J.A.; Davidson, E.; Fouch, M.E.; Doranz, B.J.; Das, S.C.; et al. Somatic Hypermutation and Framework Mutations of Variable Region Contribute to Anti-Zika Virus-Specific Monoclonal Antibody Binding and Function. *J. Virol.* **2022**, *96*, e0007122. [[CrossRef](#)] [[PubMed](#)]
4. Green, N.S.; Lin, M.M.; Scharff, M.D. Somatic hypermutation of antibody genes: A hot spot warms up. *Bioessays* **1998**, *20*, 227–234.
5. Tas, J.M.J.; Mesin, L.; Pasqual, G.; Targ, S.; Jacobsen, J.T.; Mano, Y.M.; Chen, C.S.; Weill, J.-C.; Reynaud, C.-A.; Browne, E.P.; et al. Visualizing antibody affinity maturation in germinal centers. *Science* **2016**, *351*, 1048–1054. [[CrossRef](#)] [[PubMed](#)]
6. Strohl, W.R.; Strohl, L.M. Sources of antibody variable chains. In *Therapeutic Antibody Engineering*; Elsevier: Amsterdam, The Netherlands, 2012; pp. 77–595, ISBN 9781907568374.
7. Bogen, J.P.; Elter, A.; Grzeschik, J.; Hock, B.; Kolmar, H. Humanization of Chicken-Derived Antibodies by Yeast Surface Display. *Methods Mol. Biol.* **2022**, *2491*, 335–360. [[CrossRef](#)]
8. Tabasinezhad, M.; Talebkhan, Y.; Wenzel, W.; Rahimi, H.; Omidinia, E.; Mahboudi, F. Trends in therapeutic antibody affinity maturation: From in-vitro towards next-generation sequencing approaches. *Immunol. Lett.* **2019**, *212*, 106–113. [[CrossRef](#)] [[PubMed](#)]
9. Persson, H.; Kirik, U.; Thörnqvist, L.; Greiff, L.; Levander, F.; Ohlin, M. In Vitro Evolution of Antibodies Inspired by In Vivo Evolution. *Front. Immunol.* **2018**, *9*, 1391. [[CrossRef](#)] [[PubMed](#)]
10. Fujii, I. Antibody affinity maturation by random mutagenesis. *Methods Mol. Biol.* **2004**, *248*, 345–359. [[CrossRef](#)]
11. Lou, J.; Marks, J.D. Affinity Maturation by Chain Shuffling and Site Directed Mutagenesis. In *Antibody Engineering*; Kontermann, R., Dübel, S., Eds.; Scholars Portal: Berlin/Heidelberg, Germany, 2010; pp. 377–396, ISBN 978-3-642-01143-6.
12. Smith, G.P. Filamentous fusion phage: Novel expression vectors that display cloned antigens on the virion surface. *Science* **1985**, *228*, 1315–1317. [[CrossRef](#)]
13. Boder, E.T.; Wittrup, K.D. Yeast surface display for screening combinatorial polypeptide libraries. *Nat. Biotechnol.* **1997**, *15*, 553–557. [[CrossRef](#)] [[PubMed](#)]



14. Tsuruta, L.R.; Dos, M.L.; Moro, A.M. Display Technologies for the Selection of Monoclonal Antibodies for Clinical Use. In *Antibody Engineering*; Böldicke, T., Ed.; InTech: London, UK, 2018; ISBN 978-953-51-3825-9.
15. He, M.; Khan, F. Ribosome display: Next-generation display technologies for production of antibodies in vitro. *Expert Rev. Proteomics* **2005**, *2*, 421–430. [[CrossRef](#)] [[PubMed](#)]
16. Chowdhury, P.S.; Pastan, I. Improving antibody affinity by mimicking somatic hypermutation in vitro. *Nat. Biotechnol.* **1999**, *17*, 568–572. [[CrossRef](#)]
17. Rajpal, A.; Beyaz, N.; Haber, L.; Cappuccilli, G.; Yee, H.; Bhatt, R.R.; Takeuchi, T.; Lerner, R.A.; Crea, R. A general method for greatly improving the affinity of antibodies by using combinatorial libraries. *Proc. Natl. Acad. Sci. USA* **2005**, *102*, 8466–8471. [[CrossRef](#)] [[PubMed](#)]
18. Laffly, E.; Pelat, T.; Cédrone, F.; Blésa, S.; Bedouelle, H.; Thullier, P. Improvement of an antibody neutralizing the anthrax toxin by simultaneous mutagenesis of its six hypervariable loops. *J. Mol. Biol.* **2008**, *378*, 1094–1103. [[CrossRef](#)]
19. Tillotson, B.J.; de Larrinoa, I.F.; Skinner, C.A.; Klavas, D.M.; Shusta, E.V. Antibody affinity maturation using yeast display with detergent-solubilized membrane proteins as antigen sources. *Protein Eng. Des. Sel.* **2013**, *26*, 101–112. [[CrossRef](#)]
20. van den Beucken, T.; Pieters, H.; Steukers, M.; van der Vaart, M.; Ladner, R.C.; Hoogenboom, H.R.; Hufton, S.E. Affinity maturation of Fab antibody fragments by fluorescent-activated cell sorting of yeast-displayed libraries. *FEBS Lett.* **2003**, *546*, 288–294. [[CrossRef](#)]
21. Hu, D.; Hu, S.; Wan, W.; Xu, M.; Du, R.; Zhao, W.; Gao, X.; Liu, J.; Liu, H.; Hong, J. Effective Optimization of Antibody Affinity by Phage Display Integrated with High-Throughput DNA Synthesis and Sequencing Technologies. *PLoS ONE* **2015**, *10*, e0129125. [[CrossRef](#)]
22. Igawa, T.; Tsunoda, H.; Kuramochi, T.; Sampei, Z.; Ishii, S.; Hattori, K. Engineering the variable region of therapeutic IgG antibodies. *MAbs* **2011**, *3*, 243–252. [[CrossRef](#)]
23. Sassi, A.B.; Nagarkar, R.; Hamblin, P. *Biobetter Biologics. Novel Approaches and Strategies for Biologics, Vaccines and Cancer Therapies*; Elsevier: Amsterdam, The Netherlands, 2015; pp. 199–217, ISBN 9780124166035.
24. Kareva, I.; Zutshi, A.; Gupta, P.; Kabilan, S. Bispecific antibodies: A guide to model informed drug discovery and development. *Heliyon* **2021**, *7*, e07649. [[CrossRef](#)]
25. Chen, S.; Li, J.; Li, Q.; Wang, Z. Bispecific antibodies in cancer immunotherapy. *Hum. Vaccin. Immunother.* **2016**, *12*, 2491–2500. [[CrossRef](#)] [[PubMed](#)]
26. Sheridan, C. Bispecific antibodies poised to deliver wave of cancer therapies. *Nat. Biotechnol.* **2021**, *39*, 251–254. [[CrossRef](#)] [[PubMed](#)]
27. Krishnamurthy, A.; Jimeno, A. Bispecific antibodies for cancer therapy: A review. *Pharmacol. Ther.* **2018**, *185*, 122–134. [[CrossRef](#)] [[PubMed](#)]
28. Suurs, F.V.; Lub-de Hooge, M.N.; de Vries, E.G.E.; de Groot, D.J.A. A review of bispecific antibodies and antibody constructs in oncology and clinical challenges. *Pharmacol. Ther.* **2019**, *201*, 103–119. [[CrossRef](#)]
29. Ju, X.; Zhang, H.; Zhou, Z.; Wang, Q. Regulation of PD-L1 expression in cancer and clinical implications in immunotherapy. *Am. J. Cancer Res.* **2020**, *10*, 1–11.
30. Sigismund, S.; Avanzato, D.; Lanzetti, L. Emerging functions of the EGFR in cancer. *Mol. Oncol.* **2018**, *12*, 3–20. [[CrossRef](#)]
31. Harwardt, J.; Bogen, J.P.; Carrara, S.C.; Ullitzka, M.; Grzeschik, J.; Hock, B.; Kolmar, H. A Generic Strategy to Generate Bifunctional Two-in-One Antibodies by Chicken Immunization. *Front. Immunol.* **2022**, *13*, 888838. [[CrossRef](#)]
32. Beck, A.; Wurch, T.; Bailly, C.; Corvaia, N. Strategies and challenges for the next generation of therapeutic antibodies. *Nat. Rev. Immunol.* **2010**, *10*, 345–352. [[CrossRef](#)]
33. Benatuil, L.; Perez, J.M.; Belk, J.; Hsieh, C.-M. An improved yeast transformation method for the generation of very large human antibody libraries. *Protein Eng. Des. Sel.* **2010**, *23*, 155–159. [[CrossRef](#)]
34. Bogen, J.P.; Hinz, S.C.; Grzeschik, J.; Ebenig, A.; Krahl, S.; Zielonka, S.; Kolmar, H. Dual Function pH Responsive Bispecific Antibodies for Tumor Targeting and Antigen Depletion in Plasma. *Front. Immunol.* **2019**, *10*, 1892. [[CrossRef](#)]
35. Harwardt, J.; Carrara, S.C.; Bogen, J.P.; Schoenfeld, K.; Grzeschik, J.; Hock, B.; Kolmar, H. Generation of a symmetrical trispecific NK cell engager based on a two-in-one antibody. *Front. Immunol.* **2023**, *14*, 1170042. [[CrossRef](#)] [[PubMed](#)]
36. Cochran, J.R.; Kim, Y.-S.; Olsen, M.J.; Bhandari, R.; Wittrup, K.D. Domain-level antibody epitope mapping through yeast surface display of epidermal growth factor receptor fragments. *J. Immunol. Methods* **2004**, *287*, 147–158. [[CrossRef](#)] [[PubMed](#)]
37. Bogen, J.P.; Carrara, S.C.; Fiebig, D.; Grzeschik, J.; Hock, B.; Kolmar, H. Expedient Generation of Biparatopic Common Light Chain Antibodies via Chicken Immunization and Yeast Display Screening. *Front. Immunol.* **2020**, *11*, 606878. [[CrossRef](#)] [[PubMed](#)]
38. Jumper, J.; Evans, R.; Pritzel, A.; Green, T.; Figurnov, M.; Ronneberger, O.; Tunyasuvunakool, K.; Bates, R.; Žídek, A.; Potapenko, A.; et al. Highly accurate protein structure prediction with AlphaFold. *Nature* **2021**, *596*, 583–589. [[CrossRef](#)] [[PubMed](#)]
39. Mirdita, M.; Schütze, K.; Moriawaki, Y.; Heo, L.; Ovchinnikov, S.; Steinegger, M. ColabFold: Making protein folding accessible to all. *Nat. Methods* **2022**, *19*, 679–682. [[CrossRef](#)]
40. Baek, M.; DiMaio, F.; Anishchenko, I.; Dauparas, J.; Ovchinnikov, S.; Lee, G.R.; Wang, J.; Cong, Q.; Kinch, L.N.; Schaeffer, R.D.; et al. Accurate prediction of protein structures and interactions using a three-track neural network. *Science* **2021**, *373*, 871–876. [[CrossRef](#)]

41. Evans, R.; O'Neill, M.; Pritzel, A.; Antropova, N.; Senior, A.; Green, T.; Žídek, A.; Bates, R.; Blackwell, S.; Yim, J.; et al. Protein complex prediction with AlphaFold-Multimer. *bioRxiv* **2021**. [[CrossRef](#)]
42. Mirdita, M.; Steinegger, M.; Söding, J. MMseqs2 desktop and local web server app for fast, interactive sequence searches. *Bioinformatics* **2019**, *35*, 2856–2858. [[CrossRef](#)] [[PubMed](#)]
43. Steinegger, M.; Söding, J. MMseqs2 enables sensitive protein sequence searching for the analysis of massive data sets. *Nat. Biotechnol.* **2017**, *35*, 1026–1028. [[CrossRef](#)]
44. Suzek, B.E.; Wang, Y.; Huang, H.; McGarvey, P.B.; Wu, C.H. UniRef clusters: A comprehensive and scalable alternative for improving sequence similarity searches. *Bioinformatics* **2015**, *31*, 926–932. [[CrossRef](#)]
45. Eastman, P.; Swails, J.; Chodera, J.D.; McGibbon, R.T.; Zhao, Y.; Beauchamp, K.A.; Wang, L.-P.; Simmonett, A.C.; Harrigan, M.P.; Stern, C.D.; et al. OpenMM 7: Rapid development of high performance algorithms for molecular dynamics. *PLoS Comput. Biol.* **2017**, *13*, e1005659. [[CrossRef](#)] [[PubMed](#)]
46. Vangone, A.; Bonvin, A.M.J.J. PRODIGY: A Contact-based Predictor of Binding Affinity in Protein-protein Complexes. *Bio Protoc.* **2017**, *7*, e2124. [[CrossRef](#)]
47. Xue, L.C.; Rodrigues, J.P.; Kastiris, P.L.; Bonvin, A.M.; Vangone, A. PRODIGY: A web server for predicting the binding affinity of protein-protein complexes. *Bioinformatics* **2016**, *32*, 3676–3678. [[CrossRef](#)]
48. Yan, Y.; Tao, H.; He, J.; Huang, S.-Y. The HDock server for integrated protein-protein docking. *Nat. Protoc.* **2020**, *15*, 1829–1852. [[CrossRef](#)] [[PubMed](#)]
49. Yan, Y.; Wen, Z.; Wang, X.; Huang, S.-Y. Addressing recent docking challenges: A hybrid strategy to integrate template-based and free protein-protein docking. *Proteins* **2017**, *85*, 497–512. [[CrossRef](#)]
50. Siloto, R.M.; Weselake, R.J. Site saturation mutagenesis: Methods and applications in protein engineering. *Biocatal. Agric. Biotechnol.* **2012**, *1*, 181–189. [[CrossRef](#)]
51. Bogen, J.P.; Carrara, S.C.; Fiebig, D.; Grzeschik, J.; Hock, B.; Kolmar, H. Design of a Trispecific Checkpoint Inhibitor and Natural Killer Cell Engager Based on a 2 + 1 Common Light Chain Antibody Architecture. *Front. Immunol.* **2021**, *12*, 669496. [[CrossRef](#)] [[PubMed](#)]
52. Bogen, J.P.; Storka, J.; Yanakieva, D.; Fiebig, D.; Grzeschik, J.; Hock, B.; Kolmar, H. Isolation of Common Light Chain Antibodies from Immunized Chickens Using Yeast Biopanning and Fluorescence-Activated Cell Sorting. *Biotechnol. J.* **2021**, *16*, e2000240. [[CrossRef](#)]
53. Yin, R.; Feng, B.Y.; Varshney, A.; Pierce, B.G. Benchmarking AlphaFold for protein complex modeling reveals accuracy determinants. *Protein Sci.* **2022**, *31*, e4379. [[CrossRef](#)]
54. MacLennan, I.C. Germinal centers. *Annu. Rev. Immunol.* **1994**, *12*, 117–139. [[CrossRef](#)]
55. Chan, T.D.; Brink, R. Affinity-based selection and the germinal center response. *Immunol. Rev.* **2012**, *247*, 11–23. [[CrossRef](#)] [[PubMed](#)]
56. Doria-Rose, N.A.; Joyce, M.G. Strategies to guide the antibody affinity maturation process. *Curr. Opin. Virol.* **2015**, *11*, 137–147. [[CrossRef](#)]
57. Chan, D.T.Y.; Groves, M.A.T. Affinity maturation: Highlights in the application of in vitro strategies for the directed evolution of antibodies. *Emerg. Top. Life Sci.* **2021**, *5*, 601–608. [[CrossRef](#)] [[PubMed](#)]
58. Adler, A.S.; Mizrahi, R.A.; Spindler, M.J.; Adams, M.S.; Asensio, M.A.; Edgar, R.C.; Leong, J.; Leong, R.; Roalfe, L.; White, R.; et al. Rare, high-affinity anti-pathogen antibodies from human repertoires, discovered using microfluidics and molecular genomics. *MAbs* **2017**, *9*, 1282–1296. [[CrossRef](#)] [[PubMed](#)]
59. Daugherty, P.S.; Chen, G.; Iverson, B.L.; Georgiou, G. Quantitative analysis of the effect of the mutation frequency on the affinity maturation of single chain Fv antibodies. *Proc. Natl. Acad. Sci. USA* **2000**, *97*, 2029–2034. [[CrossRef](#)]
60. Donald, J.E.; Kulp, D.W.; DeGrado, W.F. Salt bridges: Geometrically specific, designable interactions. *Proteins* **2011**, *79*, 898–915. [[CrossRef](#)]
61. Ferreira de Freitas, R.; Schapira, M. A systematic analysis of atomic protein-ligand interactions in the PDB. *Medchemcomm* **2017**, *8*, 1970–1981. [[CrossRef](#)]
62. Spassov, D.S.; Atanasova, M.; Doytchinova, I. A role of salt bridges in mediating drug potency: A lesson from the N-myristoyltransferase inhibitors. *Front. Mol. Biosci.* **2022**, *9*, 1066029. [[CrossRef](#)] [[PubMed](#)]
63. Abbate, F.; Pfarrer, C.; Jones, C.J.P.; Ciriaco, E.; Germanà, G.; Leiser, R. Age-dependent changes in the pigeon bursa of Fabricius vasculature: A comparative study using light microscopy and scanning electron microscopy of vessel casts. *J. Anat.* **2007**, *211*, 387–398. [[CrossRef](#)]
64. Houssaint, E.; Mansikka, A.; Vainio, O. Early separation of B and T lymphocyte precursors in chick embryo. *J. Exp. Med.* **1991**, *174*, 397–406. [[CrossRef](#)]
65. Kurosawa, K.; Ohta, K. Genetic diversification by somatic gene conversion. *Genes* **2011**, *2*, 48–58. [[CrossRef](#)] [[PubMed](#)]
66. Mallaby, J.; Mwangi, W.; Ng, J.; Stewart, A.; Dorey-Robinson, D.; Kipling, D.; Hershberg, U.; Fraternali, F.; Nair, V.; Dunn-Walters, D. Diversification of immunoglobulin genes by gene conversion in the domestic chicken (*Gallus gallus domesticus*). *Discov. Immunol.* **2023**, *2*, kyad002. [[CrossRef](#)] [[PubMed](#)]

- 
67. Koopmans, I.; Hendriks, D.; Samplonius, D.F.; van Ginkel, R.J.; Heskamp, S.; Wierstra, P.J.; Bremer, E.; Helfrich, W. A novel bispecific antibody for EGFR-directed blockade of the PD-1/PD-L1 immune checkpoint. *Oncoimmunology* **2018**, *7*, e1466016. [[CrossRef](#)] [[PubMed](#)]
  68. Rubio-Pérez, L.; Lázaro-Gorines, R.; Harwood, S.L.; Compte, M.; Navarro, R.; Tapia-Galisteo, A.; Bonet, J.; Blanco, B.; Lykkemark, S.; Ramírez-Fernández, Á.; et al. A PD-L1/EGFR bispecific antibody combines immune checkpoint blockade and direct anti-cancer action for an enhanced anti-tumor response. *Oncoimmunology* **2023**, *12*, 2205336. [[CrossRef](#)]

**Disclaimer/Publisher’s Note:** The statements, opinions and data contained in all publications are solely those of the individual author(s) and contributor(s) and not of MDPI and/or the editor(s). MDPI and/or the editor(s) disclaim responsibility for any injury to people or property resulting from any ideas, methods, instructions or products referred to in the content.

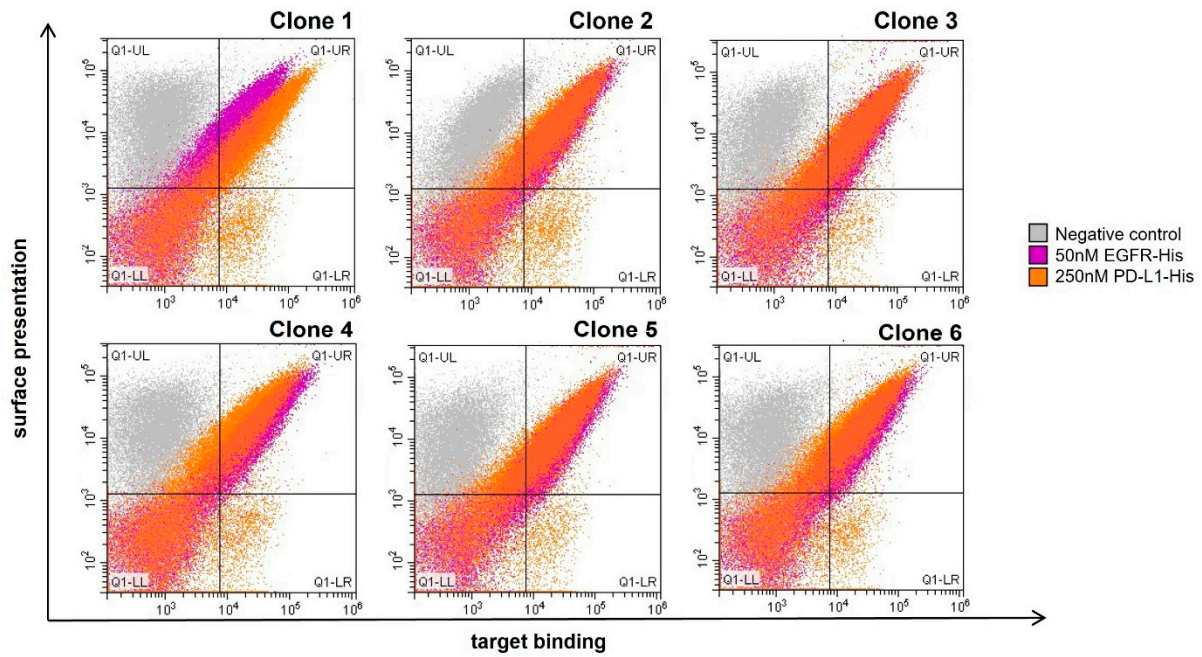


**Figure S1.** Flow cytometric analysis of six isolated yeast single clones after three consecutive rounds of FACS screening. Surface presentation is depicted on the y-axis utilizing the anti-human-Lambda PE-conjugated F(ab')<sub>2</sub> antibody, while EGFR-His<sub>6</sub> (purple) and PD-L1-His<sub>6</sub> (orange) binding is shown on the x-axis using the anti-6xHis AF647 antibody.

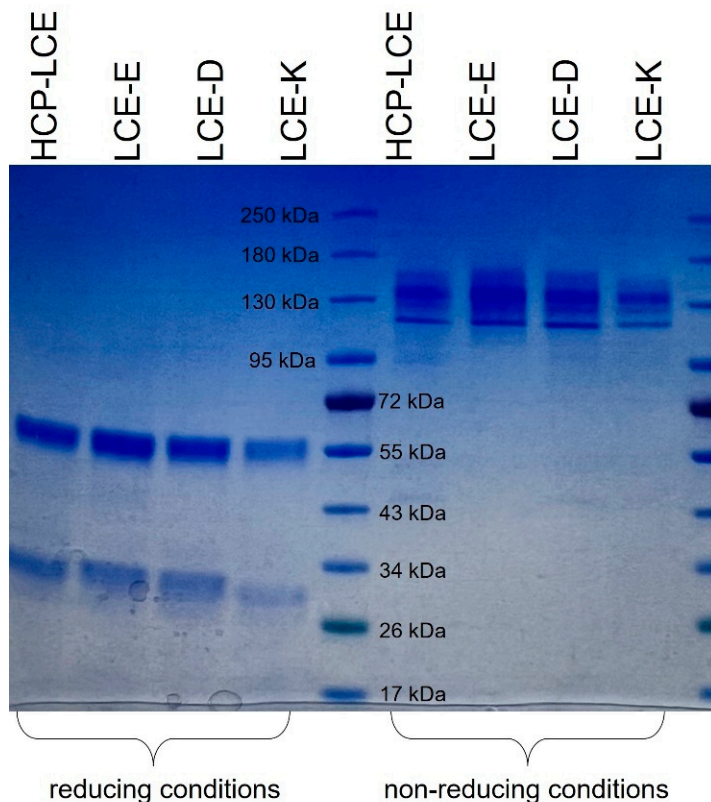


**Figure S2.** SDS-PAGE analysis of the wildtype Two-in-One antibody HCP-LCE and mutants LCE-E, LCE-D and LCE-K under reducing (left) and non-reducing conditions (right). As protein standard, Color Prestained Protein standard (New England Biolabs) was used.

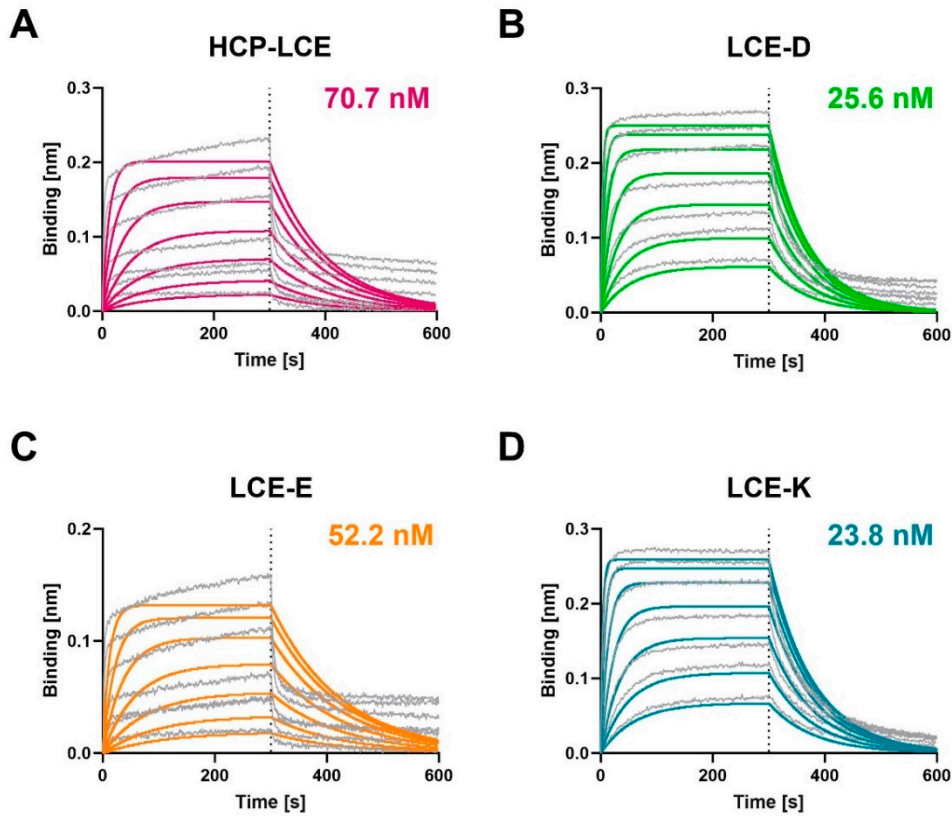


**Figure S3.** Characterization of PD-L1 binding of the HCP-LCE variants by BLI-measurements. BLI-measurements of (A) HCP-LCE, (B) LCE-D, (C) LCE-E and (D) LCE-K against PD-L1. The fit is depicted by the colored curves.

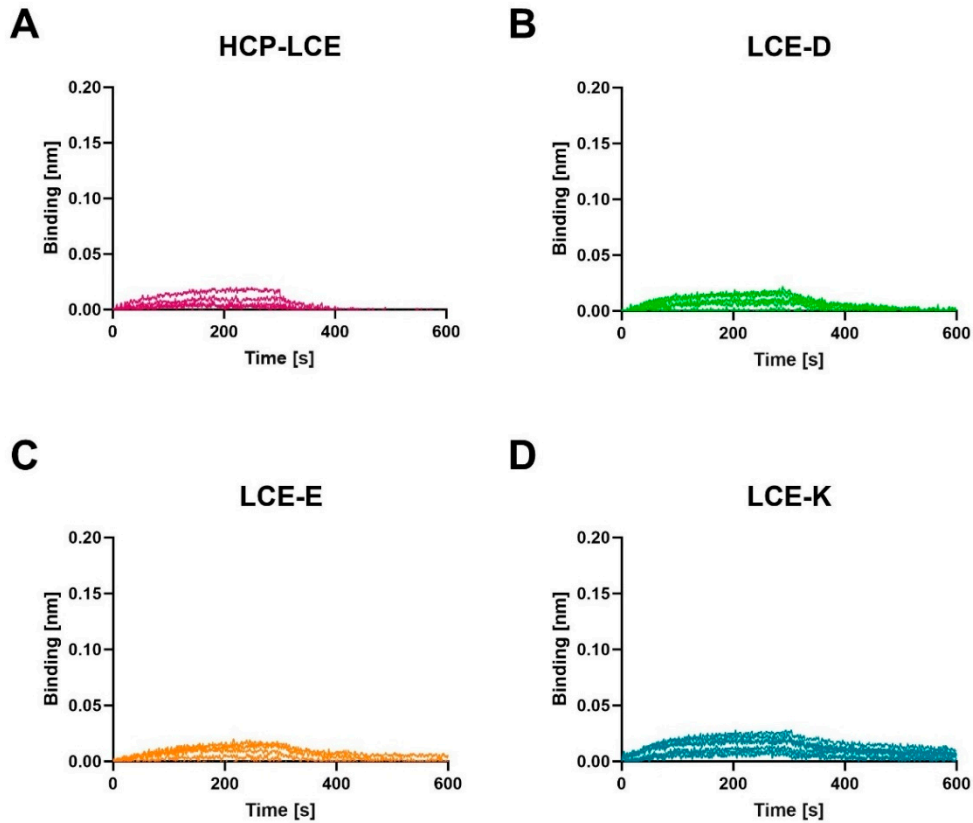


**Figure S4.** Characterization of (A) HCP-LCE, (B) LCE-D, (C) LCE-E and (D) LCE-K binding to a negative control protein by BLI-measurements.

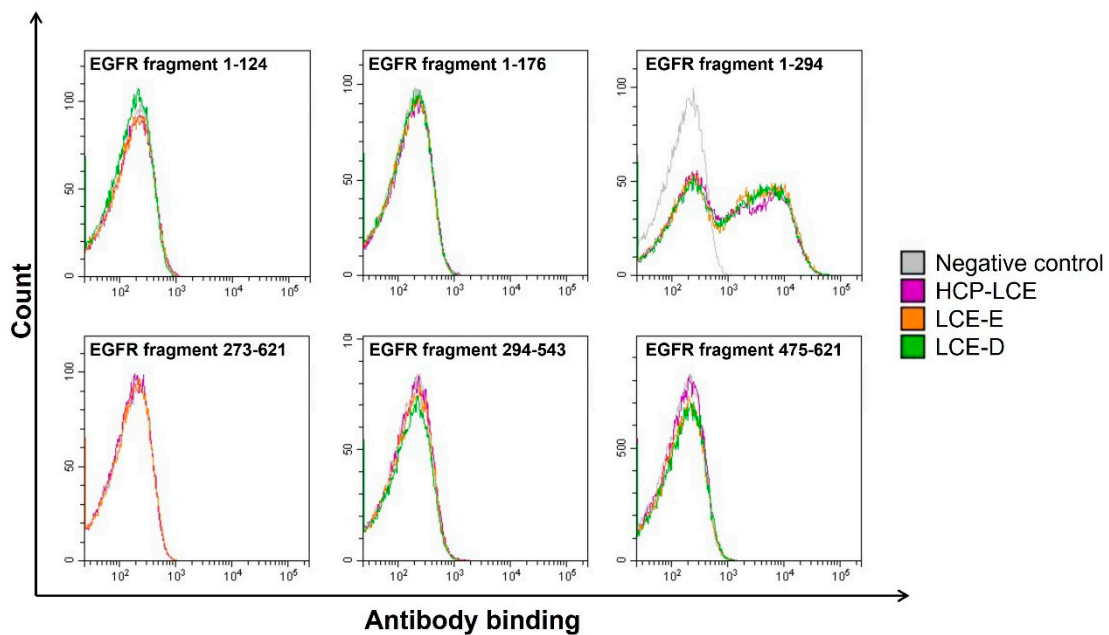


**Figure S5.** YSD-based EGFR epitope mapping. Binding of HCP-LCE (pink), LCE-E (orange) and LCE-D (green) to yeast cells expressing different truncated EGFR fragments was detected using the anti-human Fc PE-labelled antibody. Measurements

without antibody (grey) served as negative control. All antibodies target EGFR fragment 1-294.

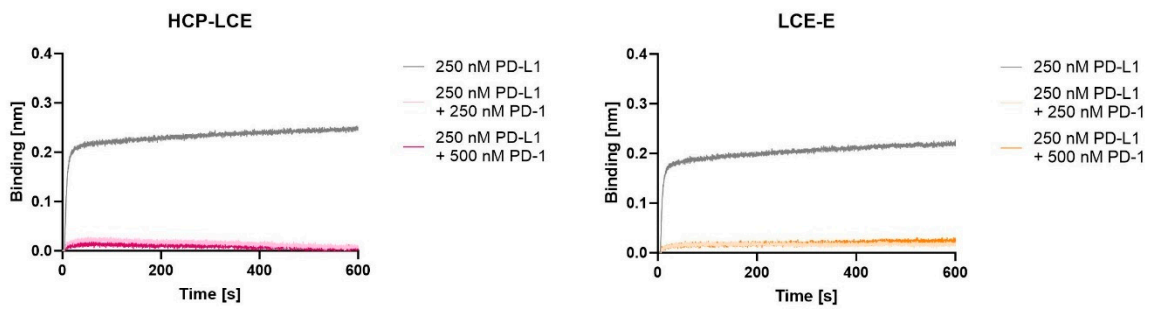


**Figure S6.** BLI-assisted PD-1 competition assay. HCP-LCE and LCE-E were loaded onto FAB2G biosensors and subsequently associated to PD-L1 pre-incubated with varying PD-1 concentrations. The antibodies do not target the PD-1/PD-L1 complex.

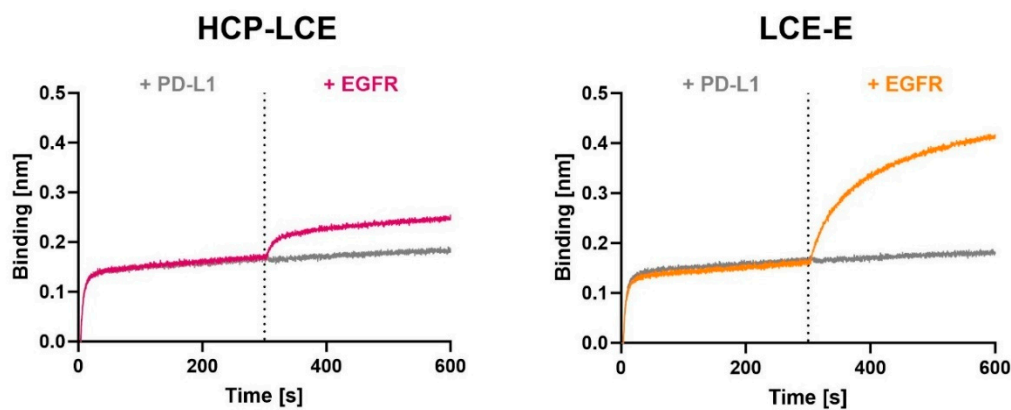


**Figure S7.** BLI-assisted simultaneous binding assay. One-armed variants of the antibodies HCP-LCE and LCE-E were loaded onto AHC biosensors and antigens were added stepwise, revealing simultaneous PD-L1 and EGFR binding.

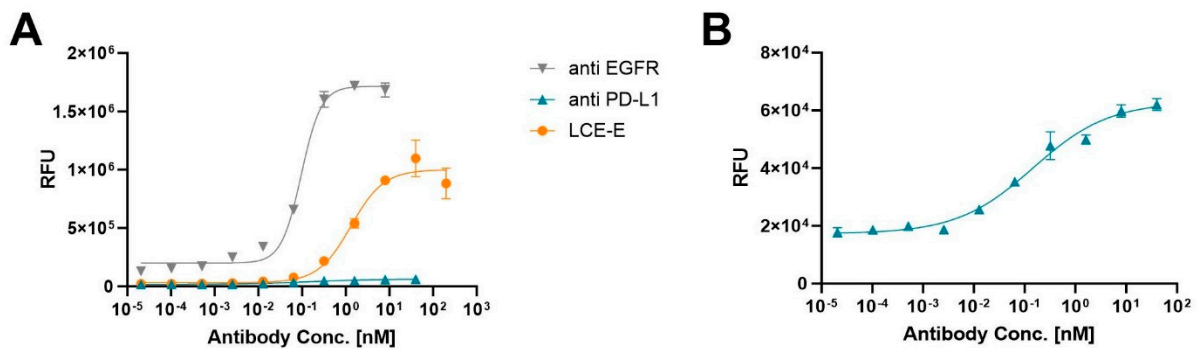


**Figure S8.** Cellular binding of a monospecific anti-EGFR (grey) and anti-PD-L1 antibody (blue) compared to LCE-E (orange) on EGFR/PD-L1 double positive A549 cells. B is a zoomed-in view of the graph shown in A.

**Cellular binding on EGFR/PD-L1 negative Jurkat cells**

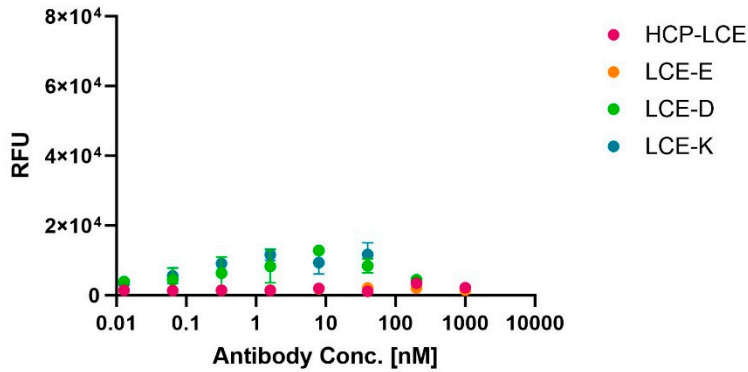


**Figure S9.** Cellular binding of the HCP-LCE variants on EGFR/PD-L1 double negative Jurkat cells. Cell titration of HCP-LCE (pink), LCE-E (orange), LCE-D (green) and LCE-K (blue) on Jurkat cells.

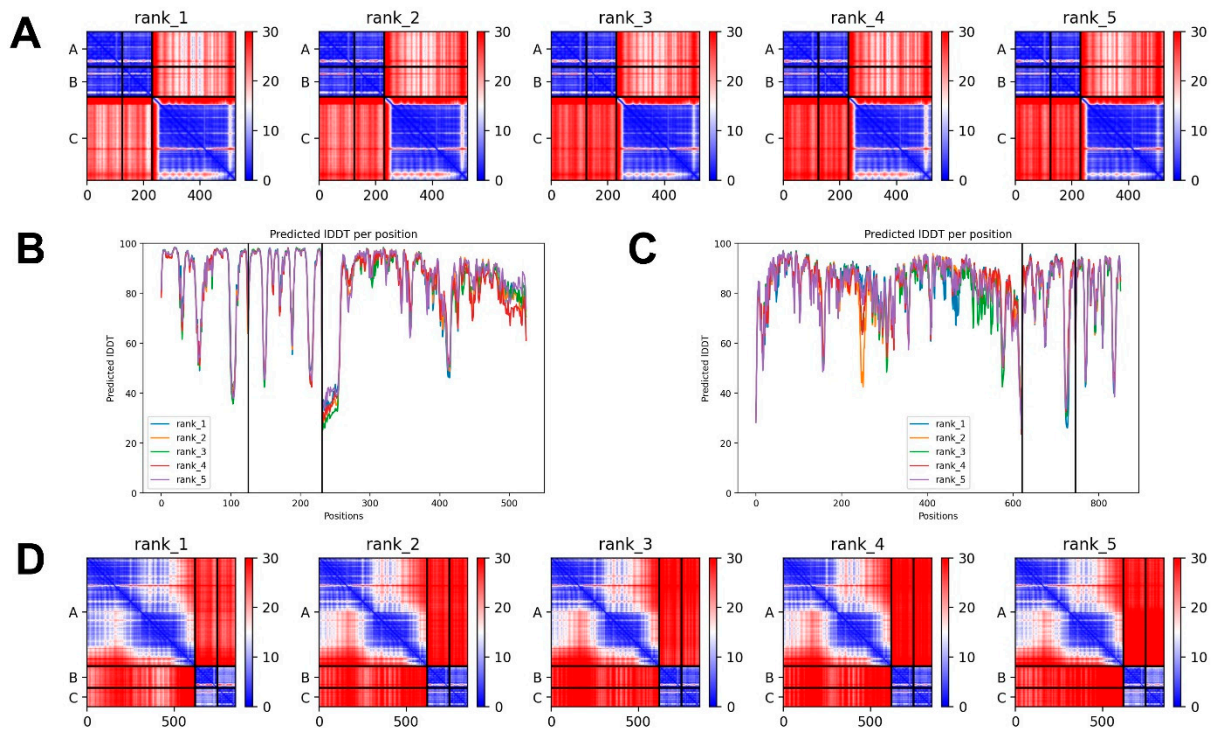


**Figure S10.** pLDDT and PAE plots generated by AlphaFold Multimer. (A) PAE plots of LCE-E and EGFR modelling, (B) pLLDT plot of LCE-E and EGFR modelling, (C) pLLDT plot of HCP-LCE and EGFR modelling, (D) PAE plots of HCP-LCE and EGFR modelling.



**Table S1.** Kinetic values calculated from switchSENSE® measurements.

analyte	surface	monitored interaction	ka [M <sup>-1</sup> s <sup>-1</sup> ]	Kd1 [s <sup>-1</sup> ]	Kd2 [s <sup>-1</sup> ]	KD1 [M]	KD2 [M]	relative dissociation amplitude 1	relative dissociation amplitude 2	t <sub>1/2</sub> [s]
HCP-LCE	PD-L1	PD-L1	4.42E+06	1.87E-02	2.66E-04	4.23E-09	6.02E-11	0.603	0.397	90
	EGFR and PD-L1	EGFR	5.08E+06	1.04E-02	6.88E-05	2.05E-09	1.36E-11	0.795	0.205	95
		PD-L1	5.29E+06	2.17E-02	5.34E-04	4.10E-09	1.01E-10	0.607	0.393	74
	EGFR	EGFR	7.28E+06	2.25E-02	3.19E-04	3.09E-09	4.39E-11	0.690	0.310	56
LCE-E	PD-L1	PD-L1	9.27E+06	1.79E-02	4.71E-04	1.94E-09	5.08E-11	0.436	0.564	269
	EGFR and PD-L1	EGFR	7.39E+06	NA	2.11E-04	NA	2.86E-11	NA	NA	3283
		PD-L1	6.15E+06	2.31E-02	4.85E-04	3.76E-09	7.88E-11	0.626	0.374	35
	EGFR	EGFR	6.78E+06	1.33E-04	1.06E-04	1.96E-11	1.56E-11	0.392	0.608	5982

**Table S2.** Kinetic values calculated from RT-IC measurements.

analyte	cell line	ka [M <sup>-1</sup> s <sup>-1</sup> ]	kd1 [s <sup>-1</sup> ]	kd2 [s <sup>-1</sup> ]	KD1 [M]	KD2 [M]	relative dissociation amplitude 1	relative dissociation amplitude 2	t <sub>1/2</sub> [s]
HCP-LCE	A431	1.37E+06	3.97E-03	1.59E-04	2.90E-09	1.16E-10	0.316	0.684	1966
		2.81E+05	3.97E-03	8.21E-05	1.41E-08	2.92E-10	0.229	0.771	5268
		1.66E+05	5.18E-03	1.21E-04	3.12E-08	7.30E-10	0.159	0.841	4291
	A549	6.70E+04	3.28E-03	6.89E-05	4.89E-08	1.03E-09	0.172	0.828	7312
		4.31E+04	4.65E-03	5.30E-05	1.08E-07	1.23E-09	0.177	0.823	9389
LCE-E	A431	3.41E+04	4.52E-03	4.17E-05	1.33E-07	1.23E-09	0.105	0.895	13960
		4.89E+04	NA	7.67E-05	NA	1.57E-09	0.000	1.000	9035
	A549	1.61E+04	NA	2.47E-05	NA	1.53E-09	0.000	1.000	28056
		2.43E+04	2.50E-03	4.71E-05	1.03E-07	1.93E-09	0.096	0.904	12573

---

#### 4.4. Better safe than sorry: Dual targeting antibodies for cancer immunotherapy

Titel:

Better safe than sorry: Dual targeting antibodies for cancer immunotherapy

Authors:

Katrin Schoenfeld\*, Julia Harwardt\* and Harald Kolmar

(\*shared first authorship)

Bibliographic data:

Journal – Biological Chemistry

Special Issue – Immune Engineering

Article published online: 01 February 2024

DOI: 10.1515/hsz-2023-0329

Copyright © 2024 Walter de Gruyter GmbH, Berlin/Boston.

Contributions by J. Harwardt:

- Literature search with K. Schoenfeld
- Summarizing data from literature and planning of the manuscript with K. Schoenfeld
- Writing of original manuscript draft and generation of figures with K. Schoenfeld

## Review

Katrin Schoenfeld, Julia Harwardt and Harald Kolmar\*

# Better safe than sorry: dual targeting antibodies for cancer immunotherapy

<https://doi.org/10.1515/hsz-2023-0329>

Received October 17, 2023; accepted January 11, 2024;  
published online February 1, 2024

**Abstract:** Antibody-based therapies are revolutionizing cancer treatment and experience a steady increase from preclinical and clinical pipelines to market share. While the clinical success of monoclonal antibodies is frequently limited by low response rates, treatment resistance and various other factors, multispecific antibodies open up new prospects by addressing tumor complexity as well as immune response actuation potentially improving safety and efficacy. Novel antibody approaches involve simultaneous binding of two antigens on one cell implying increased specificity and reduced tumor escape for dual tumor-associated antigen targeting and enhanced and durable cytotoxic effects for dual immune cell-related antigen targeting. This article reviews antibody and cell-based therapeutics for oncology with intrinsic dual targeting of either tumor cells or immune cells. As revealed in various preclinical studies and clinical trials, dual targeting molecules are promising candidates constituting the next generation of antibody drugs for fighting cancer.

**Keywords:** bispecific antibody; cancer immunotherapy; dual targeting; immune cell engager; multispecific antibody

## 1 Introduction

It took 35 years to reach an impressive milestone in therapeutic antibody discovery with the Food and Drug Administration (FDA) approval of the 100th antibody-based product in April

---

Katrin Schoenfeld and Julia Harwardt contributed equally to this work.

\***Corresponding author: Harald Kolmar**, Institute for Organic Chemistry and Biochemistry, Technical University of Darmstadt, Peter-Grünberg-Strasse 4, D-64287 Darmstadt, Germany; and Centre for Synthetic Biology, Technical University of Darmstadt, Darmstadt, Germany, E-mail: Harald.Kolmar@TU-Darmstadt.de. <https://orcid.org/0000-0002-8210-1993>

**Katrin Schoenfeld and Julia Harwardt**, Institute for Organic Chemistry and Biochemistry, Technical University of Darmstadt, Peter-Grünberg-Strasse 4, D-64287 Darmstadt, Germany

2021 (Mullard 2021). Since then, the number has steadily increased, demonstrating that antibodies have become a class of therapeutics of considerable value in recent years. In particular, antibodies are of great importance for cancer drug development, as about one in two antibodies is approved for the treatment of oncology patients. While the number of approved bispecific antibodies is relatively small (nine), interest in bi- and multispecific molecules as well as antibody-drug conjugated and cell-based therapeutics is growing rapidly, as evidenced by the large number of such molecules being investigated in various stages of research and clinical trials (>100) (Lyu et al. 2022).

Examples of novel and potent antibody-based molecules targeting various relevant antigens and key pathways of tumor growth include (i) bispecific antibodies simultaneously targeting two tumor-associated antigens (TAAs) demonstrating enhanced cancer cell selectivity and reduced tumor immune escape (Huang et al. 2020; Schubert et al. 2012), (ii) dual TAA-targeting antibody drug conjugates (ADCs) that efficiently deliver cytotoxic drugs to tumor cells (Huang et al. 2020), (iii) dual TAA-targeting CAR-T cells reducing the likelihood of antigen escape and increasing tumor cell killing activity (Sternier and Sternier 2021; Xie et al. 2022), and (iv) multispecific antibodies targeting tumors in combination with single or dual immune cell targeting which activate immune cells more intense and durable, thereby enhancing effector cell-mediated cytotoxicity (Tapia-Galisteo et al. 2023).

This review focuses on antibody and cell-based therapeutics for oncology clinical development with intrinsic dual targeting of different antigens on the same cell, thereby overcoming bottlenecks of single mode cell targeting. In this context, dual TAA-targeting bispecific antibodies, as well as dual TAA-targeting ADCs and CAR-T cells are described in chapter 2 (Table 1). Furthermore, trispecific immune cell engagers are highlighted in chapter 3, which either simultaneously target two TAAs or two immune cell-related antigens.

## 2 Bispecific dual tumor cell-targeting antibodies

In this chapter, the current status of bispecific antibodies concurrently targeting two different TAAs or different epitopes

**Table 1:** Dual targeting antibodies in preclinical and clinical development.

Drug name	Specificity	Development status	Sponsor/investigator/developer
<b>Bispecific dual tumor cell-targeting antibodies</b>			
Amivantamab (NJ-61186372)	EGFR × c-Met	FDA-approved	Janssen Biotech
MCLA-129	EGFR × c-Met	Clinical study phase 1/2 (NCT04868877; NCT04930432)	Merus
EMB-01	EGFR × c-Met	Clinical study phase 1/2 (NCT03797391; NCT05176665)	EpimAb Biotherapeutics
SI-B001	EGFR × HER3	Clinical study phase 2/3 (NCT05020769)	Sichuan Baili Pharmaceutical Co. Ltd.
MCLA-158	EGFR × LGR5	Clinical study phase 1/2 (NCT03526835)	Merus
MCLA-128 Zenocutuzumab	HER2 × HER3	Clinical study phase 2 (NCT02912949; NCT05588609)	Merus
ZW25	HER2 × HER2	Clinical study phase 2 (NCT04513665)	BeiGene
MBS301	HER2 × HER2	Clinical study phase 1 (NCT03842085)	Mabwork
KN026	HER2 × HER2	Clinical study phase 2 (NCT04165993)	Alphamab Oncology
RO6874813	FAP × DR5	Clinical study phase 1 (NCT02558140)	Roche
BI905711	DR5 × CDH17	Clinical study phase 1 (NCT04137289)	Boehringer Ingelheim
IMGS-001	PD-L1 × PD-L2	Clinical study phase 1 (NCT06014502)	ImmunoGenesis
PM8001	PD-L1 × TGF-β	Clinical study phase 2 (NCT05537051)	Biotheus Inc.
SHR-1701	PD-L1 × TGF-β	Clinical study phase 1 (NCT03710265; NCT03774979)	Jiangsu HengRui Medicine
TG-1801	CD47 × CD19	Clinical study phase 1 (NCT03804996)	TG Therapeutics
NI-1801	CD47 × MSLN	Clinical study phase 1 (NCT05403554)	NovImmune
IBI322	CD47 × PD-L1	Clinical study phase 1 (NCT04795128)	Innovent Biologics
IMM2902	CD47 × HER2	Clinical study phase 1 (NCT05805956)	ImmuneOnco Biopharmaceuticals
IMM0306	CD47 × CD20	Clinical study phase 1 (NCT05805943)	ImmuneOnco Biopharmaceuticals
<b>Dual tumor-targeting antibody-drug conjugates</b>			
bsHER2xCD63his-Duo3	HER2 × CD63	Preclinical	Goeij et al.
PRLR × HER2 BsADC	HER2 × PRLR	Preclinical	Zong et al.
ZW49	HER2 × HER2	Clinical study phase 1 (NCT03821233)	Zymeworks/BeiGene
REGN5093-M114	MET × MET	Clinical study phase 1/2 (NCT04982224)	Regeneron Pharmaceuticals
DT2219	CD19 × CD22	Clinical study phase 1/2 (NCT02370160)	Masonic Cancer Center, University of Minnesota
<b>Dual tumor-targeting chimeric antigen receptor-T cells</b>			
TanCARCD19/20 T cells	CD19 × CD20	Clinical study phase 1/2 (NCT03097770)	Chinese PLA General Hospital
CAR-20/19-T	CD19 × CD20	Clinical study phase 1 (NCT03019055)	Medical College of Wisconsin
CART19/20	CD19 × CD20	Clinical study phase 1 (NCT04007029)	Jonsson Comprehensive Cancer Center
CD19/CD22 Bicistronic CAR-T cells	CD19 × CD22	Clinical study phase 1/2 (NCT05442515)	National Cancer Institute (NCI)
CD19/CD22 dual targeted CAR-T cell	CD19 × CD22	Clinical study phase 1 (NCT05225831)	Hebei Senlang Biotechnology Inc., Ltd.
CD19/CD22-CAR-T cell	CD19 × CD22	Clinical study phase 1 (NCT03448393)	National Cancer Institute (NCI)
FasT CAR-T GC012F	BCMA × CD19	Clinical study phase 1/2 (NCT04935580)	Shanghai Changzheng Hospital
BM38 CAR-T	BCMA × CD38	Clinical study phase 1/2 (NCT03767751)	Chinese PLA General Hospital
BCMA/CS1 CAR-T	BCMA × CD319	Preclinical	Zah et al.
BCMA/GPRC5D CAR-T	BCMA × GPRC5D	Preclinical	De Larrea et al.
<b>Trispecific dual targeting immune cell engager</b>			
<b>Dual tumor cell-targeting ICEs</b>			
TCE	CD19 × CD20 × CD3	Preclinical	Wang et al.
TCE	CD19 × CD22 × CD3	Preclinical	Zhao et al.
TCE	CD19 × CD33 × CD3	Preclinical	Roskopf et al.
TCE	EGFR × EpCAM × CD3	Preclinical	Tapia-Galisteo et al.
TCE	HER2 × VEGFR2 × CD3	Preclinical	Liu et al.
NKCE	CD33 × CD19 × CD16	Preclinical	Schubert et al.

Table 1: (continued)

Drug name	Specificity	Development status	Sponsor/investigator/developer
NKCE	CD33 × CD123 × CD16	Preclinical	Kügler et al.
NKCE	CD22 × CD19 × CD16	Preclinical	Gleason et al.
NKCE	BCMA × CD2000 × CD16	Preclinical	Gantke et al.
NKCE	EGFR × PD-L1 × CD16	Preclinical	Bogen et al.
NKCE	EGFR × PD-L1 × CD16	Preclinical	Harwardt et al.
<b>Dual immune cell-targeting ICEs</b>			
<b>Dual T cell-targeting ICEs</b>			
SAR442257	CD38 × CD3 × CD28	Clinical study phase 1 (NCT04401020)	Sanofi
SAR443216	HER2 × CD3 × CD28	Clinical study phase 1 (NCT05013554)	Sanofi
<b>Dual NK cell-targeting ICEs</b>			
NKCEs	CD16 × NKp46 × CD19/CD20/EGFR	Preclinical	Innate Pharma
ANKET IPH62	CD16 × NKp46 × B7-H3	Preclinical	Innate Pharma/Sanofi
ANKET IPH6101 (SAR443579)	CD16 × NKp46 × CD123	Clinical study phase 1/2 (NCT05086315)	Innate Pharma/Sanofi
ANKET IPH6401	CD16 × NKp46 × BCMA	Clinical study phase 1/2 (NCT05839626)	Innate Pharma/Sanofi
TriNKETs	NKG2D × CD16 × TAA (e.g. HLA-E/CCR4/PD-L1/FLT3)	Preclinical	Dragonfly Therapeutics
TriNKET DF9001	NKG2D × CD16 × EGFR	Clinical study phase 1/2 (NCT05597839)	Dragonfly Therapeutics
TriNKET DF3001	NKG2D × CD16 × BCMA	Clinical study phase 1 (NCT04975399)	Bristol-Myers Squibb
TriNKET DF2001	NKG2D × CD16 × CD33	Clinical study phase 1 (NCT04789655)	Bristol-Myers Squibb
TriNKET DF1001	NKG2D × CD16 × HER2	Clinical study phase 1/2 (NCT04143711)	Dragonfly Therapeutics
<b>Tetraspecific dual targeting immune cell engager</b>			
ANKET4	NKp46 × CD16a × IL-2Rβ × CD20	Preclinical	Innate Pharma
GNC-035, GNC-038 and GNC-039	CD3 × 4-1BB × PD-L1 × ROR1/CD19/EGFRvIII	Clinical study phase 1/2 (NCT05160545; NCT04606433; NCT04794972)	Sichuan Baili/Systimmune

on the same TAA is reviewed. Dual TAA-targeting antibodies are a subclass of bispecific antibodies that offer several advantages, including increased tumor selectivity, simultaneous modulation of two functional pathways in the tumor cell and circumvention of drug resistance or immune escape mechanisms (Figure 1) (Huang et al. 2020; Schubert et al. 2012). Monospecific antibodies are frequently not able to sharply discriminate between malignant and healthy cells carrying the same target antigen which may result in on-target off-tumor toxicity (Brennan et al. 2010). The generation of bispecific dual TAA-targeting antibodies that show relatively low affinity for one or both of the antigens while binding with high affinity to tumor cells that display both targets on their cell surface, results in increased tumor selectivity (Figure 1) (Harwardt et al. 2022; Sun et al. 2021). The appropriate fine-tuning of individual affinities can result in an augmented toxic effect against the tumor while therapy-related side effects are reduced, which is associated with superior drug tolerability and safety (Bendell et al. 2018; Dheilly et al. 2017; Jiang et al. 2021). Antibodies that address two receptors expressed on tumor cells further enable simultaneous modulation of two distinct functional pathways evoking alternative cell fates (Huang et al. 2020; Temraz et al.

2016). Moreover, treatment of a multi-factorial disease like cancer with monoclonal antibodies is always at risk of causing drug resistance, particularly via tumor escape mechanisms such as antigen mutation, downregulation or shedding (Reslan et al. 2009; Vasan et al. 2019). The feature of bispecific dual TAA-targeting antibodies to target two different, individually overexpressed targets on tumor cells can contribute to risk mitigation regarding drug resistance and immune escape, e.g., via immune checkpoints such as programmed cell death protein 1 (PD-1)/PD-L1 or signal regulatory protein α (SIRPα)/CD47 (Figure 1) (Huang et al. 2020; Schubert et al. 2012). The following section outlines TAA combinations for which bispecific antibodies have been developed, focusing on those currently in clinical trials or already approved for clinical use.

## 2.1 EGFR × c-Met

The epithelial growth factor receptor (EGFR) and the mesenchymal epithelial transition factor (c-Met) are commonly expressed on tumor cells and are involved in the development and progression of various tumor types through their diverse

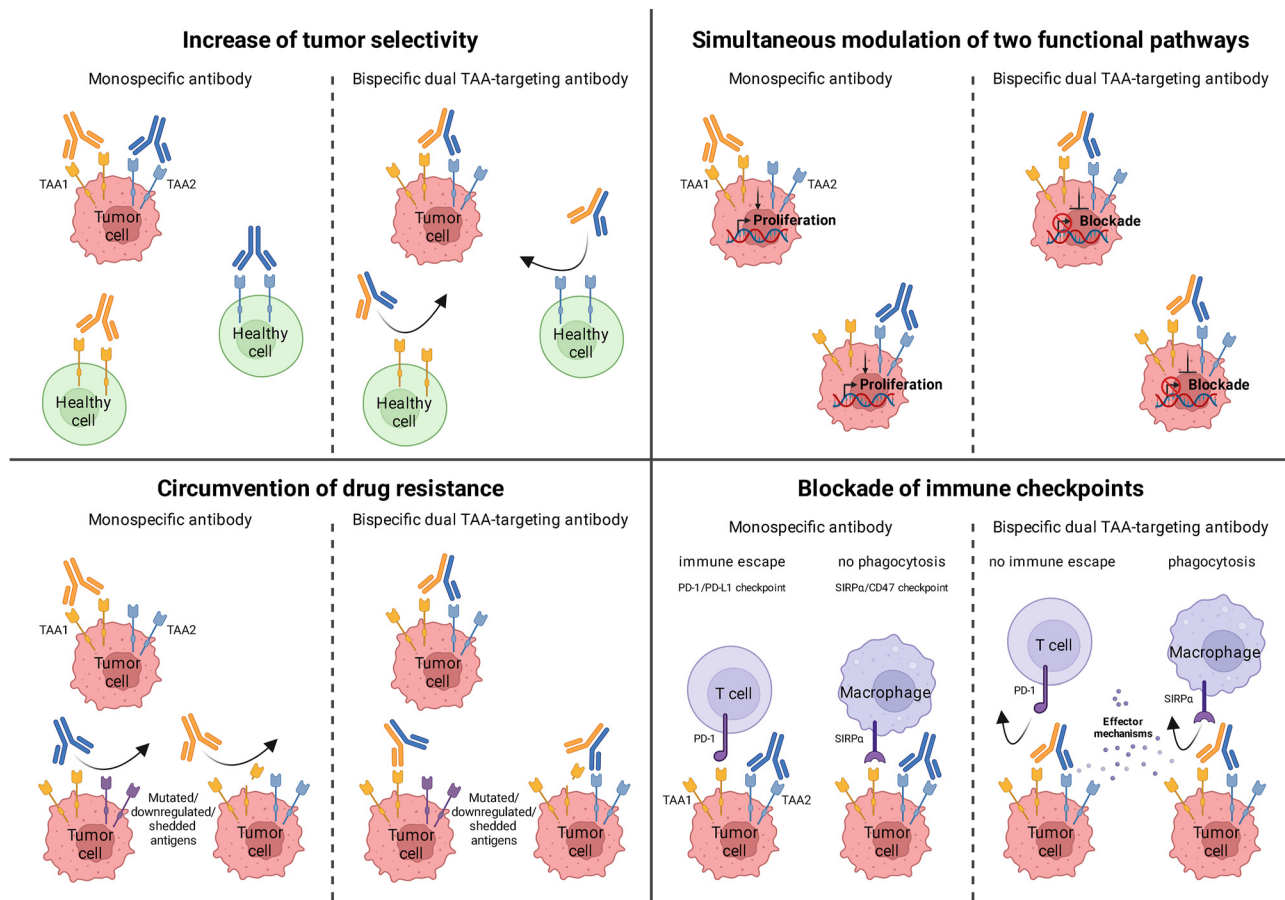


**Figure 1:** Mechanisms of bispecific dual tumor cell-targeting antibodies compared to monospecific antibodies. Bispecific dual TAA-targeting antibodies increase tumor specificity by binding to tumor cells expressing both antigens, but not to healthy cells expressing one of the antigens. They simultaneously modulate two functional pathways resulting in alternative signaling and cell fates, circumvent drug resistance and block immune checkpoints thereby preserving antibody-mediated effector mechanisms.

effects on the cell cycle, programmed cell death, and invasion (Sigmund et al. 2018; van Herpe and van Cutsem 2023). Notably, they utilize a highly overlapping repertoire of signaling adapters and downstream signaling pathways (Giovannetti and Leon 2014). Based on the signaling crosstalk between EGFR and c-Met, combinatorial inhibition of both receptors may restrict compensatory pathway activation and improve the overall efficacy of therapeutic antibodies (Moores et al. 2016). Amivantamab (JNJ-61186372) is a bispecific EGFR and c-Met-targeting antibody developed by Janssen Biotech utilizing Genmab's DuoBody® technology, that inhibits both, EGFR and c-Met signaling by blocking ligand-induced activation and inducing receptor degradation. Moreover, interaction of the amivantamab Fc domain with Fcγ receptors on natural killer (NK) cells leads to antibody-dependent cellular cytotoxicity (ADCC), and interaction with Fcγ receptors on monocytes and macrophages results in cytokine production and trogocytosis (Moores et al. 2016; Vijayaraghavan et al. 2020). Amivantamab is the first-in-class dual TAA-targeting antibody that

received FDA approval in May 2021 in the US for the treatment of adult patients with locally advanced or metastatic non-small cell lung cancer (NSCLC) harboring EGFR Exon 20 insertion mutations with progression on or after platinum-based chemotherapy (Syed 2021). The efficacy of amivantamab is partly based on its ability to target a NSCLC mutation that has historically had a poor prognosis due to innate resistance to previously approved EGFR tyrosine kinase inhibitors (Russell et al. 2023). A phase 3 study showed that the use of amivantamab in combination with chemotherapy results in superior efficacy compared to chemotherapy alone as first-line treatment of patients with advanced NSCLC with EGFR exon 20 insertions (Zhou et al. 2023). Two other EGFR- and c-Met-targeting bispecific antibodies currently undergoing clinical trials for the treatment of advanced solid tumors are represented by the full-length, common light chain (cLC), electrostatic CH3-engineered (DEKK), ADCC enhanced antibody MCLA-129, discovered by Merus (NCT04868877; NCT04930432) (Ou et al. 2022) and the tetravalent antibody EMB-01 developed by

EpimAb Biotherapeutics based on the proprietary FIT-Ig® platform (NCT03797391; NCT05176665) (Qing et al. 2022; Ren et al. 2020). Both molecules have demonstrated efficacy in multiple preclinical cancer models highlighting the synergistic function of EGFR and c-Met signaling blockade (Ou et al. 2022; Ren et al. 2020).

## 2.2 EGFR × HER3

Another member of the ErbB/HER receptor tyrosine kinase (RTK) family found in various tumor types promoting cell proliferation, is the human epidermal growth factor receptor 3 (HER3). Expression and activation of HER3 has been associated with resistance to drugs targeting EGFR (Gandullo-Sánchez et al. 2022). Therefore, dual targeting of EGFR and HER3 may be an approach to overcome this resistance and increase selectivity for EGFR/HER3 double positive tumors inhibiting both signaling pathways simultaneously (Temraz et al. 2016). Sichuan Baili Pharmaceutical Co. Ltd developed the bispecific antibody SI-B001 which is built on a tetravalent platform exhibiting two highly selective binding domains for EGFR and HER3, respectively. *In vitro*, SI-B001-mediated inhibition of tumor cell growth was stronger than that of cetuximab and dolutuzumab mAb combination (Renshaw et al. 2023). The dual blockade bispecific antibody has demonstrated encouraging anti-tumor efficacy in several xenograft models of epithelium squamous cell carcinomas (Xue et al. 2020) and is now being investigated in a clinical phase 2/3 study (NCT05020769).

## 2.3 EGFR × LGR5

To specifically trigger EGFR degradation in leucine-rich repeat-containing G-protein-coupled receptor 5 (LGR5)-positive cancer stem cells, Merus developed the human cLC IgG1 bispecific antibody, MCLA-158, against EGFR and LGR5 with enhanced ADCC activity (Herpers et al. 2022). MCLA-158 was found to be a potent inhibitor of colorectal cancer organoid growth blocking the initiation of metastasis, as well as growth in various preclinical models of cancer, including head and neck, esophagus and stomach tumors (García et al. 2023). Currently, MCLA-158 is tested in a phase 1/2 clinical trial (NCT03526835) where it demonstrates encouraging clinical efficacy (Cohen et al. 2023). Compared to other EGFR-targeting antibodies, MCLA-158 displays superior selectivity for tumor-derived organoids and an augmented therapeutic activity (Herpers et al. 2022), which is most likely caused by dual TAA targeting.

## 2.4 HER2 × HER3

Neuregulin 1 (NRG1)-mediated HER3 activation promotes asymmetric dimerization of HER3 with other members of the ErbB/RTK family, of which the HER2/HER3 dimers represent the most oncogenic ones (Klapper et al. 1999; Zhang et al. 2006). Consequently, addressing HER2/HER3 signaling is a promising therapeutic approach. The bispecific humanized full-length IgG1 antibody MCLA-128 developed by Merus targeting HER2 and HER3 is designed to block the binding of NRG1 to HER3 (Geuijen et al. 2018). One arm of the antibody binds to the HER2 receptor, optimally positioning the other arm to block the NRG1/HER3 interaction. In tumor models resistant to HER2-targeting agents, MCLA-128 effectively inhibits HER3 signaling via this “dock & block” mechanism (Geuijen et al. 2018; Schram et al. 2022). MCLA-128 demonstrated therapeutic efficacy *in vitro* and *in vivo* in various tumors harboring NRG1 fusions. The potential use of MCLA-128 as a therapy for NRG1 fusion-driven cancers is being investigated in an ongoing phase 2 trial (NCT02912949; NCT05588609) (Schram et al. 2022).

## 2.5 HER2 × HER2

Another option to improve the efficacy of an antibody by preventing resistance via dual tumor targeting is addressing two non-overlapping epitopes of the same TAA. Three so-called biparatopic antibodies targeting extracellular domains (ECDs) II and IV of HER2, which are also bound by the mAbs trastuzumab (IV) and pertuzumab (II) (Hao et al. 2019), are currently being investigated in clinical trials (NCT04513665, NCT03842085, NCT04165993). HER2 is overexpressed in many solid tumors, leading to activation of various signaling pathways that promote cell proliferation and tumorigenesis (Rubin and Yarden 2001). Since many patients experience disease progression over time after treatment with anti-HER2 agents, intrinsic and acquired resistance to approved HER2 therapies is a clinical concern (Rexer and Arteaga 2012). Biparatopic binding of the anti-HER2 antibodies effects receptor crosslinking which promotes receptor internalization and degradation. BeiGenes' ZW25 antibody, Mabworks' MBS301 antibody and Alphamab Oncologys' KN026 antibody have the potential to be used for treating HER2-positive, trastuzumab-resistant solid tumors (Huang et al. 2018; Weisser et al. 2023; Xu et al. 2023).

## 2.6 DR5 × TAA

Since dysregulated cellular apoptosis and resistance to cell death are characteristics of neoplastic initiation and

progression, the development of compounds that overcome the abnormal death regulation in tumor cells is of great therapeutic value. Activation of the extrinsic apoptotic pathway is highly dependent on hyperclustering of death receptors (DRs) on the cell surface, and therefore tumor-targeted induction of apoptosis may be achieved with antibodies binding DR5 and a TAA (Brünker et al. 2016). This was confirmed by the Roche-developed tetravalent antibody RO6874813, which targets the fibroblast activation protein (FAP) on cancer-associated fibroblasts in tumor stroma with high affinity and DR5 with low affinity (Bendell et al. 2018). Bivalent binding of both FAP and DR5 results in avidity-driven hyperclustering of DR5, further leading to induction of apoptosis in tumor cells but not in normal cells (Brünker et al. 2016). The anti-tumor efficacy of RO6874813 is strictly FAP-dependent and superior to conventional DR5 antibodies. The antibody demonstrated a favorable safety profile in patients with multiple solid tumor types in a phase 1 trial (NCT02558140), indicating that tetravalent binding of FAP and DR5 is a promising approach to overcome tumor-associated resistance to apoptosis (Bendell et al. 2018). Another TAA that shows positive effects in combination with DR5 is CDH17, a cell surface molecule member of the Cadherin superfamily of adhesion molecules (Tian et al. 2023). Boehringer Ingelheim developed the tetravalent bispecific antibody BI905711, targeting both DR5 and CDH17. The molecule triggers strong and tissue-specific DR5 activation, rendering it highly effective and strictly dependent on CDH17 expression in various colorectal xenograft models (García-Martínez et al. 2021).

## 2.7 PD-L1 × TAA

The PD-1/PD-L1 axis, representing an immune checkpoint for T cells and NK cells, is of huge interest in clinical practice as its inhibition has tremendous impact on cancer treatment outcomes (Brahmer et al. 2012; Sun et al. 2020). To overcome immune surveillance, programmed cell death 1-ligand 1 (PD-L1 or CD274) is upregulated in many malignant cancers (Ju et al. 2020). Three FDA-approved PD-L1-targeting antibodies demonstrated durable clinical benefits and long-term remissions, however, this effect has been limited to a small proportion of patients suffering from certain cancer types (Alvarez-Argote and Dasanu 2019; Kim 2017; Markham 2016; O'Donnell et al. 2017; Pang et al. 2023). Bispecific antibodies capable of simultaneously targeting another TAA may deliver advances in cancer immunotherapy. In this particular context, high expression of programmed cell death 1-ligand 2 (PD-L2 or CD273), a second ligand for PD-1, has been shown to play an important role in tumorigenesis and immune escape (Wang et al. 2023). The antibody IMGS-001

developed by ImmunoGenesis concurrently targets PD-L1 and PD-L2, which is why the molecule could benefit patients that are resistant to existing PD-(L)1 therapy by restoring immune-driven anti-tumor activity (Gagliardi et al. 2022). IMGS-001 is currently being investigated in a clinical phase 1 study (NCT06014502). Further PD-L1 × TAA molecules, including PD-L1 × PD-L2/TGF- $\beta$ , effectively providing synergistic blockade, were introduced by Biotheus (Riu Martinez et al. 2022). The transforming growth factor (TGF)- $\beta$ -addressing variant, PM8001, is constituted of a humanized anti-PD-L1 VHH domain and the ECD of TGF- $\beta$  receptor II fused to a human IgG1 Fc portion, and is currently under clinical investigation displaying promising anti-tumor activity in advanced solid tumors (NCT05537051) (Guo et al. 2022). In addition to this dual-targeting PD-L1 × TGF- $\beta$  antibody, Jiangsu HengRui Medicine developed a similar bifunctional fusion protein composed of a mAb against PD-L1 fused with the ECD of TGF- $\beta$  receptor II scrutinized as first-line therapy for PD-L1-positive advanced/metastatic NSCLC as well as for advanced solid tumors in phase 1 studies (NCT03710265; NCT03774979) (Feng et al. 2021; Liu et al. 2021). Another TAA that has been reported to be overexpressed in a variety of cancers is represented by EGFR, as described above (Sigismund et al. 2018). Co-targeting of PD-L1 and EGFR elicits immune checkpoint blockade and enhances the anti-tumor response, as demonstrated by three preclinically developed PD-L1 × EGFR bispecific antibodies. The molecules inhibit EGF-mediated proliferation, effectively block PD-1/PD-L1 interaction and induce a strong ADCC effect *in vitro* (Harwardt et al. 2022; Koopmans et al. 2018; Rubio-Pérez et al. 2023).

## 2.8 CD47 × TAA

Since the interaction of CD47 with thrombospondin-1 and SIRP $\alpha$  triggers a “don't eat me” signal on macrophages, overexpression of CD47 enables the tumor to evade immune surveillance by blocking phagocytic mechanisms (Jiang et al. 2021). However, CD47 is ubiquitously expressed on human cells which resulted in anti-CD47 antibodies causing severe anemia and thrombocytopenia. To circumvent this, bispecific antibodies were designed simultaneously targeting another tumor antigen to promote tumor-selective interaction of an affinity-optimized arm targeting CD47 (Jiang et al. 2021; Sun et al. 2021). TG-1801 is a fully humanized bispecific IgG1  $\kappa\lambda$  body developed by TG Therapeutics consisting of one arm targeting the B cell specific marker CD19, widely expressed across B cell malignancies, with high affinity, and another arm targeting CD47 with low affinity (Normant et al. 2019; Wang et al. 2012). By binding to CD19 with high affinity,



TG-1801 selectively inhibits CD47 signaling in B cells (Buatois et al. 2018) and is therefore currently undergoing a phase 1 clinical trial for B cell lymphoma patients (NCT03804996). Furthermore, the bispecific  $\kappa\lambda$  body NI-1801 was developed by NovImmune targeting Mesothelin (MSLN), which is highly expressed in many solid tumors, with high affinity and blocking CD47 with an affinity-optimized arm (Hatterer et al. 2020). Also in this case, the unbalanced affinity allows selective CD47 blockade in MSLN-expressing cells. After demonstrating an inhibitory effect on tumor growth in xenograft models *in vivo*, NI-1801 is now being investigated in a first-in-human clinical trial (NCT05403554) (Romano et al. 2022).

Another antibody based on the concept of targeting CD47 with low affinity and an additional TAA with high affinity is the anti-PD-L1/CD47 antibody IBI322 developed by Innovent Biologics. Due to optimized target selectivities, IBI322 is able to selectively bind CD47/PD-L1 double positive tumor cells, even in the presence of CD47 positive erythrocytes. Consisting of a Fab anti-CD47 arm and a 2-VHH anti-PD-L1 arm, IBI322 blocks an innate and an adaptive immune checkpoint, resulting in potent tumor inhibition (Wang et al. 2021). In a phase 1 clinical study (NCT04795128), IBI322 showed encouraging anti-tumor efficacy and a manageable safety profile, exhibiting its potential to overcome immunotherapy resistance for patients with classical Hodgkin lymphoma.

Two bispecific therapeutic fusion proteins developed by ImmuneOnco Biopharmaceuticals that also target the CD47 immune checkpoint are the anti-CD47/HER2 molecule IMM2902 and the anti-CD47/CD20 protein IMM0306. The fusion proteins consist of either a HER2- or CD20-targeting antibody containing a SIRP $\alpha$  binding domain trapped on the light chain or heavy chain, respectively (Meng et al. 2023; Yu et al. 2023; Zhang et al. 2023). The dual TAA-targeting antibodies drive several anti-tumoral killing mechanisms supporting the choice of CD47  $\times$  TAA as therapeutic targets.

## 2.9 Dual tumor-targeting antibody-drug conjugates

Antibody-drug conjugates (ADCs) combining the specificity of antibodies with the cytotoxic activity of a highly potent payload represent an attractive fast-growing drug class for anti-tumor therapies (Alley et al. 2010; Fu et al. 2022). Functionality of ADCs, composed of mAbs covalently bound to cytotoxic payloads through synthetic (cleavable) linkers, requires binding of the target antigen and subsequent internalization, lysosomal processing and release of the warhead mediating cytotoxic effects (Samantasinghar et al.

2023). The optimization of ADCs regarding the antibody portion, internalization capacity and specificity is currently addressed by the design of bispecific dual TAA-targeting ADCs (Figure 2). Such next-generation ADCs currently in preclinical development or clinical trials are outlined below.

Trastuzumab, targeting HER2 is used as first-line treatment for HER2-positive patients. Besides the mAb, two trastuzumab ADCs have been FDA-approved within the last decade which are trastuzumab emtansine (Kadcyla) for metastatic breast cancer and trastuzumab deruxtecan (Enhertu) for metastatic breast cancer and locally advanced or metastatic HER2-positive gastric or gastroesophageal adenocarcinoma (Matikonda et al. 2022). Despite the clinical successes of trastuzumab-based ADCs, improved internalization properties may result in more potent molecules since their internalization usually relies on crosslinking of HER2 while monomeric HER2 does not internalize efficiently (Baulida et al. 1996; Goeij et al. 2014). Goeij et al. developed a bispecific dual tumor cell-targeting ADC against HER2 and the lysosome-associated membrane protein 3 (LAMP3 or CD63) featuring enhanced lysosomal ADC delivery (Goeij et al. 2016). CD63 shuttles between the plasma membrane and intracellular compartments and has been reported to be overexpressed in various cancer types including cervical, breast and gastrointestinal cancer and is frequently associated with tumor metastasis (Mujic et al. 2009; Nagelkerke et al. 2011; Pols and Klumperman 2009; Sun et al. 2014). The HER2  $\times$  CD63 ADC efficiently internalized, accumulated in the lysosomes, and conjugated to the microtubule disrupting agent duostatin-3 cytotoxicity in HER2-positive tumor cells was potently mediated *in vitro* and in a xenograft model *in vivo* (Goeij et al. 2016).

In a similar manner, a bispecific MMAE-conjugated antibody was generated targeting HER2, by utilizing a trastuzumab-based arm, and prolactin preceptor (PRLR) (Zong et al. 2022). Besides the two receptors displaying crosstalk signaling in breast cancer cells, PRLR has been reported to undergo rapid internalization thereby facilitating ADC uptake (Kavarthapu et al. 2021; Piazza et al. 2009). *In vitro* studies demonstrated higher internalization efficiency and augmented anti-tumor activity compared to trastuzumab ADC in human breast cancer cell lines (Zong et al. 2022).

In terms of ADCs' tumor specificity, several bispecific ADCs have been engineered featuring dual tumor targeting using either biparatopic approaches or addressing co-expressed TAAs. Zanidatamab zovodotin (ZW49), developed by Zymeworks in collaboration with BeiGene, represents a biparatopic anti-HER2 ADC targeting subdomain II and IV of the ECD of HER2 (Jhaveri et al. 2022). Multiple mechanisms of action are described to be induced by ZW49

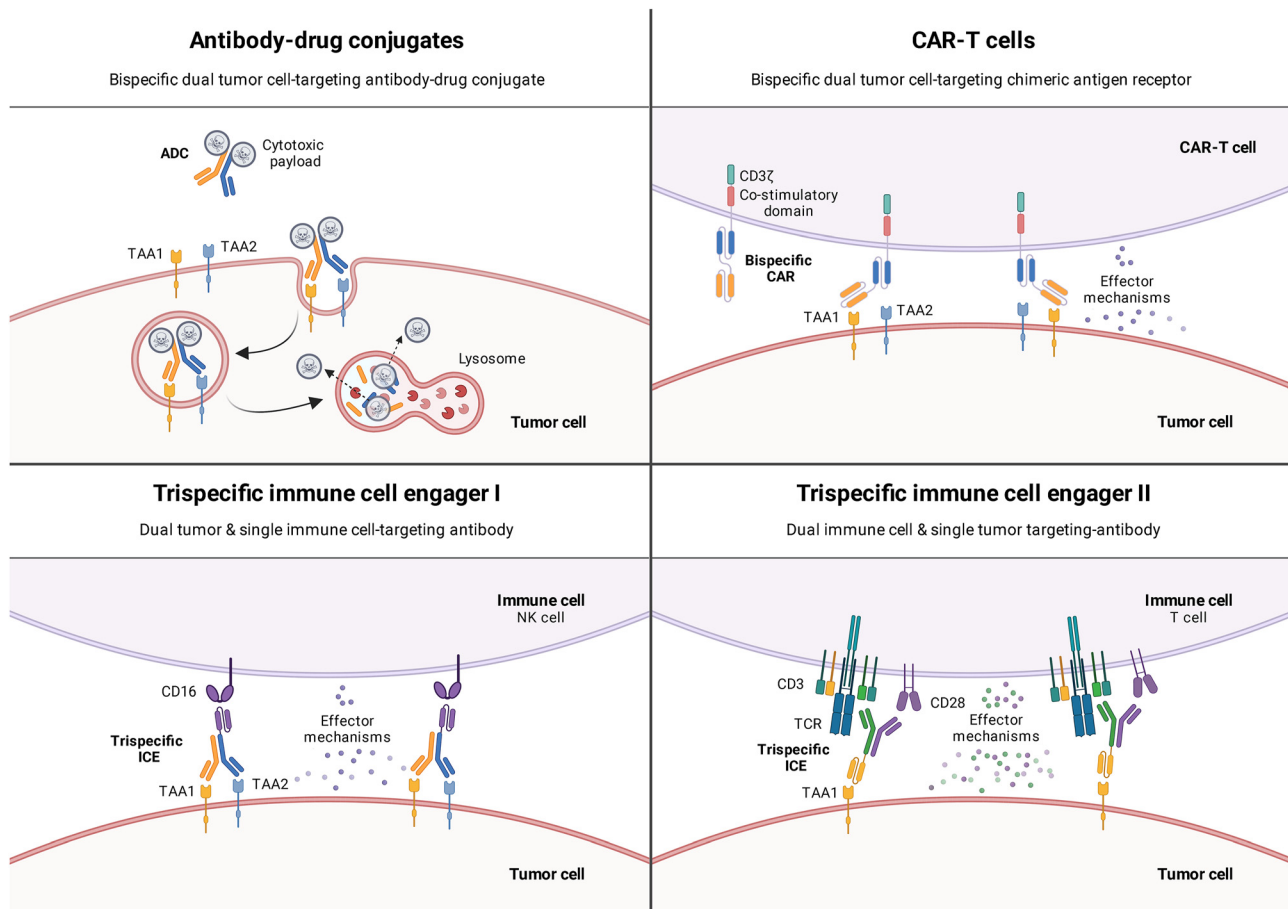


**Figure 2:** Antibody derivatives involving dual tumor cell-targeting or dual immune cell-targeting. Dual TAA-targeting ADCs efficiently deliver cytotoxic drugs to tumor cells, dual TAA-targeting CAR-T cells and dual TAA-targeting trispecific ICEs (NKCEs) enhance tumor specificity, reduce tumor immune escape and potently trigger effector mechanisms. Trispecific dual immune cell related antigen-targeting ICEs (TCEs) activate immune cells more intense and augment effector mechanisms.

including enhanced binding and receptor clustering, dual HER2 signaling blockade as well as potent effector functions (Jhaveri et al. 2022). In a first-in-human phase 1 clinical trial the molecule demonstrated a manageable safety profile with encouraging single-agent anti-tumor activity in pretreated patients with HER2-positive cancers (NCT03821233).

Furthermore, a biparatopic MET  $\times$  MET ADC (REGN5093-M114) was introduced by Regeneron Pharmaceuticals in order to achieve a functional MET pathway blockade (Drilon et al. 2022; Oh et al. 2023). Currently, the ADC is investigated in a phase 1/2 study in adult patients with MET-overexpressing NSCLC (NCT04982224).

Immunotherapies including ADC concepts involving CD19 targeting for treatment of B cell malignancies revealed encouraging results in the last years. Several anti-CD19 antibodies have recently been approved by the FDA as e.g. the Fc-engineered monoclonal antibody tafasitamab and the ADC loncastuximab tesirine (Zinzani and Minotti 2022). Additionally, CD22-addressing antibodies such as epratuzumab or

ADCs moxetumomab pasudotox (Lumoxiti) or inotuzumab ozogamicin (Besponsa) proved efficacy (Shah and Sokol 2021). There is evidence that combined targeting of both receptors is superior to monospecific binding regarding internalization properties as well as overcoming of drug resistance (Bachanova et al. 2015; Schmohl et al. 2018). The bispecific CD19  $\times$  CD22 antibody diphtheria toxin-conjugate (DT2219) demonstrated potent anti-tumor cell effects and is currently being evaluated in phase 1/2 study in patients with relapsed/refractory B lineage leukemia or lymphoma (NCT02370160) (Schmohl et al. 2018).

## 2.10 Dual tumor-targeting chimeric antigen receptor-T cells

Dual TAA-targeting therapeutic antibodies can induce tumor cell death by both direct and indirect mechanisms. Direct mechanisms include blocking of growth factor receptor

signaling, whereas indirect mechanisms require interaction with components of the host immune system, including complement-dependent cytotoxicity, antibody-dependent cellular phagocytosis and ADCC (Zahavi et al. 2018). A plethora of current strategies in immune oncology rely on simultaneous targeting of immune cells such as T cells or NK cells and tumor cells with bispecific antibodies directing patients' immune cells against cancer (reviewed in chapter 3) (Goebeler and Bargou 2020). An alternative strategy is based on reprogrammed T cells endowed with chimeric antigen receptors (CAR). CARs are synthetic receptors engineered to drive T cells to recognize and eliminate cells expressing a specific target antigen. Binding of CAR-T cells to target antigens expressed on the cell surface occurs independently of major histocompatibility complex (MHC) presentation, resulting in potent T cell activation and a strong anti-tumor response (Sadelain et al. 2013). The best-studied and clinically validated CAR-T cells target CD19, a target expressed across most B cell malignancies (Davila and Brentjens 2016; Miller and Maus 2015). However, more than 50 % of patients treated with CD19 single-targeted CAR-T cells (Si-CART) experience relapse or refractory disease (Chavez et al. 2019; Xie et al. 2022). One of the major mechanisms contributing to the development of resistance to Si-CARTs is antigen escape, possibly caused by receptor genetic mutations or epitope masking (Lemoine et al. 2021). To reduce the likelihood of antigen escape and increase tumor cell killing activity, CAR-T cells that target two TAAs concurrently are being explored (Figure 2) (Sterner and Sterner 2021; Xie et al. 2022). The following section depicts dual tumor cell-targeting CAR-T cells that have proven to be effective in preclinical models or are investigated in clinical trials.

Like CD19, CD20 is expressed in B cell-derived malignancies but is not found on hematopoietic stem cells, making it one of the most promising targets for treatment of abnormal B cells (LeBien and Tedder 2008). CD19 × CD20 dual targeting CAR-T cells have demonstrated potent and durable anti-tumor response *in vivo*, as well as a strong clinical efficacy, low toxicity, and the ability to potentially reduce antigen escape relapse in patients with relapsed/refractory non-Hodgkin lymphoma (NCT03097770; NCT03019055; NCT04007029) (Larson et al. 2022; Shah et al. 2020; Tong et al. 2020). Another approach to overcome antigen loss following CAR-T cell therapy is the simultaneous targeting of CD19 and CD22, since anti-CD22 CAR-T cells have demonstrated clinical efficacy for B cell acute lymphoblastic leukemia (B-ALL) in patients resistant to CD19-targeted CAR-T cell immunotherapy (Fry et al. 2018). However, some tumors also show reduced surface expression of CD22, and therefore CAR-T cells targeting both CD19 and CD22 may have a broader anti-tumor activity. Administration of CD19 × CD22 dual targeting

CAR-T cells to patients with relapsed/refractory B-ALL demonstrated potent anti-leukemic activity and a good safety profile (Dai et al. 2020; Jia et al. 2019; Wei et al. 2021), so these molecules are currently being studied in clinical trials (NCT05442515; NCT05225831; NCT03448393).

Although there is limited evidence from the current clinical data that relapse after anti-BCMA Si-CART therapy results from antigen loss, dual tumor cell-targeting CAR-T cells are being developed that target the B cell maturation antigen (BCMA) expressed in malignant plasma cells and CD19, CD38, CD319 or G protein-coupled receptor class C group 5 member D (GPC5D) (Fernández de Larrea et al. 2020; Mei et al. 2021; Zah et al. 2020; Zhang et al. 2019). BCMA × CD19 or CD38 dual targeting CAR-T cells showed promising clinical results whereas BCMA × CD319 or GPC5D targeting CAR-T cells were found to be effective in preclinical models (Garfall et al. 2023; Tang et al. 2022). These dual targeting CAR-T cells offer the potential to address the unmet medical need in 60 % of patients not remaining progression-free over 12 months post BCMA Si-CART treatment (Raje et al. 2019; Xie et al. 2022).

### 3 Trispecific dual targeting immune cell engager

Classical immune cell engagers (ICEs) simultaneously bind target antigens on tumor cells and immune-related molecules on endogenous effector cells, leading to the formation of an immunological synapse followed by tumor cell killing. Blinatumomab, the first US FDA-approved bispecific antibody, specific for B lymphocyte antigen CD19 and T cell co-receptor CD3 led to improved outcomes in treatment of patients with relapsed or refractory B-ALL (Jen et al. 2019). Beyond bispecific molecules, trispecific antibodies (tsAbs) have been explored by the addition of a third binding domain targeting either an additional tumor or immune cell antigen bringing forth ICEs with increased tumor specificity or enhanced immune cell responses against cancer (Figure 2) (Tapia-Galisteo et al. 2023). The following section reviews T cell engagers (TCE) and NK cell engagers (NKCE) in preclinical development or under clinical investigation binding two tumor cell targets and one immune cell target or targeting one tumor cell target and two immune cell targets.

#### 3.1 Dual tumor cell-targeting ICEs

As already described for the bispecific dual TAA-targeting mAbs, dual TAA-targeting ICEs may also prevent tumor

escape due to antigen loss and overcome antigenic heterogeneity (Figure 2). In most trispecific dual TAA-targeting TCEs, the T cell binding arm targets CD3, a molecule associated with the T cell receptor (TCR) (Clevers et al. 1988). CD3-specific antibodies are able to activate T lymphocytes directing the cytolytic activity of T cells to tumor cells, which facilitates their elimination independent of MHC specificity (Singh et al. 2021). Targeting two surface antigens on cancerous B cells, Wang et al. developed a trispecific TCE specific for CD19, CD20 and CD3 (Wang et al. 2022). For the same reason, Zhao et al. fused an anti-CD19 scFv and an anti-CD22 nanobody to an anti-CD3 Fab fragment. The trispecific CD19 × CD22 × CD3 antibody showed improved anti-tumor efficacy in a patient-derived xenograft model of B-ALL and ability to overcome immune escape compared to the corresponding bispecific (CD19 × CD3) antibody and blinatumomab (Zhao et al. 2022). Since acute leukemias with co-expression of the B lymphoid lineage marker CD19 and the myeloid lineage marker CD33 usually have a poor prognosis, Roskopf et al. generated the dual-targeting triplebody 33-3-19, which induces specific lysis of myeloid and B lymphoid cell lines, favoring CD33 and CD19 double positives over single positive leukemia cells, highlighting the potential of dual TAA-targeting agents in leukemia patients (Roskopf et al. 2016). For the treatment of colorectal cancer, a trispecific dual TAA-targeting TCE has shown promising data *in vitro* and *in vivo*. A CD3-specific scFv flanked by anti-EGFR and anti-epithelial cell adhesion molecule (EpCAM) VHH fragments enabled specific cytolysis of EGFR- and/or EpCAM-expressing cancer cells. Here, bivalent bispecific targeting of double-positive cells improved *in vitro* potency by up to 100-fold compared to single-positive cells and significantly prolonged survival *in vivo* compared to corresponding bispecific antibodies (Tapia-Galisteo et al. 2022). A similar architecture was applied by Liu et al. to fuse a HER2 and a VEGFR2 binding nanobody to an anti-CD3 Fab. The trispecific HER2 × CD3 × VEGFR2 antibody showed improved anti-tumor efficacy *in vitro* and *in vivo* compared to the corresponding bispecific antibodies alone or in combination, overcoming tumor recurrence due to antigen escape or resistance to therapy observed with the anti-HER2 antibody trastuzumab or the anti-VEGFR2 antibody ramucirumab (Liu et al. 2022).

Another type of ICEs is represented by NKCEs, molecules developed to augment tumor cell killing by NK cell inherent toxicity (Demaria et al. 2021). A large portion of dual TAA-targeting NKCEs involve the activating NK cell receptor immunoglobulin Fcγ receptor IIIa (FcγRIIIa or CD16a), naturally targeted with low affinity by the Fc region of TAA-bound IgG antibodies (Khan et al. 2020). The developed NKCEs bind CD16 with increased affinity, resulting in an

enhanced cytotoxicity and better/advanced safety profile compared to antibodies targeting CD16 with wild-type IgG1 Fc (Johnson et al. 2010; Tapia-Galisteo et al. 2023). The combination of the TAAs CD33 and CD19 with CD16 targeting also showed positive effects plugged in NKCEs as demonstrated by a single-chain triplebody generated by Schubert et al. (Schubert et al. 2011). Targeting of CD33 together with CD123 using the trispecific single-chain Fv derivative, CD33 × CD16 × CD123 induced significantly stronger NK-mediated lysis of primary leukemic cells compared to the trivalent bispecific construct CD123 × CD16 × CD123 (Kügler et al. 2010). CD22 × CD16 × CD19 trispecific tandem scFv molecule directly activated NK cells through CD16 and induced target specific cytotoxicity as well as cytokine and chemokine production resulting in the NK cell-mediated elimination of different types of leukemic cells (Gleason et al. 2012). Dual TAA-targeting trispecific NKCEs are beyond that generated for other indications such as multiple myeloma. Gantke et al. developed a monospecific anti-CD16 diabody with two scFvs at both termini, one anti-BCMA and one anti-CD200. This trispecific tetravalent aTriFlex showed increased selectivity for multiple myeloma cells and a 17-fold increase in *in vitro* potency (Gantke et al. 2017). Concurrent targeting of EGFR and PD-L1 besides CD16 with trispecific antibodies using the common light chain technology increased tumor specificity along with PD-L1/PD-1 checkpoint inhibition, resulting in a potent ADCC effect *in vitro* (Bogen et al. 2021; Harwardt et al. 2023). These data support the suggestion that trispecific antibodies involving dual tumor targeting strategies and redirection of immune cell cytotoxicity reveal augmented potencies compared to classical bispecific ICEs.

### 3.2 Dual immune cell-targeting ICEs

Besides dual tumor cell-targeting antibodies, trispecific dual immune cell-targeting molecules have been developed providing co-stimulatory signals to immune effector cells which further enhance responses against cancer (Figure 2).

### 3.3 Dual T cell-targeting ICEs

Complete activation of T lymphocytes naturally requires two signals, the first signal is derived from antigen recognition via the T cell receptor (TCR)/CD3 complex while the second signal is provided by engagement of co-stimulatory receptors (expressed on the T cell surface) (Chen and Flies 2013; Esensten et al. 2016; Mueller et al. 1989; Smith-Garvin et al. 2009). Ligation of co-stimulatory molecules such as CD28 enables T cell proliferation, differentiation and production

of cytokines necessary for adequate immune response (Boise et al. 1993; Esensten et al. 2016; Guo et al. 2008; Lindstein et al. 1989). Inhibitory receptors upregulated post T cell activation including PD-1, cytotoxic T lymphocyte-associated antigen 4 (CTLA-4) and B and T lymphocyte attenuator (BTLA) terminate T cell activation (Carreno and Collins 2003; Freeman et al. 2000; Walker and Sansom 2011). Harnessing cytotoxic properties of T cells, numerous TCEs that activate T cells *via* CD3 and redirect them to cancer cells have been developed and are currently undergoing clinical development (Zhou et al. 2021). The first CD28 superagonist TGN1412, intended to activate regulatory T cells for immune tolerance, failed in a first-in-human clinical trial inducing a dramatical cytokine release syndrome (CRS) (Suntharalingam et al. 2006; Tyrsin et al. 2016). Almost one decade later the antibody, renamed to TAB08, was forwarded to clinical studies (NCT01885624) again. Application of significantly lower CD28 superagonist doses to the patients resulted in desired T cell stimulating effects (Tabares et al. 2014).

The CD3 molecule is non-covalently associated with the TCR and participates in antigen-specific signal transduction inducing initial activation of T cells (Chen and Flies 2013). Engagement of the co-stimulatory CD28 molecule triggers alternative signal transduction pathways and thereby inhibits unresponsiveness/anergy state and activation-induced cell death (Boise et al. 1993; Crespo et al. 2013). Recently, Sanofi developed a first-in-class dual T cell activation molecule comprising CD3 and CD28 binding domains besides the tumor-related moiety which demonstrated efficient and durable T cell stimulation and potent anti-tumor activity (Seung et al. 2022; Wu et al. 2020). Two tsAb constructs differing in TAA-targeting units were designed using the cross-over dual variable (CODV) bispecific antibody format and are currently investigated in phase 1 clinical studies (NCT04401020/NCT05013554) (Steinmetz et al. 2016).

The first of the two dual TCEs (SAR442257) targets TAA CD38 for treatment of multiple myeloma and non-Hodgkin's lymphoma. T cell co-stimulation by the tsAb increased the potency and survival of T cells lysing the tumor cells and further provoked amplification of antigen-specific memory T cells *in vitro*. Besides beneficial effects of dual T cell targeting monovalent interaction towards CD28 resulted in a reduced non-specific cytokine release *in vitro* compared to the bivalent parental anti-CD28 mAb. Beyond that the CD28 specificity contributed to superior recognition of different tumor antigen level-expressing myeloma cells (CD38<sup>+</sup>/CD28<sup>+</sup>) resulting in specific and enhanced tumor cell lysis. *In vivo* administration of the tsAb resulted in suppressed myeloma growth in a humanized mouse model and displayed acceptable pharmacodynamics and toxicity in non-human primates (Wu et al. 2020). The second trispecific molecule

developed by Sanofi (SAR443216) is composed of HER2, CD3 and CD28 targeting units structurally based on their previously developed multispecific antibody platform. Overcoming current limitations of HER2-targeting monoclonal antibody therapies such as resistance in triple-negative breast cancer, the tsAb is intended to improve clinical outcomes for patients with varying HER2 level-expressing solid tumors e.g., breast or gastric cancer. Efficient stimulation of T cell activation and proliferation as well as potent anti-tumor effects against cells with low to high HER2 densities were effectuated *in vitro* by the dual TCE. Mechanisms contributing to tumor regression were shown to be exerted by CD8 T cells directly mediating tumor cell lysis *in vitro* and additionally by CD4 T cells blocking cancer cell cycle progression at G1/S and inducing pro-inflammatory responses *in vitro* and in humanized mouse models *in vivo* (Seung et al. 2022). The multispecific antibody approach providing two signals to stimulate T cells also triggers co-signaling which differs from signaling mediated by separate mAbs engaging the single receptors involved unrevealed mechanisms of T cell anti-tumor activity.

### 3.4 Dual NK cell-targeting ICEs

NK cells are key players in the innate immune system, exerting direct cytotoxic effects on infected or tumor cells and further eliciting multicellular immune responses ultimately resulting in sustained host protection (Vivier et al. 2008). The activation of NK lymphocytes is highly regulated by a set of germline-encoded stimulating and inhibitory receptors expressed on the cell membrane (Cooper et al. 2001). Equivalent to TCEs, NKCEs are bispecific molecules that bind to TAAs on tumor cells and to activating receptors on NK cells mediating potent anti-tumor immunity. The NK cell receptors to be addressed by NKCEs include CD16a, C-type lectin-like receptors natural-killer group 2, member D (NKG2D) and CD94/NKG2C, and natural cytotoxicity receptors NKp30, NKp44 and NKp46 (Demaria et al. 2021).

CD16 and NKp46 belong to the immunoglobulin superfamily, are both constituted of two extracellular Ig-like domains associated with FcR $\gamma$  and CD3 $\zeta$  ITAM-bearing polypeptides, therefore sharing protein-tyrosine kinase (PTK)-dependent signaling pathways responsible for effector cell functions (Demaria et al. 2021; Ravetch and Bolland 2001; Sivori et al. 1999). In 2019, Gauthier et al. (Innate Pharma) reported the generation of trifunctional CD16  $\times$  NKp46  $\times$  TAA antibody constructs composed of an engineered Fc for enhanced CD16 binding, a first-in-class agonist anti-NKp46 cross-mab and TAA-targeting Fabs against CD19, CD20 or EGFR (Gauthier et al. 2019). The trispecific NKCEs triggered potent cancer cell lysis by human primary NK cells *in vitro*

without inducing off-target effects or fratricidal NK cell killing. *In vivo* ADCC-mediated tumor clearance was promoted by the trifunctional antibody superior to effector-silenced versions in various preclinical mouse models of solid and invasive cancers (Gauthier et al. 2019). Based on this approach of dual NK cell engagement by CD16 and Nkp46 and targeting of different TAAs, the antibody-based NK cell engager therapeutics (ANKET<sup>®</sup>) platform has been developed by Innate Pharma (Demaria et al. 2021). In collaboration with Sanofi three drug candidates are currently under preclinical and clinical phase 1/2 investigation which incorporate TAA-targeting units against B7-H3 (IPH62), CD123 (IPH6101; NCT05086315) or BCMA (IPH6401; NCT05839626) for treatment of different types of cancer.

The activating NKG2D homodimeric receptor lacks signaling properties and mediates intracellular signal propagation via two associated DAP10 adapter proteins (which trigger the PI-3K pathway and a Grb2-Vav1-dependent pathway) (Zingoni et al. 2018). The activating NK cell receptor is featured by the ability to interact with numerous distinct ligands expressed by abnormal cells resulting in transduction of different signals and NK cell reactions. Dragonfly Therapeutics designed and patented multispecific binding proteins, referred to as TriNKETs (Trispecific NK cell Engager Therapies), that bind to NKG2D, CD16 and various TAAs such as HLA-E, CCR4, PD-L1, FLT3, EGFR, CD33, BCMA or HER2 (Baruah et al. 2020; Chang et al. 2018a, b). In general, the combination of CD16 and NKG2D engagement caused a synergistic activation of NK cells and may counteract tumor immune escape mechanisms such as CD16 downmodulation. TriNKET molecule DF9001, specific for tumor antigen EGFR, displayed improved target cell lysis compared to the parental EGFR-targeting mAbs (necitumumab, panitumumab) and is currently investigated in clinical phase 1 studies (NCT05597839) (Chang et al. 2018a). DF1001, the TriNKET progressed furthest in clinical development, targets HER2 and is currently being evaluated in phase 1/2 studies of patients with advanced solid tumors (NCT04143711).

## 4 Conclusions and prospects

In the fight against cancer, there is high demand for the development of novel therapies, with multispecific antibodies gaining importance as they can induce and combine multiple mechanisms of actions. Compared to monospecific mAbs, bispecific antibodies allow immune cell involvement or high precision tumor targeting by dual TAA binding. Attachment of another functionality results in trispecific molecules addressing either immune cells or target cancer cells with two antibody moieties. Thereby a variety of different mechanisms can be executed at the same time including immune

checkpoint blockade, simultaneous modulation of two signaling pathways, circumvention of drug resistance and immune escape or augmented immune cell activation engendering more intense and durable anti-tumor effects. Tetraspecific antibodies have recently been added to the arsenal of multispecific antibodies, including molecules derived from the Sanofi ANKET<sup>®</sup> (antibody-based NK cell engager therapeutics) platform (Demaria et al. 2022). Tetraspecific ANKETs target Nkp46, CD16a, IL-2R $\beta$  and a TAA via a single molecule inducing preferential activation and proliferation of NK cells and triggering NK cell cytotoxicity as well as cytokine and chemokine production by triple NK targeting. Besides NKCEs, tetraspecific TCEs were rendered by Sichuan Baili/Systimmune addressing CD3, 4-1BB, PD-L1 and a TAA and are currently being tested in clinical trials (NCT05160545; NCT04606433; NCT04794972) (Claus et al. 2023). The innovative molecules, not being described in scientific literature, deliver two T cell-stimulatory signals and concurrently dual target tumor cells including the blockade of an immune checkpoint. However, complex structural designs uniting diverse binding modalities also raise challenges with respect to manufacturability such as proteolysis, aggregation, incorrect assembly of multichain antibodies or low expression yields (Krah et al. 2018; Ma et al. 2020). Besides technical issues there may also be limitations regarding application of antibody drugs to humans including CRS by overstimulation of T cells or immunogenicity which requires careful pharmacologic risk assessment (Kroenke et al. 2021; Shah et al. 2023; Shimabukuro-Vornhagen et al. 2018).

In conclusion, bispecific and multispecific protein and cell-based therapies have the potential for broad use as highly effective treatment options for cancer patients, improving tumor eradication in early but also in later stages of tumor progression and reducing risk of tumor recurrence.

**Research ethics:** Not applicable.

**Author contributions:** The authors have accepted responsibility for the entire content of this manuscript and approved its submission.

**Competing interests:** The authors state no conflict of interest.

**Research funding:** None declared.

**Data availability:** Not applicable.

## References

- Alley, S.C., Okeley, N.M., and Senter, P.D. (2010). Antibody-drug conjugates: targeted drug delivery for cancer. *Curr. Opin. Chem. Biol.* 14: 529–537.
- Alvarez-Argote, J. and Dasanu, C.A. (2019). Durvalumab in cancer medicine: a comprehensive review. *Expert. Opin. Biol. Ther.* 19: 927–935.

- Bachanova, V., Frankel, A.E., Cao, Q., Lewis, D., Grzywacz, B., Verneris, M.R., Ustun, C., Lazaryan, A., McClune, B., Warlick, E.D., et al. (2015). Phase I study of a bispecific ligand-directed toxin targeting CD22 and CD19 (DT2219) for refractory B-cell malignancies. *Clin. Cancer Res.* 21: 1267–1272.
- Baruah, H., Chang, G., Cheung, A., Grinberg, A., Juo, Z., and McQuade, T. (2020). Proteins binding NKG2D, CD16 and FLT3. US201962915123P A61K39/395;A61P35/00;C07K16/28;C07K16/30;C07K16/46.
- Baulida, J., Kraus, M.H., Alimandi, M., Di Fiore, P.P., and Carpenter, G. (1996). All ErbB receptors other than the epidermal growth factor receptor are endocytosis impaired. *J. Biol. Chem.* 271: 5251–5257.
- Bendell, J., Blay, J.-Y., Cassier, P., Bauer, T., Terret, C., Mueller, C., Morel, A., Chesne, E., Xu, Z., Tessier, J., et al. (2018). Abstract A092: phase 1 trial of RO6874813, a novel bispecific FAP-DR5 antibody, in patients with solid tumors. *Mol. Cancer Ther.* 17: A092.
- Bogen, J.P., Carrara, S.C., Fiebig, D., Grzeschik, J., Hock, B., and Kolmar, H. (2021). Design of a trispecific checkpoint inhibitor and natural killer cell engager based on a 2 + 1 common light chain antibody architecture. *Front. Immunol.* 12: 669496.
- Boise, L.H., González-García, M., Postema, C.E., Ding, L., Lindsten, T., Turka, L.A., Mao, X., Nuñez, G., and Thompson, C.B. (1993). bcl-x, a bcl-2-related gene that functions as a dominant regulator of apoptotic cell death. *Cell* 74: 597–608.
- Brahmer, J.R., Tykodi, S.S., Chow, L.Q.M., Hwu, W.-J., Topalian, S.L., Hwu, P., Drake, C.G., Camacho, L.H., Kauh, J., Odunsi, K., et al. (2012). Safety and activity of anti-PD-L1 antibody in patients with advanced cancer. *N. Engl. J. Med.* 366: 2455–2465.
- Brennan, F.R., Morton, L.D., Spindeldreher, S., Kiessling, A., Allenspach, R., Hey, A., Muller, P.Y., Frings, W., and Sims, J. (2010). Safety and immunotoxicity assessment of immunomodulatory monoclonal antibodies. *MAbs* 2: 233–255.
- Brünker, P., Wartha, K., Friess, T., Grau-Richards, S., Waldhauer, I., Koller, C.F., Weiser, B., Majety, M., Runza, V., Niu, H., et al. (2016). RG7386, a novel tetravalent FAP-DR5 antibody, effectively triggers FAP-dependent, avidity-driven DR5 hyperclustering and tumor cell apoptosis. *Mol. Cancer Ther.* 15: 946–957.
- Buatois, V., Johnson, Z., Salgado-Pires, S., Papaioannou, A., Hatterer, E., Chauchet, X., Richard, F., Barba, L., Daubeuf, B., Cons, L., et al. (2018). Preclinical development of a bispecific antibody that safely and effectively targets CD19 and CD47 for the treatment of B-cell lymphoma and leukemia. *Mol. Cancer Ther.* 17: 1739–1751.
- Carreno, B.M. and Collins, M. (2003). BTLA: a new inhibitory receptor with a B7-like ligand. *Trends Immunol.* 24: 524–527.
- Chang, G.P., Cheung, A.F., Du, J., Grinberg, A., Haney, W., Sethi, D.K., Wagtmann, N., Lunde, B.M., and Prinz, B. (2018a). Proteins binding NKG2D, CD16, and EGFR, CCR4, or PD-L1. US201762546297P; US201762546300P; US201762552152P; US201762555114P; EP20180846836; WO2018US00212 A61K47/68; C07K14/705; C07K16/28; C07K16/30.
- Chang, G.P., Cheung, A.F., Haney, W., Lunde, B.M., and Prinz, B. (2018b). Proteins binding HER2, NKG2D and CD16. US201762461146P; US201816486569; WO2018US18771 A61P35/00; C07K16/28; C07K16/32.
- Chavez, J.C., Bachmeier, C., and Kharfan-Dabaja, M.A. (2019). CAR T-cell therapy for B-cell lymphomas: clinical trial results of available products. *Ther. Adv. Hematol.* 10: Article no. 2040620719841581.
- Chen, L. and Flies, D.B. (2013). Molecular mechanisms of T cell co-stimulation and co-inhibition. *Nat. Rev. Immunol.* 13: 227–242.
- Claus, C., Ferrara-Koller, C., and Klein, C. (2023). The emerging landscape of novel 4-1BB (CD137) agonistic drugs for cancer immunotherapy. *MAbs* 15: 2167189.
- Clevers, H., Alarcon, B., Wileman, T., and Terhorst, C. (1988). The T cell receptor/CD3 complex: a dynamic protein ensemble. *Annu. Rev. Immunol.* 6: 629–662.
- Cohen, E.E., Fayette, J., Daste, A., Even, C., Le Tourneau, C., Brana, I., Saada, E., Fontana, E., Iglesias, L., Kato, S., et al. (2023). Abstract CT012: clinical activity of MCLA-158 (petosemtamab), an IgG1 bispecific antibody targeting EGFR and LGR5, in advanced head and neck squamous cell cancer (HNSCC). *Cancer Res.* 83: CT012.
- Cooper, M.A., Fehniger, T.A., and Caligiuri, M.A. (2001). The biology of human natural killer-cell subsets. *Trends Immunol.* 22: 633–640.
- Crespo, J., Sun, H., Welling, T.H., Tian, Z., and Zou, W. (2013). T cell anergy, exhaustion, senescence, and stemness in the tumor microenvironment. *Curr. Opin. Immunol.* 25: 214–221.
- Dai, H., Wu, Z., Jia, H., Tong, C., Guo, Y., Ti, D., Han, X., Liu, Y., Zhang, W., Wang, C., et al. (2020). Bispecific CAR-T cells targeting both CD19 and CD22 for therapy of adults with relapsed or refractory B cell acute lymphoblastic leukemia. *J. Hematol. Oncol.* 13: 30.
- Davila, M.L. and Brentjens, R.J. (2016). CD19-Targeted CAR T cells as novel cancer immunotherapy for relapsed or refractory B-cell acute lymphoblastic leukemia. *Clin. Adv. Hematol. Oncol.* 14: 802–808.
- Demaria, O., Gauthier, L., Debroas, G., and Vivier, E. (2021). Natural killer cell engagers in cancer immunotherapy: next generation of immunoncology treatments. *Eur. J. Immunol.* 51: 1934–1942.
- Demaria, O., Gauthier, L., Vetzou, M., Blanchard Alvarez, A., Vagne, C., Habif, G., Batista, L., Baron, W., Belaïd, N., Girard-Madoux, M., et al. (2022). Antitumor immunity induced by antibody-based natural killer cell engager therapeutics armed with not-alpha IL-2 variant. *Cell Rep. Med.* 3: 100783.
- Dheilly, E., Moine, V., Broyer, L., Salgado-Pires, S., Johnson, Z., Papaioannou, A., Cons, L., Calloud, S., Majocchi, S., Nelson, R., et al. (2017). Selective blockade of the ubiquitous checkpoint receptor CD47 is enabled by dual-targeting bispecific antibodies. *Mol. Ther.* 25: 523–533.
- Drilon, A.E., Awad, M.M., Gadgeel, S.M., Villaruz, L.C., Sabari, J.K., Perez, J., Daly, C., Patel, S., Li, S., Seebach, F.A., et al. (2022). A phase 1/2 study of REGN5093-M114, a METxMET antibody-drug conjugate, in patients with mesenchymal epithelial transition factor (MET)-overexpressing NSCLC. *J. Clin. Oncol.* 40: TPS8593.
- Esensten, J.H., Helou, Y.A., Chopra, G., Weiss, A., and Bluestone, J.A. (2016). CD28 costimulation: from mechanism to therapy. *Immunity* 44: 973–988.
- Feng, J., Chen, J., Li, K., Li, X., Min, X., Li, B., Lin, L., Fang, Y., Sun, Y., Zhu, B., et al. (2021). 1278P SHR-1701, a bifunctional fusion protein targeting PD-L1 and TGF- $\beta$ , as first-line therapy for PD-L1+ advanced/metastatic NSCLC: data from a clinical expansion cohort of a phase I study. *Ann. Oncol.* 32: S995.
- Fernández de Larrea, C., Staehr, M., Lopez, A.V., Ng, K.Y., Chen, Y., Godfrey, W.D., Purdon, T.J., Ponomarev, V., Wendel, H.-G., Brentjens, R.J., et al. (2020). Defining an optimal dual-targeted CAR T-cell therapy approach simultaneously targeting BCMA and GPRC5D to prevent BCMA escape-driven relapse in multiple myeloma. *Blood Cancer Discov.* 1: 146–154.
- Freeman, G.J., Long, A.J., Iwai, Y., Bourque, K., Chernova, T., Nishimura, H., Fitz, L.J., Malenkovich, N., Okazaki, T., Byrne, M.C., et al. (2000). Engagement of the PD-1 immunoinhibitory receptor by a novel B7 family member leads to negative regulation of lymphocyte activation. *J. Exp. Med.* 192: 1027–1034.
- Fry, T.J., Shah, N.N., Orentas, R.J., Stetler-Stevenson, M., Yuan, C.M., Ramakrishna, S., Wolters, P., Martin, S., Delbrook, C., Yates, B., et al. (2018). CD22-targeted CAR T cells induce remission in B-ALL that is naive or resistant to CD19-targeted CAR immunotherapy. *Nat. Med.* 24: 20–28.

- Fu, Z., Li, S., Han, S., Shi, C., and Zhang, Y. (2022). Antibody drug conjugate: the “biological missile” for targeted cancer therapy. *Signal Transduct. Target. Ther.* 7: 93.
- Gagliardi, C., Pericle, F., Salameh, A., Blezinger, P., and Curran, M. (2022). 1333 Development of IMGS-001, a novel anti-PD-L1/PD-L2 dual specific, multi-functional antibody, to treat immune excluded tumors. In: Regular and young investigator award abstracts. BMJ Publishing Group Ltd, Boston, MA, p. A1382.
- Gandullo-Sánchez, L., Ocaña, A., and Pandiella, A. (2022). HER3 in cancer: from the bench to the bedside. *J. Exp. Clin. Cancer Res.* 41: 310.
- Gantke, T., Weichel, M., Herbrecht, C., Reusch, U., Ellwanger, K., Fucek, I., Eser, M., Müller, T., Griep, R., Molkenthin, V., et al. (2017). Trispecific antibodies for CD16A-directed NK cell engagement and dual-targeting of tumor cells. *Protein Eng. Des. Sel.* 30: 673–684.
- García, M.D., Hollebecque, A., García-Carbonero, R., Jungels, C., Smyth, E., Kato, S., Argilés, G., Martin, C.G., Magin, M., Shen, Y.-M., et al. (2023) Abstract CT156: MCLA-158 (petosemtamab), an IgG1 bispecific antibody targeting EGFR and LGR5, in advanced gastric/esophageal adenocarcinoma (GEA). *Cancer Res.* 83: CT156.
- García-Martínez, J.M., Wang, S., Weishaeupl, C., Wernitznig, A., Chetta, P., Pinto, C., Ho, J., Dutcher, D., Gorman, P.N., Kroe-Barrett, R., et al. (2021). Selective tumor cell apoptosis and tumor regression in CDH17-positive colorectal cancer models using BI 905711, a novel liver-sparing TRAILR2 agonist. *Mol. Cancer Ther.* 20: 96–108.
- Garfall, A.L., Cohen, A.D., Susanibar-Adaniya, S.P., Hwang, W.-T., Vogl, D.T., Waxman, A.J., Lacey, S.F., Gonzalez, V.E., Fraietta, J.A., Gupta, M., et al. (2023). Anti-BCMA/CD19 CAR T cells with early immunomodulatory maintenance for multiple myeloma responding to initial or later-line therapy. *Blood Cancer Discov.* 4: 118–133.
- Gauthier, L., Morel, A., Anceriz, N., Rossi, B., Blanchard-Alvarez, A., Grondin, G., Trichard, S., Cesari, C., Sapet, M., Bosco, F., et al. (2019). Multifunctional natural killer cell engagers targeting Nkp46 trigger protective tumor immunity. *Cell* 177: 1701–1713.e16.
- Geuijen, C.A.W., de Nardis, C., Maussang, D., Rovers, E., Gallenne, T., Hendriks, L.J.A., Visser, T., Nijhuis, R., Logtenberg, T., de Kruijff, J., et al. (2018). Unbiased combinatorial screening identifies a bispecific IgG1 that potently inhibits HER3 signaling via HER2-guided ligand blockade. *Cancer Cell* 33: 922–936.e10.
- Govannetti, E. and Leon, L.G. (2014). New strategies and applications for drugs targeting EGFR and c-Met. *Curr. Drug Targets* 15: 1261–1262.
- Gleason, M.K., Verneris, M.R., Todhunter, D.A., Zhang, B., McCullar, V., Zhou, S.X., Panoskaltis-Mortari, A., Weiner, L.M., Vallera, D.A., and Miller, J.S. (2012). Bispecific and trispecific killer cell engagers directly activate human NK cells through CD16 signaling and induce cytotoxicity and cytokine production. *Mol. Cancer Ther.* 11: 2674–2684.
- Goebeler, M.-E. and Bargou, R.C. (2020). T cell-engaging therapies – BiTEs and beyond. *Nat. Rev. Clin. Oncol.* 17: 418–434.
- Goeij, B.E.C.G., Peipp, M., Haij, S., van den Brink, E.N., Kellner, C., Riedl, T., de Jong, R., Vink, T., Strumane, K., Bleeker, W.K., et al. (2014). HER2 monoclonal antibodies that do not interfere with receptor heterodimerization-mediated signaling induce effective internalization and represent valuable components for rational antibody-drug conjugate design. *MAbs* 6: 392–402.
- Goeij, B.E.C.G., Vink, T., Ten Napel, H., Breij, E.C.W., Satijn, D., Wubolts, R., Miao, D., and Parren, P.W.H.I. (2016). Efficient payload delivery by a bispecific antibody-drug conjugate targeting HER2 and CD63. *Mol. Cancer Ther.* 15: 2688–2697.
- Guo, F., Iclozan, C., Suh, W.-K., Anasetti, C., and Yu, X.-Z. (2008). CD28 controls differentiation of regulatory T cells from naive CD4 T cells. *J. Immunol.* 181: 2285–2291.
- Guo, Y., Liu, B., Lv, D., Cheng, Y., Zhou, T., Zhong, Y., Hu, C., Chen, G., Wu, X., Yin, Y., et al. (2022). Phase I/IIa study of PM8001, a bifunctional fusion protein targeting PD-L1 and TGF- $\beta$ , in patients with advanced tumors. *J. Clin. Oncol.* 40: 2512.
- Hao, Y., Yu, X., Bai, Y., McBride, H.J., and Huang, X. (2019). Cryo-EM structure of HER2-trastuzumab-pertuzumab complex. *PLoS One* 14: e0216095.
- Harwardt, J., Bogen, J.P., Carrara, S.C., Ullitzka, M., Grzeschik, J., Hock, B., and Kolmar, H. (2022). A generic strategy to generate bifunctional two-in-one antibodies by chicken immunization. *Front. Immunol.* 13: 888838.
- Harwardt, J., Carrara, S.C., Bogen, J.P., Schoenfeld, K., Grzeschik, J., Hock, B., and Kolmar, H. (2023). Generation of a symmetrical trispecific NK cell engager based on a two-in-one antibody. *Front. Immunol.* 14: 1170042.
- Hatterer, E., Chauchet, X., Richard, F., Barba, L., Moine, V., Chatel, L., Broyer, L., Pontini, G., Bautzova, T., Juan, F., et al. (2020). Targeting a membrane-proximal epitope on mesothelin increases the tumoricidal activity of a bispecific antibody blocking CD47 on mesothelin-positive tumors. *MAbs* 12: 1739408.
- Herpers, B., Eppink, B., James, M.I., Cortina, C., Cañellas-Socias, A., Boj, S.F., Hernando-Momblona, X., Glodzik, D., Roovers, R.C., van de Wetering, M., et al. (2022). Functional patient-derived organoid screenings identify MCLA-158 as a therapeutic EGFR  $\times$  LGR5 bispecific antibody with efficacy in epithelial tumors. *Nat. Cancer* 3: 418–436.
- Huang, S., Li, F., Liu, H., Ye, P., Fan, X., Yuan, X., Wu, Z., Chen, J., Jin, C., Shen, B., et al. (2018). Structural and functional characterization of MBS301, an afucosylated bispecific anti-HER2 antibody. *MAbs* 10: 864–875.
- Huang, S., van Duijnhoven, S.M.J., Sijts, A.J.A.M., and van Elsas, A. (2020). Bispecific antibodies targeting dual tumor-associated antigens in cancer therapy. *J. Cancer Res. Clin. Oncol.* 146: 3111–3122.
- Jen, E.Y., Xu, Q., Schetter, A., Przepiorka, D., Shen, Y.L., Roscoe, D., Sridhara, R., Deisseroth, A., Philip, R., Farrell, A.T., et al. (2019). FDA approval: blinatumomab for patients with B-cell precursor acute lymphoblastic leukemia in morphologic remission with minimal residual disease. *Clin. Cancer Res.* 25: 473–477.
- Jhaveri, K., Han, H., Dotan, E., Oh, D.-Y., Ferrario, C., Tolcher, A., Lee, K.-W., Liao, C.-Y., Kang, Y.-K., Kim, Y.H., et al. (2022). 460MO Preliminary results from a phase I study using the bispecific, human epidermal growth factor 2 (HER2)-targeting antibody-drug conjugate (ADC) zanidatamab zovodotin (ZW49) in solid cancers. *Ann. Oncol.* 33: S749–S750.
- Jia, H., Wang, Z., Wang, Y., Liu, Y., Dai, H., Tong, C., Guo, Y., Guo, B., Ti, D., Han, X., et al. (2019). Haploidentical CD19/CD22 bispecific CAR-T cells induced MRD-negative remission in a patient with relapsed and refractory adult B-ALL after haploidentical hematopoietic stem cell transplantation. *J. Hematol. Oncol.* 12: 57.
- Jiang, Z., Sun, H., Yu, J., Tian, W., and Song, Y. (2021). Targeting CD47 for cancer immunotherapy. *J. Hematol. Oncol.* 14: 180.
- Johnson, S., Burke, S., Huang, L., Gorlatov, S., Li, H., Wang, W., Zhang, W., Tuailon, N., Rainey, J., Barat, B., et al. (2010). Effector cell recruitment with novel Fv-based dual-affinity re-targeting protein leads to potent tumor cytotoxicity and in vivo B-cell depletion. *J. Mol. Biol.* 399: 436–449.
- Ju, X., Zhang, H., Zhou, Z., and Wang, Q. (2020). Regulation of PD-L1 expression in cancer and clinical implications in immunotherapy. *Am. J. Cancer Res.* 10: 1–11.
- Kavarthapu, R., Anbazhagan, R., and Dufau, M.L. (2021). Crosstalk between PRLR and EGFR/HER2 signaling pathways in breast cancer. *Cancers* 13: 4685.
- Khan, M., Arooj, S., and Wang, H. (2020). NK cell-based immune checkpoint inhibition. *Front. Immunol.* 11: 167.
- Kim, E.S. (2017). Avelumab: first global approval. *Drugs* 77: 929–937.



- Klapper, L.N., Glathe, S., Vaisman, N., Hynes, N.E., Andrews, G.C., Sela, M., and Yarden, Y. (1999). The ErbB-2/HER2 oncoprotein of human carcinomas may function solely as a shared coreceptor for multiple stroma-derived growth factors. *Proc. Natl. Acad. Sci. U. S. A.* 96: 4995–5000.
- Koopmans, I., Hendriks, D., Samplonius, D.F., van Ginkel, R.J., Heskamp, S., Wierstra, P.J., Bremer, E., and Helfrich, W. (2018). A novel bispecific antibody for EGFR-directed blockade of the PD-1/PD-L1 immune checkpoint. *Oncoimmunology* 7: e1466016.
- Krah, S., Kolmar, H., Becker, S., and Zielonka, S. (2018). Engineering IgG-like bispecific antibodies-an overview. *Antibodies* 7: 28.
- Kroenke, M.A., Milton, M.N., Kumar, S., Bame, E., and White, J.T. (2021). Immunogenicity risk assessment for multi-specific therapeutics. *AAPS J.* 23: 115.
- Kügler, M., Stein, C., Kellner, C., Mentz, K., Saul, D., Schwenkert, M., Schubert, I., Singer, H., Oduncu, F., Stockmeyer, B., et al. (2010). A recombinant trispecific single-chain Fv derivative directed against CD123 and CD33 mediates effective elimination of acute myeloid leukaemia cells by dual targeting. *Br. J. Haematol.* 150: 574–586.
- Larson, S.M., Walthers, C., Ji, B., Ghafouri, S.N., Naparstek, J., Trent, J., Harris, C., Khericha Gandhi, M., Schweppe, T., Auerbach, M.S., et al. (2022). CD19/CD20 bispecific chimeric antigen receptor (CAR) in naïve/memory T cells for the treatment of relapsed or refractory non-Hodgkin lymphoma. *J. Clin. Oncol.* 40: 2543.
- LeBien, T.W. and Tedder, T.F. (2008). B lymphocytes: how they develop and function. *Blood* 112: 1570–1580.
- Lemoine, J., Ruella, M., and Houot, R. (2021). Born to survive: how cancer cells resist CAR T cell therapy. *J. Hematol. Oncol.* 14: 199.
- Lindstein, T., June, C.H., Ledbetter, J.A., Stella, G., and Thompson, C.B. (1989). Regulation of lymphokine messenger RNA stability by a surface-mediated T cell activation pathway. *Science* 244: 339–343.
- Liu, D., Gong, J., Liu, T., Li, K., Yin, X., Liu, Y., Wang, Y., Wang, L., Wang, W., Zhang, Y., et al. (2021). Phase 1 study of SHR-1701, a bifunctional fusion protein targeting PD-L1 and TGF- $\beta$ , in patients with advanced solid tumors. *J. Clin. Oncol.* 39: 2503.
- Liu, D., Qi, X., Wei, X., Zhao, L., Wang, X., Li, S., Wang, Z., Shi, L., Xu, J., Hong, M., et al. (2022). A Novel Her2/VEGFR2/CD3 trispecific antibody with an optimal structural design showed improved T-cell-redirecting antitumor efficacy. *Theranostics* 12: 7788–7803.
- Lyu, X., Zhao, Q., Hui, J., Wang, T., Lin, M., Wang, K., Zhang, J., Shentu, J., Dalby, P.A., Zhang, H., et al. (2022). The global landscape of approved antibody therapies. *Antib. Ther.* 5: 233–257.
- Ma, H., Ó'Fágáin, C., and O'Kennedy, R. (2020). Antibody stability: a key to performance – analysis, influences and improvement. *Biochimie* 177: 213–225.
- Markham, A. (2016). Atezolizumab: first global approval. *Drugs* 76: 1227–1232.
- Matikonda, S.S., McLaughlin, R., Shrestha, P., Lipshultz, C., and Schnermann, M.J. (2022). Structure-activity relationships of antibody-drug conjugates: a systematic review of chemistry on the trastuzumab scaffold. *Bioconjug. Chem.* 33: 1241–1253.
- Mei, H., Li, C., Jiang, H., Zhao, X., Huang, Z., Jin, D., Guo, T., Kou, H., Liu, L., Tang, L., et al. (2021). A bispecific CAR-T cell therapy targeting BCMA and CD38 in relapsed or refractory multiple myeloma. *J. Hematol. Oncol.* 14: 161.
- Meng, Y., Zhang, J., Zhao, C., Cheng, Y., Zhu, L., Song, Z., Xu, N., Wang, Z., Wang, Y., Du, Y., et al. (2023). Preliminary results of a phase I, first-in-human, dose escalation study of IMM2902 in patients with HER2-expressing advanced solid tumors. *J. Clin. Oncol.* 41: e15185.
- Miller, B.C. and Maus, M.V. (2015). CD19-Targeted CAR T cells: a new tool in the fight against B cell malignancies. *Oncol. Res. Treat.* 38: 683–690.
- Moore, S.L., Chiu, M.L., Bushey, B.S., Chevalier, K., Luistro, L., Dorn, K., Brezski, R.J., Haytko, P., Kelly, T., Wu, S.-J., et al. (2016). A novel bispecific antibody targeting EGFR and cMet is effective against EGFR inhibitor-resistant lung tumors. *Cancer Res.* 76: 3942–3953.
- Mueller, D.L., Jenkins, M.K., and Schwartz, R.H. (1989). An accessory cell-derived costimulatory signal acts independently of protein kinase C activation to allow T cell proliferation and prevent the induction of unresponsiveness. *J. Immunol.* 142: 2617–2628.
- Mujcic, H., Rzymiski, T., Rouschop, K.M.A., Koritzinsky, M., Milani, M., Harris, A.L., and Wouters, B.G. (2009). Hypoxic activation of the unfolded protein response (UPR) induces expression of the metastasis-associated gene LAMP3. *Radiother. Oncol.* 92: 450–459.
- Mullard, A. (2021). FDA approves 100th monoclonal antibody product. *Nat. Rev. Drug Discovery* 20: 491–495.
- Nagelkerke, A., Mujcic, H., Bussink, J., Wouters, B.G., van Laarhoven, H.W.M., Sweep, F.C.G.J., and Span, P.N. (2011). Hypoxic regulation and prognostic value of LAMP3 expression in breast cancer. *Cancer* 117: 3670–3681.
- Normant, E., Ribeiro, M.L., Reyes, D., Miskin, H.P., Sportelli, P., Weiss, M.S., Bosch, F., and Roue, G. (2019). The novel bispecific CD47-CD19 antibody TG-1801 potentiates the activity of Ublituximab-Umbralisib (U2) drug combination in preclinical models of B-NHL. *Hematol. Oncol.* 37: 322–323.
- O'Donnell, J.S., Long, G.V., Scolyer, R.A., Teng, M.W.L., and Smyth, M.J. (2017). Resistance to PD1/PDL1 checkpoint inhibition. *Cancer Treat. Rev.* 52: 71–81.
- Oh, S.Y., Lee, Y.W., Lee, E.J., Kim, J.H., Park, Y., Heo, S.G., Yu, M.R., Hong, M.H., DaSilva, J., Daly, C., et al. (2023). Preclinical study of a biparatopic METxMET antibody-drug conjugate, REGN5093-M114, overcomes MET-driven acquired resistance to EGFR TKIs in EGFR-mutant NSCLC. *Clin. Cancer Res.* 29: 221–232.
- Ou, S.H., Moreno García, V., Gil Bazo, I., Prenen, H., Moreno, I., Johnson, M., Castañón Álvarez, E., Nagasaka, M., Adeyemi, S., Barasa, B., et al. (2022). MCLA-129, a human anti-EGFR and anti-c-MET bispecific antibody, in patients with advanced NSCLC and other solid tumors: an ongoing phase 1/2 study. *Eur. J. Cancer* 174: S122.
- Pang, K., Shi, Z.-D., Wei, L.-Y., Dong, Y., Ma, Y.-Y., Wang, W., Wang, G.-Y., Cao, M.-Y., Dong, J.-J., Chen, Y.-A., et al. (2023). Research progress of therapeutic effects and drug resistance of immunotherapy based on PD-1/PD-L1 blockade. *Drug Resist. Updat.* 66: 100907.
- Piazza, T.M., Lu, J.-C., Carver, K.C., and Schuler, L.A. (2009). SRC family kinases accelerate prolactin receptor internalization, modulating trafficking and signaling in breast cancer cells. *Mol. Endocrinol.* 23: 202–212.
- Pols, M.S. and Klumperman, J. (2009). Trafficking and function of the tetraspanin CD63. *Exp. Cell Res.* 315: 1584–1592.
- Qing, Z., Gabrail, N., Uprety, D., Rotow, J., Han, B., Jänne, P.A., Nagasaka, M., Zheng, M., Zhang, Y., Yang, G., et al. (2022). 22P EMB-01: an EGFR-cMET bispecific antibody, in advanced/metastatic solid tumors phase I results. *Ann. Oncol.* 33: S39–S40.
- Raje, N., Berdeja, J., Lin, Y., Siegel, D., Jagannath, S., Madduri, D., Liedtke, M., Rosenblatt, J., Maus, M.V., Turka, A., et al. (2019). Anti-BCMA CAR T-cell therapy bb2121 in relapsed or refractory multiple myeloma. *N. Engl. J. Med.* 380: 1726–1737.
- Ravetch, J.V. and Bolland, S. (2001). IgG Fc receptors. *Annu. Rev. Immunol.* 19: 275–290.
- Ren, F., Wu, X., Yang, D., Wu, D., Gong, S., Zhang, Y., Lensky, S., and Wu, C. (2020) Abstract 528: EMB-01: an innovative bispecific antibody targeting EGFR and cMet on tumor cells mediates a novel mechanism to improve anti-tumor efficacy. *Cancer Res.* 80: 528.

- Renshaw, B., Khalili, J.S., Xiao, S., and Zhu, Y. (2023) Abstract 6309: anti-tumor efficacy of SI-B001, a novel EGFR × HER3 bispecific antibody, against EGFR-driven epithelial tumors alone or in combination with paclitaxel and carboplatin. *Cancer Res.* 83: 6309.
- Reslan, L., Dalle, S., and Dumontet, C. (2009). Understanding and circumventing resistance to anticancer monoclonal antibodies. *MAbs* 1: 222–229.
- Rexer, B.N. and Arteaga, C.L. (2012). Intrinsic and acquired resistance to HER2-targeted therapies in HER2 gene-amplified breast cancer: mechanisms and clinical implications. *Crit. Rev. Oncog.* 17: 1–16.
- Riu Martinez, X., Bandari, R., and Lalitha, A. (2022) American Society of Clinical Oncology (ASCO) – 58th annual meeting. Chicago/virtual – June 3–7, 2022. *Drugs Future* 47: 629.
- Romano, E., Medioni, J., La Rouge, T.D.M., Fischer, N., Bardonneau, C., Ferlin, W., Hose, D., Seckinger, A., Simonelli, M., and Curigliano, G. (2022). A Phase 1, open-label, dose finding study of NI-1801, a bispecific mesothelin × CD47 engaging antibody, in patients with mesothelin expressing solid cancers. In: Regular and young investigator award abstracts. BMJ Publishing Group Ltd, Boston, MA, p. A739.
- Roskopf, C.C., Braciak, T.A., Fenn, N.C., Kobold, S., Fey, G.H., Hopfner, K.-P., and Oduncu, F.S. (2016). Dual-targeting triplebody 33-3-19 mediates selective lysis of biphentotypic CD19+ CD33+ leukemia cells. *Oncotarget* 7: 22579–22589.
- Rubin, I. and Yarden, Y. (2001). The basic biology of HER2. *Ann. Oncol.* 12: S3–S8.
- Rubio-Pérez, L., Lázaro-Gorines, R., Harwood, S.L., Compte, M., Navarro, R., Tapia-Galisteo, A., Bonet, J., Blanco, B., Lykkemark, S., Ramírez-Fernández, Á., et al. (2023). A PD-L1/EGFR bispecific antibody combines immune checkpoint blockade and direct anti-cancer action for an enhanced anti-tumor response. *Oncoimmunology* 12: 2205336.
- Russell, M.C., Garelli, A.M., and Reeves, D.J. (2023). Targeting EGFR exon 20 insertion mutation in non-small cell lung cancer: amivantamab and mobocertinib. *Ann. Pharmacother.* 57: 198–206.
- Sadelain, M., Brentjens, R., and Rivière, I. (2013). The basic principles of chimeric antigen receptor design. *Cancer Discov.* 3: 388–398.
- Samantasinghar, A., Sunilidutt, N.P., Ahmed, F., Soomro, A.M., Salih, A.R.C., Parihar, P., Memon, F.H., Kim, K.H., Kang, I.S., and Choi, K.H. (2023). A comprehensive review of key factors affecting the efficacy of antibody drug conjugate. *Biomed. Pharmacother.* 161: 114408.
- Schmohl, J.U., Todhunter, D., Taras, E., Bachanova, V., and Vallera, D.A. (2018). Development of a deimmunized bispecific immunotoxin dDT2219 against B-cell malignancies. *Toxins* 10: 32.
- Schram, A.M., Odintsov, I., Espinosa-Cotton, M., Khodos, I., Sisso, W.J., Mattar, M.S., Lui, A.J.W., Vojnic, M., Shameem, S.H., Chauhan, T., et al. (2022). Zenocutuzumab, a HER2xHER3 bispecific antibody, is effective therapy for tumors driven by NRG1 gene rearrangements. *Cancer Discov.* 12: 1233–1247.
- Schubert, I., Kellner, C., Stein, C., Kügler, M., Schwenkert, M., Saul, D., Mentz, K., Singer, H., Stockmeyer, B., Hillen, W., et al. (2011). A single-chain triplebody with specificity for CD19 and CD33 mediates effective lysis of mixed lineage leukemia cells by dual targeting. *MAbs* 3: 21–30.
- Schubert, I., Stein, C., and Fey, G.H. (2012). Dual-targeting for the elimination of cancer cells with increased selectivity. *Antibodies* 1: 2–18.
- Seung, E., Xing, Z., Wu, L., Rao, E., Cortez-Retamozo, V., Ospina, B., Chen, L., Beil, C., Song, Z., Zhang, B., et al. (2022). A trispecific antibody targeting HER2 and T cells inhibits breast cancer growth via CD4 cells. *Nature* 603: 328–334.
- Shah, D., Soper, B., and Shopland, L. (2023). Cytokine release syndrome and cancer immunotherapies – historical challenges and promising futures. *Front. Immunol.* 14: 1190379.
- Shah, N.N., Johnson, B.D., Schneider, D., Zhu, F., Szabo, A., Keever-Taylor, C.A., Krueger, W., Worden, A.A., Kadan, M.J., Yim, S., et al. (2020). Bispecific anti-CD20, anti-CD19 CAR T cells for relapsed B cell malignancies: a phase 1 dose escalation and expansion trial. *Nat. Med.* 26: 1569–1575.
- Shah, N.N. and Sokol, L. (2021). Targeting CD22 for the treatment of B-cell malignancies. *ImmunoTargets Ther.* 10: 225–236.
- Shimabukuro-Vornhagen, A., Gödel, P., Subklewe, M., Stemmler, H.J., Schlöber, H.A., Schlaak, M., Kochanek, M., Böll, B., and von Bergwelt-Baildon, M.S. (2018). Cytokine release syndrome. *J. Immunother. Cancer* 6: 56.
- Sigismund, S., Avanzato, D., and Lanzetti, L. (2018). Emerging functions of the EGFR in cancer. *Mol. Oncol.* 12: 3–20.
- Singh, A., Dees, S., and Grewal, I.S. (2021). Overcoming the challenges associated with CD3+ T-cell redirection in cancer. *Br. J. Cancer* 124: 1037–1048.
- Sivori, S., Pende, D., Bottino, C., Marcenaro, E., Pessino, A., Biassoni, R., Moretta, L., and Moretta, A. (1999). Nkp46 is the major triggering receptor involved in the natural cytotoxicity of fresh or cultured human NK cells. Correlation between surface density of Nkp46 and natural cytotoxicity against autologous, allogeneic or xenogeneic target cells. *Eur. J. Immunol.* 29: 1656–1666.
- Smith-Garvin, J.E., Koretzky, G.A., and Jordan, M.S. (2009). T cell activation. *Annu. Rev. Immunol.* 27: 591–619.
- Steinmetz, A., Vallée, F., Beil, C., Lange, C., Baurin, N., Beninga, J., Capdevila, C., Corvey, C., Dupuy, A., Ferrari, P., et al. (2016). CODV-Ig, a universal bispecific tetraivalent and multifunctional immunoglobulin format for medical applications. *MAbs* 8: 867–878.
- Sterner, R.C. and Sterner, R.M. (2021). CAR-T cell therapy: current limitations and potential strategies. *Blood Cancer J.* 11: 69.
- Sun, J., Chen, Y., Lubben, B., Adebayo, O., Muz, B., and Azab, A.K. (2021). CD47-targeting antibodies as a novel therapeutic strategy in hematologic malignancies. *Leuk. Res. Rep.* 16: 100268.
- Sun, L., Zhang, L., Yu, J., Zhang, Y., Pang, X., Ma, C., Shen, M., Ruan, S., Wasan, H.S., and Qiu, S. (2020). Clinical efficacy and safety of anti-PD-1/PD-L1 inhibitors for the treatment of advanced or metastatic cancer: a systematic review and meta-analysis. *Sci. Rep.* 10: 2083.
- Sun, R., Wang, X., Zhu, H., Mei, H., Wang, W., Zhang, S., and Huang, J. (2014). Prognostic value of LAMP3 and TP53 overexpression in benign and malignant gastrointestinal tissues. *Oncotarget* 5: 12398–12409.
- Suntharalingam, G., Perry, M.R., Ward, S., Brett, S.J., Castello-Cortes, A., Brunner, M.D., and Panoskaltis, N. (2006). Cytokine storm in a phase 1 trial of the anti-CD28 monoclonal antibody TGN1412. *N. Engl. J. Med.* 355: 1018–1028.
- Syed, Y.Y. (2021). Amivantamab: first approval. *Drugs* 81: 1349–1353.
- Tabares, P., Berr, S., Römer, P.S., Chuvpilo, S., Matskevich, A.A., Tyrsin, D., Fedotov, Y., Einsele, H., Tony, H.-P., and Hünig, T. (2014). Human regulatory T cells are selectively activated by low-dose application of the CD28 superagonist TGN1412/TAB08. *Eur. J. Immunol.* 44: 1225–1236.
- Tang, Y., Yin, H., Zhao, X., Jin, D., Liang, Y., Xiong, T., Li, L., Tang, W., Zhang, J., Liu, M., et al. (2022). High efficacy and safety of CD38 and BCMA bispecific CAR-T in relapsed or refractory multiple myeloma. *J. Exp. Clin. Cancer Res.* 41: 2.
- Tapia-Galisteo, A., Compte, M., Álvarez-Vallina, L., and Sanz, L. (2023). When three is not a crowd: trispecific antibodies for enhanced cancer immunotherapy. *Theranostics* 13: 1028–1041.
- Tapia-Galisteo, A., Sánchez Rodríguez, Í., Aguilar-Sopeña, O., Harwood, S.L., Narbona, J., Ferreras Gutierrez, M., Navarro, R., Martín-García, L., Corbacho, C., Compte, M., et al. (2022). Trispecific T-cell engagers for dual tumor-targeting of colorectal cancer. *Oncoimmunology* 11: 2034355.

- Temraz, S., Mukherji, D., and Shamseddine, A. (2016). Dual targeting of HER3 and EGFR in colorectal tumors might overcome anti-EGFR resistance. *Crit. Rev. Oncol. Hematol.* 101: 151–157.
- Tian, W., Zhao, J., and Wang, W. (2023). Targeting CDH17 with chimeric antigen receptor-redirected T cells in small cell lung cancer. *Lung* 201: 489–497.
- Tong, C., Zhang, Y., Liu, Y., Ji, X., Zhang, W., Guo, Y., Han, X., Ti, D., Dai, H., Wang, C., et al. (2020). Optimized tandem CD19/CD20 CAR-engineered T cells in refractory/relapsed B-cell lymphoma. *Blood* 136: 1632–1644.
- Tyrsin, D., Chuvpilo, S., Matskevich, A., Nemenov, D., Römer, P.S., Tabares, P., and Hünig, T. (2016). From TGN1412 to TAB08: the return of CD28 superagonist therapy to clinical development for the treatment of rheumatoid arthritis. *Clin. Exp. Rheumatol.* 34: 45–48.
- van Herpe, F. and van Cutsem, E. (2023). The role of cMET in gastric cancer-A review of the literature. *Cancers* 15: 1976.
- Vasan, N., Baselga, J., and Hyman, D.M. (2019). A view on drug resistance in cancer. *Nature* 575: 299–309.
- Vijayaraghavan, S., Lipfert, L., Chevalier, K., Bushey, B.S., Henley, B., Lenhart, R., Sendekci, J., Beqiri, M., Millar, H.J., Packman, K., et al. (2020). Amivantamab (JNJ-61186372), an Fc enhanced EGFR/cMet bispecific antibody, induces receptor downmodulation and antitumor activity by monocyte/macrophage trogocytosis. *Mol. Cancer Ther.* 19: 2044–2056.
- Vivier, E., Tomasello, E., Baratin, M., Walzer, T., and Ugolini, S. (2008). Functions of natural killer cells. *Nat. Immunol.* 9: 503–510.
- Walker, L.S.K. and Sansom, D.M. (2011). The emerging role of CTLA4 as a cell-extrinsic regulator of T cell responses. *Nat. Rev. Immunol.* 11: 852–863.
- Wang, K., Wei, G., and Liu, D. (2012). CD19: a biomarker for B cell development, lymphoma diagnosis and therapy. *Exp. Hematol. Oncol.* 1: 36.
- Wang, S., Peng, L., Xu, W., Zhou, Y., Zhu, Z., Kong, Y., Leung, S., Wang, J., Yan, X., and Mi, J.-Q. (2022). Preclinical characterization and comparison between CD3/CD19 bispecific and novel CD3/CD19/CD20 trispecific antibodies against B-cell acute lymphoblastic leukemia: targeted immunotherapy for acute lymphoblastic leukemia. *Front. Med.* 16: 139–149.
- Wang, Y., Du, J., Gao, Z., Sun, H., Mei, M., Wang, Y., Ren, Y., and Zhou, X. (2023). Evolving landscape of PD-L2: bring new light to checkpoint immunotherapy. *Br. J. Cancer* 128: 1196–1207.
- Wang, Y., Ni, H., Zhou, S., He, K., Gao, Y., Wu, W., Wu, M., Wu, Z., Qiu, X., Zhou, Y., et al. (2021). Tumor-selective blockade of CD47 signaling with a CD47/PD-L1 bispecific antibody for enhanced anti-tumor activity and limited toxicity. *Cancer Immunol. Immunother.* 70: 365–376.
- Wei, G., Zhang, Y., Zhao, H., Wang, Y., Liu, Y., Liang, B., Wang, X., Xu, H., Cui, J., Wu, W., et al. (2021). CD19/CD22 dual-targeted CAR T-cell therapy for relapsed/refractory aggressive B-cell lymphoma: a safety and efficacy study. *Cancer Immunol. Res.* 9: 1061–1070.
- Weisser, N.E., Sanches, M., Escobar-Cabrera, E., O’Toole, J., Whalen, E., Chan, P.W.Y., Wickman, G., Abraham, L., Choi, K., Harbourne, B., et al. (2023). An anti-HER2 biparatopic antibody that induces unique HER2 clustering and complement-dependent cytotoxicity. *Nat. Commun.* 14: 1394.
- Wu, L., Seung, E., Xu, L., Rao, E., Lord, D.M., Wei, R.R., Cortez-Retamozo, V., Ospina, B., Posternak, V., Uliniski, G., et al. (2020). Trispecific antibodies enhance the therapeutic efficacy of tumor-directed T cells through T cell receptor co-stimulation. *Nat. Cancer* 1: 86–98.
- Xie, B., Li, Z., Zhou, J., and Wang, W. (2022). Current status and perspectives of dual-targeting chimeric antigen receptor T-cell therapy for the treatment of hematological malignancies. *Cancers* 14: 3230.
- Xu, J., Ying, J., Liu, R., Wu, J., Ye, F., Xu, N., Zhang, Y., Zhao, R., Xiang, X., Wang, J., et al. (2023). KN026 (anti-HER2 bispecific antibody) in patients with previously treated, advanced HER2-expressing gastric or gastroesophageal junction cancer. *Eur. J. Cancer* 178: 1–12.
- Xue, J., Kong, D., Yao, Y., Yang, L., Yao, Q., Zhu, Y., Ding, Y., Yang, F., Gong, J., Shen, L., et al. (2020). Prediction of human pharmacokinetics and clinical effective dose of SI-B001, an EGFR/HER3 Bi-specific monoclonal antibody. *J. Pharm. Sci.* 109: 3172–3180.
- Yu, J., Li, S., Chen, D., Liu, D., Guo, H., Yang, C., Zhang, W., Zhang, L., Zhao, G., Tu, X., et al. (2023). IMM0306, a fusion protein of CD20 mAb with the CD47 binding domain of SIRPα, exerts excellent cancer killing efficacy by activating both macrophages and NK cells via blockade of CD47-SIRPα interaction and FcγR engagement by simultaneously binding to CD47 and CD20 of B cells. *Leukemia* 37: 695–698.
- Zah, E., Nam, E., Bhuvan, V., Tran, U., Ji, B.Y., Gosliner, S.B., Wang, X., Brown, C.E., and Chen, Y.Y. (2020). Systematically optimized BCMA/CS1 bispecific CAR-T cells robustly control heterogeneous multiple myeloma. *Nat. Commun.* 11: 2283.
- Zahavi, D., AlDeghaither, D., O’Connell, A., and Weiner, L.M. (2018). Enhancing antibody-dependent cell-mediated cytotoxicity: a strategy for improving antibody-based immunotherapy. *Antib. Ther.* 1: 7–12.
- Zhang, B., Li, S., Chen, D., Liu, D., Guo, H., Yang, C., Zhang, L., Zhang, W., Tu, X., Peng, L., et al. (2023) Abstract 2938: preclinical development of a novel bispecific mAb-Trap fusion protein, IMM2902, targeting both HER2 and CD47 as cancer immunotherapy. *Cancer Res.* 83: 2938.
- Zhang, H., Gao, L., Liu, L., Wang, J., Wang, S., Gao, L., Zhang, C., Liu, Y., Kong, P., Liu, J., et al. (2019). A Bcma and CD19 bispecific CAR-T for relapsed and refractory multiple myeloma. *Blood* 134: 3147.
- Zhang, X., Gureasko, J., Shen, K., Cole, P.A., and Kuriyan, J. (2006). An allosteric mechanism for activation of the kinase domain of epidermal growth factor receptor. *Cell* 125: 1137–1149.
- Zhao, L., Li, S., Wei, X., Qi, X., Liu, D., Liu, L., Wen, F., Zhang, J.-S., Wang, F., Liu, Z.-L., et al. (2022). A novel CD19/CD22/CD3 trispecific antibody enhances therapeutic efficacy and overcomes immune escape against B-ALL. *Blood* 140: 1790–1802.
- Zhou, C., Tang, K.-J., Cho, B.C., Liu, B., Paz-Ares, L., Cheng, S., Kitazono, S., Thiagarajan, M., Goldman, J.W., Sabari, J.K., et al. (2023). Amivantamab plus chemotherapy in NSCLC with EGFR exon 20 insertions. *N. Engl. J. Med.* 389: 2039–2051.
- Zhou, S., Liu, M., Ren, F., Meng, X., and Yu, J. (2021). The landscape of bispecific T cell engager in cancer treatment. *Biomark. Res.* 9: 38.
- Zingoni, A., Molfetta, R., Fionda, C., Soriani, A., Paolini, R., Cippitelli, M., Cerboni, C., and Santoni, A. (2018). NKG2D and its ligands: “one for all, all for one”. *Front. Immunol.* 9: 476.
- Zinzani, P.L. and Minotti, G. (2022). Anti-CD19 monoclonal antibodies for the treatment of relapsed or refractory B-cell malignancies: a narrative review with focus on diffuse large B-cell lymphoma. *J. Cancer Res. Clin. Oncol.* 148: 177–190.
- Zong, H.-F., Zhang, B.-H., and Zhu, J.-W. (2022). Generating a bispecific antibody drug conjugate targeting PRLR and HER2 with improving the internalization. *Pharmaceut. Fronts* 4: e113–e120.

---

## 5. Danksagung

---

An dieser Stelle möchte ich mich bei allen Personen von ganzem Herzen bedanken, die mich auf meinem bisherigen Weg und insbesondere während der Anfertigung dieser Arbeit begleitet und unterstützt haben!

An erster Stelle möchte ich **Prof. Dr. Harald Kolmar** danken. Danke, dass du mir ermöglicht hast meine Doktorarbeit in deinem Arbeitskreis anzufertigen. Deine unzähligen neuen Ideen und die spannenden Diskussionen über neue und bestehende Projekte haben mich inspiriert und motiviert viele Ideen auszutesten. Danke für den Freiraum, den du mir gelassen hast, für das große Vertrauen in meine Arbeit und für die riesige Unterstützung und Fürsprache.

Außerdem möchte ich mich bei **PD Dr. Björn Hock** bedanken, nicht nur für die Übernahme des 1. Fachprüfers meiner Disputation, sondern auch für die Zeit, die du dir für wissenschaftliche Diskussionen genommen hast. Von deiner von der biopharmazeutischen Industrie geprägten Sichtweise auf Projekte konnte ich viel lernen.

**PD Dr. Stefan Schülke** und **Prof. Dr. Beatrix Süß** danke ich für die Übernahme des 2. Gutachters, bzw. der 2. Fachprüferin meiner Disputation.

Danke **Dr. Jan Bogen**, dass du nicht aufgegeben hast mich während der Betreuung meiner Masterarbeit davon zu überzeugen eine Doktorarbeit anzufertigen. Danke für deine unermüdliche Unterstützung, für alles, was du mir beigebracht hast und für die Möglichkeit aufbauend auf deinem Projekt weiterzuarbeiten.

**Dr. Stefania Carrara** danke ich für die Unterstützung und Zusammenarbeit bei einer Vielzahl von Projekten und für die unzähligen wissenschaftlichen Diskussionen. Du hattest immer ein offenes Ohr für mich, egal ob es um laborbezogene oder anderweitige Probleme ging, und ich konnte mich immer auf deine Hilfe verlassen.

Danke **Katrin Schoenfeld** und **Carolin Dombrowsky**, dass ihr das Studium vom aller ersten Tag an bis zur Doktorarbeit mit mir zusammen durchgezogen habt. Ich bin unendlich dankbar, dass ich euch als meine Freunde während dieser Zeit immer an meiner Seite hatte. Danke für die Zusammenarbeit bei spannenden Projekten, die gemeinsamen Meetings und die Unterstützung bei Problemen aller Art. Die gemeinsame Zeit als *Triplikat* im Labor, auf Konferenzen und bei diversen Freizeitveranstaltungen werde ich nie vergessen.

---

**Michael Ulitzka** möchte ich für die strukturierte Zusammenarbeit an dem NK-Projekt, zahlreiche kulinarische Tipps und diverse Lebensweisheiten danken. Von dir habe ich viel gelernt, an das ich in Zukunft sicher oft zurückdenken werde.

Den *Bitsches* **Dr. Sebastian Bitsch** und **Peter Bitsch** danke ich für die unzähligen Momenten, in denen ihr mich durch eure positive Art und die verrücktesten Aktionen zum Lachen gebracht habt. Auch für die legendären Tischkickerspiele und die Ratschläge zu den unterschiedlichsten Problemen bin ich euch sehr dankbar.

Den *Felices* **Felix Geyer** und **Felix Meiser** möchte ich für die gute Zusammenarbeit und die Unterstützung, besonders im Hinblick auf computerbasierte Modellierung, bzw. für die Fortführung einiger Projekte danken. Ich wünsche euch für die restliche Promotion nur das Beste und hoffe, dass ihr mich ab und zu auf ein Feierabendbier im Labor willkommen heißen werdet.

**Janine Becker** und **Dana Schmidt** danke ich für die Hilfe, sowie für die organisatorischen Arbeiten im Labor und für die Kaffeekränzchen im Büro. Danke, dass ihr immer ein offenes Ohr für mich hattet und für euer Vertrauen und eure Offenheit in jeglicher Hinsicht.

**Barbara Diestelmann** und **Cecilia Gorus** danke ich für die Hilfe bei bürokratischen und administrativen Aufgaben, bzw. für die Bemühung das Chaos im Arbeitskreis so gering wie möglich zu halten und jedes „Guten Morgen, Julia“.

Außerdem möchte ich dem gesamten *Ferring Team* **Dr. Julius Grzeschik**, **Dr. David Fiebig**, **Dr. Lukas Deweid** und **Dr. Benjamin Mattes** für die Unterstützung besonders zu Beginn meiner Promotion und die vielen Dinge, die ich von euch lernen durfte, danken.

**Vera Molkenthin** danke ich für die gute Zusammenarbeit, welche zu einer gemeinsamen Publikation geführt hat.

**Dr. Ataurehman Ali**, **Adrian Bloch**, **Ingo Bork**, **Dr. Adrian Elter**, **Dr. Desislava Elter**, **Alessandro Emmanuello**, **Dr. Simon Englert**, **Dr. Jan Habermann**, **Dominic Happel**, **Dr. Steffen Hinz**, **Sarah Hofmann**, **Dr. Jorge Lerma Romero**, **Dr. Arturo Macarrón**, **Dr. Hendrik Schneider** und allen weiteren ehemaligen und aktiven Mitgliedern der *Arbeitsgruppe Kolmar* danke ich für die unvergessliche Zeit im Labor, auf Konferenzen oder im Kleinwalsertal. Dank euch allen habe ich mich ab dem ersten Tag in der Arbeitsgruppe sehr wohl gefühlt.

---

Ein besonderer Dank gilt **meiner Familie**. Meinen Eltern **Birgit Harwardt** und **Christof Harwardt**, sowie meinem Bruder **Fabian Harwardt** und meinem Mann **Marcel Zänger** danke ich für die bedingungslose Unterstützung während meines gesamten Studiums. Danke, dass ihr mich zu dem Menschen gemacht habt der ich heute bin und mir ermöglicht habt, all meinen Träumen nachzugehen. Ihr habt mir beigebracht niemals aufzugeben, egal wie schwer der Weg auch scheinen mag. Danke für die Geduld und das Verständnis, wenn ich meine Arbeit mit nach Hause genommen habe und für die unzähligen aufbauenden Worte in schwierigen Phasen. Danke, dass ihr immer für mich da seid und es immer wieder schafft mich zu motivieren. Ohne euch, wäre das alles nicht ansatzweise möglich gewesen.

---

---

## 6. Affirmations

---

### Erklärung laut Promotionsordnung

#### §8 Abs. 1 lit. c PromO

Ich versichere hiermit, dass die elektronische Version meiner Dissertation mit der schriftlichen Version übereinstimmt und für die Durchführung des Promotionsverfahren vorliegt.

#### §8 Abs. 1 lit. d PromO

Ich versichere hiermit, dass zu einem vorherigen Zeitpunkt noch keine Promotion versucht wurde und zu keinem früheren Zeitpunkt an einer in- oder ausländischen Hochschule eingereicht wurde. In diesem Fall sind nähere Angaben über Zeitpunkt, Hochschule, Dissertationsthema und Ergebnis dieses Versuches mitzuteilen.

#### §9 Abs. 1 PromO

Ich versichere hiermit, dass die vorliegende Dissertation selbstständig und nur unter Verwendung der angegebenen Quellen verfasst wurde.

#### §9 Abs. 2 PromO

Die Arbeit hat bisher noch nicht zu Prüfungszwecken gedient.

Darmstadt, den 10. Juni 2024

-----  
Julia Harwardt



## Erklärung zum Eigenanteil an den Veröffentlichungen der kumulativen Dissertation

Im Folgenden ist aufgelistet, mit welchem Anteil ich an den Veröffentlichungen beteiligt war.

Mein Anteil an der folgenden Veröffentlichung beträgt 40%

1] **Harwardt J\***, Bogen JP\*, Carrara SC, Ulitzka M, Grzeschik J, Hock B, Kolmar H (2022). A Generic Strategy to Generate Bifunctional Two-in-One Antibodies by Chicken Immunization. *Frontiers in Immunology*, 10.3389/fimmu.2022888838.

Mein Anteil an der folgenden Veröffentlichung beträgt 80%

2] **Harwardt J**, Carrara SC, Bogen JP, Schoenfeld K, Grzeschik J, Hock B, Kolmar H (2023). Generation of a symmetrical trispecific NK cell engager based on a two-in-one antibody. *Frontiers in Immunology*, 10.3389/fimmu.2023.1170042.

Mein Anteil an der folgenden Veröffentlichung beträgt 70%

3] **Harwardt J**, Geyer FK, Schoenfeld K, Baumstark D, Molkenhuth V, Kolmar H (2024). Balancing the Affinity and Tumor Cell Binding of a Two-in-One Antibody Simultaneously Targeting EGFR and PD-L1. *Antibodies*, 10.3390/antib13020036.

Mein Anteil an der folgenden Veröffentlichung beträgt 45%

4] Schoenfeld K\*, **Harwardt J\***, Kolmar H (2024). Better safe than sorry: Dual targeting antibodies for cancer immunotherapy. *Biological Chemistry*, 10.1515/hsz-2023-0329.

\*geteilte Erstautorenschaft

Mein Anteil an der folgenden Patentanmeldung beträgt 30%

Kolmar H, **Harwardt J**, Bogen JP, Carrara SC, Ulitzka M (2023). TWO IN ONE – ANTIBODIES BINDING TO EGFR/PD-L1-DOUBLE POSITIVE CELLS. EP4238992A1.

Darmstadt, den 07. Mai 2024

-----  
Julia Harwardt





## Erklärung zur Begutachtung der Veröffentlichung

Prof. Dr. Harald Kolmar

-----  
Referent

PD Dr. Stefan Schülke

-----  
Co-Referent

07. Mai 2024

-----  
Datum

Weder Referent (Prof. Dr. Harald Kolmar) noch Co-Referent (PD Dr. Stefan Schülke) der vorliegenden kumulativen Doktorarbeit waren an der Begutachtung nachstehender Veröffentlichungen beteiligt:

1] A Generic Strategy to Generate Bifunctional Two-in-One Antibodies by Chicken Immunization. *Frontiers in Immunology*, 10.3389/fimmu.2022888838.

2] **Harwardt J**, Carrara SC, Bogen JP, Schoenfeld K, Grzeschik J, Hock B, Kolmar H (2023). Generation of a symmetrical trispecific NK cell engager based on a two-in-one antibody. *Frontiers in Immunology*, 10.3389/fimmu.2023.1170042.

3] **Harwardt J**, Geyer FK, Schoenfeld K, Baumstark D, Molkenhuth V, Kolmar H (2024). Balancing the Affinity and Tumor Cell Binding of a Two-in-One Antibody Simultaneously Targeting EGFR and PD-L1. *Antibodies*, 10.3390/antib13020036.

4] Schoenfeld K\*, **Harwardt J\***, Kolmar H (2024). Better safe than sorry: Dual targeting antibodies for cancer immunotherapy. *Biological Chemistry*, 10.1515/hsz-2023-0329.

Darmstadt, den 07. Mai 2024

-----  
Referent

Prof. Dr. Harald Kolmar

-----  
Co-Referent

PD Dr. Stefan Schülke